Entanglement and Symmetry Breaking

PhD Thesis: Physics Area (TPP)

Candidate: Amartya Harsh Singh

Supervisor: Prof. Francesco Benini, Prof. Laura Donnay

Academic Year 2025–2026

Declaration

I hereby declare that, except where specific reference is made to the work of others, the contents of this thesis are original and have not been submitted in whole or in part for consideration for any other degree or qualification in this, or another university. This thesis is based on the following works:

- Entanglement asymmetry in conformal field theory and holography (Francesco Benini, Victor Godet, **Amartya Harsh Singh** (arXiv 2407.07969), PTEP 2025 6 [1]

- Entanglement Asymmetry for Higher and Noninvertible symmetries (Francesco Benini, Pasquale Calabrese, Michele Fossati, **Amartya Harsh Singh**, Marco Venuti (arXiv 2509.16311) [2]

Abstract

This thesis studies (generalized) symmetry breaking in states via entanglement measures. Specifically, we study a relative entropy between a given state and a suitably defined symmetric version of the same state; obtained by applying a quantum channel made of the topological operators implementing the symmetry. We study this for both excited states in CFTs as well as symmetry breaking vacua. In the first part, following [1], we study a perturbative version of this asymmetry in CFTs for a $U(1)$ symmetry in various geometries, and study the relaxation of such states in real time while displaying a quantum Mpemba effect. We also study the holography of entanglement asymmetry. In the second part, following [2], we study the symmetrization process for non-invertible symmetries in two spacetime dimensions. We identify the different symmetry algebras that act on a circle or interval hilbert space, and prescribe a universal, unique symmetrization procedure to compute symmetry breaking. We study examples in both CFTs and gapped symmetry breaking states.

Contents

List of Figures

Chapter 1

Invitation

The purpose of this informal invitation[1] is to contextualize the core quantity which is the object of this thesis- *Entanglement Asymmetry* [1–3]. We want to motivate the present understanding that symmetries on their own are not enough to classify quantum phases of matter; a crucial role is played by the entanglement structure of states. We will do so by reviewing some paradigmatic examples from condensed matter physics that have shaped modern day research into generalized symmetries and quantum information. The hope is to convince the reader that it is a sensible exercise to try to find quantities that combine symmetry breaking and entanglement measures. Much of this is this is based on [4–6].

1.1 Quantum Ising chain

Consider what is probably the dearest Hamiltonian to a condensed matter physicst: the *Ising model in transverse field*

$$H = -J\sum_i \sigma_i^z\sigma_{i+1}^z - h\sum_i \sigma_i^x \tag{1.1.1}$$

The Hamiltonian has a global $\mathbb{Z}_2$ symmetry generated by

$$U = \prod_i \sigma_i^x.$$

Its vacua are easy to write in the extreme cases:

- $J = 0:\ \ |\Omega_+\rangle = |+...+\rangle$
- $h = 0:\ \ |\Omega\rangle = \alpha|\uparrow\uparrow..\rangle + \beta|\downarrow\downarrow..\rangle \equiv \alpha|\Omega_\uparrow\rangle + \beta|\Omega_\downarrow\rangle$

[1] which, like all invitations, can be declined

So, as we tune the parameters from $h >> J$ to $J >> h$, we find that the nature of vacua (in the thermodynamic limit) is very different: the system goes from a unique gapped vacuum $|\Omega_+\rangle$ which is $\mathbb{Z}_2$ invariant, to a 2 dimensional manifold of gapped vacua $|\Omega_\uparrow\rangle, |\Omega_\downarrow\rangle$ which are exchanged by the $\mathbb{Z}_2$ symmetry. This change can only happen if the gap closes at some point; i.e. there is a *phase transition*. The phase transition happens at precisely $J = h$. In particular, as long as $J < h$, we have a unique gapped vacuum, although it is no longer a product state $|\Omega_+\rangle$ away from $J = 0$. Similarly, as long as $h < J$, we continue to have a 2 dimensional ground state manifold of gapped vacua, but they are not just spanned by product states. Below, we continue to use the (slight abuse of) notation $|\Omega_+\rangle, |\Omega_{\uparrow,\downarrow}\rangle$ for the vacua in the $h > J$ and $h < J$ regions respectively.

Landau's paradigm says that there must be a local observable charged under the symmetry that distinguishes the two phases. In fact, note that the local operator σ_z^i is charged under this symmetry

$$U\sigma_i^z U^{-1} = -\sigma_i^z$$

And it probes the difference between the two vacua

$$\langle\Omega_+|\sigma_z|\Omega_+\rangle = 0, \quad \langle\Omega_{\uparrow\downarrow}|\sigma_z^i|\Omega_{\uparrow\downarrow\rangle} \neq 0 \quad (= 1 \text{ for } h = 0) \tag{1.1.2}$$

The crucial point is that the equation $\langle\Omega_+|\sigma_z|\Omega_+\rangle = 0$ is *exact*; this vanishing is *protected* by the $\mathbb{Z}_2$ symmetry under which the vacuum is symmetric, but the operator is charged.

So we see that Landau's theory describes very well the phases in this simplest but crucial spin chain, via $\mathbb{Z}_2$ symmetry breaking of the vacua.

Before we move on to more involved examples, let us make a remark about finite sized systems versus ground states in the thermodynamic limit.

Consider the case $h = 0$. On the finite chain (with periodic boundary conditions), we saw that we have 2 ground states $|\Omega_{\uparrow\downarrow}\rangle$ which are degenerate. In fact, their linear combinations are also valid ground states on the finite chain. [2] Suppose one takes a linear combination; then the order paramater can actually vanish:

[2] $h = 0$ is a bit peculiar; for $h > 0$, actually, the degeneracy is slightly lifted on a finite chain. There is a unique, symmetric ground state on a finite chain which is a dressed (by spin flip corrections) version of the symmetric state $|\Omega_\uparrow\rangle + |\Omega_\downarrow\rangle$. The first excited state is a dressed version of the antisymmetric state $|\Omega_\uparrow\rangle + |\Omega_\downarrow\rangle$. However this splitting is lifted in the thermodynamic limit, and we have two vacua (which are thermodynamic limits of linear combinations of the above states). This subtlety doesn't affect the subsequent arguments, so we stick to the simpler to illustrate case of $h = 0$.

$$|\Omega\rangle_{sym} \equiv \frac{1}{\sqrt{2}}(|\Omega_\uparrow\rangle + |\Omega_\downarrow\rangle) \qquad {}_{sym}\langle\Omega|\sigma_z^i|\Omega\rangle_{sym} = 0 \tag{1.1.3}$$

So, on what basis (pun intended) are we claiming that this is a symmetry breaking state? The key point is that symmetry breaking is a feature of *infinite* volume or the *thermodynamic limit*; where such linear combinations don't make sense as the two symmetry breaking vacua belong to different *superselection sectors*. The number of superselection sectors is the dimension of the (finite chain) ground state manifold. But then, how does one pick two representative "basis" vectors to label the superselection sectors? Are $|\Omega_{\uparrow\downarrow}\rangle$ the correct basis vectors that in the thermodynamic limit become the degenerate vacua? Or is it some other linear combination? Here is where physics enters, and we require *cluster decomposition*; i.e. the correlators factorize at large distances. In this simple case of product states at $h = 0$, it is simple to see that if we pick an arbitrary linear combination $|\Omega'\rangle = \alpha|\Omega_\uparrow\rangle + \beta|\Omega_\downarrow\rangle$, then cluster decomposition says

$$\langle\Omega'|\sigma_z^i\sigma_z^j|\Omega'\rangle - \langle\Omega'|\sigma_z^i|\Omega'\rangle\langle\Omega'|\sigma_z^j|\Omega'\rangle = 0 \iff |\Omega'\rangle \in \{|\Omega_\uparrow\rangle, |\Omega_\downarrow\rangle\} \tag{1.1.4}$$

(in general states, the above equation is required when $|i - j| \to \infty$, but that is immaterial here due to product state nature). This analysis doesn't change much for the case $h \neq 0$. There, in the thermodynamic limit (see footnote 2 for the subtlety on finite chain) , the clustering states $|\Omega_{\uparrow\downarrow}\rangle$ are not exact product states anymore, but have a small amount of entanglement because of the spin flipping effect of $h \neq 0$. So we learn that the *clustering* vacua are indeed a special *orthonormal* basis, which flow to the actual vacua in the thermodynamic limit. Later, when we study entanglement asymmetry for spontaneous symmetry breaking 9, we will focus our attention on such states.

Let us note that, from the entanglement point of view, both the gapped vacua are *short range entangled*. Being gapped systems, these vacua both display an *area law* for entanglement. In contrast, at the critical point, we have a critical system, with a *logarithmic* growth of entanglement.

1.2 Heisenberg chains

There is a natural (and equally famous) generalization of the the discrete $\mathbb{Z}_2$ symmetric Ising chain, to the continuous symmetry $SU(2)$. It is the *Heisenberg chain* [3]:

$$H = -J \sum_i \vec{S}_i \cdot \vec{S}_{i+1} \tag{1.2.1}$$

Here, $\vec{S}_i$ is an onsite $(2s+1)$ dimensional representation of $SU(2)$, describing a chain of spin-s particles. For integer spins, we consider $SO(3)$ as the faithful symmetry [4]. The sign of J is crucial. For $J > 0$, we have a ferromagnetic interaction. The ground state spontaneously breaks $SU(2) \to U(1)$ [5], and the resulting phase is therefore gapless. The ground state is the trivial product state with all spins pointing in the same direction. This state has no entanglement, and is quite dull by all practical means.

Instead, the *antiferromagnetic* case $J < 0$ is much more interesting. The underlying reason is that the ground state is now a highly entangled state. To see this, note that this sign of the coupling encourages neighboring spins to be *anti-aligned*. The classical ground state would be a so called *Neel state* $|\uparrow\downarrow\uparrow\downarrow ..\rangle$ which is not an eigenstate of the hamiltonian; so the quantum state is actually a superposition of many such states: this is the reason it is highly entangled. Note also that the total spin in any such state has to be zero.

For the case of *half integer spins*, a surprising answer emerges comes from the famous (Affleck) Lieb Schulz Matthis theorem[6]:

A half-integer (per unit cell) 1D system ***cannot*** *simultaneously have a unique ground state, be gapped, and preserve rotation and translation symmetry.*

Therefore for *half integer spins*, the Heiseberg antiferromagnet chain is actually gapless, if it has a unique ground state. In fact, for $s = \frac{1}{2}$, this system is actually *integrable* and can be solved exactly via the *Bethe Ansatz* [7], demonstrating rigorously that the system is indeed gapless. With the evidence from Bethe Ansatz and Leib-Schulz-Matthis-Affleck, it was clear that half integer antiferromagnetic spin chains were gapless when the ground state is unique, and it seemed to be natural to expect this for all spins.

---

[3] In particular, this is the XXX or the isotropic spin chain; more general couplings for the different $SU(2)$ generators are also often considered

[4] Note that for integers spins, the $\mathbb{Z}_2$ center of the $SU(2)$ symmetry acts trivially, so the representation is not faithful as an $SU(2)$ representation but it is faithful as an $SO(3) \cong SU(2)/\mathbb{Z}_2$ representation

[5] This is at zero temperature, so Mermin Wagner doesn't forbid this

[6] Leib-Schulz-Mattis proved it for spin 1/2; Leib and Affleck then proved it for all half integer spins

However, Haldane made a remarkable conjecture [8, 9] that *the 1D Heisenberg antiferromagnetic chain is gapless for half integer spins, but gapped for integer spins*, so they are quite different! He argued that there is a crucial difference between the effective nonlinear sigma models for integer and half integer terms. There is a topological term in the action that turns on only for half integer spins, and renders such systems gapless.

Unlike spin 1/2, it is not possible to solve the system exactly and verify the conjecture, except for $s = 1/2$. Fortunately, AKLT conjured up a closely related model [10, 11], which turns out to be exactly solvable[7] and in the same phase as the Haldane chain . This model has the Hamiltonian

$$H = -J \sum \left(\vec{S}_i \cdot \vec{S}_{i+1} + \frac{1}{3} (\vec{S}_i \cdot \vec{S}_{i+1})^2 \right) \quad (J < 0) \tag{1.2.2}$$

where $\vec{S}_i$ are the spin 1 $SO(3)$ representations. The ground state is made by *dimerizing* a pair of virtual spin 1/2s on each site into a spin 1 triplet onsite, while the extremal spin-1/2s on each such dimer are (maximally) entangled with its neighbouring site to form a spin singlet on the 'bond' connecting the onsite triplets. This is not a product state, and it is nicely written as a matrix product state (MPS) [8] It is perhaps best to see it in pictures

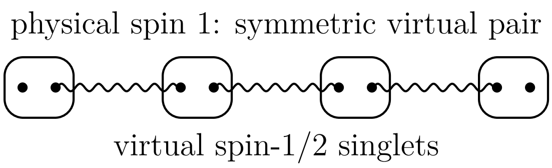

Figure 1.1: Valence-bond construction of the periodic AKLT state. Each rounded box is the projection of two virtual spin-1/2s onto a physical spin 1; each wavy line is a virtual singlet.

On a closed chain, the hamiltonian can be shown to be *gapped*, verifying Haldane's conjecture. In fact, since the ground state is exactly known, one can show that the correlation length is finite $(1/\log 3)$:

$$\langle \vec{S}_i \cdot \vec{S}_j \rangle \sim (-1)^{|i-j|} e^{-|i-j| \log 3} \tag{1.2.3}$$

But there's much more. A finite correlation length indicates that the spins are uncorrelatated at large enough distances, but there is something different in this

[7] More precisely, its ground state is known exactly, and a few excited states. It cannot really be fully diagonalized

[8] in fact the construction described above is a standard way to get an MPS representation from Project Entangled Pairs (PEPs), where one introduces virtual degrees of freedom on each site such that they are maximally entangled with neighbouring sites. Then one projects onto the physical Hilbert space on the physical site via an intertwiner from the virtual to physical hilbert space.

gapped state as compared to the trivially gapped state of e.g. the Ising chain that we saw earlier. To start with, this state has entanglement, and is not a dull product state with all spins pointing in the same direction. But it is not completely disordered either: there is still a hidden antiferromagnetic order here, but one that a local operator cannot probe. Consider the state formed by the virtual bonds which are spin singlets; the AKLT state is formed by applying a projector/intertwiner to the spin-1 Hilbert space on this virtual state. This state is a product of qubits. We can assign a 'domain wall' to each such qubit to track them, going up through $|\uparrow\downarrow\rangle$, down through $|\downarrow\downarrow\rangle$ and skipping the $|\uparrow\downarrow\rangle, |\downarrow\uparrow\rangle$ states. However, what goes up must come down, and there is an operator that can keep track of the number of domain walls D between sites i, j, without talking about the length it took the wall that goes up to come down: $\prod_i^j \exp(i\pi S_i^z) = (-1)^D$. Clearly then, this operator carries some information about an order, but this operator is *nonlocal.* Indeed, the Haldane phase can be captured by the *nonlocal string order parameter* [12]:

$$\lim_{|i-j|\to\infty} \langle S_i^z \prod_{i+1}^{j-1} \exp(i\pi S_i^z) S_j^z \rangle \neq 0 \tag{1.2.4}$$

in the AKLT ground state. Note an important lesson: there is no symmetry breaking and the system naively looks disordered from a local order parameter point of view; however there is a hidden order which can be probed by *non-local* order parameters like the string order parameter above. Crucial for this behaviour was a nontrivial entanglement pattern in the ground state.

There is another remarkable phenomenon going on here. On an *open* chain, it is clear by construction of the AKLT picture above, that there remain 'dangling' spin-1/2 degrees of freedom on the boundary where you cut the system-on an open chain the state is therefore $4-$ fold degenerate due to boundary conditions. But these boundary spin 1/2s are a *projective* representation of $SO(3)$- the boundary theory has a 'tHooft anomaly. In fact, these spins come in doublets at either end, and are robust and cannot be removed (i.e. gapped out) by any symmetry preserving perturbations. This is a hallmark feature of the Haldane spin 1 chain.

This phase of matter is a gapped phase, but it is clearly special from several points of view. The ground state break any symmetry by choosing a special order, but carries some kind of long range order that can be probed only by non-local order parameters. More dramatic is the fact that if you cut this state at some position, then the bulk remains gapped but you find edge spins that carry a t'hooft anomaly for the theory. Such phases of matter are called *symmetry protected topological/trivial* phases (SPTs), where the choice trivial/topological is left to one's taste.

The characteristic feature of such states is a unique, symmetry preserving gapped ground state on closed manifolds, presence of (short ranged) entanglement, and anomalous gapless edge theories when the theory is studied on an open manifold. Such states are almost trivial, in that they can be adiabatically deformed to the trivially gapped phase; but the obstruction is to do this *while preserving the symmetry*.[9]

1.3 Hall effects and new surprises

Haldane's chain is a classic example of an SPT phase. By definition, this phase becomes trivial if one allows deformations that break the $SO(3)$ symmetry. It turns out that there is another popular system that exhibits similar features, but reveals something deeper in the classification of phases that is missed if we only consider the $SO(3)$ symmetry of the Haldane chain.

Consider electrons confined to move along a plane, with a strong magnetic field that pierces the plane. If there is a current along some direction on the plane, then the magnetic field induces a *transverse voltage* along the orthogonal direction. This defines a *hall conductivity/resistivity* along the transverse axis. This is the classical hall effect. Experimentally, in the 80s, it was found that this resistivity shows remarkable quantization [13, 14]. In one of the most groundbreaking developments in theoretical condensed matter physics, this quantization and in particular its robustness was understood as a topological phenomenon. Without going into all the details, let us quickly sketch the argument.

The quantum mechanics of a particle of charge e and mass m in the presence of a magnetic field $B = \nabla \times \vec{A}$ is described by a hamiltonian

$$H = (\vec{p} - e\vec{A})^2/2m$$

Suppose the particle moves in the XY plane, and the magnetic field threads through, $\vec{B} = B\hat{e}_z$. In the *Landau gauge*, the vector potential may be chosen to be $\vec{A} = (0, Bx, 0)$. In this gauge, there is no explicit t or y dependence in the wavefunction $\psi(x, y, t)$; so those directions enjoy translation invariance. We can therefore make a plane wave ansatz in those directions, writing eigenfunctions of the hamiltonian as

$$\psi_n(x, y, t) = e^{iE_n t} e^{ik_n y} \phi_n(x)$$

[9] In fact, The spin-1 Haldane phase is protected by any one of several symmetries:SO(3) spin rotations, the dihedral group generated by π rotations, time reversal. If all protecting symmetries are relaxed, the AKLT state can be joined to a product state through gapped parent Hamiltonians.

It turns out that the equation for $\phi_n(x)$ a (shifted) harmonic oscillator, with the spectrum

$$E_n = \frac{eB}{m}(n+\frac{1}{2}) \qquad n = 0, 1, 2, ..$$

with no dependence on k_n, the dual variable to y. This is a *huge degeneracy.* These degenerate states are called *Landau levels.* It turns out that an almost semiclassical computation (the Drude model) can already predict that if ν of these Landau levels are filled in the presence of a magnetic field, then the Hall conductivity's[10] off diagonal components are

$$\sigma_{xy} = \nu \frac{e^2}{2\pi\hbar} \qquad \nu \in \mathbb{Z} \tag{1.3.1}$$

Does this already explain the observed plateaux? Not quite. The above equation works only when the electron density and external magnetic field B is precisely tuned to fill ν Landau levels. But the striking feature is the persistence of the plateau at a given ν even if we change B. It turns out the reason for this robustness is entirely different, and indeed the reason for the quantization too is much deeper than merely filling out an integer number of Landau levels.

The plateaux can be attributed to the presence of disorder in the sample, that provides a random perturbation to the Hamiltonian and actually lifts the vasts degeneracy in the Landau levels, and gives rise to two distinct kinds of charge carriers: those trapped in local extrema of the disorder-inclusive potential, and those can actually travel across the sample and transport current (and therefore contribute to conductivity). The plateau in Hall conductivity exist because changing the magnetic field will not immediately populate new states that can transport charge; but they will instead get trapped in the local extrema within the sample, keeping the conductivity fixed.

However, note that the same explanation now makes quantization a problem- the notion of a sharp, integer valued Landau level contributing to the conductivity is gone; some of its electrons can be trapped. So how is there a quantization? Here is where topology enters.

The setup is to consider the sample on a (unit, say) torus, with a uniform field $B\hat{e}_z$ that pierces the sample. Now, we turn on fluxes Φ_x, Φ_y that thread the two cycles of the torus. These fluxes trigger a current J_x, J_y: what we have done is perturb the original hamiltonian by a term

[10]Recall that its a tensor, with 4 components

$$\delta H_i = -\sum_{i=x,y} J_i \Phi_i$$

Note that we have a vector potential $\vec{A} = (\Phi_x, \Phi_y + Bx, 0)$. The spectrum is unchanged if the fluxes are of the form $\Phi_{x,y} = \frac{2\pi\hbar}{e}\mathbb{Z}$.

These fluxes trigger some current; what is it? The *Kubo formula* gives us the conductivity induced by such a perturbation, in terms of the matrix elements $\sigma_{xy} \sim \mathrm{Im}(\langle 0|J_x|n\rangle\langle n|J_y|0\rangle)/(E_n - E_0)^2$. The crucial observation is that these matrix elements are actually related to a *Berry curvature*. Recall that if we have a family of Hamiltonians $H(\lambda_i)$ depending on some parameters λ_i, then the adiabatic theorem guarantees that for a slow enough [11] motion in parameter space, the state continues to be stuck in an eigenstate if it started in one. This means that if one goes in a loop, the particle returns to the same state as it started. However, states are defined modulo phases, and the phase here is actually physical, being a phase *difference* between the initial and final wavefunctions. This phase can be captured by a holonomy in parameter space:

$$|\psi(2\pi)\rangle = \exp\Big(i\oint d\lambda^i \mathcal{A}_i(\lambda)\Big)|\psi(0)\rangle \quad \mathcal{A}_i(\lambda_i) \equiv i\langle\psi_0(\lambda)|\partial_{\lambda^i}|\psi_0(\lambda)\rangle \tag{1.3.2}$$

where $\psi_0(\lambda)$ is the instantaneous ground state when moving along the parameter space. $\mathcal{A}$ is called the Berry connection, from which one may define a Berry curvature $\mathcal{F}_{ij} = \partial_{[i}\mathcal{A}_{j]}$. It turns out that this curvature has a very curious property: it flux through a closed surface is always quantized

$$\oint \mathcal{F}_{ij} dS^{ij} = 2\pi\mathbb{Z}$$

The integer appearing is the famous *Chern number*. What is going on is that we are thinking of the space of wavefunctions as a complex line bundle over the space of parameters. Such bundles can be classified by Chern numbers; a nonzero Chern number indicates that the bundle is nontrivial i.e. there is no global section, and a loop in parameter space doesn't necessarily lift to a loop of states in the total space.

In our case, the parameter space is characterized by the fluxes we are threading $\Phi_{x,y}$. The Berry connection and curvature is is

$$\mathcal{A}_i = i\langle\psi_0(J_i)|\partial_{J_i}|\psi_0(J_i)\rangle, \quad \mathcal{F}_{ij} = \partial_{[J_i}\mathcal{A}_{j]} \tag{1.3.3}$$

[11]This depends on the details of the gap in the spectrum- the point is to be slow enough to avoid level crossing

where $|\psi_0(J_i)\rangle$ is the ground state accounting for the perturbation in the Hamiltonian with the fluxes. We remarked earlier that such fluxes are only effective modulo integer multiples of $2\pi\hbar/e$. This means that the parameter space of $J_{x,y}$ is a torus $S^1 \times S^1$ (with cycles of circumference $2\pi\hbar/e$). We can then find the averaged conductivity by averaging over the contributions from the entire parameter space; this produces the Chern number of this Berry curvature:

$$\sigma_{xy} = -\frac{e^2}{\hbar}\int_{S^1\times S^1} d^2\Phi \mathcal{F}_{xy} = -\frac{e^2}{2\pi\hbar}\mathbb{Z}$$

this is underlying topological origin for the integer quantum hall effect.

This is all very nice, but perhaps the most interesting part of this story is the physics going on at the boundary of the sample. Note that classically, for a finite rectangular sheet of (mobile) electrons pierced by a strong magnetic field, one expects the Lorentz force to make the electrons move in a circle with *fixed orientation* (depending on the direction of the magnetic field); and therefore when they reach the edge of the sample, they are forced to move in a fixed direction along the edge of the sample. In fact this intuition is correct, and the system hosts *chiral gapless edge modes*. These edge modes are much like the edge modes we saw earlier in the Haldane chain, and one can indeed think of the setup we just described as one describing an SPT phase protected by $U(1)$ symmetry (its this current that allows the coupling to background gauge fields, the response to which is probed by the conductivity).

But there is a surprise, as always. In fact, many characters in the above story are not so important to understand the topological mechanism of quantized hall conductance. For instance, one doesn't need a magnetic field[12] and Landau levels in this story: a *Chern insulator* displays quantized hall conductance even in zero external magnetic field (so no Landau levels); this quantization is called the *TKNN invariant* [14]. The Chern number in this case is classifing the ground state bundles over the torus of electron (on a periodic lattice's) momenta. More importantly, thinking of these phase merely as $U(1)$ SPT phase misses something very crucial: the gapless edge modes and the quantization of Hall conductivity have are not just an artifact of an electromagnetic response. In particular, one can break the $U(1)$ symmetry in the setup above and then there is no conductivity to define. Yet, there are gapless edge modes on a Chern insulator, just because the edge is an interface between the sample with nonzero Chern number and the vacuum; such an interface cannot be trivial. In fact, the conductivity probes the electromagnetic response of the sample, but the chiral edge modes are actually probing the *gravitational* response

[12] Just to be clear, the conductivity is a response to external perturbing fluxes, which we must put. What is not essential to put is the external field B that was creating the Landau levels.

of the sample, which is something much more fundamental. Note the difference in comparison to the Haldane chain: the edge spins there can be gapped out by a symmetry breaking perturbation. However, in the case of Chern insulators/Hall effect; the chiral edge modes cannot disappear: what's really protecting them is their *chirality*.

The usual SPT picture misses this crucial aspect of this phase; we need a more fundamental characterization. This is provided by the notion of *invertibility*. Consider what happens if take two Chern insulators, with chern numbers C and $(-C)$ respectively, and pile one on top of the other. What this does is bring together two *opposite* chirality edge modes together. But now the edge can be gapped out by the usual means of adding a dirac mass term that couples the two chiralities! This is often represented by an equation like

$$\mathcal{I} \boxtimes \mathcal{I}^{-1} \simeq \mathcal{E}$$

Where $\mathcal{I}$ is our invertible phase with inverse $\mathcal{I}^{-1}$, and $\mathcal{E}$ is supposed to denote the *trivial gapped phase*(product state). The notation $\simeq$ means that it can be reached via local deformations without closing the gap. Formally, one says that gapped phases of matter form a *monoid under stacking*, with the unit element being the trivial phase $\mathcal{E}$. Within this monoid lies the *group* of invertible phases labelled by $\mathcal{I}$.

What is common between the Chern insulator, and the Haldane phase, then? There are edge modes, but their robustness is of different origin and different nature. There are topological invariants that characterize both systems, but one has to do with anomalous symmetries and the other has to do with Berry phases. What is common however, is that both states display short range entanglement. In the case of Haldane phase, this entanglement structure is protected by symmetries; if you allow breaking them then you can deform the state adiabatically through a series of gapped states, into a trivial product state with no entanglement. However, for a chern insulator, this simply cannot be done! It can only be trivialized by stacking. Clearly, the nature of entanglement and the mechanisms that protect it are quite different in both cases, and they represent quite different phenomena.

1.4 Long range topological order

This is not the end. One feature that we saw emerge repeatedly was short range entanglement. Since this nomenclature exists, it is natural to expect that there also exists *long range entanglement*. In fact, we find it if we just think a little bit harder about the integer quantum hall case from before. After the experimental results of the 80s, new measurements a few years later revealed the existence of fractional-quantized conductances [15, 16], for instance $\nu = 1/3$. What did we miss in the description of the integer quantum hall effect? How to explain these fractions?

First, the picture earlier never spoke of inter-electron interactions. These are important to explain the FQHE. Moreover, we saw earlier that the conductance was related to the fact that once a Landau level is fully filled (the filling fraction $\nu \in \mathbb{Z}$), the system behaves like an insulator because of the gap between the Landau levels. A crucial feature of full Landau levels is that the many-body state is uniquely specified [13]; because of fermi statistics, if the Landau level is fully occupied, then each degenerate state is occupied exactly once. However, if instead we have only a *fractional* filling (say $\nu = 1/3$), then there is an enormous degeneracy to choose from when putting the electrons into a Landau level. Now, (Coulombic) interactions are important. They lift this degeneracy, and produces a *highly entangled* state describing the ground state; often described by the *Laughlin wavefunction* [16]:

$$\psi(z_1, ..z_n) = \prod_{i<j}(z_i - z_j)^m \exp\left(-\frac{eB}{4\hbar}|z_i|^2\right) \tag{1.4.1}$$

where $1/m$ is the filling fraction $\nu = 1/m$ of the Landau level. n is the total number of electrons[14]. Note that the gaussian part of this wavefunction is what expects from Landau levels (which are essentially harmonic oscillators, as we argued earlier). The factor $(z_i - z_j)^m$ out front are there to enforce fermi statistics: m must be odd to enforce anti-commutation. Moreover, $m > 1$ suppresses the amplitude for two electrons to get close to each other; this enforces coulumbic repulsion. It is really remarkable that such a simple ansatz captures the essence of FQHE.

This wavefunction is the ground state of our sample. Some exotic things happen if we consider *excitations* on top of it. An ansatz for an excited state (*quasi-hole*) localized at η is

$$\psi_{exc}(\eta, z_i) = \prod(z_i - \eta)\psi(z_1, .., z_n) \tag{1.4.2}$$

What this wavefunction is doing is suppressing the probability of finding an electron at the site η. This hole can be thought of as excising a small hole at η and adiabatically inserting a magnetic flux through it. This flux creates a transverse hall current, and pushes the electrons away; creating a deficit of negative charge. This can be thought of as an excitation-the quasi hole. What is remarkable is that

[13]The slater determined is fixed

[14]Given a total external flux Φ that is piercing our sample, there are roughly $e\Phi/h$ one particle in each Landau level; this is the degeneracy of a given level. The filling fraction of that level is the $\nu = n/(e\Phi/h)$

this hole carries a charge e/m, not e [17]. This is because the hall conductivity determines the charge transport, and for the Laughlin state, we have

$$\sigma_{xy} = \frac{1}{m}\frac{e^2}{2\pi\hbar} \qquad j_r = \sigma_{xy}E_\theta \qquad E_\theta = -\frac{1}{2\pi r}\frac{d\Phi(t)}{dt} \tag{1.4.3}$$

Integrating this current, one finds a charge transported $\Delta Q = e/m$. This is the famous charge fractionalization.

We can now consider a pair of quasi holes,

$$\psi_{2\ exc} = \prod_i (z_i - \eta_1)(z_i - \eta_2)\psi(z_1, .., z_n) \tag{1.4.4}$$

We can ask what happens to this state when we exchange $\eta_1 \leftrightarrow \eta_2$. Note that in general, this phase has to be computed via the Berry phase accumulated as one particle circles the other. It is therefore captured by the first fundamental group of the configuration space (of, say, 2 particles). In ≥ 3 spatial dimensions, the fundamental group is just the permutation group. However, in $2+1$ dimensions, it is instead the *braid group*. The geometrical reason is that in 2 spatial dimensions, there is not enough room to undo a winding, whereas in 3 spatial dimensions, the windings can be undone because of the extra available direction.

Fixing η_1, we can compute the berry phase $\mathcal{A}_\eta = i\frac{\langle\psi(\eta)|\partial_\eta\psi(\eta)\rangle}{\langle\psi|\psi\rangle}$ for the state $\psi_{2\ exc}$ as a function of η_2. This produces a braiding phase $\gamma = \oint \mathcal{A} = 2\pi/m$. We learn that these excitations have fractional statistics! [17] These are *anyons*.

These exotic properties make the FQHE very different from IQHE. The presence of anyons are also responsible for other striking features, such as ground state degeneracy on a torus. This phase has has m ground states on a torus. These are not directly visible in the Laughlin wavefunction; they are globally distinct states distinguished by noncontractible anyon Wilson loops. Local operators cannot distinguish them in the thermodynamic limit. Moreover, they display a striking entanglement feature due to the presence of anyons. For a simply connected region with a smooth boundary in a gapped $2+1$-dimensional topologically ordered phase,

$$S_A = \alpha\frac{|\partial A|}{\epsilon} - \gamma + O(e^{-L/\xi}), \qquad \gamma = \log\mathcal{D}, \qquad \mathcal{D} = \sqrt{\sum_a d_a^2}, \tag{1.4.5}$$

where d_a are the anyon quantum dimensions [18]. The Laughlin $U(1)_m$ theory has m Abelian anyon types, each with $d_a = 1$, and hence

$$\gamma = \frac{1}{2}\log m. \tag{1.4.6}$$

The universal term enters the entropy as $-\gamma$. It cannot be generated or removed by a finite-depth local circuit, just as such a circuit cannot remove the braiding data or topology-dependent ground-state degeneracy. This is the long-range entanglement of intrinsic topological order. [15] This is a universal term that could only be global information about the state, invisible to local contributions to entanglement such as the area law term. These states are called *long range entangled.* Unlike the integer quantum hall effect, this phase is *not* invertible; stacking cannot remove anyons. We thus found ourselves another phase with exotic phenomena that the conventional landau paradigm would have missed, but it has a curious entanglement structure that characterizes it.

With this preamble that illustrates the intricate interplay of symmetries and entanglement, let us now turn to the subject of the thesis.

[15] Conversely, $\gamma = 0$ does not imply triviality: an invertible chiral phase such as a Chern insulator has no fractional anyons but can still be obstructed from a product state by its chiral central charge.

Chapter 2

Introduction

Symmetries are a powerful and universal tool in quantum field theory (QFT), applicable beyond the perturbative regime. In particular, it is useful to be able to detect whether symmetries are broken in a given quantum state. For instance, in the Landau paradigm one distinguishes different phases of a theory according to how symmetries are realized and possibly spontaneously broken in ground states. As another example, excited states produced by quenches can exhibit interesting physics revealed by symmetry breaking and its restoration (or lack thereof) during time evolution due to relaxation. The standard approach to detect symmetry breaking uses order parameters, *i.e.*, expectation values of (usually local) operators. This is a valid approach, but there are alternatives that might have advantages.

One alternative approach, proposed in [3] to study the dynamics of out-of-equilibrium states, is named "entanglement asymmetry." It builds on quantum-information methods, and it is equivalent to previously introduced quantities in different contexts, namely the "asymmetry" of [19–21] and the "entropic order parameter" of [22–25]. For example, given a state and a subregion of space A, the entanglement asymmetry ΔS with respect to a symmetry group G is defined as the relative entropy between the reduced density matrix on A and its average over the action of G. This definition applies to both continuous and discrete, Abelian and non-Abelian groups. A few advantages of asymmetry include the following: it does not require one to identify a suitable order parameter for the symmetry; it has an extra dependence on a subsystem, or subregion, A; it is faithful, meaning that $\Delta S > 0$ if and only if the state breaks the symmetry. Notably, entanglement asymmetry is a measure of symmetry breaking rather than of entanglement itself, as it can be nonzero even for states with vanishing entanglement.

By now, entanglement asymmetry has been studied from the perspectives of both condensed-matter and high-energy physics. On the condensed-matter front, it was applied to a variety of systems, including ground states with explicit [26–31] and spontaneous [32] symmetry breaking, matrix product states [33], integrable systems [26, 34–36], and quantum circuits [37, 38], to name a few. It shed light on out-of-equilibrium dynamics, in particular revealing a "quantum Mpemba effect" taking place under time evolution [3] (see [39] for a review), later experimentally confirmed [40]. On the high-energy front, asymmetry was studied in certain excited states in conformal field theories (CFTs) [1, 41, 42]. Besides, a holographic dual was proposed for a class of perturbative states [1]. In [43–46] the asymmetry with respect to $U(1)$ and $SU(N)$ symmetries was computed in the Page model of radiating black holes, yielding a cousin of the Page curve. In [2, 47] it was studied for generalized symmetries. In [48] its connection to topological entanglement entropy was studied, and in [49] it was studied for gauge theories. In this thesis, we will be concerned with the works in [1, 2].

2.1 Definitions

Entanglement asymmetry is a quantum-information-based measure of symmetry breaking in pure or mixed states. Given a density matrix ρ, in order to quantify how much this breaks the symmetry, we compare it with a symmetrized version of itself, that we call ρ_{S}. Entanglement asymmetry is then defined as the relative entropy

$$\Delta S[\rho] \equiv S[\rho \| \rho_{\mathsf{S}}] \equiv \mathrm{Tr}\Big(\rho\,(\log \rho - \log \rho_{\mathsf{S}})\Big) \ . \tag{2.1.1}$$

Because of the properties of ρ_{S}, entanglement asymmetry can also be written [50], as we show below around (7.1.9) in general, as a difference

$$\Delta S[\rho] = S[\rho_{\mathsf{S}}] - S[\rho] \ , \tag{2.1.2}$$

where $S[\rho] \equiv -\,\mathrm{Tr}(\rho \log \rho)$ is the von Neumann entropy. From standard properties of relative entropy, it follows that entanglement asymmetry is nonnegative, $\Delta S[\rho] \geq 0$, and that it vanishes if and only if $\rho = \rho_{\mathsf{S}}$. One can also define Rényi asymmetries, characterized by an index n:[1]

$$\Delta S^{(n)}[\rho] = \frac{1}{1-n} \log \frac{\mathrm{Tr}(\rho_{\mathsf{S}}^n)}{\mathrm{Tr}(\rho^n)} \ . \tag{2.1.3}$$

[1]If ρ is a pure state, this reduces to the Rényi entropy, which is nonnegative (independently of the details of the symmetrization procedure). For a generic state, it has been proven in [50, 51] that the Rényi asymmetries are nonnegative for every n for the case of a $U(1)$ symmetry. The proof therein generalizes to any Abelian algebra, because the symmetrizer still takes the form (8.1.4).

The entanglement asymmetry is reproduced in the limit $n \to 1$. Some properties of Rényi asymmetries are explored in appendix 5.1.13.

Given a Hilbert space $\mathcal{H}$ and a density matrix $\rho \in \mathrm{End}(\mathcal{H})$, in order to obtain the symmetrized version of ρ we need to construct a *symmetrizer* map $\mathsf{S} \in \mathrm{End}\big(\mathrm{End}(\mathcal{H})\big)$ such that

$$\mathsf{S} \colon \rho \mapsto \rho_{\mathsf{S}} \, . \tag{2.1.4}$$

The symmetrizer is characterized by the following properties:

1. It is a linear projector, in particular $(\rho_{\mathsf{S}})_{\mathsf{S}} = \rho_{\mathsf{S}}$.
2. Its image is symmetry-invariant, namely $\mathcal{X}_a \, \rho_{\mathsf{S}} = \rho_{\mathsf{S}} \, \mathcal{X}_a$ for all $\mathcal{X}_a \in \mathcal{A}$.
3. If ρ is already symmetry-invariant, then $\rho_{\mathsf{S}} = \rho$.
4. It is trace-preserving, namely $\mathrm{Tr}(\rho_{\mathsf{S}}) = \mathrm{Tr}(\rho)$.
5. It maps density matrices to density matrices: $\rho_{\mathsf{S}}^{\dagger} = \rho_{\mathsf{S}}$ and $\rho_{\mathsf{S}} \geq 0$.

Notice that while properties 1. – 4. only depend on the product structure on $\mathcal{A}$, property 5. also depends on its $*$-structure.

Properties 1. – 3. can be more compactly stated as follows: S is a linear projector to the vector space of operators that commute with the algebra $\mathcal{A}$. Indeed, property 2. states that the image of S is contained in the space of commuting operators, while property 3. states that commuting operators are contained in the image of S. Properties 4. and 5., on the other hand, guarantee that ρ_{S} is a normalized density matrix (as long as ρ is) so that it makes sense to compute its von Neumann or Rényi entropies.

An intuitive picture for the action of the symmetrizer is the following. Decomposing the Hilbert space $\mathcal{H}$ into a direct sum of irreducible representations of $\mathcal{A}$ (with multiplicities), we can decompose both ρ and ρ_{S} into blocks that map irreducible representations to irreducible representations. Property 2. states that ρ_{S} commutes with every element of the algebra $\mathcal{A}$. Then, Schur's lemma (see, *e.g.*, [52]) implies that every block of ρ_{S} that connects two different irreducible representations must be the zero map, and that every block of ρ_{S} that connects two equal irreducible representations must be proportional to the identity. In App. A.6.2 we show that the action of the symmetrizer S on ρ is precisely that of setting to zero the blocks that connect different irreducible representations, and to replace the blocks that connect equal irreducible representations with blocks proportional to the identity matrix, with a prefactor such that the trace of each block is preserved. See Fig. 2.1 for a graphical representation.

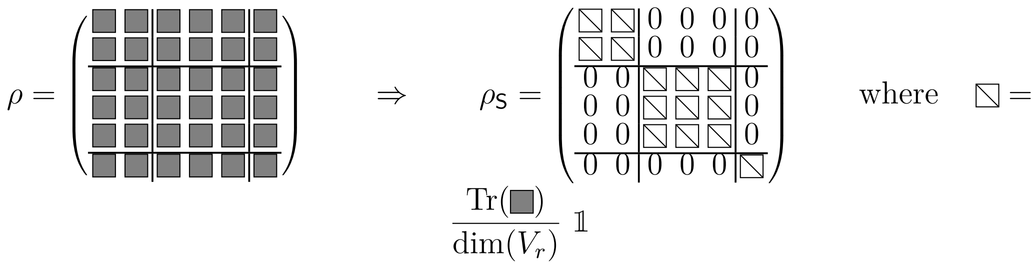

Figure 2.1: The Hilbert space splits as $\mathcal{H} = \bigoplus_r n_r V_r$ where V_r is the r-th irreducible representation of $\mathcal{A}$, while n_r is its degeneracy. A similar block decomposition applies to density matrices. The symmetrizer acts by setting to zero the off-diagonal blocks, and keeping sub-blocks proportional to the identity on the diagonal.

2.2 Outline and Summary

In this thesis, we are studying two broad settings:

- Perturbative Entanglement asymmetry for $U(1)$ in CFTs and Holography
- Entanglement Asymmetry for finite (generalized) symmetries in $1+1$D

Let us provide a brief outline here; the detailed outline will be presented in the chapters when necessary.

Chapter 5 starts with studying the asymmetry for a class of excited states in CFTs, created by local operator insertion. In perturbation theory, the result for the asymmetry is universal. We first do it via the replica trick in 2D CFTs, for some specific choice of conformal weights for the excited. Exploiting its connection with perturbative relative entropy, we are able to extend these results to any dimensions and any conformal weights.

In chapter 6, we exploit the holographic dual of perturbative relative entropy to extract a perturbative bulk dual for the asymmetry. The result depends on a current through the entanglement wedge, and is quite natural.

In Chapter 7 we begin a systematic generalization of entanglement asymmetry to generalized symmetries. We explain how the symmetry algebras acting on Hilbert spaces have special features that allow a concrete notion of symmetrizing a state.

In 8, we elaborate on generalized symmetry actions in $1+1$D theories which produce the aforementioned algebras, both on the circle (tube and fusion algebra) and interval Hilbert spaces (strip algebra).

In 9 we study the asymmetry for ground states to probe spontaneous symmetry breaking. In 10, we study several examples for asymmetry for excited states in 2D CFTs with groups and non-invertible symmetries both.

In addition, there are two chapters with some material to acquaint the reader with the necessary background. In Chapter 3 we give an introduction to entanglement entropy calculations in CFTs and holography. In Chapter 4 we give an introduction for generalized symmetries in $2D$, the axioms of the unitary fusion categories that describe them. This chapter is not necessary until chapter 7 is encountered.

Chapter 3

Background I: Entanglement and Holography

Entanglement is a hallmark of quantum mechanical phenomena, ultimately coming from the notion of superposition of states. In many body quantum systems and quantum field theories, it is actually quite subtle to be able to define 'regions' between which we are trying to measure entanglement. We are mostly interested in *bipartite entanglement*, although there are other notions one can use. The standard way to quantify this is *entanglement entropy*.

Consider a theory in $(d+1)$ dimensions, quantized on a manifold of the form $\mathcal{M}_d \times \mathbb{R}$, with $\mathcal{M}$ a closed (spatial) manifold for simplicity. Associated with this foliation is a *Hilbert space* on $\mathcal{M}_d$, on which states of the theory live. It is convenient to represent these states not as vectors but as (hermitian) operators $\rho \in \mathrm{End}(\mathcal{H})$, called *density matrices*. These are always assumed to be normalized $\mathrm{Tr}(\rho) = 1$. We ignore such issues here ρ needn't be a pure state, i.e. expressible in the form $\rho = |\psi\rangle\langle\psi|$ for a single vector $|\psi\rangle \in \mathcal{H}$; it is generally a sum of such terms and therfore is a clearly more general notion of states than vectors.

Given an observable of the theory, its expectation value in a given state is given by

$$\langle \mathcal{O} \rangle_\rho \equiv \mathrm{Tr}(\rho \mathcal{O}) \tag{3.0.1}$$

Given a state i.e. density matrix ρ (of, for instance, a many body quantum system or a QFT), we may define its *von-Neumann entropy*by

$$S(\rho) = -\mathrm{Tr}(\rho \log \rho) \tag{3.0.2}$$

It is always non-negative, and vanishes for a pure state.

Given such a state, suppose we wanted to restrict our attention only to a subregion A and ask what does the state look like for an observer who only has access to A. This is not a made up situation; a classic example of this setting is an evaporating black hole, where one only has access to the degrees of freedom outside the horizon. To answer this question, one starts by partitioning the hilbert space as

$$\mathcal{H} = \mathcal{H}_A \otimes \mathcal{H}_{A^c} \tag{3.0.3}$$

Actually, this assumption is in general false because one must keep track of what goes on at the *entangling surface* ∂A; which is a subtlety we will briefly address in 3.4. For the moment, we assume we have managed such a partition. Then, one defines the *reduced density matrix*

$$\rho_A \equiv \mathrm{Tr}_{A^c}\, \rho \quad \langle \mathcal{O}_A \otimes \mathbf{1}_{A^c} \rangle_{\mathcal{M}} = \mathrm{Tr}_{\mathcal{H}_A \otimes \mathcal{H}_{A^c}}(\rho(\mathcal{O}_A \otimes \mathbf{1}_{A^c})) = \mathrm{Tr}_{\mathcal{H}_A}(\rho_A \mathcal{O}_A) \tag{3.0.4}$$

which works as the effective state to compute observables localised to the subregion A. Note that $\mathrm{Tr}_{\mathcal{H}_A}(\rho_A) = 1$ still and it remains self adjoint [1], But this partial tracing cannot make one forget the fact that degrees of freedom in A and A^c are actually generally *entangled*; and even if the total state ρ was pure to begin with, the reduced state ρ_A is in general *mixed*, i.e. like a thermal state. This is ofcourse related to the fact that outside the horizon of an evaporating black hole, one finds (Hawking) radiation.

A quantity that characterizes this entanglement is precisely the *entanglement entropy* of the reduced density matrix; defined as the von Neumann entropy

$$S(\rho_A) = -\,\mathrm{Tr}(\rho_A \log \rho_A) \tag{3.0.5}$$

In summary, an observer that can access only a subregion of an entangled state will find themselves in a mixed state.

How does one define a density matrix in a quantum field theory? Let us find out.

Path integral A path integral is a machine to compute quantum mechanical transition amplitudes between two states. Schematically, given some field(s) $\psi(x,t)$ and their configurations $|\psi_{1,2}\rangle$ fixed on slices t_1, t_2

$$\langle \psi_2 | e^{-\tau H|} | \psi_1 \rangle = \int_{\psi(0)=\psi_1}^{\psi(\tau)=\psi_1} [D\psi]\ e^{-S_E[\psi]} \tag{3.0.6}$$

[1] Partial trace is a CPTP operation [53]

We can think of this equation as the evaluation of a wavefunction(al) on a ket

$$\Psi(\tau) = e^{-\tau H}|\psi_1\rangle \qquad \langle\psi_2|e^{-\tau H|}|\psi_1\rangle = \Psi(\tau)[\psi_2] \tag{3.0.7}$$

This is telling us that given a past boundary condition $|\psi_1\rangle$, the path integral is a way to encode time evolution until time τ. It prepares a wavefunctional $\psi(\tau)$on the slice τ. Be definition, a wavefunctional eats a state and gives a number. This is the number the path integral computes. We can therefore use the path integral to produce states (vectors),

$$\Psi[\cdot] = \int_{\psi(0)=\psi_1}^{\psi(\tau)=\cdot} [D\psi]\; e^{-S_E[\psi]} \tag{3.0.8}$$

This prepares a ket, which feeds on a bra. Note also that this state is *unnormalized*. Typically this is not an issue as we are interested in *correlation functions* and not partition functions, so such normalizations always cancel out. We can also do the inverse time evolution, and prepare a bra. Together, this prepares an (unnormalized) density matrix ρ, which, being a matrix, feeds on two vectors and spits out a number. This is illustrated in the figure below 3.1

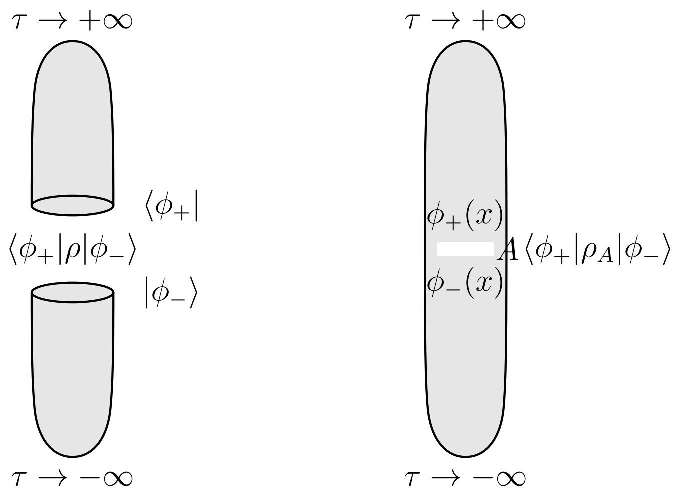

Figure 3.1: Euclidean representations of the vacuum (reduced) density matrix. Left panel shows a 'global' state preparation. Right panel shows the geometry cut open along the interval A, with boundary data ϕ_+ and ϕ_- specified on the two sides of the slit.

Note that the wavefunctional depended on the choice of *initial* state ψ_1 i.e. a *past boundary condition*. In euclidean spacetime, there is a canonical choice of these past boundary conditions- the *vacuum* state $|0\rangle$. This is achieved by inserting the past boundary condition in the infinite past: Euclidean evolution always damps a generic linear combination to the vacuum

$$e^{-\tau H}\left(\sum c_n|n\rangle\right) \simeq c_0|0\rangle \qquad \text{as } \tau \to \infty \tag{3.0.9}$$

A standard way to encode this point at infinity in a picture is to attach a 'euclidean cap' in the path integral [2]. This picture is meant to say that spacetime has been compactified by adding a point at infinity. Then, as long as there are no other insertions in the path integral, the state produced is the vacuum. Note that the argument for euclidean damping requires the initial state has an overlap with the vacuum: inserting just a (nonzero) *eigenstate* $|n\rangle$ escapes this argument, although the state has almost vanishing norm as long as the energy $E_n \neq 0$ when $\tau \to \infty$. Normalized states, however, can be defined. For example, in a CFT, if one inserts a primary operator at past infinity, one gets a primary state, not the vacuum. If one inserts a generic combination, then one gets the state of the lowest weight. These different situations can be captured by inserting the relevant primary at the point at infinity; producing a primary state on the cut slice. The vacuum corresponds to inserting the identity i.e. nothing. We can also produce *excited states* by inserting inserting a local operator $\mathcal{O}$ at some finite time. If they were primaries, then one obtains a complicated combination of descendents on the cut slice; pushing this insertion in the far past damps out everything but the primary. These insertions at finite τ typically lead to state that is *not* an energy eigenstate, and therefore is a model for an out of equilibrium state, since it is not left invariant by Lorentzian time evolution. These states will be our prototype for studying entanglement asymmetry in CFTs.

Let us remark that for artistic reasons, in the rest of the thesis we will not be drawing this Hartle-Hawking style picture for the vacuum state, and will adopt the more conventional picture where path integrals are drawn on a plane. It is to always be remembered, however, that such path integrals only make sense when spacetime has been compactified with the point at infinity; otherwise one needs to explicitly specify the boundary conditions there. This point at infinity will be crucial when we later perform maneuvers on topological lines to compute Renyi asymmetries, and indeed even in the replica trick of 2D CFTs.

Modular hamiltonian This is a good opportunity to introduce a concept that we will later use in 5.3. We remarked that a reduced density matrix is in general a mixed state and therefore has thermal behaviour. It is then useful to introduce a

[2]This cap can also be attached to Lorentzian path integrals, as a way to regulate them. In particular, the euclidean path integral is used to prepare a well defined state, which is stitched onto some Lorentzian time slice, from where one can carry out Lorentzian evolution with e^{-itH} and observe the real time dependence of the state.

fictitious thermal ensemble (at unit temperature) with a hamiltonian H_A, for which the reduced density matrix ρ_A is the Gibbs state:

$$\rho_A = \frac{e^{-H_A}}{\mathrm{Tr}(e^{-H_A})} \qquad H_A : \text{modular hamiltonian} \tag{3.0.10}$$

In fact, being a hermitian positive operator, such a representation for ρ_A is guaranteed to exist. In general, one cannot hope for the operator H_A to have some nice, local expression; after all ρ_A is going to be some complicated object.

However, there is a very special (and thankfully, ubiquitous) situation in which H_A is actually a simple, local quantity with a geometric interpretation. Starting from the *vacuum* state in Minkowski space (t, x_i), we may define the spatial subregion of interest to be the half space $x^1 \geq 0$. Associated to this slice is the region of spacetime called the *Rindler wedge*, defined as the region $x^1 \geq |t|$ in minkowski space. For instance, in $\mathbb{R}^{1,d}$, we may do a change of coordinates

$$t = r \sinh \eta \qquad x_1 = r \cosh \eta \qquad x_1 \geq |t| \tag{3.0.11}$$

that maps the $x_1 \geq |t|$ wedge of minkowski space $ds^2 = -dt^2 + dx_i^2$ to Rindler space

$$ds^2_{\text{Rindler}} = -r^2 d\eta^2 + dr^2 + dx_i^2 \tag{3.0.12}$$

Note that this is a nonlinear transformation; an observer at rest in Rindler spacetime is uniformly acclerating in Minkowski spacetime. Moreover, at $r = 0$ there is a *Rindler horizon* which is a forbidden region of spacetime; this is the kind of setting where reduced density matrices are natural.

It is actually natural to guess what the modular hamiltonian must be: note that the metric 6.1.12 has a manifest isometry of η translations, generated by $-i\partial_\eta$. This is precisely the modular hamiltonian. The easiest way to see this is to wick rotate to Euclidean space with $\tau = i\eta$, so that τ becomes an angular coordinate $\tau \sim \tau + 2\pi$. [3] In this geometry, the density matrix elements have the interpretation of 'time evolution' along the angular direction; establishing that the modular hamiltonian is the generator $H_A = \partial_\tau$. Note that if one goes back to Lorentzian, then the modular hamiltonian

$$H_A = -i\partial_\eta = i(t\partial_{x_1} + x_1\partial_t) \tag{3.0.13}$$

[3] The reader might recognise that this is the same trick to compute temperature of a black hole; more generally a Lorentzian metric with a horizon. One maps to a (smooth) Euclidean spacetime where the singularity caps off smoothly, and enforces a periodicity condition like above to avoid conical singularities. The period determines the black hole temperature.

becomes the boost generator. This is the famous *Bisognano-Wichmann* theorem [54, 55] , valid for Rindler spacetimes any QFT.

A useful way to write the modular hamiltonian is to use the fact that if a metric has a killing vector ξ^μ; then one obtains the associated conserved charge by integrating the stress tensor along this direction. One writes, for the boost generator ξ^μ,

$$H = \int d\Sigma^\mu \xi^\nu T_{\mu\nu} = \int_{x^1>0,t=0} x_1 T_{00} \tag{3.0.14}$$

It might feel unsettling that the subregion in Rindler wedge is actually infinite. Incredibly, there is a very useful conformal map between the Rindler geometry and (finite!) ball-shaped regions. In a conformal field theory, therefore, this map can be exploited to actually write down a local modular hamiltonian for such ball shaped regions. Recall that in *any* QFT, the *Rindler wedge* admits a local modular hamiltonian in the form of the boost generator [54, 55]. However, as explained in [56], there exists a *conformal map* from the rindler wedge $x^1 > 0$ in flat space, to the causal development of A [4]. This is given by [56]

$$x^\mu \to \frac{x^\mu - (x\cdot x)c^\mu}{1 - 2x\cdot c + (x\cdot x)(c\cdot c)} + 2R^2 c^\mu \quad c^\mu = (0, (2R)^{-1}, 0, 0, ..) \tag{3.0.15}$$

Now, in a CFT (and only in a CFT), we can use the above conformal transformation to write the modular hamiltonian as a conformal transform of the rindler boost. This is how one obtains the famous expression for the modular hamiltonian for a ball shaped region (of radius R) in a CFT [56]:

$$H_A = 2\pi \int_A d^d x\ \zeta^0(x) T_{00}(x) \quad \zeta^0(x) = \frac{(R^2 - |\vec{x}|^2)}{2R}$$

Here $\zeta_\mu = -\frac{2\pi}{R}(tx\partial_i) + \frac{\pi}{R}(R^2 - t^2 - \vec{x}^2)\partial_t$ is the boundary modular flow inside the causal diamond of the ball-shaped region.

This makes the computation of entanglement entropy for such regions in CFTs remarkably elegant. In fact, this region can further be mapped to other spaces, like hyperbolic space at finite temperature. We will be using these transformations in section 5.4 to compute the entanglement asymmetry in these various geometries.

[4]This is the set of all points through which every causal curve passing through the point also passes through A

3.1 Replica trick

So far we were quite formal; how does one actually ever compute such an entanglement entropy? In a QFT with infinitely many degrees of freedom, it makes little sense to compute quantities like $\log\rho$. Instead, a powerful technique exists to compute something more tractable. This requires introducing the *Renyi entropies*, labelled by a parameter n:

$$S_n(\rho_A) = \frac{1}{1-n}\log\mathrm{Tr}(\rho_A^n) \quad \lim_{n\to 1} S_n(\rho_A) = S(\rho_A) = -\lim_{n\to 1}\partial_n \log\mathrm{Tr}(\rho_A^n) \tag{3.1.1}$$

It is understood that S_n is first defined for $n \in \mathbb{Z}_+$, and then the result is analytically continued to $n \in \mathbb{R}$ to take the limit $n \to 1$ and get the entanglement entropy. Renyi entropies carry more information about the state than the entanglement entropy does. In terms of the modular hamiltonian, the state ρ_A^n is a state at inverse temperature n. Renyi entropy obeys some interesting constraints to, for instance $\partial_n S_n \leq 0$, where these inequalities have an interpretation as thermodynamic constraints on an equilibrium system.

The main practical application of Renyi entropy is that the quantity

$$\mathrm{Tr}_A(\rho_A^n) = Z_n(A)/Z(A)^n \tag{3.1.2}$$

has a natural interpretation as a partition function on an $n-$sheeted manifold, with branch points at the entangling surface ∂A. This is illustrated in figure 3.1

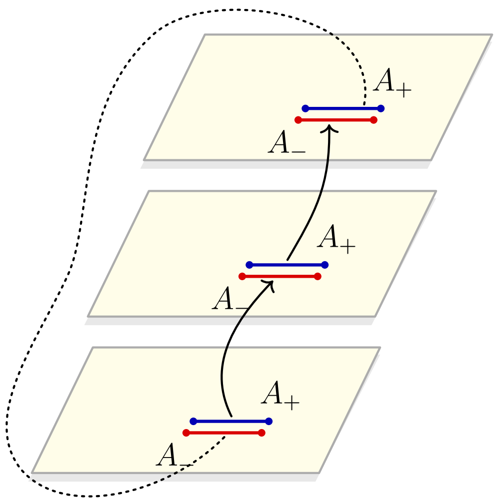

Figure 3.2: The Euclidean geometry for computing matrix elements of powers of the reduced density matrix ρ_A and its trace. Three replicated path integrals are glued cyclically along the banks A_+ and A_-. The dotted line represents the final identification used in taking the trace.

This manifold is the $n-$fold cover of the original manifold, formed by gluing n copies of the original spacetime along the cut A. $Z(A)$ is the partition function of the single sheet.

Note that this manifold has conical singularities with a deficit $2\pi(1-n)$ at the branch points ∂A, as one needs to go around by $2\pi n$ to cover a loop around them. This is a partition functions on curved manifolds-worse-on singular manifolds. It is not fun to calculate: one has to adopt regularization procedures (most commonly heat kernel), and the computation becomes pretty complicated very quickly. One can organize the UV divergences as an expansion in the diffeomorphism invariants constructed from the curvature tensor of the curved manifold. This is already an indication that the entanglement entropy has something to do with conformal anomalies; which arise in a similar expansion.

Let us note that there are two ways to think of this partition function :

$$
\begin{aligned}
&\mathrm{Tr}(\rho_A^n) = \\
&\qquad \int_{\mathcal{R}_n,\mathrm{b.c}} [D\phi] e^{-S_E(\phi)_{\mathcal{R}_n}}, \qquad \phi(0_i^-, A_i) = \phi(0_{i+1}^+, A_{i+1}) \text{ gluing one theory} \\
&\qquad \int_{\hat{\mathbb{C}},\mathrm{b.c}} \prod [D\phi] e^{-\sum_i^n S_E(\phi_i)_{\hat{\mathbb{C}}}}, \qquad \phi_i(0^-, A) = \phi_{i+1}(0^+, A) \text{ gluing many theories}
\end{aligned}
$$

The first approach is called *worldsheet* replica, the second is called *target space* replica. The latter has the advantage of being framed on a simple manifold $\hat{\mathbb{C}}$ (the compactified complex plane i.e. Riemann sphere) instead of its branched covering $\mathcal{R}_n$.

In replica target space, these boundary conditions enforce the $\mathbb{Z}_n$ symmetry of *cyclic* permutations [5] $\phi_i \to \phi_{i+1}$. This global symmetry is implemented by a $\mathbb{Z}_n$ topological defect that straddles A. However, at the endpoints ∂A, this defect must end. In the case of $1+1$ dimensions, for instance, it will end at local operators; these are the famous *twist operators* [6] of [57]. The key idea is that we can then write this partition function in target space replica perspective, as

$$
\begin{aligned}
\mathrm{Tr}(\rho_A^n) = \int_{\hat{\mathbb{C}},\mathrm{b.c}} \prod [D\phi] e^{-\sum_i^n S_E(\phi_i)_{\hat{\mathbb{C}}}} &= \int_{\hat{\mathbb{C}}} \prod [D\phi] e^{-\sum_i^n S_E(\phi_i)_{\hat{\mathbb{C}}}} \tau(u)\tau^\dagger(v) && (3.1.3) \\
&= \langle \mathcal{T}(u)\mathcal{T}^\dagger(v)\rangle_{\hat{\mathbb{C}}} && (3.1.4)
\end{aligned}
$$

[5] And not arbitrary ones, that would make the symmetry S_n

[6] In higher dimensions, the boundary ∂A is connected, so its not a local operator anymore and the situation is not simple

where now note that the integration measure after the second equality no longer has the specification of'(b.c)': the insertion of twist operators $\mathcal{T}, \mathcal{T}^\dagger$ is implementing those conditions. This is now just a 2 point correlator on $\hat{\mathbb{C}}$; which is a very nice object in a CFT. But so far, it is some abstract operator we know nothing about, so how do compute this two point function?

As always, there is something magical about $2D$. Here we are dealing with Riemann *surfaces*, as opposed to generic manifolds. There are powerful theorems in complex analysis that allow one to solve the issue of conical singularities on these surfaces, by going . This goes by the name 'uniformization theorem': it says that *every simply connected Riemann surface* $\tilde{X}$ *is conformally equivalent to either the unit disc* $\mathbb{D}^2$*, the complex plane* $\mathbb{C}$*, or the Riemann sphere* $\hat{\mathbb{C}}$. In fact, this powerful theorem allows a classification of every *connected* Riemann surface X, which are always obtained by the free, proper and holomorphic action of a discrete group Γ, $X = \tilde{X}/\Gamma$.

Let us exploit this theorem in a famous setting, as an instructive warm up for the kind of computations will have to do later.

3.2 Single interval in CFT$_2$

Consider a single interval of length ℓ in a 2D CFT, chosen to be $[u, v]$. We want to compute its Renyi entropy, for which we go to the replicated worldsheet picture. This is branched Riemann surface with n sheets and genus zero. It has 2 branch points at the entangling surfaces at u, v, each with ramification n (i.e. all n sheets meet at the branch points). This surface has to be an n fold branched covering of some universal covering space, which can only be a disc, a sphere, or the plane. But our Riemann surface is compact (thanks to the point at infinity, which is always crucial and must be remembered), and therefore, being genus zero, it can only be a covering of the sphere. Indeed, the Riemann-Hurwitz theorem says that if X is an $n-$ fold branched covering of B (base), with p labeling the branch points each of ramification e_p, then their genus g_X, g_B are related as

$$2g_X - 2 = (2g_B - 2)n + \sum_p (e_p - 1) \qquad \Longrightarrow \; g_B = 0 \tag{3.2.1}$$

where for our surface, $g_X = 0$ and we have 2 branch points with $e_p = n$ each. So our branched covering is topologically just a sphere; therefore the uniformization of this surface will also be a map to the sphere.

Crucially, in a CFT$_2$, such a conformal covering map is a symmetry of the theory;

and therefore the nasty partition function on the branched Riemann surface can be mapped to a simple one on the nicest possible manifold-the sphere. Let us see this explicitly.

Let w be the multivalued coordinate on the Riemann surface $\mathcal{R}_n$, where the the branch cut is along the real axis at $[u, v]$. This surface is a branched covering for the sphere labelled by coordinate z. The explicit relation between them is

$$z = \left(\frac{w-u}{w-v}\right)^{1/n} \tag{3.2.2}$$

Note that we first map the region $[u, v]$ to the half line[7], and then kill the monodromy around them by taking the power $1/n$. Under this transformation, the (holomorphic) stress tensor of the theory transforms with a Schwarzian term

$$T(w) = \left(dz/dw\right)^2 T(z) + \frac{c}{12}\{z, w\} \qquad \{z, w\} \equiv \frac{(z'''z' - \frac{3}{2}z''^2)}{z'^2} \tag{3.2.3}$$

Its the Schwarzian term that keeps track of the fact that we might be mapping a curved space ($\mathcal{R}_n$) to one with no curvature (the sphere). Using that $\langle T(z)\rangle_{\hat{\mathbb{C}}} = 0$, we find that

$$\langle T(w)\rangle_{\mathcal{R}_n} = \frac{c}{24}\left(1 - \frac{1}{n^2}\right)\frac{(v-u)^2}{(w-u)^2(w-v)^2} \tag{3.2.4}$$

Note that so far we were using the worldhseet replica picture. At this point, the trick is to switch to *target space* replica. We consider n decoupled copies of the theory, but now defined . $\hat{\mathbb{C}}$. Note that in such a theory, the stress tensor is the sum of the decoupled copies $T^{(n)} = nT$. Then, the content of the replica trick is that, for any operator $\mathcal{O}(w, i)$ inserted on sheet i on $\mathcal{R}_n$, we can write the correlation function as

$$\langle \mathcal{O}(w(z), i)...\rangle_{\mathcal{L}, \mathcal{R}_n} = \frac{\langle \mathcal{T}_n(u)\mathcal{T}_n^{\dagger}(v)\mathcal{O}_i(z)\rangle_{\mathcal{L}^{(n)}, \hat{\mathbb{C}}}}{\langle \mathcal{T}_n(u)\mathcal{T}_n^{\dagger}(v)\rangle_{\mathcal{L}^{(n)}, \hat{\mathbb{C}}}} \tag{3.2.5}$$

where $\mathcal{O}_i$ is an operator on the sphere that belongs to the ith theory. [8] This allows us to recast 3.2.4 via 3.2.5 into

[7] Rindler strikes again; ofcourse, not by accident. As said before, it is conformally equivalent to a ball i.e. an interval in $2D$

[8] Also, $\mathcal{T}(u, \bar{u})$ is not a holomorphic operator, we are suppressing the $\bar{u}$ to avoid clutter

$$\frac{\langle \mathcal{T}_n(u,\bar{u})\ \mathcal{T}_n^{\dagger}(v,\bar{v})\ T^{(n)}(z(w))\rangle_{\mathcal{L}^{(n)},\hat{\mathbb{C}}}}{\langle \mathcal{T}_n(u,\bar{u})\ \mathcal{T}_n^{\dagger}(v,\bar{v})\rangle_{\mathcal{L}^{(n)},\hat{\mathbb{C}}}} = \frac{c(n^2-1)}{24n}\frac{(v-u)^2}{(w-u)^2(w-v)^2} \tag{3.2.6}$$

But this has constructed for us an equation that is the leading terms in the Ward identity between the stress tensor and two primaries $\mathcal{T}, \mathcal{T}^{\dagger}$ [58]; we read off the scaling dimensions

$$\Delta(\mathcal{T}_n) = \Delta(\mathcal{T}_n^{\dagger}) = \frac{c}{12}(n-\frac{1}{n}) \equiv \Delta_n \tag{3.2.7}$$

With this, let us return to our replica geometry that computes the Renyi entropy. By construction ,

$$\mathrm{Tr}(\rho_A^n) = \frac{Z_n(A)}{Z(A)^n} = \langle \mathcal{T}_n(u)\mathcal{T}_n^{\dagger}(v)\rangle = \left(\frac{\epsilon}{|u-v|}\right)^{2\Delta_n} \tag{3.2.8}$$

Where the normalization was inserted to make the final result dimensionless, as it must be. The notation ϵ is not an accident, it is related to the regulating procedure. We ignored the subtleties of Hilbert space factorization, and put a local twist operator at ∂A where there was a conical singularity in the equivalent replica picture. As we will explain in 3.4, in the picture on $\hat{\mathbb{C}}$, we have to cut out ϵ-sized discs at ∂A. This shrinking process amounts to replacing the 'boundary state' at the entangling disc by a series of local operators, by the state operator correspondence. This series is organized in an expansion in $\epsilon^{\Delta}\mathcal{O}_{\Delta}$. The lowest lying operator in that expansion is the twist operator $\mathcal{T}$, which is capturing the leading term.

Taking the limit $n \to 1$ gives the famous result

$$S(\rho_A) = \frac{c}{3}\log\frac{\ell}{\epsilon} + ... \tag{3.2.9}$$

Let us note that the reason for such universal behaviour was that the two point function in a CFT is universal, upto a normalization which was indeed the source of the regulator ϵ. This doesn't work for higher dimensions, since such a conformal map doesn't exist to uniformize the Riemann surface. Moreover, even in 2D, this argument doesn't straightforwardly extend to more than one interval. For instance, for two intervals, the Riemann-Hurwitz theorem says that for the $n = 2$ replica manifold, the genus of the replica space is 1 i.e. it is *torus*. Moreover, with 4 branch points, we have 4 point functions of twist fields; and this is no longer a universal object. One therefore has to compute the actual replica partition function, regulating the singularities, using techniques developed in [59].

Area law A remarkable feature of entanglement entropy is that it is not entirely extensive like thermal entropy; it usually scales as an *area* instead of a *volume*. This is usually called the *area law*. In a gapped system, the underlying intuition is simple. Such systems have a finite correlation length ξ and exponentially decaying correlations. This means that the bipartite entanglement essentially comes only from those degrees of freedom that straddle the entangling surface ∂A; the other ones are too far away to be meaningfully correlated. Increasing the system size doesn't matter except for the increase in the area of ∂A. Thus, the general expectation is

$$S(\rho_A) \simeq \frac{\text{Area}(\partial A)}{\epsilon^{d-2}} \qquad \text{area law for entanglement} \tag{3.2.10}$$

The exact coefficient is scheme-dependent. Here ϵ is a length scale introduced for dimensional reasons. On a lattice, this is provided naturally by the lattice spacing. In the continuum, it is to be thought of as a UV regulator; related to the scheme dependence of the overall coefficient.. We will have more to say about this in 3.4. This is a powerful result; for instance, in gapped $1D$ chains, it predicts that the entanglement entropy saturates to a constant value (as the entangling surface is just two points). The area law is rigorously proved in $1+1D$ by [60]. There might be other interesting subleading corrections, such as topological entanglement entropy [18].

In a gapless system, though, we may expect other important subleading corrections, because the correlators only show a power law decay instead of exponential; there is no correlation length that can cut off interactions at some finite scale. This expectation is in fact true; and CFTs show important subleading corrections to the area law. In *even* d, these corrections are logarithmic, and universal. In d *odd*, these corrections are finite and universal. Schematically,

$$S_A = c_{d-2}\frac{\text{Area}(\partial A)}{\epsilon^{d-2}} + \frac{c_{d-4}}{\epsilon^{d-4}} + ... + c_0 \log\frac{\ell}{\epsilon} + .. \qquad \text{even } d \tag{3.2.11}$$

$$S_A = c_{d-2}\frac{\text{Area}(\partial A)}{\epsilon^{d-2}} + \frac{c_{d-4}}{\epsilon^{d-4}} + ... + \frac{c_1}{\epsilon} + (-1)^{(d-1)/2}F \qquad \text{odd } d \tag{3.2.12}$$

where ℓ is the characteristic lengthscale of the system (the volume of the system A scales as l^{d-1}). The crucial point is that for even d, c_0 is a universal quantity, depending on the weyl anomaly coefficients of the CFT [9]. For instance, in $d = 2$ $c_0 = c/3$, the central charge. In $d = 4$, it is a combination of a and c anomalies. In $d =$(odd), ofcourse, there is no Weyl anomaly, so such a logarithm doesn't appear. What appears, for instance in $d = 3$, is the sphere partition function $F = -Z_{S^3}$,

[9] This is transparent from the replica method where these curvature invariants enter to regulate conical singularities on the replica manifold

which is also universal. This observation will also be the starting point for the holographic dual of entanglement, which we now outline.

3.3 Towards holographic entanglement

The area law for entanglement entropy taught us that the entropy is really associated to a *codimension-two area*, since A is codimension-1 in spacetime.

This observation is striking if one recalls the Bekenstein–Hawking formula. A stationary black hole has entropy

$$S_{\mathrm{BH}} = \frac{\mathrm{Area}(\mathcal{B})}{4G_N}, \tag{3.3.1}$$

where $\mathcal{B}$ is a spatial cross-section of the horizon; for an eternal stationary black hole, the natural choice is the bifurcation surface. So black hole thermodynamics tells us that gravitational entropy is also measured by the area of a codimension-two surface in spacetime. This parallel is one of the basic motivations behind holographic entanglement entropy, and the *Ryu-Takayanagi* formula [61, 62].

Bekenstein Hawking to Ryu Takayanagi Let us outline the motivation for why a Ryu Takayanagi surface exists. The underlying reason is black hole entropy is characterized by a horizon, but horizons don't need black holes. As we have seen before, observers restricted to subregions of spacetime also have horizons: the standard example is the Rindler horizon we encountered earlier. Is there a natural surface on this horizon that computes the entanglement entropy of the Rindler space, much like the bifurcation surface of the black hole horizon computes the black hole entropy? The key observation is that there is a sharp characterization of this bifurcation surface in the black hole horizon- it is where the horizon's Killing vector degenerates. What is the counterpart of this Killing vector in the Rindler setup? We have seen it before-it is the modular flow. It turns out that there is indeed a surface where this field degenerates; this is the Ryu Takayanagi surface.

Let us elaborate. Consider a stationary black hole whose horizon is generated by a Killing vector ξ^μ. In the maximally extended geometry, the future and past Killing horizons intersect on the bifurcation surface $\mathcal{B}$.

The horizon of a stationary black hole (like Schwarzschild) is a null hypersurface, and is characterized by a Killing vector field that generates translations along this surface. The Killing field vanishes there,

$$\xi^\mu\Big|_{\mathcal{B}} = 0. \tag{3.3.2}$$

For instance, in a Schwarzchild black hole in Eddington-Finkelstein coordinates,

$$ds^2 = -(1-\frac{2GM}{r})dv^2 + 2dvdr + r^2 d\Omega_2^2 \qquad \xi = \partial_v, \qquad \xi^2 = \frac{2GM}{r} - 1$$

so the killing field is null on the horizon. In fact, it can be shown that it is exactly zero as a vector field on the $2-$sphere $\mathcal{B}$[10] Wald's construction [63] explains why black hole entropy has a natural geometric definition. This Killing symmetry is associated with a charge in $\mathcal{B}$ via Noether's theorem. Wald's insight was that this Noether charge is the black hole entropy, and it reproduces the Bekenstein formula.

To construct this charge note that for a diffeomorphism-invariant Lagrangian L, the variation can be written schematically as

$$\delta L = E(\phi)\,\delta\phi + d\Theta(\phi, \delta\phi), \tag{3.3.3}$$

where $E(\phi) = 0$ denotes the equations of motion and Θ is the pre-symplectic potential.

Given a vector field ξ^μ, the corresponding diffeomorphism variation and its associated Noether current is

$$\delta_\xi \phi = \mathcal{L}_\xi \phi. \qquad J_\xi = \Theta(\phi, \mathcal{L}_\xi \phi) - \xi \cdot L. \tag{3.3.4}$$

On shell, $dJ_\xi = 0$ is conserved [11], so locally

$$J_\xi = dQ_\xi, \tag{3.3.5}$$

where Q_ξ is the Noether charge $(d-2)$-form.

For our stationary black hole, take ξ^μ to be the Killing field generating the horizon. On the bifurcation surface,

$$\xi^\mu = 0, \qquad \nabla_\mu \xi_\nu = \kappa\, \epsilon_{\mu\nu}, \tag{3.3.6}$$

where $\epsilon_{\mu\nu}$ is the binormal [12] to $\mathcal{B}$.

Wald [63] made the elegant identification of the black hole entropy with the corresponding Noether charge. For a Lagrangian that depends on the Reimann

[10] In these coordinates, that surface is at $v \to -\infty$. It is cleaner in to see this in Kruskal coordinates, but we avoid those details here.

[11] Explicitly, $dJ_\xi = -E\mathcal{L}_\xi\phi$ where E is the EOM

[12] This is defined as $\epsilon_{\mu\nu} = u_{[\mu}n_{\nu]}$ where $u^2 < 0, n^2 > 0, u \cdot n = 0$ are two normal vectors to $\mathcal{B}$. It is $\epsilon^2 = -2$. For Schwarzchild, in usual coordinates, it is simple $\epsilon_{tr} = 1$.

tensor but not its derivatives, becomes:

$$S_{\text{Wald}} = \frac{2\pi}{\kappa}\int_{\mathcal{B}} Q_\xi = -2\pi\int_{\mathcal{B}} \frac{\partial L}{\partial R_{\mu\nu\rho\sigma}}\epsilon_{\mu\nu}\epsilon_{\rho\sigma} \tag{3.3.7}$$

For Einstein gravity,

$$L = \frac{1}{16\pi G_N} R\,\epsilon, \tag{3.3.8}$$

the Wald formula reduces precisely to the Bekenstein formula, showing it to be a special case (Einstein gravity) of a much deeper relation between black hole entropy and Noether charge.

3.4 The Ryu–Takayanagi formula

Guided by the black hole formula, we look for a bulk codimension-two surface

Let us start with a remarkable computation. Consider an interval defined at some time slice $t = 0$ in CFT_2, like the previous section. If this CFT was holographic, we can imagine that it lives on the conformal boundary of an AdS_3 spacetime. Suppose we are in a static situation [13] where the CFT is in its ground state. This means the bulk is empty AdS_3. The ground state of the CFT is entangled; one can compute the entanglement entropy of the interval as above. Let us ask what is a natural quantity that one may compute in the bulk, that only takes as its data this subsystem i.e. the interval. Perhaps one would consider drawing a geodesic through the bulk that connects the endpoints of this interval. Let us compute its length.

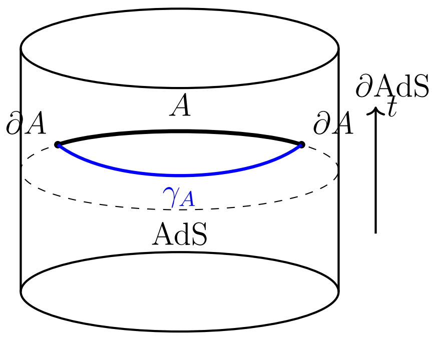

The interval $A = [u, v]$ lives on the boundary. The RT surface γ_A is the bulk geodesic ending at u and v.

Let us work in Poincaré AdS_3, where L is the radius of AdS:

$$ds^2 = \frac{L^2}{z^2}\left(dz^2 - dt^2 + dx^2\right).$$

[13]there is a time dependent, although more complicated, version of this [62]. The final result is almost identical, so we stick to the simpler setting

By time translation invariance, choose the CFT state to live on a constant-time slice, say, $t = 0$. The bulk geodesic must also lie on the same such slice[14] . The induced metric on this surface is

$$ds^2_{t=0} = \frac{L^2}{z^2}\left(dz^2 + dx^2\right).$$

Take the boundary interval of length ℓ to be $A = \left[-\frac{\ell}{2}, \frac{\ell}{2}\right]$. A bulk curve can be written as $z = z(x)$, and its arclength can simply be computed as

$$\text{Length} = L\int_{-\ell/2}^{\ell/2} dx\, \frac{\sqrt{1+(z')^2}}{z}, \qquad z' = \frac{dz}{dx}.$$

Here is a nice trick to compute this. Note that since this functional has no explicit x-dependence, there is a conserved quantity:

$$\mathcal{L} - z'\frac{\partial \mathcal{L}}{\partial z'} = \frac{1}{z\sqrt{1+(z')^2}} = \frac{1}{z_*},$$

where z_* is the maximum depth reached by the curve, where $z' = 0$. Hence

Integrating,

$$x = \pm\sqrt{z_*^2 - z^2} + \text{const}.$$

By symmetry the turning point is at $x = 0$, $z = z_*$, so the solution is a semicircle. The endpoints are at $x = \pm\ell/2$, so one finds the geodesic is

$$x^2 + z^2 = \left(\frac{\ell}{2}\right)^2.$$

The geodesic length diverges near the AdS boundary $z = 0$, so we need to regulate the action at $z = \epsilon$. This is the familiar fact that UV divergences in the CFT are IR divergences in the bulk. We get

$$\text{Length} = 2L\int_{\epsilon}^{z_*} \frac{dz}{z\sqrt{1 - z^2/z_*^2}} = 2L\log\frac{2z_*}{\epsilon} + O(\epsilon).$$

Now use the AdS/CFT dictionary, $c = \frac{3L}{2G_N}$ [15]

[14] In fact, a constant time slice in *AdS* is *totally geodesic*, meaning any geodesic that is tangent to it at any point, stays within the slice. The slice $t = 0$ has reflection symmetry, so there is a conserved charge $\dot{t}(\lambda)/z^2 = \text{constant}$, for some affine parametrization $t(\lambda)$. Unless this constant was zero, $t(\lambda)$ would be monotonic, so the geodesic would never return to the $t = 0$ slice

[15] Or the Brown-Henneaux relation, which actually predates AdS/CFT

we find a beautiful result

$$\frac{\mathrm{Length}(\gamma_A)}{4G_N} = \frac{c}{3}\log\frac{\ell}{\epsilon}.$$

This is exactly the CFT$_2$ result for the entanglement entropy of a single interval in the vacuum.

So the bulk geodesic reproduces the boundary entropy perfectly. This is in tune with the lessons we learnt from black hole. Naturally generalizing this observation to general dimensions, we are looking for a bulk-codimension 2 surface γ_A satisfying

$$\partial\gamma_A = \partial A. \tag{3.4.1}$$

In addition, γ_A must be homologous to A: there should exist a bulk region Σ_A such that

$$\partial\Sigma_A = A \cup \gamma_A. \tag{3.4.2}$$

For a static bulk geometry, Ryu and Takayanagi [61] proposed that γ_A is the minimal-area surface satisfying these conditions, and

$$S_A = \frac{\mathrm{Area}(\gamma_A)}{4G_N} \tag{3.4.3}$$

In a time-dependent spacetime, the correct generalization is the Hubeny–Rangamani–Takayanagi prescription: the relevant surface is no longer minimal on a preferred spatial slice but extremal in the full Lorentzian spacetime [62].

Many facts about entanglement entropy which are convulated from a quantum information perspective, become very natural geometry facts. Consider the classic example of (strong) subadditivity.

Take two overlapping boundary intervals

$$A = [x_1, x_3], \qquad B = [x_2, x_4], \qquad x_1 < x_2 < x_3 < x_4.$$

Let γ_A and γ_B be the minimal geodesics for A and B.

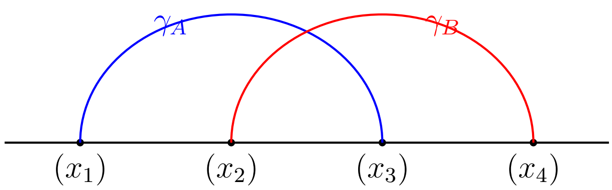

These two curves intersect in the bulk. Now cut them at the intersection point and reconnect the pieces. This produces two new curves: one joining x_1 to x_4, and one joining x_2 to x_3.

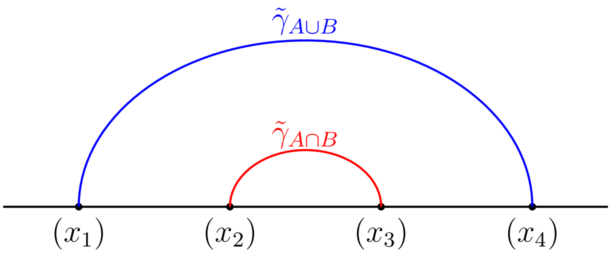

These recombined curves are not necessarily minimal, but they are homologous to $A \cup B$ and $A \cap B$. Therefore

$$\text{Length}(\gamma_{A\cup B}) \leq \text{Length}(\tilde{\gamma}_{A\cup B}), \qquad \text{Length}(\gamma_{A\cap B}) \leq \text{Length}(\tilde{\gamma}_{A\cap B}).$$

On the other hand, by construction,

$$\text{Length}(\tilde{\gamma}_{A\cup B}) + \text{Length}(\tilde{\gamma}_{A\cap B}) = \text{Length}(\gamma_A) + \text{Length}(\gamma_B).$$

Putting these together,

$$\text{Length}(\gamma_{A\cup B}) + \text{Length}(\gamma_{A\cap B}) \leq \text{Length}(\gamma_A) + \text{Length}(\gamma_B).$$

Dividing by $4G_N$, the RT formula gives

$$S(A \cup B) + S(A \cap B) \leq S(A) + S(B)$$

This is precisely *strong subadditivity*. Ordinary subadditivity follows immediately, since $S(A \cap B) \geq 0$.

Hilbert-space factorization in continuum QFT Suppose we divide a spatial slice into a region A and its complement $\bar{A}$. In ordinary quantum mechanics one would like to write

$$\mathcal{H} = \mathcal{H}_A \otimes \mathcal{H}_{\bar{A}},$$

and then define the reduced density matrix by

$$\rho_A = \text{Tr}_{\mathcal{H}_{\bar{A}}}\, \rho.$$

In continuum quantum field theory this apparently innocent construction is subtle: for a sharp spatial region, the Hilbert space generally does *not* factorize in this way.

Intuitively, this is because the entangling surface ∂A cannot really 'divide' degrees of freedom in a continuum, since they exist at arbitrarily small scales, and will always straddle any surface ∂A you might try to draw. On a lattice Λ, there is a finite UV cutoff given by the lattice spacing ϵ. For a theory whose degrees of freedom live on lattice sites, the Hilbert space takes the form

$$\mathcal{H}_\epsilon = \bigotimes_{i \in \Lambda} \mathcal{H}_i.$$

If A is a subset of lattice sites, this immediately gives

$$\mathcal{H}_\epsilon = \mathcal{H}_{A,\epsilon} \otimes \mathcal{H}_{\bar{A},\epsilon}, \qquad \mathcal{H}_{A,\epsilon} = \bigotimes_{i \in A} \mathcal{H}_i.$$

Hence the reduced density matrix

$$\rho_{A,\epsilon} = \operatorname{Tr}_{\bar{A}} \rho_\epsilon$$

is an honest trace-class operator.

Physically, the cutoff removes modes with wavelength shorter than ϵ; there are no degrees of freedom probing lengthscales smaller than ϵ, and the entangling surface can be 'resolved' clearly.

If one attempts to take the continuum limit $\epsilon \to 0$, something goes wrong. The vacuum contains correlations across ∂A at arbitrarily short distance, so new entangled modes keep appearing as the cutoff is lowered to zero; we expose ourselves to new entangled degrees of freedom in a continuous way. The limiting Hilbert space therefore does not inherit a canonical factorization

$$\mathcal{H} \overset{\text{not}}{=} \mathcal{H}_A \otimes \mathcal{H}_{\bar{A}}.$$

In algebraic QFT, one would say that a continuum QFT associates to A a local von Neumann algebra $\mathcal{A}(A) \subset B(\mathcal{H})$. If a tensor factorization existed in the usual sense, one would expect that $\mathcal{A}(A)$ is a type-I algebra. Local algebras in relativistic continuum QFT, however, are generically type III.

In gauge theories, things are still subtle. Even at finite lattice spacing, the *physical*, gauge-invariant Hilbert space need not factorize, as gauge constraints correlate the two sides of the entangling surface. For instance, consider a Wilson line, which is certainly a gauge invariant state before trying to do a bipartition. If it extended across the entangling surface, then cutting it open would produce open Wilson lines across the cut, which are not gauge invariant. Something must be put by hand on their endpoints to restore their gauge invariance and therefore presence in the hilbert space. This is the main idea for introducing 'edge modes' at the entangling surface where the Wilson lines can 'end', to produce an extended hilbert space that may then be factorized.

In practice one therefore introduces a UV regulator first. One way to think about the regulator is to replace the sharp entangling surface by a small physical boundary of thickness ϵ, and to specify a boundary condition a there. This defines a cutting map

$$\iota : \mathcal{H} \longrightarrow \mathcal{H}_{A,a} \otimes \mathcal{H}_{\bar{A},a}.$$

For a state $|\Psi\rangle$, the regulated reduced density matrix is then

$$\rho_{A,\epsilon} = \mathrm{Tr}_{\mathcal{H}_{\bar{A},a}} \left(\iota |\Psi\rangle\langle\Psi| \iota^{\dagger} \right).$$

On an ordinary spin lattice the natural "clear-cut" decomposition corresponds simply to $\iota = 1$. In a continuum theory, however, the map ι, and hence the precise definition of the factorization, contains information about how the UV theory is cut at ∂A. In section 8.2, we will return to this point more explicitly.

One computes the desired quantity at finite ϵ, and only afterwards studies the limit $\epsilon \to 0$. The density matrix itself need not have a continuum limit, and neither does its entropy. Nevertheless, universal or suitably renormalized combinations can have a well-defined limit. This makes relative entropy an especially interesting quantity, of which entanglement asymmetry will be an example.

Chapter 4

Background II: Categorical Symmetries

By now, it has become well known that the best way to think about symmetries of a theory, is by looking at the topological operators of the theory [64, 65]. When there is continuous symmetry with a Noether current $\partial_\mu j^u$ available, it can always be used to construct an operator that implements the associated symmetry (with parameter α) on the Hilbert space $U_\alpha(\Sigma) = e^{i\alpha \int d\Sigma^\mu j_\mu}$. If the symmetry was a continuous group, then this operator is unitary. But not all symmetries are continuous, and there is no analogous procedure to construct the operator that acts on the Hilbert space. However, there is certainly *some* operator that must be implementing the symmetry. The fundamental observation is that such an operator must be *topological*; in the Noether construction it follows from the conservation law. Once symmetry is phrased this way, there is no compelling reason to insist that every line have an inverse. The resulting noninvertible symmetries are not entirely exotic; they appear naturally after gauging finite non-Abelian groups, in Kramers–Wannier duality, and among the Verlinde lines of rational conformal field theories.

In $1+1$ D, the data of topological operators implementing 0-form symmetries is captured by a *unitary fusion category*. We shall restrict our attention to this setup. A good reference for the reader interested in higher form symmetries in [66].

We usually meet a symmetry as a unitary operator U_g where $g \in G$ is a group element, satisfying

$$U_g U_h = U_{gh}, \qquad U_g^{-1} = U_{g^{-1}}, \qquad [U_g, H] = 0. \tag{4.0.1}$$

This is an excellent definition, but in two spacetime dimensions it hides a useful piece of geometry. A finite internal symmetry element g can be represented by an oriented codimension-one topological defect line L_g. Placing L_g across a spatial slice gives the operator U_g. Moving the line in Euclidean spacetime does not change a correlator, provided that it does not cross an insertion. Fusion of parallel lines is just group multiplication,

$$L_g \otimes L_h \simeq L_{gh}, \qquad L_g \otimes L_{g^{-1}} \simeq \mathbf{1}. \tag{4.0.2}$$

This defect formulation is the natural starting point for generalized global symmetries.

We never required that the action be invertible; indeed we may have for some lines $\mathcal{L}_a, \mathcal{L}_b$

$$\mathcal{L}_a \otimes \mathcal{L}_b \simeq \bigoplus_c N_{ab}{}^c \mathcal{L}_c, \qquad N_{ab}{}^c \in \mathbb{Z}_{\geq 0}, \tag{4.0.3}$$

with several terms on the right-hand side. The line still commutes with the Hamiltonian and can still be freely deformed, but it need not act by a unitary or even an invertible operator. These lines can be split, fused, deformed, etc freely: this data is captured by a unitary fusion category [65,67].

Before moving on to the technicalities, let us motivate why it is actually quite natural that not all symmetries can be grouplike, following [65]. Consider a two-dimensional theory $\mathcal{T}$ carrying a finite, non-anomalous group symmetry G[1]. Gauge it, and call the result $\mathcal{T}/G$. If G is Abelian, the gauged theory has the familiar dual symmetry $\widehat{G}$ (its Pontryagin dual), which is also a finite abelian group. We can re-gauge this theory, and this returns us the original theory.

Since G is abelian, it is guaranteed that $\hat{G}$ is an abelian group. It is simply the group of one dimensional $U(1)$ characters of G. What replaces $\widehat{G}$ when G is non-Abelian? Something should already ring alarm bells, since non-abelian groups don't have just one dimensional representations; so the gauged theory cannot have an abelian group symmetry like before.

The gauged theory contains topological Wilson lines labelled by irreducible representations R of G. Bringing two Wilson lines together tensors their representations,

$$W_R \otimes W_S \simeq \bigoplus_T N_{RS}{}^T W_T, \qquad R \otimes S \cong \bigoplus_T N_{RS}{}^T T. \tag{4.0.4}$$

The dual symmetry of $\mathcal{T}/G$ is therefore $\mathrm{Rep}(G)$, not in general an ordinary group [65]. If G is Abelian, every irreducible representation is one-dimensional and $\mathrm{Rep}(G)$ reduces to the group-like category associated with $\widehat{G}$. If G is non-Abelian, some

[1]These arguments are true also in higher dimensions and for p form symmetries, where the dual symmetry is a $d-p-2$ for symmetry

irreducible representation R has dimension greater than one, and

$$R \otimes R^* \cong \mathbf{1} \oplus (\text{other representations}). \tag{4.0.5}$$

Hence W_R has no fusion inverse. Noninvertibility has appeared simply because we gauged an ordinary symmetry.

This also teaches us another lesson: the Wilson lines retain the information lost by summing over G gauge fields; an appropriate regauging of the $\mathrm{Rep}(G)$ symmetry recovers $\mathcal{T}$. For a general fusion category this gauging operation is not canonical: one must choose suitable algebraic data that allows one to form a consistent mesh of topological lines. This extra structure is clearly something that goes beyond just the fusion rules of the topological defects.

Just to have an example to keep in mind as we define things concretely below, consider $\mathrm{Rep}(G)$ again as a unitary fusion category.

Its objects are finite-dimensional unitary representations of G; morphisms are G-intertwiners; tensor product is the ordinary tensor product of representations; simple objects are irreducible representations; and duality is the dual representation.

For an irreducible representation R, $\dim(R) = \dim_{\mathbb{C}} R$,

and therefore

$$\dim \mathrm{Rep}(G) = \sum_{R \in \mathrm{Irr}(G)} (\dim R)^2 = |G|.$$

4.1 Symmetry categories in two dimensions

We provide a brief review of 0-form symmetries that can be realised in theories in $1 + 1D$. We will use the Euclidean formulation of these theories. As we discussed earlier, in many interesting and natural cases, such symmetries are not group-like. The data for such symmetries is described by a *unitary fusion category* [65, 67]. Let us emphasize that when we say symmetries are captured by unitary fusion categories here, we mean the underlying data that characterizes the bare bones of the symmetry, before committing to quantizing a given theory on a specific manifold and thus defining the symmetry *action* on Hilbert space. Depending on the setup, this category acts on the Hilbert spaces with various *algebras*. We will consider them in turn in Chapter 8.

In $1 + 1D$, a zero form symmetry must be implemented by a codimension 1 operator i.e. *line operators*. Moreover, being topological, these line operators can do many other maneuvers such as fusing, splitting, etc. The data that describes the lines and manipulations on them is captured by a *unitary fusion category* $\mathcal{C}$. A standard example is the Verlinde lines in an RCFT. The operators charged under this symmetry are pointlike i.e. local operators; for the Verlinde lines these would be the primaries. The modular S-matrix of the RCFT captures how the primaries transform under the symmetry. More generally, this notion is captured by *linking* of *Fusion algebra* Fus($\mathcal{C}$), see the left panel of figure 4.1.

Figure 4.1: Linking (left) and Lasso(right) actions

Importantly, these lines cannot arbitrarily 'end'; one needs to specify some boundary conditions at the endpoints. In case the line ends at a generic spacetime point, the endpoint hosts *twisted sector operators*. These operators are theory dependent. A standard example is the disorder operator in the Ising RCFT, which is twisted by the $\mathbb{Z}_2$ line. These operators are not the usual local operators as they cannot exist without the line; and they certainly don't need to be topological. For instance, the disorder operator carries a nonzero conformal dimension; it costs energy to move it in space unlike the $\mathbb{Z}_2$ that emanates from it and be deformed for free. What is the analog of the 'linking' procedure for such operators? It turns out that one needs a more complicated action that requires also the data about fusion and splitting of these lines. This is the so called *lasso* action of the *Tube algebra*Tube($\mathcal{C}$); see the right panel of figure 4.1.

A related notion is *twisted sector Hilbert space*. When the lines are inserted along the spatial slice, they are topological upto linking action with the operators, and this constrains correlation functions through Ward identities. Instead, if they are placed along the time direction, then they act like the worldline of a pointlike defect placed on the spatial manifold. The state on that spatial slice can then no longer describes the vacuum sector of the theory; we have added a defect in space and it changes the quantization problem entirely. This leads to a *twisted sector hilbert space*.

It can also happen that we find special boundary conditions where the line *can* end topologically; but the boundary condition is not a local operator but an extended state. One needs additional data about how the line terminates on such a state and possibly alters it: this data specifies a *module category* $\mathcal{M}$ of $\mathcal{C}$. Note that this data only depends on the symmetry; whether such boundary conditions can actually *realized* in a physical theory is a dynamical question [2]

4.2 The axioms of a unitary fusion category

A unitary fusion category is a $\mathbb{C}$-linear semisimple rigid monoidal category with finitely many simple objects, simple tensor unit, and a compatible positive †-structure. Let us spell out this mouthful, and list the axioms.

Objects and morphisms The building blocks of a category $\mathcal{C}$ are (isomorphism classes of) its *objects* $Ob(\mathcal{C})$, and *morphisms* $Mor(\mathcal{C})$ between them. The set of morphisms between two objects $a, b \in Ob(\mathcal{C})$ is denoted $\mathrm{Hom}_{\mathcal{C}}(a, b)$. We further require that is is a finite-dimensional complex vector space[3]. There is a zero object $0 \in Ob(\mathcal{C})$ with $\mathrm{Hom}_{\mathcal{C}}(0, 0) = 0$ as a vector space.

These morphisms are equipped with an associative $\mathbb{C}$-linear composition operation;

$$f_i \in \mathrm{Hom}(a_i, a_{i+1}) \quad \text{then} \quad f_1 \circ (f_2 \circ f_3) = (f_1 \circ f_2) \circ f_3)$$

Every object a possesses a unique *identity morphism* $\mathrm{id}_a \in \mathrm{Hom}(a, a)$. Physically, morphisms are topological point operators living at junctions of defect lines.

Additivity We are interested in *Abelian* categories [4] with the notion of a *direct sum*. Given $a_1, a_2 \in Ob(\mathcal{C})$, there exists a *unique* (upto a unique isomorphism) $b \in Ob(\mathcal{C})$ with maps

$$h_{1,2} : b \to a_{1,2}, \quad k_{1,2} : a_{1,2} \to b \ \text{ s.t. } \ h_i k_i = \mathrm{id}_{a_i} \text{ and } k_1 h_1 + k_2 h_2 = \mathrm{id}_b$$

Then, the object satisfying the above property is defined to be

$$b \equiv a_1 \oplus a_2 \in Ob(\mathcal{C}) \tag{4.2.1}$$

This endows $\mathcal{C}$ with an abelian ring $\oplus$ over $\mathbb{Z}_{\geq 0}$. The notion of adding objects allows one to define *simple* objects as those that cannot be written as a direct sum of other objects. Equivalently,

[2] It is believed to be possible in CFTs, see section 4.3 in [68]

[3] The jargon is $\mathcal{C}$ is *enriched* in $\mathrm{Vect}_{\mathbb{C}}$ or $\mathbb{C}-$linear

[4] Strictly, what we describe an additive category; an abelian category further requires some constraints on the kernel and cokernel morphisms. We suppress such details here, see [69]

$$\mathrm{Hom}(a,a) \simeq \mathbb{C} \iff a \text{ is simple} \tag{4.2.2}$$

These are the building blocks of the category. Physically, a direct sum means that the line carries a finite superselection label; its correlator is the sum of the correlators for the summands. In the twisted sector perspective, the hilbert space associated to $a \oplus b$ is $\mathcal{H}_a \oplus \mathcal{H}_b$. Note that non-integer coefficients don't make any sense in this construction; we gave a concrete meaning to the symbol $a \oplus b$, and we can iteratively give meanings only to similar integer coefficient sums.

In a fusion category, one requires that the identity $\mathbf{1}_{\mathcal{C}}$ be a simple object (otherwise we have a *multi*fusion category).

Finiteness and semisimplicity $\mathcal{C}$ is *finite* if there are finitely many isomorphism classes of simple objects. *Semisimplicity* is the requirement that every object is a finite direct sum of simple objects:

$$x \simeq \bigoplus_{a \in \mathrm{Irr}(\mathcal{C})} N_a \, a, \qquad N_a \in \mathbb{Z}_{\geq 0},$$

Functors Given 2 categories $\mathcal{C}, \mathcal{D}$ with their respective objects and morphisms; a *functor* $\mathcal{F}$ maps $Ob(\mathcal{C}) \to Ob(\mathcal{C})$ and $Mor(\mathcal{C}) \to Mor(\mathcal{D})$ such that for every $a_i \in Ob(\mathcal{C})$ and morphisms $f_i \in \mathrm{Hom}(a_i, a_{i+1})$

$$\mathcal{F}(\mathrm{id}_{a_i}) = \mathrm{id}_{\mathcal{F}(a_i)} \quad \mathcal{F}(f_1 \circ_{\mathcal{C}} f_2) = \mathcal{F}(f_1) \circ_{\mathcal{D}} \mathcal{F}(f_2)$$

We can similarly define bifunctors and multifunctors, depending on how many arguments they take.

Particularly useful is the concept of a *natural transformation* of functors. Given two functors $\mathcal{F}, \mathcal{G} : \mathcal{C} \to \mathcal{D}$, and some $a \in Ob(\mathcal{C})$; we can construct the morphism $\eta_a : \mathcal{F}(a) \to \mathcal{G}(a)$ in $\mathcal{D}$. We can consider then the family of all such morphisms, one for each $a \in \mathcal{C}$, satisfying

$$\eta_b \circ \mathcal{F}(f) = \mathcal{G}(f) \circ \eta_a \quad \text{where } f \in \mathrm{Hom}_{\mathcal{C}}(a,b)$$

If $\forall a \in Ob(\mathcal{C})$, η_a is an isomorphism in $\mathcal{D}$, then we call this transformation a *natural isomorphism*.

Monoidal categories A monoidal category $\{\mathcal{C}, \otimes, \mathbf{1}_{\mathcal{C}}, , \alpha\}$ is a category equipped with a bilinear *bifunctor* $\otimes : \mathcal{C} \otimes \mathcal{C} \to \mathcal{C}$ satisfying

$$(f_2 \otimes g_2) \circ (f_1 \otimes g_1) = (f_2 \circ f_1) \otimes (g_2 \circ g_1).$$

There is a tensor unit object $(\mathbf{1}_{\mathcal{C}},)$ with an isomorphism $: \mathbf{1}_{\mathcal{C}} \otimes \mathbf{1}_{\mathcal{C}} \simeq \mathbf{1}_{\mathcal{C}}$ (which is arbitrary, and will be suppressed usually) and natural isomorphisms

$$\lambda_a : \mathbf{1} \otimes a \xrightarrow{\sim} a, \qquad \rho_a : a \otimes \mathbf{1} \xrightarrow{\sim} a.$$

In a *strict* monoidal category, these isomorphisms are the identity map.

Monoidal and semisimple structure allows one to define a *fusion ring*

$$a \otimes b \simeq \bigoplus_c N_{ab}{}^c\, c, \qquad N_{ab}{}^c \in \mathbb{Z}_{\geq 0}.$$

Equivalently,

$$N_{ab}{}^c = \dim_{\mathbb{C}} \mathrm{Hom}(a \otimes b, c).$$

Associativity of this ring requires

$$\sum_e N_{ab}{}^e N_{ec}{}^d = \sum_f N_{bc}{}^f N_{af}{}^d.$$

This allows us to define, for instance, trivalent junctions

$$m \in \mathrm{Hom}(a \otimes b, c).$$

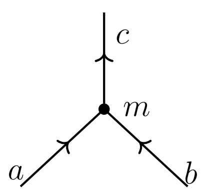

Associator It is important that the fusion ring is *not* the whole symmetry category: it forgets the junction spaces and the associator/F-symbols. Tensor product need not be strictly associative. Instead there are natural isomorphisms

$$\alpha_{a,b,c} : (a \otimes b) \otimes c \xrightarrow{\sim} a \otimes (b \otimes c).$$

Graphically this is the elementary F-move:

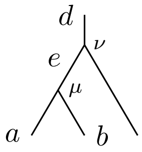

$$= \sum_{f,\rho,\sigma} \left[F^{d}_{abc}\right]_{(e;\mu\nu)(f;\rho\sigma)}$$

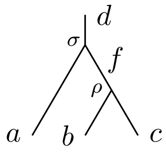

$$. \qquad (4.2.3)$$

After bases are chosen in the junction spaces, the matrix elements of α are the F-symbols. They are the amplitudes for the local recoupling move that changes one fusion tree into another. This is physical information not contained in the integers ${N_{ab}}^{c}$.

The associator is natural: inserting junction operators and then recoupling gives the same answer as recoupling first and inserting the induced junctions. It must also be compatible with erasing the invisible line. This is the triangle identity,

$$(\mathrm{id}_a \otimes \lambda_b) \circ \alpha_{a,\mathbf{1},b} = \rho_a \otimes \mathrm{id}_b\,. \tag{4.2.4}$$

Both sides remove an invisible segment from $(a \otimes \mathbf{1}) \otimes b$.

There are two sequences of recouplings that take four parenthesized lines from $((a \otimes b) \otimes c) \otimes d$ to $a \otimes (b \otimes (c \otimes d))$. Since the final line network is the same, the answers must agree:

$$\alpha_{a,b,c\otimes d} \circ \alpha_{a\otimes b,c,d} = (\mathrm{id}_a \otimes \alpha_{b,c,d}) \circ \alpha_{a,b\otimes c,d} \circ (\alpha_{a,b,c} \otimes \mathrm{id}_d). \tag{4.2.5}$$

This is, in a basisc, the *pentagon identity*:

$$\alpha_{a,b,c\otimes d} \circ \alpha_{a\otimes b,c,d} = (\mathrm{id}_a \otimes \alpha_{b,c,d}) \circ \alpha_{a,b\otimes c,d} \circ (\alpha_{a,b,c} \otimes \mathrm{id}_d)$$

It is best read as path-independence of local topological manipulations. In an ordinary group symmetry the associator may carry a three-cocycle; its cohomology class is precisely the $1+1$-dimensional 't Hooft anomaly.

Duality and rigidity $\mathcal{C}$ is *rigid* if every object a possesses a dual object a^*, physically obtained by reversing the orientation of the line. One has

$$(a^*)^* \simeq a, \qquad (a \otimes b)^* \simeq b^* \otimes a^*.$$

There are evaluation maps

$$\epsilon^R_a : a \otimes a^* \to \mathbf{1}, \qquad \epsilon^L_a : a^* \otimes a \to \mathbf{1},$$

and coevaluation maps

$$\eta_a^R : \mathbf{1} \to a^* \otimes a, \qquad \eta_a^L : \mathbf{1} \to a \otimes a^*.$$

which can be drawn as

Let us note that the existence of a (unique, upto unique isomorphism) dual is a feature of rigid categories, and is something special. More generally, one has the notion of a left dual a^* or a right dual ${}^*a$ for an object $a \in Ob(\mathcal{C})$; with their respective evaluation and coevaluation maps, say,

$$\epsilon'^L_a : a^* \otimes a \to \mathbf{1}, \qquad \epsilon'^R_a : a \otimes^* a \to \mathbf{1}$$

and the reversed arrows for coevaluations. By definition, it is clear that

$$\epsilon'^L_a = \epsilon'^R_{a^*},$$

and the same for coevaluations; meaning a^* is the right dual of ${}^*a$, and similarly one is the left dual of the other. If, either one exists, then it is unique upto an unique isomorphism [69], Proposition 2.10.5. If an object possesses both left and right duals, then the object is called rigid. Note that for such an object

$${}^*({}^*a) \simeq (a) \simeq (a^*)^* \qquad \text{pivotal structure}$$

If every object in a monoidal category is rigid, then that category is called rigid. Note that $\mathbf{1}^* =^* \mathbf{1} = \mathbf{1}$ always, where the evaluation and coevaluations morphisms are $, ^{-1}$.

In a rigid category, such an isomorphism lets one define a dual (without qualifiers left/right) for any object a; conventionally denoted a^*. It is important to keep track of this isomorphism since its not an equality: this the *pivotal structure* p_a

$$p_a : a \xrightarrow{\sim} (a^*)^*$$

this allows one to define something that is *both* a left right dual, with (co)evaluations maps defined so that

$$\epsilon_a^R = \epsilon_{a^*}^L \circ (p_a \otimes \mathbf{1}) = \epsilon_{a^*}^L \circ (1 \otimes p_{a^*}^{-1}) \qquad \eta_a^R = (\mathbf{1} \otimes p_a^{-1}) \circ \epsilon_{a^*}^L = (p_{a^*} \otimes \mathbf{1}) \circ \epsilon_{a^*}^L$$

These are the maps defined earlier.

They satisfy the zig-zag, or snake, identities. For example,

$$(\epsilon_a^R \otimes \mathrm{id}_a) \circ \alpha^{-1}_{a,a^*,a} \circ (\mathrm{id}_a \otimes \eta_a^R) = \mathrm{id}_a,$$

with the analogous equation for a^*.

Graphically,

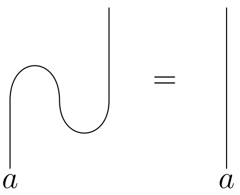

this is a part of the broader requirement of *isotopy invariance* of diagrams of defects. Note that an orientation of a line was never part of the datum; it is a shorthand for keeping track of the pivotal structures involved. An orientation reversed line doesn't really exist as it is because orientation is not part of the category data; it is a shorthand for inserting some pivotal structure. So one has to be very careful when interpreting lines as their duals oriented oppositely, inside diagrams; the morphisms must all be chosen in the appropriate way to be internally consistent.

Let us also remark that in general one can have a *Frobenius Schur indicator* in theories where there is also an isomorphism between $a \simeq a^*$, so this equality can differ by a phase. If this isomorphism doesn't exist, then the indicator is pure gauge and there is always a basis of morphisms in which we can forget it. However, in many important examples like Tambara-Yamagami categories, one has to be careful. In practice, one always chooses a trivial Schur indicator (for example, the symmetry of the Ising CFT is the the Tambara-Yamagami category over $\mathbb{Z}_2$ with a trivial Schur indicator chosen by hand) to have full isotopy invariance. See Chapter 14 in [70] for a nice discussion.

Quantum trace/dimension In a rigid monoidal category with a pivotal structure p, we may construct the following element of $\mathrm{End}(\mathbf{1}_\mathcal{C})$:

$$\mathrm{Tr}(p) \in \mathrm{End}(\mathbf{1}_\mathcal{C}) : \mathbf{1} \xrightarrow{\eta_a^L} a \otimes a^* \xrightarrow{p \otimes \mathrm{id}_{a^*}} a^{**} \otimes a^* \xrightarrow{\epsilon_{a^*}^L} \mathbf{1} \tag{4.2.6}$$

This is technically a left trace; there exists also a right trace when using right duals. They are related by a dual pivotal structure which is fixed by $(p_a)^* = p_{a^*}^{-1}$; so we can commit to just one. Evaluating this morphism on a specific object of the category defines its *quantum dimension*

$$\dim(a) \equiv \mathrm{Tr}(p_a) \in \mathrm{End}(\mathbf{1}_{\mathcal{C}}) \tag{4.2.7}$$

Note that this number is a map from $\mathbf{1}$ to itself, and $\mathbf{1}$ is a simple object in a fusion category (by definition); so this object must simply be a (complex) number.

The sequence of maps in the definition of the trace is often represented through closing a line into a loop produces a scalar:

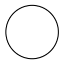 $a \quad = \quad \dim(a)$.

This is really to be interpreted as a, a^* fusing into the identity via the (co)evaluation morphisms, and a pivotal structure being used to rewrite this fusion as a single a (or a^*) going into a loop.

The pivotal structure p is further called *spherical* if

$$\dim(a) = \dim(a^*)$$

or equivalently the left and right traces are the same. The word ‘spherical’ indicates that on a sphere, a closed loop is unambiguous, whether it is evaluated clockwise or counter-clockwise.

Shrinking concentric loops shows that quantum dimension is a one-dimensional representation of the fusion ring,

$$\dim(a)\dim(b) = \sum_c {N_{ab}}^c \dim(c), \tag{4.2.8}$$

The total dimension of the category is

$$\dim(\mathcal{C}) = \sum_{a \in \mathrm{Irr}(\mathcal{C})} \dim(a)^2$$

Note that if the category in question was a braided category in $2+1$D, then this number captures the topological entanglement entropy of the ground state over which the excitations are the lines (anyons).

Henceforth, we will denote the quantum dimensions as $\dim(a) = d_a = \dim(a^*)$

The unitary or † structure We now demand some additional structure: For every pair a, b there is a conjugation map

$$\dagger : \mathrm{Hom}(a,b) \longrightarrow \mathrm{Hom}(b,a), \qquad f \longmapsto f^\dagger,$$

such that $(g \circ f)^\dagger = f^\dagger \circ g^\dagger, \qquad (f \otimes g)^\dagger = f^\dagger \otimes g^\dagger$

The associators may then be chosen unitarily, so that

$$\alpha^\dagger_{a,b,c} = \alpha^{-1}_{a,b,c}.$$

Evaluation and coevaluation are then necessarily related by this Hermitian conjugation

$$\eta^R_{a^*} = (\epsilon^L_a)^\dagger, \qquad \eta^L_{a^*} = (\epsilon^R_a)^\dagger.$$

Crucially, one imposes positivity:

$$f^\dagger \circ f \geq 0.$$

For a simple object a, since $f \in \mathrm{Hom}_{\mathcal{C}}(a,a) \simeq \mathbb{C}$, positivity implies

$$f^\dagger f = \lambda\, \mathrm{id}_a, \qquad \lambda \geq 0.$$

Consequently,

$$d_a > 0$$

for every nonzero object a. This is the categorical origin of the positivity of quantum dimensions in a unitary fusion category. Moreover, consider the fusion matrices

$$(N_a)^c{}_b = N_{ab}{}^c.$$

Then the positive vector $v_b = \dim(b)$ obeys

$$N_a v = \dim(a)\, v.$$

By Perron–Frobenius, for a unitary fusion category, $\dim a > 0$ is the Perron–Frobenius eigenvalue[5] of N_a. The same argument applies to $\dim(a^*)$, so actually unitarity implies sphericity [66].

Moreover, because $a \otimes a^*$ contains $\mathbf{1}$, positivity gives

$$d_a^2 = 1 + \sum_{c \neq \mathbf{1}} N_{aa^*}{}^c d_c \geq 1. \tag{4.2.9}$$

Thus $d_a \geq 1$ for a simple line, and $d_a = 1$ precisely when $a \otimes a^* \simeq \mathbf{1}$, namely when a is invertible. For example, the Ising duality line implements a non-invertible symmetry,

[5] For a matrix with non-negative entries $M_{ij} \geq 0$, there is always an eigenvector $M\vec{v} = \lambda_{PF}\vec{v}$, $v_i > 0$ of positive entries, whose eigenvalue λ_{PF} is the largest eigenvalue of the matrix, called Perron–Frobenius eigenvalue

and carries a quantum dimension of $\sqrt{2}$.

There is a useful CFT proof that d_a is nonnegative [67]. Consider the two torus amplitudes

$$Z^a(\tau,\overline{\tau}) = \mathrm{Tr}_{\mathcal{H}}\left(\widehat{L}_a q^{L_0-c/24}\overline{q}^{\overline{L}_0-\overline{c}/24}\right), \tag{4.2.10}$$
$$Z_a(\tau,\overline{\tau}) = \mathrm{Tr}_{\mathcal{H}_a}\left(q^{L_0-c/24}\overline{q}^{\overline{L}_0-\overline{c}/24}\right). \tag{4.2.11}$$

Here $\mathcal{H}_a$ is the Hilbert space on a circle with an a-defect point. A modular S transformation exchanges the two cycles of the torus and hence exchanges these two descriptions. In the low-temperature channel, the unique vacuum contribution to Z^a is d_a times the universal vacuum Boltzmann factor. In the crossed channel, Z_a is an ordinary trace over the positive-norm Hilbert space $\mathcal{H}_a$, so its spectral coefficients are nonnegative. Matching the leading terms gives

$$d_a \geq 0. \tag{4.2.12}$$

For a nonzero simple line in a unitary compact CFT one in fact has $d_a > 0$.

4.3 Physical consequences

Let us illustrate the use of all this machinery in some concrete physical settings, to illustrate how they teach us some physics. Let us illustrate with some basic examples the physical consequences of generalized symmetries. The critical Ising CFT gives the smallest useful example. In a diagonal rational CFT, the Verlinde lines are labelled by chiral primaries and act on the sector i with eigenvalue S_{ai}/S_{0i}; their fusion is governed by the Verlinde algebra [71]. The Ising CFT is an example of such a system.

It has three distinguished simple topological lines: the invisible line $\mathbf{1}$, the invertible spin-flip line η, and the Kramers–Wannier duality line $\mathcal{N}$. Their fusion rules are

$$\eta\otimes\eta \simeq \mathbf{1}, \qquad \eta\otimes\mathcal{N} \simeq \mathcal{N}\otimes\eta \simeq \mathcal{N}, \qquad \mathcal{N}\otimes\mathcal{N} \simeq \mathbf{1}\oplus\eta. \tag{4.3.1}$$

The last equation makes $\mathcal{N}$ noninvertible. It is the continuum defect that implements Kramers–Wannier order–disorder duality [72,73]. For this noninvertible line, (4.3.1) immediately provides the quantum dimension exceeding one:

$$d_{\mathcal{N}}^2 = d_{\mathbf{1}} + d_\eta = 2, \qquad d_{\mathcal{N}} = \sqrt{2}. \tag{4.3.2}$$

The local Virasoro primaries are $\mathbf{1}$, the energy operator ε, and the order operator σ, with weights

$$(h,\overline{h})_{\mathbf{1}}=(0,0),\qquad (h,\overline{h})_{\varepsilon}=\left(\frac{1}{2},\frac{1}{2}\right),\qquad (h,\overline{h})_{\sigma}=\left(\frac{1}{16},\frac{1}{16}\right). \tag{4.3.3}$$

As an operator on the ordinary, untwisted Hilbert space, the $\mathcal{N}$ line acts diagonally on these three conformal families

$$\mathcal{L}_{\mathcal{N}}|\mathbf{1}\rangle=\sqrt{2}|\mathbf{1}\rangle,\qquad \mathcal{L}_{\mathcal{N}}|\varepsilon\rangle=-\sqrt{2}|\varepsilon\rangle,\qquad \mathcal{L}_{\mathcal{N}}|\sigma\rangle=0. \tag{4.3.4}$$

where we have used the notation $\mathcal{L}_a$ to emphasize that this is a representation of the fusion category on the circle hilbert space, that maps the abstract object a to an operator $\mathcal{L}_a \in \mathrm{End}(\mathcal{H})$. Notice the zero eigenvalue. Moreover, if we sweep $\mathcal{N}$ through the local order field σ, it produces the disorder field μ, which is attached to the spin-flip line η. In other words, the natural action of a noninvertible line relates untwisted and twisted sectors; it is not simply an automorphism of the local operator algebra. In fact, the way the category acts on this *extended* Hilbert space including twisted sectors, is via the Tube algebra, which we will review in section 8.1.1.

This observation has physical consequences i.e. selection rules. Nucleate a small $\mathcal{N}$ loop in a correlator, sweep it through three insertions of ε, and shrink it on the other side. Each crossing contributes a minus sign, while the same loop factor appears before and after. Therefore

$$\langle\varepsilon(z_1,\overline{z}_1)\varepsilon(z_2,\overline{z}_2)\varepsilon(z_3,\overline{z}_3)\rangle=0. \tag{4.3.5}$$

The ordinary $\mathbb{Z}_2$ symmetry cannot explain this because ε is even. Similarly, sweeping $\mathcal{N}$ through a correlator containing two order fields relates an order correlator to a disorder correlator-for instance their two point functions must be the same: indeed they have the same conformal dimension. In fact, they belong to a 2 dimensional irrep of the tube algebra, which commutes with the conformal symmetry. Note that such constraints between twisted and untwisted sector correlators would be missed without invoking the tube algebra and non-invertible symmetries.

As another example, let a CFT be perturbed by a relevant scalar operator ϕ. A topological line is preserved by the deformation when ϕ commutes with it. Since the vacuum is invariant under the symmetry,

$$\mathcal{L}_a|\phi\rangle=d_a|\phi\rangle. \tag{4.3.6}$$

In the path integral picture, one imagines the ground state prepared by a cylinder path integral capped at infinity by a euclidean section. Then, the line $\mathcal{L}_a$ acting on the cut where the (symmetric!) state lives, can be pushed all the way to infinity and shrunk there, producing the quantum dimension. The line then remains topological along the flow. Its fusion rules, junction recouplings, and defect spin-selection rules survive to the infrared. This is a notion of *rigidity* of categorical data under RG.

Suppose a preserved line a has $d_a \notin \mathbb{Z}_{\geq 0}$ and assume, for contradiction, that the infrared is trivially gapped with a unique vacuum. The low-energy theory is then the trivial two-dimensional TQFT. Evaluate its torus partition function in two channels:

- with a wrapping the spatial cycle, it is the trace of $\widehat{L}_a$ on the one-dimensional vacuum space, hence it equals d_a;
- after a modular S transformation, a wraps the Euclidean-time cycle, so the same path integral equals $\dim \mathcal{H}_a$, the dimension of the a-twisted Hilbert space.

Therefore

$$d_a = \dim \mathcal{H}_a \in \mathbb{Z}_{\geq 0}, \tag{4.3.7}$$

which is a contradiction. A preserved line of nonintegral quantum dimension therefore forbids a unique trivially gapped infrared. The flow must remain gapless or end in a gapped phase with vacuum degeneracy (more generally, a nontrivial infrared TQFT) [67].

Chapter 5

Asymmetry for U(1) in CFTs

In this chapter we are interested in computing entanglement asymmetry in conformal quantum field theories (CFTs) with a $U(1)$ global symmetry in general dimensions d. In case the CFT is holographic, we will explore a gravity dual in chapter 6.1

In QFT, entanglement entropy is a well known measure of bipartite entanglement. However, it is known to suffer from UV divergences that come from the highly entangled modes across the entangling surface. Recall that for relative entropy, instead, the divergences cancel out and we expect to obtain a well-defined observable; therefore, *Entanglement asymmetry*, by being a relative entropy, is a good quantity to study.

In CFTs the vacuum does not spontaneously break the symmetry [1], thus we ought to consider some excited state. Let us remark that Entanglement asymmetry in CFTs in which the symmetry is explicitly broken has been studied in [28]; our setup is different, where the symmetry is really there and implemented by topological operators.

Here we study a class of "coherent states", partially motivated by holography [74–76]:

$$|\Psi\rangle = e^{i\lambda V}|0\rangle\,, \tag{5.0.1}$$

obtained by acting on the vacuum with $e^{i\lambda V}$ in Euclidean time, where V is a primary local operator of charge 1.[2] We choose to work in a perturbative expansion in λ, and show that $\Delta S = \lambda^2 \Delta S^{(2)} + O(\lambda^4)$. We compute the leading contribution $\Delta S^{(2)}$ in three different ways:

[1] a broken phase is characterized by an algebra of topological operators that project one onto the different superselection sectors. A CFT only has a unique topological local operator-the identity.

[2] Similar states have been studied in [41].

1. By first computing the Renyi asymmetries

$$\Delta S_n = \frac{1}{1-n}\Big(\log \mathrm{Tr}\, \rho_Q^n - \log \mathrm{Tr}\, \rho^n\Big) \tag{5.0.2}$$

   using the replica method of [57, 77, 78], and then taking the limit $n \to 1$.
2. By exploiting an integral representation for the leading perturbative contribution to relative entropy, also called Fisher information [76, 79].
3. By computing the Renyi asymmetries in terms of correlation functions of V and $V^\dagger$ that include twist operators [57].

The result is a "universal expression" for the entanglement asymmetry, that depends on the dimension Δ of V and on the location of its insertion in Euclidean space.

It turns out that both $\Delta S^{(2)}$ and $\Delta S_n^{(2)}$ behave as two-point functions. This allows us (for instance as in [80]) to exploit conformal transformations to determine the entanglement asymmetry in a variety of geometries, for different choices of the subsystem A: for the "Rindler" geometry in which A is an infinite half-space; for finite spherical subregions A in infinite volume as well as in finite volume on S^{d-1}; for spherical subregions on the hyperbolic plane $\mathbb{H}^{d-1}$ at finite temperature; for finite intervals on the real line at finite temperature in $d = 2$.

Following [80, 81], we are also able to use conformal transformations and analytic continuation to determine the time evolution of entanglement asymmetry, starting from a coherent state (that we regard as originating from a local quench). As expected from thermalization, the asymmetry of a subsystem decreases with time since the excited state relaxes. Interestingly, however, we observe that a universal quantum Mpemba effect takes place. It would be interesting to identify an underlying mechanism responsible for the Mpemba effect in CFTs (as done in [34] for integrable systems).

5.1 Symmetrization for $U(1)$

Let us review the definition of entanglement asymmetry proposed in [3].[3] Consider a quantum system which can be divided into two parts A and B in such a way that the Hilbert space factorizes: $\mathcal{H} = \mathcal{H}_A \otimes \mathcal{H}_B$. Consider the case that there exists a charge operator Q that generates a $U(1)$ action on the Hilbert space,[4] and that the

[3] The authors of [50] considered a very similar quantity, but for global states.

[4] In most cases, and here too, the $U(1)$ action is a global symmetry of the quantum system. However the Hamiltonian of the system does not enter into the definition of entanglement asymmetry and therefore one could consider $U(1)$ actions that are not symmetries, as for instance in [28].

charge operator can be factorized as well

$$Q = Q_A \otimes \mathbb{1}_B + \mathbb{1}_A \otimes Q_B\,. \tag{5.1.1}$$

This is a subtle assumption we are making; typically such a factorization can be done only after choosing specific boundary conditions at the entangling surface. For non-anomalous grouplike symmetries, it turns out that this can always be achieved in a natural way[5]. Given a (normalized) density matrix ρ_{tot}, which could represent a pure ($\rho_{\text{tot}} = |\psi\rangle\langle\psi|$) or a mixed state, one constructs the reduced density matrix on A, namely $\rho = \operatorname{Tr}_B \rho_{\text{tot}}$, and its entanglement entropy is given by the von Neumann entropy $S = -\operatorname{Tr}(\rho \log \rho)$. If the state ρ_{tot} is an eingenstate of Q, namely $[\rho_{\text{tot}}, Q] = 0$ and thus the symmetry is unbroken, then $[\rho, Q_A] = 0$ and thus ρ takes a block-diagonal form in a basis of eigenspaces of Q_A. Then the entanglement entropy S can be resolved into the contributions $S(q)$ from each charge sector: this is called symmetry-resolved entanglement entropy [82–84]. On the other hand, if the symmetry is broken in the subsystem A and thus $[\rho, Q_A] \neq 0$, one can quantify the amount of breaking in the following way. One constructs a projected reduced density matrix

$$\rho_Q = \textstyle\sum_{q\in\mathbb{Z}} \Pi_q\, \rho\, \Pi_q\,, \tag{5.1.2}$$

where Π_q is the projector to the eigenspace of Q_A with charge q. This is essentially the matrix ρ with all off-diagonal blocks set to zero. The quantity (5.1.2) can be recast in a more elegant form by using the Fourier transform of the projector $\Pi_q = \int_0^{2\pi} \frac{d\alpha}{2\pi}\, e^{i\alpha(Q_A - q)}$, hence

$$\rho_Q = \int_0^{2\pi} \frac{d\alpha}{2\pi} e^{-i\alpha Q_A}\, \rho\, e^{i\alpha Q_A}\,. \tag{5.1.3}$$

This is the average of ρ over the adjoint action of the group $U(1)$, and it naturally generalizes to discrete as well as non-Abelian groups [27, 28, 32, 33]. Notice that ρ_Q is a density matrix, namely it is Hermitian, semi-positive definite, and $\operatorname{Tr}\rho_Q = 1$. The entanglement asymmetry is defined as the difference between the entanglement entropies of ρ_Q and ρ [3]:

$$\Delta S = S[\rho_Q] - S[\rho] = \operatorname{Tr}(\rho \log \rho) - \operatorname{Tr}(\rho_Q \log \rho_Q)\,. \tag{5.1.4}$$

[5]For the curious reader, this is what we do. Cut out the entangling discs at ∂A and impose strongly symmetric boundary conditions c.f. 8.2.2. In the replica geometry, one has a bunch of lines fusing on the disc. These can be disentangled by trivial $\tilde{F}$ moves, and since the replica constructions ensures that all group lines fuse to the identity, in the end we can disentangle them all from the disc, and shrink it away. What is left is just the usual group lines, restricted on the subregion A.

One easily verifies that the entanglement asymmetry is equivalent to the relative entropy of ρ with respect to ρ_Q [50]:

$$\Delta S = \mathrm{Tr}\Big(\rho\,(\log\rho - \log\rho_Q)\Big) = S(\rho\,\|\,\rho_Q)\,. \tag{5.1.5}$$

This makes ΔS a good measure of symmetry breaking. Indeed, as it follows from the properties of relative entropy: $\Delta S \geq 0$, and $\Delta S = 0$ if and only if $\rho = \rho_Q$ namely if $[\rho, Q_A] = 0$ so that the symmetry is unbroken in A.

The entanglement asymmetry can be obtained from Renyi entanglement asymmetries using the replica trick [57, 77]. The Renyi entanglement asymmetries are defined as

$$\Delta S_n = \frac{1}{1-n}\log\frac{\mathrm{Tr}\big(\rho_Q^n\big)}{\mathrm{Tr}(\rho^n)}\,. \tag{5.1.6}$$

The entanglement asymmetry is obtained from the limit $\Delta S = \lim_{n\to 1}\Delta S_n$. The moments $\mathrm{Tr}\big(\rho_Q^n\big)$ are easily obtained from (5.1.3). By a change of integration variables, they can be written as [3, 50]:

$$\mathrm{Tr}\big(\rho_Q^n\big) = \int_0^{2\pi}\frac{d\gamma_1\ldots d\gamma_{n-1}}{(2\pi)^{n-1}}\,X_n(A,\gamma) \tag{5.1.7}$$

where we defined the so-called charged moments

$$X_n(A,\gamma) = \mathrm{Tr}\Big[\rho\, e^{i\gamma_1 Q_A}\,\rho\, e^{i\gamma_2 Q_A}\,\cdots\,\rho\, e^{i\gamma_{n-1}Q_A}\,\rho\, e^{-i(\gamma_1+\ldots+\gamma_{n-1})Q_A}\Big]\,. \tag{5.1.8}$$

We could formally define $\gamma_n \equiv -(\gamma_1 + \ldots + \gamma_{n-1})$ so that $\sum_{j=1}^n \gamma_j = 0$. Thus, the charged moments implement all insertions of elements of $U(1)$ that multiply to the identity.

We are interested in studying entanglement asymmetry in quantum field theories, following [57]. In particular, we will use the path integral over replicas in order to define and compute traces of density matrices. It is well known that the definition of entanglement entropy we presented is plagued by UV divergences when used in quantum field theory, as opposed to quantum mechanics. The situation improves for entanglement asymmetry (as it does in general for relative entropies) because the divergences cancel among the numerator and denominator of (5.1.6), at least as long as the symmetry breaking is spontaneous, or explicit but soft.

We consider states ρ_{tot} that have a Euclidean path-integral representation. In particular, given a spatial manifold $\mathcal{M}$, the state ρ_{tot} is produced by the path integral on some Euclidean manifold, possibly with operator insertions, with a cut along a copy of $\mathcal{M}$. We call this geometry $\mathcal{G}$. Schematically, the matrix elements of such a state are

$$\langle\phi_-|\rho_{\rm tot}|\phi_+\rangle = \frac{1}{Z}\int_{\substack{\text{geometry } \mathcal{G} \\ \varphi(0^-,\mathcal{M})=\phi_- \\ \varphi(0^+,\mathcal{M})=\phi_+}} \mathcal{D}\varphi\,(\dots)\,e^{-S[\varphi]}\,. \tag{5.1.9}$$

Here $(t_{\rm E},\mathcal{M})$ are Euclidean coordinates with $t_{\rm E}$ the Euclidean time and the cut at $t_{\rm E}=0$, $\phi_\mp$ are Dirichlet boundary conditions for the fields, $(\dots)$ are possible operator insertions, while Z is the partition function on $\mathcal{G}$ with the cut closed so as to guarantee that $\operatorname{Tr}\rho_{\rm tot}=1$. The reduced density matrix ρ is obtained by partially closing the cut along B while keeping it open along $A\subset\mathcal{M}$. The moments of ρ are computed by

$$\operatorname{Tr}(\rho^n) = \frac{Z_n(A)}{Z^n}\,. \tag{5.1.10}$$

Here $Z_n(A)$ is the Euclidean path integral of the theory on a manifold $\mathcal{G}_n$ obtained by gluing together n identical copies of $\mathcal{G}$ (possibly with operator insertions) along the cut A, in such a way that the lower part of the cut on the n-th copy is glued to the upper part of the cut on the $(n+1)$-th copy. Then $Z\equiv Z_1(A)$ is the path integral on $\mathcal{G}$ (possibly with operator insertions) with the cut completely closed.

In order to compute the charged moments $X_n(A,\gamma)$ of ρ_Q we need to insert the operators $e^{i\gamma_j Q_A}$ into the trace [28]. In the path-integral description they are the topological codimension-one surfaces $U_\gamma[A]$, also called symmetry defects, that implement the $U(1)$ action on the Hilbert space [64], placed along the cut A. They are

$$U_\gamma[A] = \exp\left(i\gamma\int_A \star J\right) \qquad \text{labelled by } \gamma\in[0,2\pi)\cong U(1)\,, \tag{5.1.11}$$

where J is the conserved $U(1)$ current operator, while $\star$ is the Hodge star operation. Thus

$$X_n(A,\gamma) = \frac{Z_n(A,\gamma)}{Z^n}\,. \tag{5.1.12}$$

Here $Z_n(A,\gamma)$ is the path integral on $\mathcal{G}_n$ with the insertion of topological symmetry defects $U_{\gamma_j}[A]$ along each of the gluings from one replica to the next. In the original geometry $\mathcal{G}$ it may appear that the operator $U_\alpha[A]$ has a boundary along ∂A, and in general the boundaries of symmetry defect operators are *not* topological. However on the covering geometry $\mathcal{G}_n$ there are n symmetry defects that join along ∂A and with parameters γ_j that sum up to $0\in U(1)$, therefore in this case the junction of defects is topological as well.

Notice that $Z_1(A,\gamma)=Z$.

Eventually, the path-integral formula for the Renyi asymmetries is

$$\Delta S_n = \frac{1}{1-n}\log\frac{\frac{1}{(2\pi)^{n-1}}\int d\vec{\gamma}\;Z_n(A,\gamma)}{Z_n(A)}\,, \tag{5.1.13}$$

where $d\vec{\gamma}$ is a shorthand notation for $d\gamma_1 \dots d\gamma_{n-1}$. Similar partition functions with topological defects were recently considered in [85] to study entanglement entropy in symmetric product orbifold CFTs.

There exists an alternative computational approach in which one considers n replicas of the theory, as opposed to n replicas of the Euclidean geometry. In this approach one computes the path integral of the theory in the presence of twist fields placed along ∂A that implement the gluing of one copy of the theory to the next as one crosses A [57]. In the context of entanglement asymmetry, the twist fields are dressed by the endpoints of a suitable symmetry defect placed along A [28, 32]. We illustrate and utilize this approach in section 5.6.

Let us explain why in the general case, we use a worldsheet replica approach, and not the target space replica approach i.e. twist fields. This is because we are studying entropies of excited states; therefore in the twist field approach we would end up computing a $4-$ point function of two insertions and two twist fields. This is not universal; and can only be done in specific cases, like the fermion case which we will explore in section 5.6. In the original Cardy-Calabrese computation [57, 78] the system considered was the ground state, so only the (universal) two point function of twist fields matters.

5.2 Replicas and Renyi Asymmetry in CFT$_2$

We are interested in the computation of entanglement asymmetry in CFTs with a $U(1)$ symmetry.

Since the vacuum of a CFT does not exhibit spontaneous symmetry breaking, we should consider some excited state. Here, we study a class of "coherent states" obtained by acting on the vacuum with a local operator $\mathcal{O}(z) = e^{i\lambda V(z)}$ inserted along Euclidean time.[6] Here V is a primary operator with fixed charge under Q, that for simplicity we take to be 1, while λ is a small real parameter. The state is thus

$$|\psi\rangle = \mathcal{O}(z_-)\,|0\rangle = e^{i\lambda V(z_-)}\,|0\rangle\,, \qquad \rho_{\text{tot}} = |\psi\rangle\langle\psi| = e^{i\lambda V(z_-)}\,|0\rangle\langle 0|\,e^{-i\lambda V^\dagger(z_+)}\,. \tag{5.2.1}$$

Here z_- is the insertion point in the Euclidean past, while z_+ is its specular image

[6] More precisely, one should define $\mathcal{O}$ as a smeared operator $\mathcal{O} = e^{i\int d^dz\,\lambda(z)\,V(z)}$ obtained by integrating $V(z)$ on a region of spacetime in the Euclidean past. The resulting excited coherent state is $|\psi\rangle = e^{i\int d^dz\,\lambda(z)\,V(z)}|0\rangle$. This construction parallels the holographic setup discussed in Sec. 6.1. As the smearing function $\lambda(z)$ is concentrated on a smaller and smaller support, limiting to a Dirac delta function, the operator $\mathcal{O}$ develops divergences. There are no divergences, however, at linear order in λ and therefore, with some abuse, we will keep using the notation $\mathcal{O}(z) = e^{i\lambda V(z)}$ for $\mathcal{O}$, with the above understanding in mind.

$$\langle \phi_- |\, \rho \,| \phi_+ \rangle \quad = \quad \frac{1}{Z}$$

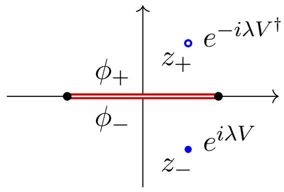

Figure 5.1: Path-integral preparation of the reduced density matrix ρ for the excited coherent states $|\psi\rangle$.

under the inversion of Euclidean time. We give a graphical representation of the path integral in Fig. 5.1. Since the operator $\mathcal{O}$ does not have definite charge, the state breaks the symmetry. This class of states is particularly natural from the point of view of holography, as we discuss in Section 6.1, and has already been studied for instance in [74–76].

Given a spatial manifold $\mathcal{M}$, the state is prepared by the Euclidean path integral on $\mathbb{R} \times \mathcal{M}$ (where the first factor is Euclidean time t_E) with a cut at $t_\mathrm{E} = 0$, the insertion of $\mathcal{O}(z_-)$ at a point z_- with $t_\mathrm{E} < 0$, and the insertion of $\mathcal{O}^\dagger(z_+)$ where z_+ is the point obtained from z_- by $t_\mathrm{E} \mapsto -t_\mathrm{E}$. We can then write the Renyi asymmetry (5.1.13) in terms of correlation functions:

$$\Delta S_n = \frac{1}{1-n} \log \frac{\frac{1}{(2\pi)^{n-1}} \int d\vec{\gamma}\, \left\langle \mathcal{O}_1 \mathcal{O}_1^\dagger \mathcal{L}_{\gamma_1} \cdots \mathcal{O}_n \mathcal{O}_n^\dagger \mathcal{L}_{\gamma_n} \right\rangle_{\mathcal{G}_n}}{\left\langle \mathcal{O}_1 \mathcal{O}_1^\dagger \cdots \mathcal{O}_n \mathcal{O}_n^\dagger \right\rangle_{\mathcal{G}_n}} \,. \tag{5.2.2}$$

Here $\mathcal{O}_j \equiv \mathcal{O}(z_{j-})$ is the operator inserted in the j-th replica, while $\mathcal{L}_{\gamma_j}$ is the topological symmetry defects placed along the gluing from the j-th to the $(j+1)$-th replica. See also [41] where some Renyi asymmetries were discussed as correlation functions.

For now, we will content ourselves with computing the entanglement asymmetry at leading order in a perturbative expansion at small λ, *i.e.*, in a limit in which the symmetry is only slightly broken. Calling Δ the dimension of the primary V, notice that λ has dimensions of length$^\Delta$ and thus we study a limit in which λ is small compared to the Euclidean distance between the insertion point z_- and the cut A. In the denominator of (5.2.2) we find

$$\left\langle \mathcal{O}_1 \mathcal{O}_1^\dagger \ldots \mathcal{O}_n \mathcal{O}_n^\dagger \right\rangle_{\mathcal{G}_n} = 1 + \lambda^2 \sum_{j,k} \left\langle V(z_{j-})\, V^\dagger(z_{k+}) \right\rangle_{\mathcal{G}_n} + O(\lambda^4) \,. \tag{5.2.3}$$

Notice that there are no terms with odd powers of λ because of charge conservation in the vacuum. Besides, at order λ^2 we never pick up the product of two V's or two $V^\dagger$'s at the same point and therefore we do not have to worry about divergences. In the numerator of (5.2.2) we have a correlator in the presence of the symmetry

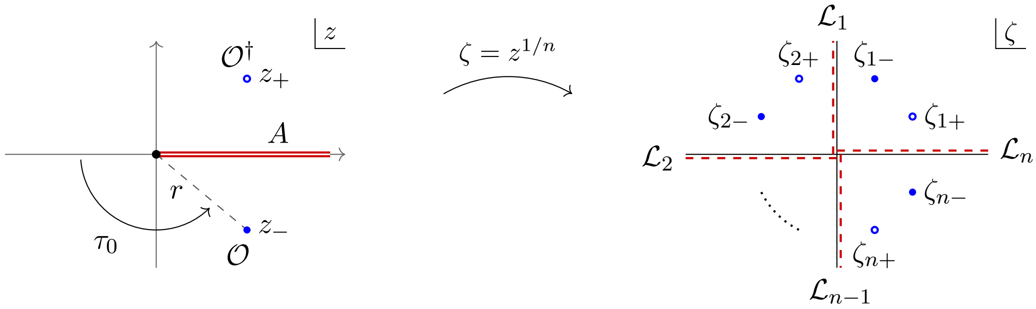

Figure 5.2: Left: physical z-plane of the Rindler geometry, with insertions of $\mathcal{O}$ at $z_- = r\, e^{-i(\pi-\tau_0)}$ and $\mathcal{O}^\dagger$ at $z_+ = z_-^*$. Right: covering ζ-plane, in the case $n = 4$. The conformal map is $\zeta = z^{1/n}$.

defects $\mathcal{L}_{\gamma_j}$. Since they are topological, we can swipe them through the replicas until they are all moved to the same sheet, and then we can collapse them on top of each other. Since the parameters sum up to zero, they disappear. However, when they cross a local operator, the correlator picks up a phase. We thus find

$$\left\langle \mathcal{O}_1 \mathcal{O}_1^\dagger \mathcal{L}_{\gamma_1} \dots \mathcal{O}_n \mathcal{O}_n^\dagger \mathcal{L}_{\gamma_n} \right\rangle_{\mathcal{G}_n} = 1 + \lambda^2 \sum_{j,k} e^{i\theta_{jk}} \left\langle V(z_{j-})\, V^\dagger(z_{k+}) \right\rangle_{\mathcal{G}_n} + O(\lambda^4)\,, \quad (5.2.4)$$

where $\theta_{jk} = \sum_{i=j}^{k-1} \gamma_i$ if $k > j$, or $\theta_{jk} = -\sum_{i=k}^{j-1} \gamma_i$ if $k < j$, or $\theta_{jk} = 0$ if $j = k$. Once we integrate in $d\vec{\gamma}$, all terms in the summation with a nontrivial phase are projected out, therefore the summation reduces to $j = k$:

$$\frac{1}{(2\pi)^{n-1}} \int d\vec{\gamma}\, \left\langle \mathcal{O}_1 \mathcal{O}_1^\dagger \mathcal{L}_{\gamma_1} \dots \mathcal{O}_n \mathcal{O}_n^\dagger \mathcal{L}_{\gamma_n} \right\rangle_{\mathcal{G}_n} = 1 + \lambda^2 \sum_j \left\langle V(z_{j-}) V^\dagger(z_{j+}) \right\rangle_{\mathcal{G}_n} + O(\lambda^4)\,. \quad (5.2.5)$$

In other words, the integral projects to covering geometries in which the total charge vanishes copy by copy, not just globally in the union of copies. From (5.2.2) we eventually obtain

$$\Delta S_n = \frac{\lambda^2}{n-1} \sum_{j \neq k}^{n} \left\langle V(z_{j-}) V^\dagger(z_{k+}) \right\rangle_{\mathcal{G}_n} + O(\lambda^4)\,. \quad (5.2.6)$$

This gives the leading perturbative contribution to the Renyi asymmetries.

Two-point functions on the replicated geometries $\mathcal{G}_n$ are non-trivial because the branching loci ∂A create curvature singularities. The two-dimensional case is special because, in certain cases, the singularities can be removed by a conformal transformation. We thus consider a 2d CFT, and the case that A is the semi-infinite line to the right of the origin. Using a complex coordinate $z = z_2 + iz_1$ (where z_1 is Euclidean time and z_2 is space) we take $A = \{z \in \mathbb{R}_+\}$. We call this case the *Rindler geometry*, as in Fig. 5.2 left (we will consider other geometries in Section 5.4).

We can then compute correlators on $\mathcal{G}_n$ by exploiting a conformal covering map $\zeta = z^{1/n}$. Two-point functions transform as

$$\Big\langle V(z_{j-})\,V^\dagger(z_{k+})\Big\rangle_{\mathcal{G}_n} = \left|\frac{d\zeta}{dz}(\zeta_{j-})\,\frac{d\zeta}{dz}(\zeta_{k+})\right|^{\Delta} \Big\langle V(\zeta_{j-})V^\dagger(\zeta_{k+})\Big\rangle_{\mathbb{C}}\,, \tag{5.2.7}$$

where Δ is the dimension of V. We parametrize the insertion points $z_\pm$ as

$$z_- = r\,e^{-i(\pi-\tau_0)}\,, \qquad z_+ = r\,e^{i(\pi-\tau_0)}\,, \qquad r>0\,, \quad 0<\tau_0<\pi\,. \tag{5.2.8}$$

On the covering ζ-plane we take

$$\zeta_{j-} = r^{1/n}e^{i\left[2\pi\left(j-\frac{1}{2}\right)+\tau_0\right]/n}\,, \qquad \zeta_{j+} = r^{1/n}e^{i\left[2\pi\left(j-\frac{1}{2}\right)-\tau_0\right]/n}\,. \tag{5.2.9}$$

The twist lines $\mathcal{L}_j$ (before being removed) run along the semi-infinite lines with $\arg(\zeta) = 2\pi j/n$, as depicted in Fig. 5.2 right. The two-point functions on the covering geometries $\mathcal{G}_n$ are

$$\Big\langle V(z_{j-})\,V^\dagger(z_{k+})\Big\rangle_{\mathcal{G}_n} = \frac{1}{n^{2\Delta}\; r^{2\Delta(n-1)/n}\left|\zeta_{j-}-\zeta_{k+}\right|^{2\Delta}}\,. \tag{5.2.10}$$

Writing the Renyi asymmetry as $\Delta S_n = \lambda^2 \Delta S_n^{(2)} + O(\lambda^4)$, the leading term from (5.2.6) is

$$\Delta S_n^{(2)} = \frac{n^{-2\Delta}}{n-1}\,\frac{1}{r^{2\Delta}}\sum_{j\neq k}^{n} \frac{1}{\left|2\sin\left(\frac{\tau_0+(j-k)\pi}{n}\right)\right|^{2\Delta}}\,. \tag{5.2.11}$$

In order to compute the leading contribution $\Delta S^{(2)}$ to the entanglement asymmetry we need to analytically continue (5.2.11) to complex values of n and then take the limit $n\to 1$. This means that we need to perform the sum explicitly. We were able to do that only for some integer values of 2Δ, using the Mellin transform

$$\frac{1}{\sin(\pi x)} = \frac{1}{\pi}\int_{\mathbb{R}} ds\,\frac{e^{sx}}{1+e^s} \qquad \text{for } 0<\mathbb{R}\mathrm{e}(x)<1\,. \tag{5.2.12}$$

In Appendix A.1 we perform the computation for $\Delta = \frac{1}{2}, 1, \frac{3}{2}, 2$. For instance, for $\Delta = 1$ the Renyi asymmetry of the Rindler geometry takes the form

$$\Delta = 1: \qquad \Delta S_n^{(2)} = \frac{1}{4r^2}\,\frac{n}{n-1}\left(\frac{1}{\sin^2(\tau_0)} - \frac{1}{n^2\sin^2\left(\frac{\tau_0}{n}\right)}\right), \tag{5.2.13}$$

therefore the entanglement asymmetry is

$$\Delta = 1: \qquad \Delta S^{(2)}_{\text{Rindler}} = \frac{1}{2r^2\sin^2(\tau_0)}\left(1 - \frac{\tau_0}{\tan(\tau_0)}\right). \tag{5.2.14}$$

In the next section we will determine $\Delta S^{(2)}_{\text{Rindler}}$ for all $\Delta \in \mathbb{R}_+$.

5.3 Asymmetry as relative entropy

We can make progress in the computation of the leading contribution to the entanglement asymmetry of coherent states in a perturbative expansion in λ — in general dimension d — by using that entanglement asymmetry is a relative entropy; in this case with respect to the vacuum state in a Rindler space.

Given two density matrices ρ_0, ρ_1, their relative entropy is defined as

$$S(\rho_1 \,\|\, \rho_0) = \text{Tr}(\rho_1 \log \rho_1) - \text{Tr}(\rho_1 \log \rho_0)\,. \tag{5.3.1}$$

Consider a continuous family $\rho(\lambda) = \rho_0 + \lambda\,\delta\rho + O(\lambda^2)$, normalized so that $\text{Tr}\,\rho(\lambda) = 1$. Then, the relative entropy $S\big(\rho(\lambda)\,\|\,\rho_0\big)$ starts at second order in λ and at that order it is given by

$$\frac{1}{2}\frac{d^2}{d\lambda^2} S\big(\rho(\lambda)\,\|\,\rho_0\big) = F\big(\delta\rho, \delta\rho\big)_{\rho_0}\,, \tag{5.3.2}$$

where the quantity $F(\delta\rho_1, \delta\rho_2)_{\rho_0}$ is symmetric in its arguments and is called the Fisher information metric around ρ_0. There exists an integral formula for it, see [7] *e.g.* Appendix B of [76]:

$$F\big(\delta\rho_1, \delta\rho_2\big)_{\rho_0} = \frac{1}{4}\int_{-\infty}^{\infty} \frac{ds}{1+\cosh(s)}\, \text{Tr}\Big[\delta\rho_1\, \rho_0^{-\frac{1}{2}-\frac{is}{2\pi}}\, \delta\rho_2\, \rho_0^{-\frac{1}{2}+\frac{is}{2\pi}}\Big]. \tag{5.3.3}$$

[7] The starting point is that, from definition, we explicitly have

$$\frac{1}{2}\frac{d^2}{d\lambda^2} S\big(\rho(\lambda)\,\|\,\rho_0\big) = \frac{1}{2}\,\text{Tr}\left[\delta^{(1)}\rho \log\Big(\rho_0 + \delta^{(1)\rho}\Big)\right]$$

The trick is to then get rid of the logarithm by using the following identities

$$\log x = -\int_{\mathbb{R}_+} \frac{ds}{s}(e^{-sx} - e^{s}), \qquad \frac{d}{d\epsilon}e^{A+\epsilon B} = \int_0^1 dx\; e^{Ax}\; B\; e^{(1-x)A}$$

The result is a double integral

$$\frac{1}{2}\frac{d^2}{d\lambda^2} S\big(\rho(\lambda)\,\|\,\rho_0\big) = \int_0^1 dx \int ds\, \text{Tr}\left(\delta\rho_1 e^{-xs\rho_0}\;\delta\rho_1\; e^{-(1-x)s\rho_0}\right)$$

Both this integral and the integral in 5.3.3 can be done by diagonalizing ρ_0, and shown to agree. Thus the formula.

This formula is valid even if $\rho(\lambda)$ is not Hermitian, as long as it is normalized.

Whether this formula is useful in a QFT is a different question. It turns out that if the state ρ_0 had a geometric, local modular flow, then the above Fisher information actually reduces to a computation of correlation functions. If we were in a CFT, then this correlation function is likely to be computable. We will see how this happens explicitly in our case.

In our setup the reduced density matrix ρ is

$$\rho = \sigma + \lambda\, \sigma\, (iV - iV^\dagger) + O(\lambda^2)\,, \tag{5.3.4}$$

where $\sigma = \mathrm{Tr}_B\, |0\rangle\langle 0|$ is the reduced density matrix of the vacuum. Since the vacuum does not break the symmetry while $\sum_q \Pi_q\, \sigma V\, \Pi_q = 0$, we obtain that the projection ρ_Q differs from the vacuum only at second order in λ: $\rho_Q = \sigma + O(\lambda^2)$. We already noticed that the entanglement asymmetry can be written as a relative entropy $\Delta S = S(\rho \,\|\, \rho_Q)$. Using again that σ commutes with Q_A, we can also write the asymmetry as $\Delta S = S(\rho \,\|\, \sigma) - S(\rho_Q \,\|\, \sigma)$. Since ρ_Q is equal to σ at first order in λ, the second term does not contribute at leading order. We thus obtain

$$\Delta S = \lambda^2\, S^{(2)}(\rho \,\|\, \sigma) + O(\lambda^4)\,. \tag{5.3.5}$$

We apply this formula to the Rindler geometry in $d \geq 2$ dimensions. The spatial slice is $\mathbb{R}^{d-1}$, the subsystem A is a half-space, and the entangling surface ∂A is a $(d-2)$-dimensional plane. We use a complex coordinate z for the spatial direction orthogonal to the entangling surface and the Euclidean time direction, and y_i for the other coordinates (if any). The state is obtained from the vacuum with the insertion of $\mathcal{O} = e^{i\lambda V}$ at z_- and $\mathcal{O}^\dagger = e^{-i\lambda V^\dagger}$ at $z_+ = z_-^*$, both on the plane $y_i = 0$. We could more generally consider insertions at two generic points, not necessarily related by complex conjugation.[8] We will be interested in the case

$$z_- = r\, e^{-i(\pi - \tau_-)} = r\, e^{i\theta_-}\,, \qquad\qquad z_+ = r\, e^{i(\pi - \tau_+)} = r\, e^{i\theta_+}\,. \tag{5.3.6}$$

The reduced density matrix σ of the vacuum in the Rindler geometry is special because its modular Hamiltonian K defined by $\sigma = e^{-K}$ is local and geometric: it generates a counterclockwise rotation of the complex coordinate z around the

[8] In this case the Euclidean path integral prepares a non-Hermitian matrix.

entangling surface. We can thus write the state ρ as

$$\begin{aligned}\rho &= e^{-\left(1-\frac{\theta_-}{2\pi}\right)K}\, e^{i\lambda V}\, e^{-\frac{\theta_--\theta_+}{2\pi}K}\, e^{-i\lambda V^\dagger}\, e^{-\frac{\theta_+}{2\pi}K} \\ &= \sigma + i\lambda\,\sigma\, e^{\frac{\theta_-}{2\pi}K}\, V\, e^{-\frac{\theta_-}{2\pi}K} - i\lambda\,\sigma\, e^{\frac{\theta_+}{2\pi}K}\, V^\dagger\, e^{-\frac{\theta_+}{2\pi}K} + O(\lambda^2) \\ &= \sigma + i\lambda\,\sigma\, V(z_-) - i\lambda\,\sigma\, V^\dagger(z_+) + O(\lambda^2)\,,\end{aligned} \tag{5.3.7}$$

as already written in (5.3.4). To this state we apply (5.3.2)–(5.3.3). Taking into account charge conservation, we obtain two terms which however are equal using the change of variable $s \to -s$ and the cyclicity of the trace:

$$\Delta S^{(2)}_{\text{Rindler}} = \frac{1}{2}\int \frac{ds}{1+\cosh(s)}\,\mathrm{Tr}\Big[\sigma\, V^\dagger(z_+)\,\sigma^{-\frac{1}{2}-\frac{is}{2\pi}}\,\sigma\, V(z_-)\,\sigma^{-\frac{1}{2}+\frac{is}{2\pi}}\Big]\,. \tag{5.3.8}$$

Shifting the integration contour as $s \to s + \pi i(1-\varepsilon)$ where ε is an infinitesimal positive quantity that specifies a contour prescription, the integral is recast as

$$\Delta S^{(2)}_{\text{Rindler}} = -\frac{1}{4}\int \frac{ds}{\sinh^2\!\left(\frac{s}{2}-i\varepsilon\right)}\,\mathrm{Tr}\Big[\sigma\,\sigma^{-\frac{is}{2\pi}}\, V(z_-)\,\sigma^{\frac{is}{2\pi}}\, V^\dagger(z_+)\Big]\,. \tag{5.3.9}$$

The trace contains operators time-ordered with respect to modular time and is thus a two-point function. With $s=0$, if we take two generic ordered points $z_j = e^{u_j + i\theta_j}$ we have

$$\begin{aligned}\mathrm{Tr}\Big[\sigma\, V(z_1)\, V^\dagger(z_2)\Big] &= \Big\langle V(z_1)\, V^\dagger(z_2)\Big\rangle = \frac{1}{|z_1-z_2|^{2\Delta}} = \\ &= \frac{1}{\Big[2\, e^{u_1+u_2}\Big(\cosh(u_1-u_2)-\cos(\theta_1-\theta_2)\Big)\Big]^\Delta} \equiv G_\Delta(u_1,\theta_1,u_2,\theta_2)\,.\end{aligned} \tag{5.3.10}$$

Since $V(z_-) = e^{\frac{\theta_-}{2\pi}K}\, V(r,0)\, e^{-\frac{\theta_-}{2\pi}K}$ we see that $\sigma^{-\frac{is}{2\pi}}\, V(z_-)\,\sigma^{\frac{is}{2\pi}}$ has the net effect of shifting $\theta_- \to \theta_- + is$. The trace in (5.3.9) is then $G_\Delta(u,\theta_-+is,u,\theta_+) = G_\Delta(u,\pi+\tau_-+is,u,\pi-\tau_+)$ in terms of our parametrization. We obtain the formula:

$$\Delta S^{(2)}_{\text{Rindler}} = -\int_{-\infty}^{+\infty} \frac{ds}{4\, r^{2\Delta}\sinh^2\!\left(\frac{s}{2}-i\varepsilon\right)\Big[-4\sinh^2\!\left(\frac{s}{2}-i\tau_0\right)\Big]^\Delta} \tag{5.3.11}$$

where $\tau_0 = \frac{1}{2}(\tau_+ + \tau_-)$.

As we describe in Appendix A.2, the integral in (5.3.11) can be analytically performed in terms of a hypergeometric function. Let us define the function:[9]

$$I_\Delta(x) = \frac{\sqrt{\pi}\,\Gamma(\Delta+1)}{4^\Delta\,\Gamma\big(\Delta+\frac{1}{2}\big)}\left(1-\big(1-x^2\big)\frac{\Delta}{\Delta+\frac{1}{2}}\,{}_2F_1\Big[1,\tfrac{1}{2}-\Delta,\tfrac{3}{2}+\Delta;-x^2\Big]\right). \quad (5.3.12)$$

Then

$$\Delta S^{(2)}_{\text{Rindler}} = \frac{1}{r^{2\Delta}}\,I_\Delta\Big(\tan\big(\tfrac{\tau_0}{2}\big)\Big). \quad (5.3.13)$$

The entanglement asymmetry of the Rindler geometry starts at a finite value for $\tau_0 = 0$ and increases monotonically with a divergence at $\tau_0 = \pi$ with the following behaviors:[10]

$$\lim_{\tau_0\to 0}\,\Delta S^{(2)}_{\text{Rindler}} = \frac{\sqrt{\pi}\,\Gamma(\Delta+1)}{2\,(2r)^{2\Delta}\,\Gamma\big(\Delta+\frac{3}{2}\big)}\,, \qquad \Delta S^{(2)}_{\text{Rindler}} \underset{\tau_0\to\pi}{\sim} \frac{2\pi\Delta}{(2r)^{2\Delta}\,\sin^{2\Delta+1}(\tau_0)}\,. \quad (5.3.14)$$

This is illustrated in Fig. 5.3 where we plot the function $I_\Delta\big(\tan(\tau_0/2)\big)$ for different values of Δ. For semi-integer values of Δ we found alternative expressions for (5.3.11) in terms of trigonometric functions. For $\Delta \in \frac{1}{2}+\mathbb{Z}_{\geq 0}$ we found the expressions:

$$\Delta S^{(2)}_{\text{Rindler}} = \frac{\pi\,\Delta}{(4r)^{2\Delta}\,\cos^{2\Delta+1}\big(\frac{\tau_0}{2}\big)}\left[1+\sum_{k=1}^{\Delta-\frac{3}{2}}\frac{\big(\Delta-\frac{1}{2}-k\big)\big(\Delta-\frac{3}{2}+k\big)!}{k!\,\big(\Delta-\frac{1}{2}\big)!}\,\cos^{2k}\Big(\frac{\tau_0}{2}\Big)\right]. \quad (5.3.15)$$

The summation is finite and contributes only for $\Delta \geq \frac{5}{2}$. For $\Delta \in \mathbb{Z}_{\geq 1}$ we found:

$$\Delta S^{(2)}_{\text{Rindler}} = \frac{2\Delta}{(2r)^{2\Delta}\,\sin^{2\Delta}(\tau_0)}\left[1-\frac{\tau_0}{\tan(\tau_0)}-\sum_{k=1}^{\Delta-1}\frac{(2k-2)!!}{(2k+1)!!}\,\sin^{2k}(\tau_0)\right]. \quad (5.3.16)$$

The summation is finite and contributes only for $\Delta \geq 2$. These expressions match with those we already found in $d = 2$ for $\Delta = \frac{1}{2}, 1, \frac{3}{2}, 2$ using the replica method (see Appendix A.1).

5.4 Other geometries

For the class of states (5.2.1) and at leading order in λ, it is clear from (5.2.6) that both Renyi and entanglement asymmetries behave as two-point functions. This means that in a CFT we can exploit conformal transformations to determine the asymmetry

[9] Recall that ${}_2F_1(a,b,c;z) = \sum_{n=0}^{\infty}\frac{(a)_n(b)_n}{(c)_n}\frac{z^n}{n!}$ and in particular ${}_2F_1(a,b,c;0) = 1$. The analytic continuation for $|z| \geq 1$ has a branch cut from 1 to ∞ along the positive real axis.

[10] They follow from $\lim_{x\to 0} I_\Delta(x) = \dfrac{\sqrt{\pi}\,\Gamma(\Delta+1)}{2^{2\Delta+1}\,\Gamma(\Delta+3/2)}$ and $I_\Delta(x) \sim \dfrac{\pi\,\Delta}{16^\Delta}\,x^{2\Delta+1}$ for $x \to +\infty$.

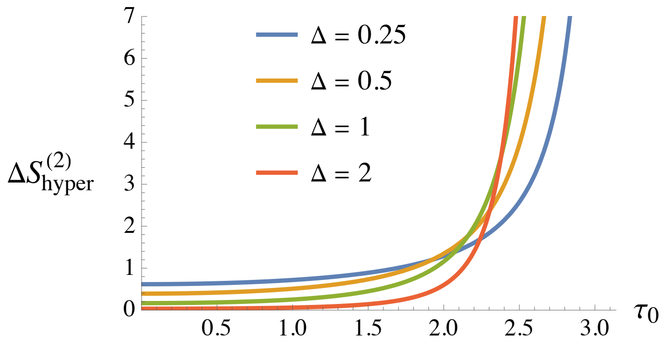

Figure 5.3: The function $I_\Delta\big(\tan\big(\frac{\tau_0}{2}\big)\big)$ that describes $\Delta S^{(2)}_{\text{Rindler}}$ and $\Delta S^{(2)}_{\text{hyper}}$, plotted for different values of Δ as a function of $\tau_0 \in [0, \pi)$.

in geometries other than the Rindler one.[11] In this section we will compute the entanglement asymmetry of finite spherical regions A in arbitrary dimensions, both in infinite volume, in a finite spherical volume, and in the hyperbolic plane at finite temperature.[12]

By analytic continuation from Euclidean to Lorentzian time, we will also be able to compute the time evolution of entanglement asymmetry in those geometries. Thus entanglement asymmetry can be used to study dynamics: starting with a state that explicitly breaks the symmetry (in our setup regarded as a local quench at $t = 0$) we can study the dynamical restoration of the symmetry as expected from thermalization. In the context of quantum spin chains, entanglement asymmetry was used in [3] and subsequent works to provide a quantitative framework to study the Mpemba effect [86–88] — the observation that states father away from equilibrium can relax faster. We observe a similar effect for the coherent states in CFTs in general dimensions.

First of all, we can use the computation of Section 5.3 of the entanglement asymmetry (5.3.13) of a CFT$_d$ in the Rindler geometry to determine the asymmetry of a thermal state in hyperbolic space. We already introduced flat coordinates $\{z_1, z_2, y_{i=1,\dots,d-2}\}$ on $\mathbb{R}^d$, where z_1 is Euclidean time, so that the subsystem A is the half-space $A = \{z_1 = 0, z_2 \geq 0\}$. We also introduced a complex coordinate

$$z = z_2 + iz_1 = r\, e^{i\tau} \tag{5.4.1}$$

so that the metric takes the form $ds^2_{\text{Rindler}} = dr^2 + r^2 d\tau^2 + dy^2_{1,\dots,d-2}$ with $\tau \cong \tau + 2\pi$. Without loss of generality, we took the insertions at $z_\pm$ with $y_i = 0$, as in (5.3.6).

[11] This is the same as what was done in [57, 78, 80] for the entanglement entropy.

[12] In $d = 2$ dimensions, the hyperbolic plane at finite temperature is identical to the standard real line at finite temperature.

We now perform a conformal (Weyl) transformation to $S^1 \times \mathbb{H}^{d-1}$:

$$ds^2_{\text{hyper}} = d\tau^2 + \frac{dr^2 + dy^2_{1,\dots,d-2}}{r^2} = \frac{1}{r^2}\, ds^2_{\text{Rindler}}\,. \tag{5.4.2}$$

This maps the subsystem A of the Rindler geometry to the whole hyperbolic space $\mathbb{H}^{d-1}$ at $\tau = 0$. Since entanglement asymmetry transforms as a two-point function, it follows that $\Delta S^{(2)}_{\text{hyper}} = r^{2\Delta} \Delta S^{(2)}_{\text{Rindler}}$ and therefore

$$\Delta S^{(2)}_{\text{hyper}} = I_\Delta\Big(\tan\Big(\tfrac{\tau_0}{2}\Big)\Big) \tag{5.4.3}$$

where $\tau_0 = \frac{1}{2}(\tau_- + \tau_+)$ and I_Δ is as in (5.3.12). This is the entanglement asymmetry of an excited thermal state (with inverse temperature $\beta = 2\pi$) on the hyperbolic plane. It only depends on τ_0 (related to the Euclidean time of the insertions with respect to the cut) and not on the location on the hyperbolic plane because of its $SO(d-1,1)$ isometry.

It is convenient to rewrite the metric on the hyperbolic geometry as

$$ds^2_{\text{hyper}} = d\tau^2 + du^2 + \sinh^2(u)\, d\Omega^2_{d-2} = \frac{dz\, d\bar{z}}{|z|^2} + \frac{1}{4}\left|z - \frac{1}{z^*}\right|^2 d\Omega^2_{d-2} \tag{5.4.4}$$

where $z = e^{u+i\tau}$ is some other complex coordinate,[13] while $d\Omega^2_{d-2}$ is the angular metric on a unit sphere S^{d-2}. Notice that in $d > 2$ we take $u \geq 0$ and so $|z| \geq 1$, while in $d = 2$ we can neglect $d\Omega^2_{d-2}$ but take $u \in \mathbb{R}$. We consider a conformal (holomorphic) transformation

$$z = f(w) \qquad \text{where} \qquad w = r + it_{\text{E}} \tag{5.4.5}$$

and t_{E} is Euclidean time. The metric takes the form

$$ds^2_{\text{hyper}} = \left|\frac{f'(w)}{f(w)}\right|^2 \left[dw\, d\bar{w} + \frac{\big(|f|^2 - 1\big)^2}{4|f'|^2}\, d\Omega^2_{d-2}\right] \equiv \Omega^2\, ds^2_{\text{geom}}\,. \tag{5.4.6}$$

This allows us to obtain the asymmetry in other geometries. We will be interested in transformations such that the coefficient of $d\Omega^2_{d-2}$ is only a function of r and not

[13] The coordinate change from (5.4.2) to (5.4.4) is $(1 + r^2 + \vec{y}^2)/2r = \cosh(u)$, $(1 - r^2 - \vec{y}^2)/2r = \sinh(u)\, \theta_{d-1}$, $y^j/r = \sinh(u)\, \theta_j$ for $j = 1, \dots, d-2$, so that $\theta_{a=1,\dots,d-1} \in S^{d-2}$ satisfy $\sum_a \theta_a^2 = 1$.

of t_{E}. In any case, the conformal factor Ω and the parameter x are given by

$$\Omega = \left|\frac{f'(w_-)}{f(w_-)}\right| , \qquad x \equiv \tan\left(\frac{\tau_0}{2}\right) = -i\,\frac{z_- + |z_-|}{z_- - |z_-|} = -i\,\frac{f(w_-) + |f(w_-)|}{f(w_-) - |f(w_-)|} \,. \tag{5.4.7}$$

We thus obtain the general formula

$$\Delta S^{(2)}_{\text{geom}} = \Omega^{2\Delta}\, I_\Delta(x)\,. \tag{5.4.8}$$

5.4.1 Asymmetry for a finite subregion

The choice

$$z = f(w) = \frac{w+\ell}{\ell - w} \tag{5.4.9}$$

in (5.4.6) gives the flat metric $ds^2_{\text{geom}} = dt_{\mathrm{E}}^2 + dr^2 + r^2 d\Omega^2_{d-2}$ on $\mathbb{R}^d$. In $d>2$ dimensions, the preimage of the hyperbolic plane is the spherical region $A = \left\{t_{\mathrm{E}} = 0,\, r^2 \leq \ell^2\right\}$ of radius ℓ that we will call a disk. In $d=2$ it is convenient to take $r \in \mathbb{R}$ and then the subsystem A is the finite interval $r \in [-\ell, \ell]$. Using (5.4.7)–(5.4.8) we can thus compute the entanglement asymmetry of a finite spherical subregion. The conformal factor and the variable x in this case read:

$$\Omega = \frac{2\ell}{\left|w_-^2 - \ell^2\right|} \,, \qquad x = \frac{2\ell\,\mathbb{I}\mathrm{m}(w_-)}{\ell^2 - |w_-|^2 - |w_-^2 - \ell^2|} \,, \tag{5.4.10}$$

in terms of the insertion point w_-, and $\Delta S^{(2)}_{\text{disk}} = \Omega^{2\Delta} I_\Delta(x)$ according to (5.4.8).

These formulas simplify if we take the insertion point w_- to lie along the imaginary axis $\mathbb{R}\mathrm{e}(w) = 0$. This is a vertical line (along Euclidean time) that goes through the center of the disk. Let us set[14]

$$w_- = -i\eta \tag{5.4.11}$$

in terms of a real parameter $\eta \in \mathbb{R}_+$. Then

$$\Omega = \frac{2\ell}{\ell^2 + \eta^2} \qquad \text{and} \qquad x = \tan\left(\frac{\tau_0}{2}\right) = \frac{\ell}{\eta}\,. \tag{5.4.12}$$

We thus obtain the following compact expression for the entanglement asymmetry of a disk in infinite volume:

$$\Delta S^{(2)}_{\text{disk}} = \left(\frac{2\ell}{\ell^2 + \eta^2}\right)^{2\Delta} I_\Delta\left(\frac{\ell}{\eta}\right). \tag{5.4.13}$$

[14] This corresponds to $e^{i\tau_0} = (i\eta - \ell)/(i\eta + \ell)$.

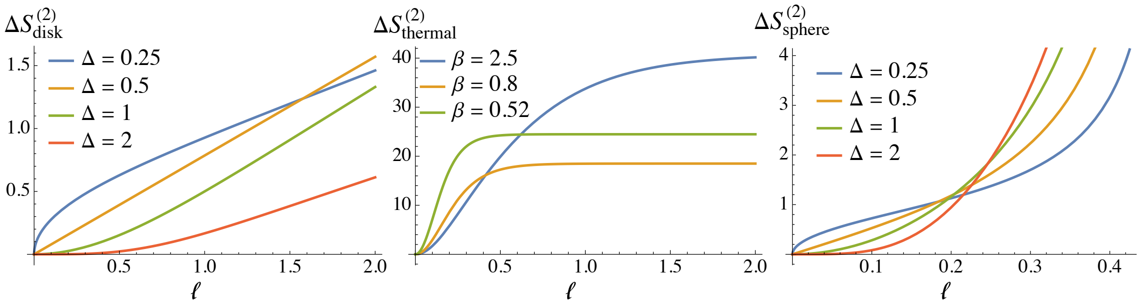

Figure 5.4: Entanglement asymmetries in various geometries for insertions along the imaginary lines. Left: asymmetry $\Delta S^{(2)}_{\text{disk}}$ of a finite subregion as function of ℓ, for $\eta = 1$. Center: asymmetry $\Delta S^{(2)}_{\text{thermal}}$ at finite temperature β^{-1} as function of ℓ, for $\Delta = 1$ and $\eta = \frac{1}{4}$. Right: asymmetry $\Delta S^{(2)}_{\text{sphere}}$ in finite volume as function of ℓ, for $L = 1$ and $\eta = \frac{1}{3}$ (central line).

In section 5.6 we perform a check of this result by computing it in 2d from a four-point function of V, $V^\dagger$ and two twist operators (as in [57]), instead of using geometric replicas. In Fig. 5.4 (left) we plot the behavior of $\Delta S^{(2)}_{\text{disk}}$ with ℓ for some values of the parameters. The expression in (5.4.13) has the following asymptotic behaviors:

$$\ell \ll \eta : \quad \Delta S^{(2)}_{\text{disk}} \simeq \frac{\sqrt{\pi}\,\Gamma(\Delta+1)}{2\,\Gamma\big(\Delta+\frac{3}{2}\big)}\,\frac{\ell^{2\Delta}}{\eta^{4\Delta}}\,, \qquad\qquad \eta \ll \ell : \quad \Delta S^{(2)}_{\text{disk}} \simeq \frac{\pi\Delta}{4^{\Delta}}\,\frac{\ell}{\eta^{2\Delta+1}}\,. \tag{5.4.14}$$

In particular $\Delta S^{(2)}$ increases and diverges as ℓ for large intervals. We believe that this behavior will be corrected asymptotically by higher-order contributions to ΔS. Notice also that $\Delta S^{(2)}$ is dimensionful, in accord with the fact that $\Delta S = \lambda^2 \Delta S^{(2)} + O(\lambda^4)$ and λ has dimensions of length$^\Delta$. A natural normalization (that we will use later on) would be to fix λ in units of η^Δ.

5.4.2 Asymmetry at finite temperature and in finite volume

The choice

$$z = f(w) = \frac{\sinh\big(\pi(w+\ell)/\beta\big)}{\sinh\big(\pi(\ell-w)/\beta\big)}\,, \tag{5.4.15}$$

which implies the identification $w \cong w + i\beta$, when plugged in (5.4.6) gives

$$ds^2_{\text{geom}} = dt_{\text{E}}^2 + dr^2 + \frac{\beta^2}{4\pi^2}\sinh^2\!\left(\frac{2\pi r}{\beta}\right) d\Omega^2_{d-2}\,. \tag{5.4.16}$$

This is the metric on $S^1_\beta \times \mathbb{H}^{d-1}$, where the Euclidean time circle has radius β. In $d > 2$ dimensions we take $r \geq 0$ and the preimage of the hyperbolic plane is the spherical region $A = \{t_{\text{E}} = 0, r^2 \leq \ell^2\}$ inside $\mathbb{H}^{d-1}$. This geometry therefore describes an excited thermal state (with temperature β^{-1}) on the hyperbolic plane $\mathbb{H}^{d-1}$ (with curvature proportional to β^{-2}), reduced to a spherical subsystem A. Since the state lives on the hyperbolic plane, it does not originate from the standard thermal vacuum. On the other hand, in $d = 2$ dimensions we take $r \in \mathbb{R}$ and the geometry is just $S^1_\beta \times \mathbb{R}$ while the subsystem A is the interval $r \in [-\ell, \ell]$: this is a finite subsystem in the standard thermal setup. The entanglement asymmetry is given by (5.4.7)–(5.4.8).

For insertions along the imaginary axis $w_- = -i\eta$ (we take $0 < \eta < \beta/2$) namely along the Euclidean circle that goes through the center of the disk A, we find

$$\Delta S^{(2)}_{\text{thermal}} = \left(\frac{2\pi\beta^{-1} \sinh(2\pi\ell/\beta)}{\cosh(2\pi\ell/\beta) - \cos(2\pi\eta/\beta)} \right)^{2\Delta} I_\Delta\left(\frac{\tanh(\pi\ell/\beta)}{\tan(\pi\eta/\beta)} \right) . \tag{5.4.17}$$

We plot it in Fig. 5.4 (center) for some values of the parameters. In the limit $\beta \gg \ell, \eta$ we recover the case (5.4.13) of a disk in infinite volume. For $\ell \gg \beta$ we have $\tau_0 \simeq \pi(1 - 2\eta/\beta)$ and therefore the asymmetry asymptotes to a constant:

$$\Delta S^{(2)}_{\text{thermal}} \simeq (2\pi/\beta)^{2\Delta} I_\Delta\big(\cot(\pi\eta/\beta)\big) \qquad\qquad \text{for } \ell \gg \beta \, . \tag{5.4.18}$$

This reproduces (5.4.3) for $\beta = 2\pi$.

The choice

$$z = f(w) = \frac{\sin\big(\pi(w+\ell)/L\big)}{\sin\big(\pi(\ell - w)/L\big)} \tag{5.4.19}$$

with $0 < \ell < L/2$ in (5.4.6) gives

$$ds^2_{\text{geom}} = dt^2_{\text{E}} + dr^2 + \frac{L^2}{4\pi^2} \sin\left(\frac{2\pi r}{L}\right)^2 d\Omega^2_{d-2} \, . \tag{5.4.20}$$

This is the metric on $\mathbb{R} \times S^{d-1}$ where the sphere has circumference L. Notice that (5.4.19) implies the identification $w \cong w + L$. In $d > 2$ dimensions we take $0 \leq r \leq \frac{L}{2}$ and the preimage of the hyperbolic plane is the spherical region $A = \{t_{\text{E}} = 0, r^2 \leq \ell^2\}$ inside the sphere S^{d-1}. In $d = 2$ we take $r \cong r + L$ and A is the interval $r \in [-\ell, \ell]$ inside this circle. This geometry allows us to evaluate the asymmetry of a spherical disk in finite volume. The general formula is (5.4.7)–(5.4.8).

We consider two interesting cases in which the expressions simplify. One is of insertions along the imaginary axis $w_- = -i\eta$ which is the Euclidean time line through the center of the disk. We call this the central line, and we find

$$\Delta S^{(2)}_{\text{sphere}} = \left(\frac{2\pi L^{-1} \sin(2\pi\ell/L)}{\cosh(2\pi\eta/L) - \cos(2\pi\ell/L)} \right)^{2\Delta} I_\Delta\left(\frac{\tan(\pi\ell/L)}{\tanh(\pi\eta/L)} \right) . \tag{5.4.21}$$

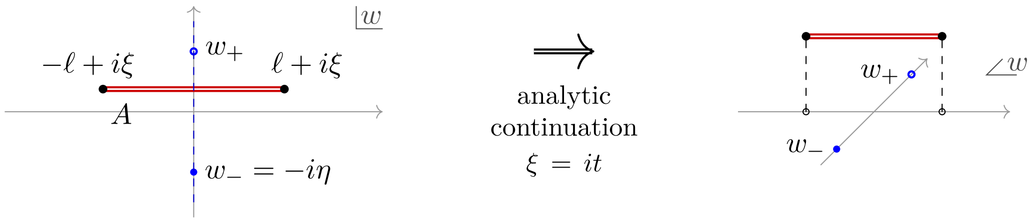

Figure 5.5: The time evolution of entanglement asymmetry can be computed by first shifting the cut A along the Euclidean time direction by ξ, and then performing analytic continuation $\xi = it$ to Lorentzian time t.

We plot it in Fig. 5.4 (right) for some values of the parameters. Notice that $2\pi\ell/L < \tau_0 < \pi$. For $L \gg \ell, \eta$ we recover the asymmetry (5.4.13) of a disk in infinite volume. For $\ell \to L/2$ (*i.e.*, if the subspace A is the whole space) the asymmetry $\Delta S^{(2)}$ diverges, however we believe that this is an artefact of the perturbative expansion. On the other hand, for $\eta \to \infty$ the asymmetry vanishes because the Euclidean time evolution projects the state to the ground state, which is symmetric.

The other case is of insertions along the axis $\mathbb{R}\text{e}(w) = \frac{L}{2}$ that we parametrize as $w_- = \frac{L}{2} - i\eta$. This is the Euclidean time line that goes through the antipodal point on the sphere with respect to the center of the disk, and we call it the antipodal line. We find

$$\Omega = \frac{2\pi L^{-1} \sin(2\pi\ell/L)}{\cosh(2\pi\eta/L) + \cos(2\pi\ell/L)}\,, \qquad x = \tan\left(\frac{\tau_0}{2}\right) = \tan(\pi\ell/L)\tanh(\pi\eta/L)\,, \tag{5.4.22}$$

and $\Delta S^{(2)}_{\text{sphere}} = \Omega^{2\Delta} I_\Delta(x)$. In this case $0 < \tau_0 < 2\pi\ell/L$.

5.5 Time dependence and relaxation

As in [80, 81] we can use conformal transformations and analytic continuation to obtain the time evolution of entanglement asymmetry, as follows. One first computes the entanglement asymmetry of a configuration in which the cut A is shifted by ξ along the Euclidean time direction, as in Fig 5.5. In our setup, this is equivalent to a geometry in which A is left untouched at $t_{\text{E}} = 0$ but the insertions are shifted as $\mathcal{O}(w_- - i\xi)$ and $\mathcal{O}^\dagger(w_-^* - i\xi)$. Since such a configuration is not specular with respect to the spatial slice of the cut at $t_{\text{E}} = 0$, the path integral prepares a "density matrix"

$$\rho_\xi = \text{Tr}_B\left(e^{-(\eta+\xi)H}\,\mathcal{O}\,|0\rangle\langle 0|\,\mathcal{O}^\dagger\,e^{-(\eta-\xi)H}\right) \tag{5.5.1}$$

(where $\eta = |\,\mathbb{I}\text{m}\,w_-|$) which, for real ξ, is not Hermitian. In order to compute the asymmetry of ρ_ξ in general one needs to extend the evaluation of the integral in

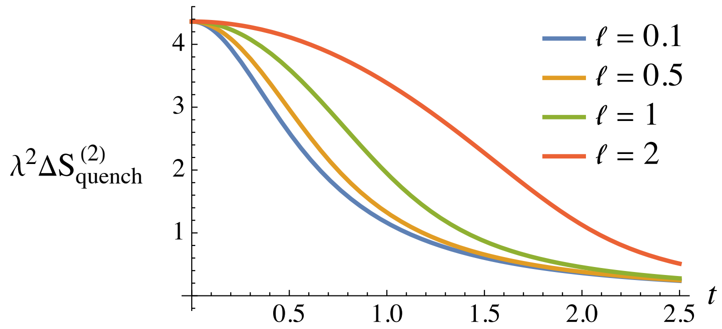

Figure 5.6: Time evolution of the entanglement asymmetry $\lambda^2 \Delta S^{(2)}_{\text{quench}}(t)$ of a disk after a local quench, for $\eta = 0.6$, $\Delta = 0.5$, and different values of the disk radius ℓ. We normalized $\lambda^2 \propto \ell^{-1}$ in order to have the same initial value. Notice that larger subsystems thermalize more slowly.

(5.3.9) (that computes the asymmetry in the Rindler geometry) to the case that $z_\pm$ have different absolute values. In the thermal hyperbolic geometry, this corresponds to having $\mathcal{O}, \mathcal{O}^\dagger$ inserted at different points on the hyperbolic plane. Then one takes the analytic continuation $\xi = it$. Now the configuration is specular with respect to the spatial slice, the cut is shifted in the Lorentzian time direction, and the path integral is performed along a Schwinger-Keldysh contour. This setup can be regarded as a local quench:[15] at $t = 0$ the system is in an excited state prepared by the Euclidean path integral, and for $t > 0$ is relaxes towards the vacuum.

In the special cases that the orbits of $w_- - i\xi$ and $w_+ - i\xi$ (as we vary ξ) have $|z_-| = |z_+|$ in the Rindler geometry (or equivalently $u_- = u_+$ in the thermal hyperbolic geometry), we can use (5.3.11). These special cases are precisely the “imaginary lines” we already discussed in the previous sections. Let us discuss the various cases separately.

Finite spherical subregion. We consider the geometry of Section 5.4.1 with a spherical subsystem $A = \{t_{\text{E}} = 0, r^2 \leq \ell^2\}$ in $\mathbb{R}^d$ and insertions along the imaginary axis $\mathbb{R}\text{e}(w) = 0$. With insertions at $w_- = -i(\eta + \xi)$ and $w_+ = i(\eta - \xi)$ we find

$$\tan\left(\frac{\tau_-}{2}\right) = \frac{\ell}{\eta + \xi}\,, \qquad \tan\left(\frac{\tau_+}{2}\right) = \frac{\ell}{\eta - \xi}\,. \tag{5.5.2}$$

Including the conformal factors, the entanglement asymmetry takes the form:

$$\Delta S^{(2)} = \left[\frac{4\ell^2}{\left(\ell^2 + (\eta+\tau)^2\right)\left(\ell^2 + (\eta-\tau)^2\right)}\right]^{\Delta} I_\Delta\left(\tan^2\left(\tfrac{\tau_0}{2}\right)\right) \tag{5.5.3}$$

[15]We call the quench “local” (as opposed to “global”) because it is localized in space and it produces an inhomogeneous state.

where $\tau_0 = \frac{1}{2}(\tau_- + \tau_+)$. We then perform the analytic continuation $\xi = it$ and obtain

$$\Delta S^{(2)}_{\text{quench}} = \left| \frac{2\ell}{\ell^2 + (\eta + it)^2} \right|^{2\Delta} I_\Delta(x) \tag{5.5.4}$$

where

$$x = \tan\left[\mathbb{R}\mathrm{e}\arctan\left(\frac{\ell}{\eta + it}\right)\right] = \frac{\ell^2 - \eta^2 - t^2 + \sqrt{\left(\ell^2 - \eta^2 - t^2\right)^2 + 4\ell^2\eta^2}}{2\ell\eta}\,. \tag{5.5.5}$$

Both the conformal factor Ω and x are as in (5.4.10) but evaluated at $w_- = t - i\eta$. This describes the time evolution of entanglement asymmetry after a local quench. We plot $\lambda^2 \Delta S^{(2)}_{\text{quench}}(t)$ for a choice of Δ, η and different values of ℓ in Fig. 5.6. Using a normalization of λ^2 so as to have the same initial value for the asymmetry, we see that larger subsystems thermalize more slowly. We will explore other physical consequences of (5.5.4) in Section 5.5.1.

Finite temperature. For the finite-temperature geometry $S^1_\beta \times \mathbb{H}^{d-1}$ of Section 5.4.2 and insertions along the imaginary axis, proceeding as before we find

$$\Delta S^{(2)}_{\text{T quench}} = \left| \frac{2\pi\beta^{-1}\sinh(2\pi\ell/\beta)}{\cosh(2\pi\ell/\beta) - \cos\big(2\pi(\eta + it)/\beta\big)} \right|^{2\Delta} I_\Delta(x) \tag{5.5.6}$$

with

$$x = \tan\left[\mathbb{R}\mathrm{e}\arctan\left(\frac{\tanh(\pi\ell/\beta)}{\tan\big(\pi(\eta + it)/\beta\big)}\right)\right]. \tag{5.5.7}$$

The parameter x can also be expressed as in (5.4.7) with $w_- = t - i\eta$.

Finite volume. For the geometry $\mathbb{R} \times S^{d-1}$ of Section 5.4.2 and insertions along the imaginary axis (that we called the central line), we find

$$\Delta S^{(2)}_{\text{L quench}} = \left| \frac{2\pi L^{-1}\sin(2\pi\ell/L)}{\cosh\big(2\pi(\eta + it)/L\big) - \cos(2\pi\ell/L)} \right|^{2\Delta} I_\Delta(x) \tag{5.5.8}$$

with

$$x = \tan\left[\mathbb{R}\mathrm{e}\arctan\left(\frac{\tan(\pi\ell/L)}{\tanh\big(\pi(\eta + it)/L\big)}\right)\right]. \tag{5.5.9}$$

One can obtain a similar expression for insertions along the antipodal line. In both cases the parameter x can also be expressed as in (5.4.7) with $w_- = t - i\eta$.

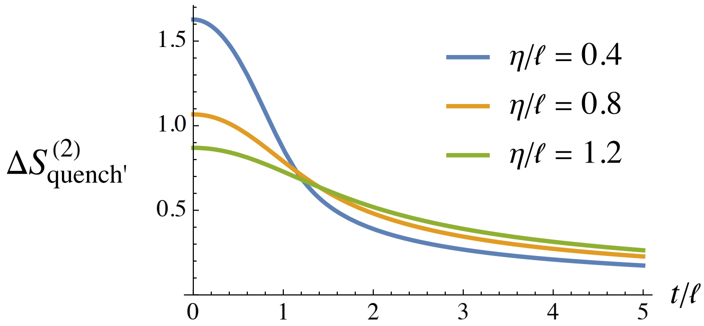

Figure 5.7: Thermalization curves $\Delta S^{(2)}_{\text{quench}'}(t) \equiv \eta^{2\Delta}\Delta S^{(2)}_{\text{quench}}(t)$ for states created with different values of η at fixed $\Delta = 0.2$. We observe the Mbempa effect between any two such curves.

5.5.1 Mpemba effect

Excited states (that are not eigenstates of the hamiltonian) are interesting because time evolution relaxes them: this is an expected thermalization; so they can be considered a toy model for out of equilibrium states. A curious feature that was observed in [3] was that sometimes, this rate of relaxation is more the further away from equilibrium you are; and this is probed by the asymmetry of such states. They dubbed this the 'quantum Mpemba effect'. In this section we analyze some physical consequences of the time evolution of entanglement asymmetry. Before doing that, notice that the primary operator V has dimensions of mass$^{\Delta}$ while λ has dimensions of length$^{\Delta}$. It is then more natural to parametrize

$$\lambda = \epsilon\, \eta^{\Delta} \tag{5.5.10}$$

in terms of a (small) dimensionless parameter ϵ. This is the normalization we will use in the rest of this section, hence the entanglement asymmetry takes the form

$$\Delta S = \epsilon^2\, \eta^{2\Delta}\, \Omega^{2\Delta}\, I_{\Delta}(x) + O(\epsilon^4) \tag{5.5.11}$$

at leading order in ϵ.

Let us first study the case of a finite subsystem in infinite volume given by (5.5.4). Since the conformal factor and the parameter x behave as $\Omega \sim 2\ell/t^2$ and $x \sim \eta\ell/t^2$ for large t, at late times the asymmetry is controlled by the constant $I_{\Delta}(0)$ and more precisely

$$\Delta S \;\sim\; \epsilon^2\, \frac{\sqrt{\pi}\,\Gamma(\Delta+1)}{2\,\Gamma(\Delta+3/2)} \left(\frac{\eta\ell}{t^2}\right)^{2\Delta} \qquad \text{for } t \to \infty\,. \tag{5.5.12}$$

Defining a thermalization timescale t_* as the time at which ΔS gets reduced by a factor of e, we obtain

$$t_* = \sqrt{\eta\ell}\; e^{1/4\Delta}\,. \tag{5.5.13}$$

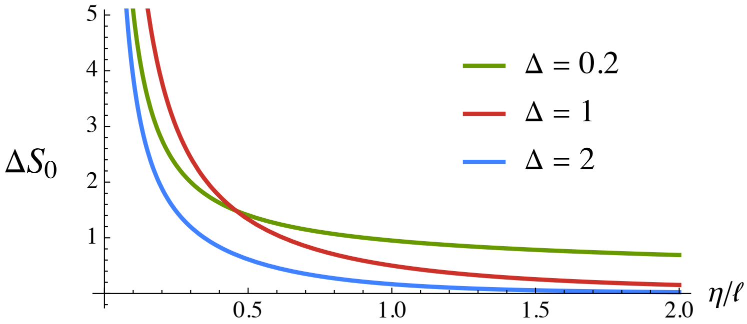

Figure 5.8: The initial value $\Delta S_0(\eta) = \eta^{2\Delta} \Delta S^{(2)}_{\text{disk}}$ is a decreasing function of η for any fixed Δ. Since the thermalization timescale t_* is an increasing function of η, we always observe the Mpemba effect among states of different η and same Δ, as illustrated in Fig. 5.7.

We see that thermalization is slower if we increase η while it is faster if we increase the conformal dimension Δ. The two parameters η, Δ label the class of states we consider, and it is interesting to compare the thermalization of different states.

Consider two symmetry-breaking states ρ, ρ' and compare how fast they thermalize. How much these states break the symmetry is quantified by the initial value ΔS_0 of the asymmetry at $t = 0$. The speed at which they thermalize is quantified by the corresponding thermalization timescales t_* and t'_*. The Mpemba effect [86–88] occurs when, despite the symmetry being more broken, the thermalization timescale is shorter. This can be expressed using a quantity

$$m = \frac{\Delta S'_0 - \Delta S_0}{t'_* - t_*} \,. \tag{5.5.14}$$

If $m \geq 0$ the state starting at a higher ΔS_0 takes more time to equilibrate and there is no Mpemba effect. If $m < 0$, instead, that state relaxes faster, the curves cross, and the Mpemba effect takes place.

If we consider a one-parameter family of states, m evaluated for infinitesimally closed states is related to the derivative of ΔS_0 with respect to the parameter. The sign of the derivative governs whether the Mpemba effect occurs locally around a given state. The result is that the Mpemba effect occurs only in some regions of parameter space. To illustrate this point we analyze two cases: varying η at fixed Δ, and varying Δ at fixed η. In the first case we always observe the Mpemba effect, while in the second case we only observe it using subsystems with $\ell > \eta$ and for sufficiently small conformal dimensions.

Varying η at fixed Δ. This is illustrated in Fig. 5.7. We always observe the Mpemba effect because any two curves cross. This can be understood from the fact that the initial value $\Delta S_0(\eta)$ is a decreasing function of η (see Fig. 5.8) and that the

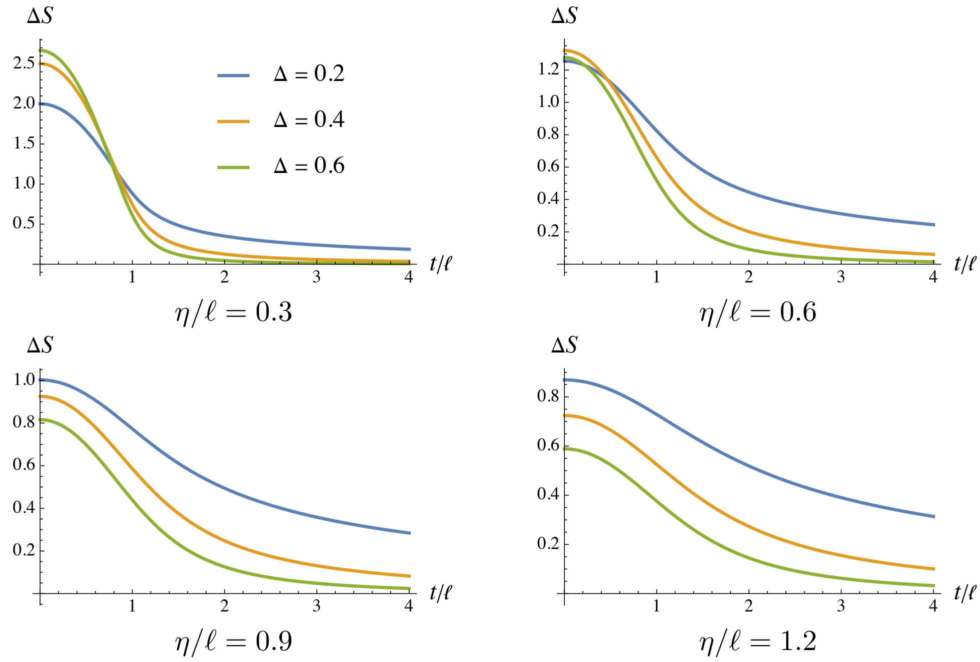

Figure 5.9: Thermalization for different values of Δ and η. We observe different behaviors in different regions of parameter space. The Mpemba effect is only visible in the two upper plots.

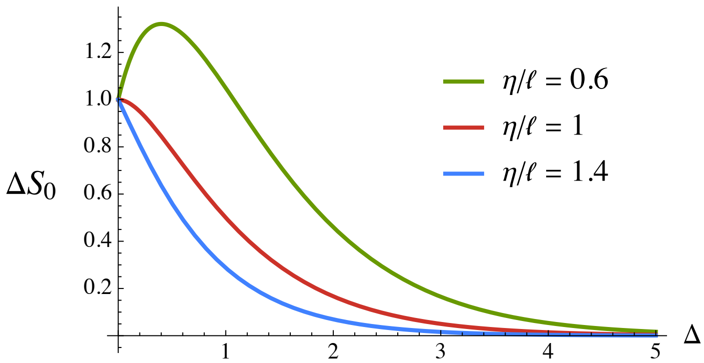

Figure 5.10: The curve $\Delta S_0(\Delta) = \eta^{2\Delta} \Delta S^{(2)}_{\text{disk}}$ has two different shapes depending on the value of the parameter η. For $\eta \geq \ell$ it is decreasing, while for $\eta < \ell$ it first increases and then decreases.

thermalization timescale t_* is an increasing function of η.

Varying $\boldsymbol{\Delta}$ at fixed $\boldsymbol{\eta}$. As illustrated in Fig. 5.9, we observe two different behaviors depending on the values of the parameters. The two regimes originate from two different profiles of the initial-value curve $\Delta S_0(\Delta)$ plotted in Fig. 5.10. If the dimension Δ is above a critical value Δ_*, then the Mpemba effect does not take place. If $\Delta < \Delta_*$ then there is Mpemba effect, but this is only visible in subsystems A with $\ell > \eta$. This is because at least one of the two conformal dimensions must be below the value Δ_* at which ΔS_0 has a maximum: The condition to observe the Mpemba effect is that $\Delta < \Delta'$ with $\Delta S_0(\Delta) < \Delta S_0(\Delta')$ which is possible only if $\Delta < \Delta_*$ and only in the region $\ell > \eta$.

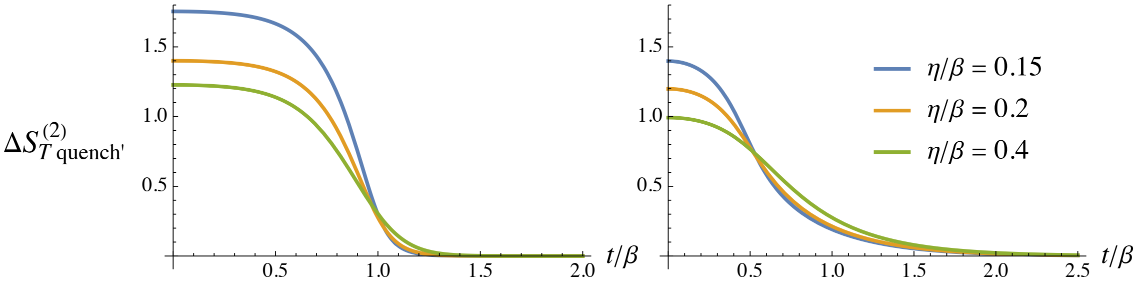

Figure 5.11: Relaxation of entanglement asymmetry $\Delta S^{(2)}_{\mathrm{T\,quench}'}(t) = \eta^{2\Delta}\Delta S^{(2)}_{\mathrm{T\,quench}}(t)$ at finite temperature β^{-1}, for different values of the parameters. Left plot: $\Delta = 1$ and $\ell/\beta = 1$. Right plot: $\Delta = 0.2$ and $\ell/\beta = \frac{1}{2}$.

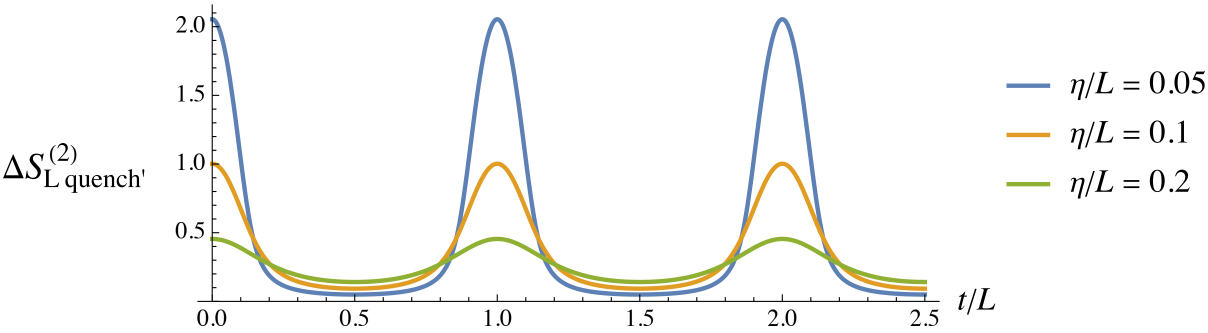

Figure 5.12: Thermalization in finite volume described by $\Delta S^{(2)}_{\mathrm{L\,quench}'}(t) = \eta^{2\Delta}\Delta S^{(2)}_{\mathrm{L\,quench}}(t)$ for different values of η. We chose $\Delta = 1$ and subsystem size $\ell = L/8$. We observe a periodic behavior with period L.

Finite temperature or volume

Next, we can study the finite-temperature case given by $\Delta S^{(2)}_{\mathrm{T\,quench}}(t)$ in (5.5.6). At late times the conformal factor behaves as $\Omega \sim 4\pi T \sinh(2\pi T\ell)\, e^{-2\pi T t}$ where $T = \beta^{-1}$ is the temperature, while $x \to 0$. This means that at non-vanishing temperature the late-time asymmetry decays exponentially:

$$\Delta S \;\sim\; \epsilon^2 \frac{\sqrt{\pi}\,\Gamma(\Delta+1)}{2\,\Gamma(\Delta+3/2)} \Big(2\pi T\eta \sinh(2\pi T\ell)\Big)^{2\Delta} e^{-4\pi\Delta T t} \qquad \text{for } t\to\infty\,. \tag{5.5.15}$$

The natural thermalization timescale is

$$t_* = \frac{1}{\Delta T}\,. \tag{5.5.16}$$

The entanglement asymmetry is approximately constant for small times, and then it decays exponentially as illustrated in Fig. 5.11. For what regards the Mpemba effect, there are four possible regimes depending on the shape of the curve $\Delta S_0(\Delta)$, distinguished by whether $\lim_{\Delta\to\infty}\Delta S_0$ vanishes or diverges, and by the sign of $\partial_\Delta \Delta S_0|_{\Delta=0}$. The four phases are:

- ΔS_0 is a monotonously decreasing function of Δ: we never see the Mpemba effect.
- ΔS_0 first increases and then it decays with Δ: we observe the Mpemba effect for sufficiently small conformal dimensions.
- ΔS_0 is monotonously increasing with Δ: we always observe the Mpemba effect.
- ΔS_0 is first decreasing and then diverging with Δ: we see the Mpemba effect for sufficiently large conformal dimensions.

Finally, let us briefly study the time evolution of entanglement asymmetry in finite volume. In Fig. 5.12 we plot the time dependence of $\Delta S^{(2)}_{\mathrm{L\ quench}}(t)$ in (5.5.8) for different values of the parameter η (that controls insertions along the central line) and a choice of Δ. We observe that the asymmetry is periodic with period L (the circumference of the sphere) and thus it never thermalizes. Although oscillations and partial revivals are expected in systems in finite volume (see for instance [89] for a discussion in two-dimensional rational CFTs), we do not expect exact periodicity in a generic CFT. We believe that this is an artefact of the perturbative expansion, that will be corrected by higher-order terms.

5.6 Twist operator approach

As in [57], the Renyi asymmetries can be computed by making use of replicated theories, as opposed to replicated geometries. Given a theory $\mathcal{S}$, we consider a theory $\mathcal{S}^{(n)}$ made of n decoupled copies of $\mathcal{S}$. Since $\mathcal{S}^{(n)}$ has a permutation symmetry that exchanges the copies, it also has a codimension-two twist operator $\mathcal{T}_n$ such that when we circle around it we go from one copy to the next, cyclicly. More precisely, $\mathcal{T}_n$ is the (non-topological) boundary of a codimension-one topological symmetry defect such that the fields on the two sides are glued with a cyclic permutation. If theory $\mathcal{S}$ has a $U(1)$ symmetry, the previous symmetry defect can be combined with other symmetry defects that implement independent $U(1)$ actions on each copy of $\mathcal{S}$ in $\mathcal{S}^{(n)}$. This generates a dressed twist operator $\mathcal{T}_{n,\gamma}$ that permutes the copies and besides acts with $e^{i\gamma_j Q_A}$ on the j-th copy. The twist operators relevant for the computation of Renyi asymmetries have $\sum_j \gamma_j = 0 \bmod 2\pi$. Similarly to (5.1.13), the Renyi asymmetry is then given by a ratio of correlation functions, one with the insertion of the dressed twist fields, and one with the standard twist fields:

$$\Delta S_n = \frac{1}{1-n} \log \frac{\frac{1}{(2\pi)^{n-1}} \int d\vec{\gamma} \left\langle \mathcal{T}_{n,\gamma}[\partial A] \, \dots \right\rangle}{\left\langle \mathcal{T}_n[\partial A] \, \dots \right\rangle} \,. \tag{5.6.1}$$

The twist fields are placed along the boundaries of the cut A. The dots stand for possible operator insertions used to construct the state.

In two dimensions the symmetry defects are lines and the twist operators are pointlike, therefore (5.6.1) boils down to the computation of certain correlation functions. In this section we use (5.6.1) to compute the Renyi asymmetry of a 2d free Dirac fermion Ψ with respect to its vector-like $U(1)$ symmetry, in coherent states generated by the primary[16] $V = \psi_L \psi_R$ with $\Delta = 1$, for an interval $A = [-\ell, \ell]$. This computation will reproduce (5.4.13) for $\Delta = 1$, as well as a conformal transformation of (5.2.13).

The theory $\mathcal{S}^{(n)}$ is given by n copies Ψ_k ($k = 1, \ldots, n$) of the 2d free Dirac fermion. The twist operator $\mathcal{T}_{n,\gamma}(u)$ implements the boundary condition[17]

$$\begin{aligned} \Psi_k\Big(u + e^{2\pi i} w\Big) &= e^{i\gamma_k}\, \Psi_{k+1}(u + w) \qquad\qquad \text{for } k = 1, \ldots, n-1 \\ \Psi_n\Big(u + e^{2\pi i} w\Big) &= (-1)^{n+1} e^{-i(\gamma_1 + \ldots + \gamma_{n-1})} \Psi_1(u + w) \end{aligned} \tag{5.6.2}$$

around u. The twist operator $\mathcal{T}^\dagger_{n,\gamma}$ implements the opposite boundary condition. Writing $\gamma_k = \alpha_{k+1} - \alpha_k$, the boundary conditions are diagonalized by the fields

$$\tilde{\Psi}_l = \frac{1}{\sqrt{n}} \sum_{k=1}^{n} \exp\left(-2\pi i\, \frac{2l - n - 1}{2n}\, k + i\, \alpha_k \right) \Psi_k \tag{5.6.3}$$

in the sense that

$$\tilde{\Psi}_l\Big(u + e^{2\pi i} w\Big) = e^{2\pi i m_l}\, \tilde{\Psi}_l(u + w) \qquad \text{with} \qquad m_l = \frac{2l - n - 1}{2n} \,. \tag{5.6.4}$$

Notice that in the diagonalizing basis the twists do not depend on the γ_k's. We decompose the Dirac fermion $\Psi = \binom{\psi_L}{\psi_R}$ into left- and right-moving parts, and the two fields ψ_L and ψ_R have the same charge under $U(1)$. Then the scalar primary we use to construct the excited coherent states is $V = \psi_L \psi_R$.

In order to construct the twist operators we use bosonization. For each copy $\tilde{\Psi}_l$ we introduce a compact scalar[18] $\varphi \cong \varphi + 2\pi$ and decompose it into left- and

[16] It can be written as $V = \Psi^\mathsf{T} C \Psi$ where C is the charge conjugation matrix.

[17] This computation is adapted from Section 2.4 of [90]. The minus signs in the second line are due to the fact that we are dealing with fermions, as in thermal partition functions, as explained in Section 2 of [91].

[18] Take $S = \frac{1}{8\pi} \int d^2\sigma\, \partial_\mu \varphi \partial^\mu \varphi$ with $\varphi \cong \varphi + 2\pi R$. The operators $\mathcal{O}_{n,w} = e^{in\varphi/R} e^{iwR\tilde{\varphi}/2}$ (where the dual scalar $\tilde{\varphi}$ is defined by $\partial_\mu \tilde{\varphi} = \epsilon_{\mu\nu} \partial^\nu \varphi$) have conformal dimensions and spin

$$h_{n,w} = \frac{1}{2}\left(\frac{n}{R} + \frac{wR}{2} \right)^2 , \qquad \bar{h}_{n,w} = \frac{1}{2}\left(\frac{n}{R} - \frac{wR}{2} \right)^2 \qquad \Delta_{n,w} = \frac{n^2}{R^2} + \frac{w^2 R^2}{4} \,, \qquad s_{n,w} = nw \,. \tag{5.6.5}$$

T-duality maps $R \leftrightarrow 2/R$. The case $R = 1$ gives the bosonization of the Dirac fermion. Indeed $\mathcal{O}_{\frac{1}{2},1} = \tilde{\psi}_L$ and $\mathcal{O}_{-\frac{1}{2},-1} = \tilde{\psi}^\dagger_L$ are the left-moving fermion while $\mathcal{O}_{\frac{1}{2},-1} = \tilde{\psi}_R$ and $\mathcal{O}_{-\frac{1}{2},1} = \tilde{\psi}^\dagger_R$ are the right-moving fermion.

right-moving parts: $\varphi = \varphi_L + \varphi_R$ and $\tilde{\varphi} = \varphi_L - \varphi_R$. An operator $\mathcal{O} = e^{i\epsilon_L \varphi_L} e^{i\epsilon_R \varphi_R}$ has dimensions $(h, \bar{h}) = \left(\epsilon_L^2/2, \epsilon_R^2/2\right)$. It follows that the fermions are

$$\tilde{\psi}_L = e^{i\varphi_L} \ , \qquad \tilde{\psi}_L^\dagger = e^{-i\varphi_L} \ , \qquad \tilde{\psi}_R = e^{i\varphi_R} \ , \qquad \tilde{\psi}_R^\dagger = e^{-i\varphi_R} \ . \tag{5.6.6}$$

The current that implements the shift symmetry $\varphi \to \varphi + \text{const}$ is $J_\mu = \frac{1}{2\pi}\partial_\mu \varphi$ and the charge operator is $Q = \int \star J = \frac{1}{2\pi}\int d\tilde{\varphi}$. The twist operator lives at the end of a symmetry defect. Thus the operator that implements a twist by $e^{2\pi i\epsilon}$ along the positive real axis, which lives at the left end of the line $e^{2\pi i \epsilon Q}$, is $e^{i\epsilon\tilde{\varphi}} = e^{i\epsilon\varphi_L} e^{-i\epsilon\varphi_R}$ with dimensions $(h, \bar{h}) = \left(\frac{\epsilon^2}{2}, \frac{\epsilon^2}{2}\right)$ and $\Delta = \epsilon^2$. To resolve possible ambiguities, we insist that the twist operator is the ground state of the twisted sector. This means that we take $\epsilon \in \left[-\frac{1}{2}, \frac{1}{2}\right]$. Let us call σ_l the twist operator in the l-th copy that implements a twist by $e^{2\pi i m_l}$. The full twist operator is

$$\mathcal{T}_{n,\gamma} = \prod_{l=1}^n \sigma_l = \prod_{l=1}^n e^{i m_l \tilde{\varphi}_l} \tag{5.6.7}$$

and its conformal dimension is

$$\Delta\Big[\mathcal{T}_{n,\gamma}\Big] = \sum_{l=1}^n m_l^2 = \frac{n^2-1}{12n} \,. \tag{5.6.8}$$

This reproduces the dimension of the twist fields in the case of central charge $c = 1$ [57] and shows that such a dimension does not depend on the parameters γ_k [32].

Let us now compute the Renyi asymmetries of the coherent states created by V, for a finite subset $A = [-\ell, \ell]$ as in Section 5.4.1. For simplicity we take the insertions along the imaginary axis: $w_- = -i\eta$ and $w_+ = i\eta$. The correlator we need to compute is thus

$$\mathcal{A} = \left\langle \mathcal{T}_{n,\gamma}(-\ell)\ \mathcal{T}_{n,\gamma}^\dagger(\ell) \left(\prod_{j=1}^n e^{i\lambda V_j(-i\eta)}\right) \left(\prod_{j=1}^n e^{-i\lambda V_j^\dagger(i\eta)}\right) \right\rangle_{\mathcal{S}^{(n)},\mathbb{C}} . \tag{5.6.9}$$

Here V_j is the primary in the j-th copy, and we put identical insertions in each copy. In (5.6.1) there is one such correlator in the numerator integrated over $\vec{\gamma}$, and one such correlator in the denominator with $\vec{\gamma} = 0$. We expand the correlator in λ. At zero-th order we have

$$\mathcal{A}^{(0)} = \left\langle \mathcal{T}_{n,\gamma}(-\ell)\ \mathcal{T}_{n,\gamma}^\dagger(\ell) \right\rangle = \frac{1}{(2\ell)^{2\Delta_\mathcal{T}}} \tag{5.6.10}$$

where $\Delta_{\mathcal{T}} = (n^2-1)/12n$. At second order we have

$$\mathcal{A}^{(2)} = \Big\langle \mathcal{T}_{n,\gamma}\, \mathcal{T}^{\dagger}_{n,\gamma} \sum\nolimits_{k_1,k_2} \Big(V_{k_1}\, V^{\dagger}_{k_2} \Big) \Big\rangle\,, \tag{5.6.11}$$

where we left the dependence on positions implicit in order not to clutter. We expand each of the fields in the diagonalizing basis:[19] the twist operators are as in (5.6.7) while

$$\begin{aligned} V_{k_1} &= \frac{1}{n}\sum_{j_1,j_2} \exp\Big(\quad \frac{2\pi i}{n}\Big(j_1+j_2-n-1\Big)k_1 - 2i\alpha_{k_1}\Big)\, \tilde{\psi}_{Lj_1}\tilde{\psi}_{Rj_2} \\ V^{\dagger}_{k_2} &= \frac{1}{n}\sum_{j_3,j_4} \exp\Big(-\frac{2\pi i}{n}\Big(j_3+j_4-n-1\Big)k_2 + 2i\alpha_{k_2}\Big)\, \tilde{\psi}^{\dagger}_{Lj_3}\tilde{\psi}^{\dagger}_{Rj_4}\,. \end{aligned} \tag{5.6.12}$$

When we substitute in the correlator (5.6.11) we obtain six sums. However if we insert $\tilde{\psi}_{Lj_1}$ then there must also be $\tilde{\psi}^{\dagger}_{Lj_1}$ or else the correlator vanishes, which means that we restrict to $j_3 = j_1$. Similarly we restrict to $j_4 = j_2$. We thus find

$$\begin{aligned} \mathcal{A}^{(2)} = \frac{1}{n^2}\sum_{k_1,k_2,j_1,j_2} &\exp\Big[\frac{2\pi i}{n}\Big(j_1+j_2-n-1\Big)(k_1-k_2) - 2i\Big(\alpha_{k_1}-\alpha_{k_2}\Big)\Big] \times \\ &\times \Big\langle \Big(\prod\nolimits_l e^{im_l\tilde{\varphi}_l}\, e^{-im_l\tilde{\varphi}_l}\Big)\, \tilde{\psi}_{Lj_1}\tilde{\psi}_{Rj_2}\tilde{\psi}^{\dagger}_{Lj_1}\tilde{\psi}^{\dagger}_{Rj_2} \Big\rangle\,. \end{aligned} \tag{5.6.13}$$

In the numerator the integrals over $\vec{\gamma}$, equivalent to integrals over $\vec{\alpha}$, impose $k_1 = k_2$. In the denominator there are no such integrals. So at order λ^2 we are left with a sum over $k_1 \neq k_2$ (and no α's). We need to compute each term of this sum.

To compute the correlators we use the Coulomb gas formalism, *i.e.*, we separately compute the left- and right-moving contributions. The holomorphic part of a correlator is

$$\Big\langle e^{i\epsilon_1\varphi_L}(z_1)\ldots e^{i\epsilon_n\varphi_L}(z_n) \Big\rangle = \prod\nolimits_{i<j}^{n} (z_i - z_j)^{\epsilon_i\epsilon_j}\,. \tag{5.6.14}$$

---

[19] The inverse to (5.6.3) is $\Psi_k = \dfrac{1}{\sqrt{n}}\displaystyle\sum_{l=1}^{n} \exp\Big(2\pi i\, \frac{2l-n-1}{2n}\, k - i\,\alpha_k\Big)\, \tilde{\Psi}_l$.

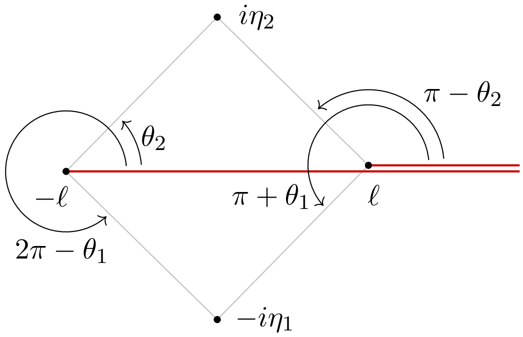

Figure 5.13: Phases involved in the 4-point function $\big\langle e^{i\epsilon\varphi_L}(-\ell)\, e^{-i\epsilon\varphi_L}(\ell)\, e^{i\varphi_L}(-i\eta_1)\, e^{-i\varphi_L}(i\eta_2)\big\rangle$.

The left-moving part of the correlator is given by

$$\begin{aligned}
\mathcal{A}^{(2)}_{L,k_1k_2} &= \frac{1}{n}\sum_{j_1=1}^{n}\Big\langle\Big(\prod\nolimits_l e^{im_l\varphi_{Ll}}(-\ell)\, e^{-im_l\varphi_{Ll}}(\ell)\Big)\, e^{i\varphi_{Lj_1}}(-i\eta)\, e^{-i\varphi_{Lj_1}}(i\eta)\Big\rangle\, e^{2\pi i\,\frac{2j_1-n-1}{2n}(k_1-k_2)} \\
&= \Big(\prod_{l\neq j_1}(2\ell)^{-m_l^2}\Big)\frac{1}{n}\sum_{j_1=1}^{n}\frac{(2\ell)^{-m_{j_1}^2}}{2i\eta}\left[\frac{(i\eta-\ell)(-i\eta+\ell)}{(i\eta+\ell)(-i\eta-\ell)}\right]^{m_{j_1}} e^{2\pi i\,\frac{2j_1-n-1}{2n}(k_1-k_2)} \qquad (5.6.15)\\
&= \frac{n^{-1}}{(2\ell)^{\Delta_\mathcal{T}}\,(2i\eta)}\sum_{j_1=1}^{n} e^{2\pi i\,\frac{2j_1-n-1}{2n}\left(k_1-k_2+\frac{\tau_0}{\pi}\right)} = \frac{1}{(2\ell)^{\Delta_\mathcal{T}}\,(2i\eta)}\,\frac{\sin\!\Big(\pi(k_1-k_2)+\tau_0\Big)}{n\sin\!\Big(\frac{\pi(k_1-k_2)+\tau_0}{n}\Big)}\ ,
\end{aligned}$$

where $\tau_0 = 2\arctan(\ell/\eta)$. To correctly evaluate the second line we placed the cut of each twist operator on the right, and this unambiguously fixes all phases. In particular:

$$\begin{aligned}
\Big\langle e^{i\epsilon\varphi_L}(-\ell)\, e^{-i\epsilon\varphi_L}(\ell)\, e^{i\varphi_L}(-i\eta_1)\, e^{-i\varphi_L}(i\eta_2)\Big\rangle &= \frac{1}{(2\ell)^{\epsilon^2}\, i(\eta_1+\eta_2)}\,\frac{(i\eta_2-\ell)^\epsilon(-i\eta_1+\ell)^\epsilon}{(i\eta_2+\ell)^\epsilon(-i\eta_1-\ell)^\epsilon} \\
= \frac{1}{(2\ell)^{\epsilon^2}\, i(\eta_1+\eta_2)}\,\frac{e^{i(\pi-\theta_2)\epsilon}\, e^{i(2\pi-\theta_1)\epsilon}}{e^{i\theta_2\epsilon}\quad e^{i(\pi+\theta_1)}} &= \frac{1}{(2\ell)^{\epsilon^2}\, i(\eta_1+\eta_2)}\, e^{i(2\pi-2\theta_1-2\theta_2)\epsilon}\ ,
\end{aligned} \qquad (5.6.16)$$

where $\tan\theta_j = \eta_j/\ell$ and $0<\theta_j<\frac{\pi}{2}$. Here it is important and all angles are taken from the cut (towards the right) going counterclockwise. See Fig. 5.13. In our example we take $\theta_1=\theta_2\equiv\theta$ and, defining $\tan(\tau_0/2)=\ell/\eta$, we have $\theta=(\pi-\tau_0)/2$. The right-moving part of the correlator is similar, however: $\varphi_{Lj}\to\varphi_{Rj}$; the twist operator is $e^{-i\epsilon\varphi_R}$; all dependences are on the anti-holomorphic coordinates. This is the same as mapping $\epsilon\to-\epsilon$ and $\eta\to-\eta$, and it gives:

$$\mathcal{A}^{(2)}_{R,k_1k_2} = \frac{1}{(2\ell)^{\Delta_\mathcal{T}}\,(-2i\eta)}\,\frac{\sin\!\Big(\pi(k_1-k_2)+\tau_0\Big)}{n\sin\!\Big(\frac{\pi(k_1-k_2)+\tau_0}{n}\Big)}\ . \qquad (5.6.17)$$

Putting the two contributions together, we find

$$\mathcal{A}^{(2)}_{k_1k_2} = \frac{1}{(2\ell)^{2\Delta_T}\,4\eta^2}\,\frac{\sin^2(\tau_0)}{n^2\sin^2\!\left(\frac{\pi(k_1-k_2)+\tau_0}{n}\right)}\,. \tag{5.6.18}$$

The expansion of (5.6.1) in λ gives

$$\begin{aligned}\Delta S_n &= \frac{1}{1-n}\log\frac{\mathcal{A}^{(0)}+\lambda^2\frac{1}{(2\pi)^n}\int d\vec{\alpha}\,\sum_{k_1k_2}\mathcal{A}^{(2)}_{k_1k_2}(\vec{\alpha})+O(\lambda^4)}{\mathcal{A}^{(0)}+\lambda^2\sum_{k_1k_2}\mathcal{A}^{(2)}_{k_1k_2}(0)+O(\lambda^4)}\\ &= \frac{1}{1-n}\log\frac{1+\frac{\lambda^2}{\mathcal{A}^{(0)}}\sum_k\mathcal{A}^{(2)}_{kk}+O(\lambda^4)}{1+\frac{\lambda^2}{\mathcal{A}^{(0)}}\sum_{k_1k_2}\mathcal{A}^{(2)}_{k_1k_2}+O(\lambda^4)} = \frac{\lambda^2}{n-1}\sum_{k_1\neq k_2}^{n}\frac{\mathcal{A}^{(2)}_{k_1k_2}}{\mathcal{A}^{(0)}}+O(\lambda^4)\,.\end{aligned} \tag{5.6.19}$$

The sum over $k_1\neq k_2$ is essentially the same one that we already encountered in (A.1.1) for $\Delta=1$. Therefore at quadratic order:

$$\Delta S^{(2)}_n = \frac{1}{n-1}\,\frac{1}{4\eta^2}\left(n-\frac{\sin^2(\tau_0)}{n\sin^2(\tau_0/n)}\right)\,. \tag{5.6.20}$$

This is indeed the Renyi asymmetry of an interval in the case $\Delta=1$, that one obtains by performing a conformal transformation from the Rindler geometry and using (5.2.13). The limit $n\to 1$ gives $\Delta S^{(2)}_{\text{disk}} = \big(1-\tau_0\cot(\tau_0)\big)/2\eta^2$ that reproduces (5.4.13).

Chapter 6

Towards Holography

The AdS/CFT correspondence [92–94] provides a non-perturbative definition of quantum gravity in AdS space in terms of a CFT that lives at the boundary, such that the bulk direction emerges from the strongly-coupled many-body dynamics of the CFT. This means that interesting questions often come in two avatars: one from a field theory perspective, and one from a gravity perspective. Often one perspective is simpler to work out than the other (thereby making this duality not merely a curiousity but also something useful) and this means that it worthwhile to study *both* CFTs and quantum gravity in AdS, instead of just one. Quantum information theory has long been recognized to play a primary role in understanding the emergence of the bulk. A famous example is the Ryu–Takayanagi formula [61], that shows that complicated quantum-information quantities in the CFT can translate to simple geometric observables in AdS, which sometimes can be derived using a gravitational version of the replica trick [95–97]. Thus, it is natural to expect that entanglement asymmetry is also dual to a simple quantity in the bulk. In this chapter we provide some evidence for this, at leading order in the parameter λ.

In the context of AdS/CFT, what is the holographic dual to entanglement asymmetry? At leading order in λ, entanglement asymmetry is Fisher information, and the latter has a known holographic dual [79] given by a suitable integral of the so-called symplectic flux in the entanglement wedge. We observe that such a quantity can be recast in a suggestive form:

$$\Delta S^{(2)} = 2\pi\, \partial_{\tau_0} \left(\int_{\widetilde{A}} \star F - \int_{A} \star F \right). \tag{6.0.1}$$

Here F is the field strength of the bulk gauge field dual to the $U(1)$ symmetry of the CFT, A is the chosen spatial subsystem at the boundary, $\widetilde{A}$ is the Ryu–Takayanagi surface (homologous to A) that describes entanglement entropy, while

τ_0 is the boundary location of the insertion of V along the modular flow. This formula thus contains all the ingredients that we expect to be important in the holographic evaluation of entanglement asymmetry. We hope to be able to address the higher-order terms, and to obtain a better physical understanding of this formula, in future work.

6.1 Holographic setup

A holographic CFT$_d$ on $\mathbb{R}^d$ is dual to a bulk gravitational theory in Euclidean AdS$_{d+1}$ with metric (in Poincaré coordinates):

$$ds^2 = \frac{dz^2 + dx_1^2 + \ldots + dx_d^2}{z^2}\,. \tag{6.1.1}$$

On the boundary we consider states obtained by turning on a source for a charged primary operator V in the Euclidean past:

$$|\psi\rangle = e^{i\int d^d x\, \lambda(x)\, V(x)}\,|0\rangle\,. \tag{6.1.2}$$

Such states are of particular interest in holography because they correspond to classical bulk states (see [76] and references therein). When V is charged under a $U(1)$ symmetry, the state $|\psi\rangle$ has nontrivial entanglement asymmetry.

The charged primary V of conformal dimension Δ is dual to a complex scalar field ϕ in the bulk, and its source $\lambda(x)$ corresponds to a boundary condition

$$\lim_{z\to 0} z^{\Delta-d}\,\phi(z,x) = \lambda(x)\,. \tag{6.1.3}$$

The matter theory in the bulk has Euclidean action:

$$S = \int dz\, d^d x\,\sqrt{g}\left(\frac{1}{4}F_{\mu\nu}F^{\mu\nu} + \left|D_\mu\phi\right|^2 + m^2|\phi|^2\right), \tag{6.1.4}$$

where $D_\mu\phi = \nabla_\mu\phi - ieA_\mu\phi$ and the mass is related to the dimension of V via the formula $m^2 = \Delta(\Delta - d)$. The equations of motion are

$$\left(D_\mu D^\mu - m^2\right)\phi = 0\,, \qquad \nabla^\nu F_{\mu\nu} = j_\mu \qquad \text{with} \qquad j_\mu = -i\left(\phi^\dagger D_\mu\phi - \phi\, D_\mu\phi^\dagger\right), \tag{6.1.5}$$

where j_μ is the bulk current. The solution that satisfies the boundary condition

(6.1.3) can be written as [94, 98]:

$$\phi(z, x) = \int d^d x' \, K_E(z, x \,|\, x')\, \lambda(x') \tag{6.1.6}$$

where the bulk-to-boundary propagator is (for $\Delta > d/2$):

$$K_E(z, x \,|\, x') = C_\Delta \left(\frac{z}{z^2 + (x - x')^2} \right)^{\Delta} . \tag{6.1.7}$$

The value of C_Δ that reproduces (6.1.3) is $C_\Delta = \Gamma(\Delta)/\big(\pi^{d/2}\,\Gamma(\Delta - d/2)\big)$.[1] However, with that value, the resulting two-point function of the dual complex scalar operator V has coefficient $c = 2\,(2\Delta - d)\,\Gamma(\Delta)/\big(\pi^{d/2}\,\Gamma(\Delta - d/2)\big)$ (see the Appendix of [98]). In the field theory analysis we normalized the operator V so that its two-point function has coefficient 1. In order to have the same normalization in holography, we should rescale the field ϕ by $c^{-1/2}$. This is the same as rescaling K_E, namely, as taking

$$C_\Delta = \sqrt{\frac{\Gamma(\Delta)}{4\,\pi^{d/2}\,\Gamma\big(\Delta + 1 - \frac{d}{2}\big)}} \tag{6.1.8}$$

in (6.1.7). Notice that the unitarity bound guarantees that $\Delta + 1 - \frac{d}{2} > 0$.

We focus on states where the operator is inserted at a single point:

$$\lambda(x) = \lambda\, \delta^d(x - x_0)\,, \tag{6.1.9}$$

and we take $\lambda \in \mathbb{R}$. We consider spherical regions A in the CFT, such that the modular hamiltonian is local and related to the boost generators of half-space by a conformal transformation [56]. As explained in Section 5.4, the reduced density matrix of A can be obtained by using a different time slicing of $\mathbb{R}^d$. This corresponds to writing the metric of $\mathbb{R}^d$ as a conformal transformation of $S^1 \times \mathbb{H}^{d-1}$, namely as

$$ds^2 = \Omega^{-2} \left(d\tau^2 + du^2 + \sinh^2(u)\, d\Omega^2_{d-2} \right) \tag{6.1.10}$$

as we already did in Section 5.4.1. The conformal factor (5.4.10) in these coordinates (for $\ell = 1$) is

$$\Omega = \cosh(u) + \cos(\tau)\,. \tag{6.1.11}$$

The spherical region A is mapped to the whole hyperbolic plane $\mathbb{H}^{d-1}$ at $\tau = 0$. In the bulk this slicing means writing the AdS metric using coordinates adapted to the

[1] For the case $\Delta = \frac{d}{2}$ in which the mass is at the Breitenlohner-Freedman bound, the asymptotic behavior and the normalizations are different [98].

Rindler wedge:

$$ds^2 = (\rho^2 - 1)\, d\tau^2 + \frac{d\rho^2}{\rho^2 - 1} + \rho^2 \left(du^2 + \sinh^2(u)\, d\Omega_{d-2}^2\right) \tag{6.1.12}$$

with $\rho > 1$. In these coordinates the bulk-to-boundary propagator (6.1.7) in the embedding formalism reads

$$K_E\Big(\rho, \tau, Y \,\Big|\, \tau', Y'\Big) = \frac{C_\Delta}{\left(-2\rho\, Y \cdot Y' - 2\sqrt{\rho^2 - 1}\, \cos(\tau - \tau')\right)^{\Delta}}\,. \tag{6.1.13}$$

Here $Y = \left(Y_0, Y_{a=1,\dots,d-1}\right)$ are coordinates on the hyperboloid $\mathbb{H}^{d-1}$, they solve the constraint $Y \cdot Y \equiv -Y_0^2 + \sum_a Y_a^2 = -1$ and are parametrized as $Y = \left(\cosh(u), \sinh(u)\, \theta_a\right)$ with $\sum_a \theta_a^2 = 1$ so that $\theta_a \in S^{d-2}$ (see Appendix A.3 and App. A of [76] for more details). The Rindler horizon is at $\rho = 1$ and the asymptotic boundary is at $\rho = \infty$. The prescription of [76], as we review below, requires us to construct a real-time solution for the bulk fields. In particular, the bulk solution is constructed by analytically continuing the propagator (6.1.13) to $\tau \to it$. It is then useful at this stage to perform the analytic continuation $\tau = it$ to Lorentzian signature in (6.1.12) as well, where t is the Lorentzian Rindler time. In these coordinates the bulk modular flow in the Rindler wedge is represented by the manifest Killing symmetry

$$\xi = 2\pi\, \partial_t\,. \tag{6.1.14}$$

The prescription of [76] then, given a spherical region in the CFT$_d$ on $S^1 \times \mathbb{H}^{d-1}$ as before and a one-parameter family of excited states $\rho_A = \sigma_A\Big(1 + i\int d^dx\, \lambda(x)\, V(x) + \text{h.c.} + \dots\Big)$, requires us to construct bulk solutions consistent with the operator insertions on the boundary. In hyperbolic coordinates, (6.1.6) reads

$$\phi(\rho, t, Y) = \int d\tau'\, dY'\; K_E\Big(\rho, it, Y \,\Big|\, \tau', Y'\Big)\, \lambda(\tau', Y') \tag{6.1.15}$$

with K_E as defined in (6.1.13) but analytically continued to $\tau \to it$.

Let us construct these solutions explicitly in Lorentzian AdS$_{d+1}$. The boundary CFT has delta-function sources corresponding to the Euclidean insertion of two conjugate operators V at $\tau' = -(\pi - \tau_0)$ and $V^\dagger$ at $\tau' = (\pi - \tau_0)$. Without loss of generality we take $u' = 0$. The solution takes the form $\phi(\rho, t, u) = \lambda\, K_E\Big(\rho, it, u \,\Big|$

$\tau_0 - \pi, 0\big)$ and similarly for $\phi^\dagger$:

$$\begin{aligned}
\phi &= \frac{\lambda\, C_\Delta}{\Big(2\rho\cosh(u) + 2\sqrt{\rho^2-1}\,\cos(it-\tau_0)\Big)^\Delta}\,,\\
\phi^\dagger &= \frac{\lambda\, C_\Delta}{\Big(2\rho\cosh(u) + 2\sqrt{\rho^2-1}\,\cos(it+\tau_0)\Big)^\Delta}\,.
\end{aligned} \tag{6.1.16}$$

Notice that inserting the boundary operators at specular points $\tau' = \mp(\pi - \tau_0)$ automatically ensures that the bulk solutions are complex conjugate to each other.

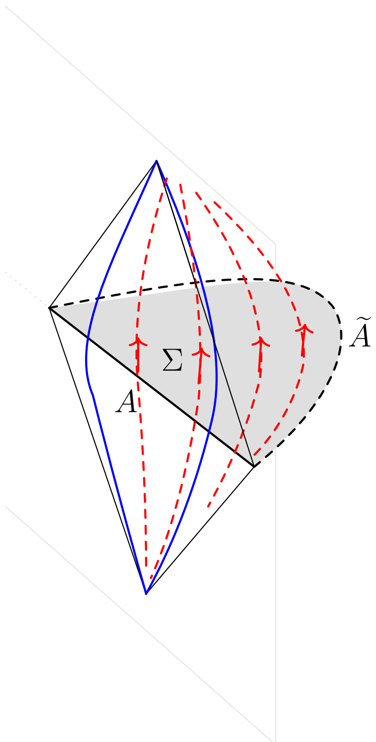

Figure 6.1: AdS Rindler wedge associated to ball shaped boundary region A. Blue curves are the boundary modular flow ζ^μ and the red curves are the bulk modular flow ξ^μ

6.1.1 Asymmetry as canonical energy

We saw that, at leading order, entanglement asymmetry is equal to perturbative relative entropy. This is a generalization of a result known as the *first law of entanglement entropy*, which is a constraint between the variation of entanglement entropy and its associated modular hamiltonian. At first order in perturbations, there is no relative entropy. At second order in perturbation, it kicks in, and was shown in [76, 79] to be holographically dual to canonical energy, first defined by Hollands and Wald [99] and then generalized in [100, 101]. These results were an extension of older work in [63, 102] in the context of black hole mechanics, using the gravitational phase space variational calculus. We provide a discussion of some of these basic features in A.4 for the interested reader.

The perturbative relative entropy defines a metric on the space of perturbations, known as the "quantum Fisher" or Bogoliubov–Kubo–Mori metric. We therefore conclude that the leading-order entanglement asymmetry is given by the canonical energy, where we are interested in the particular case of scalar primary operator insertions on the boundary, and corresponding dual bulk scalar fields. The canonical energy is defined as a particular symplectic flux of on-shell fields, evaluated on a codimension-one surface in the entanglement wedge which is bounded by the Ryu–Takayanagi surface $\widetilde{A}$ on one side and by the boundary subsystem A on the other side. Since the symplectic flux is conserved, we are free to choose any such surface and we choose the $t = 0$ spatial slice of the entanglement wedge.[2] We denote such a surface as Σ, whose boundary is $\partial\Sigma = A \cup \widetilde{A}$. The bulk formula for the entanglement asymmetry is

$$\Delta S = \int_{\Sigma} \star\,\boldsymbol{\omega}(\phi, \mathcal{L}_{\xi}\phi) + O(\lambda^4)\,, \tag{6.1.17}$$

where ϕ is taken of order λ. Here ξ is the vector field of bulk modular flow, which in Rindler coordinates is (6.1.14), while $\mathcal{L}_{\xi}$ is a Lie derivative. This is visualized in 6.1.

The symplectic current $\boldsymbol{\omega}$ is a one-form, quadratic in the on-shell bulk fields (6.1.16). We also expect corrections suppressed by G_N and e obtained by taking into account the gravitational and gauge fields.

The symplectic current can be derived by writing the variation of the bulk Lagrangian under a field variation [103]:

$$\delta\mathscr{L} = E_{\phi}\,\delta\phi + \nabla^{\mu}\Theta_{\mu}[\delta\phi]\,, \tag{6.1.18}$$

where E_{ϕ} are the equations of motion. The quantity Θ_{μ} that produces a total derivative is called the pre-symplectic current. The symplectic current is then defined as [103]:

$$\boldsymbol{\omega}_{\mu}\Big(\delta_1\phi, \delta_2\phi\Big) = \delta_1\Theta_{\mu}[\delta_2\phi] - \delta_2\Theta_{\mu}[\delta_1\phi]\,. \tag{6.1.19}$$

For the bulk action (6.1.4), and working in the approximation that only the complex scalar field is turned on at leading order, we find:

$$\begin{aligned} \Theta_{\mu}[\delta\phi] &= (D_{\mu}\phi)\,\delta\phi^{\dagger} + (D_{\mu}\phi^{\dagger})\,\delta\phi\,, \\ \boldsymbol{\omega}_{\mu}\Big(\phi_1, \phi_2\Big) &= (D_{\mu}\phi_1)\,\phi_2^{\dagger} + (D_{\mu}\phi_1^{\dagger})\,\phi_2 - (D_{\mu}\phi_2)\,\phi_1^{\dagger} - (D_{\mu}\phi_2^{\dagger})\,\phi_1\,. \end{aligned} \tag{6.1.20}$$

[2] The choice made in [76] is instead that Σ is the horizon of the entanglement wedge.

The surface Σ is at $t=0$. This surface has normal vector $n = (\rho^2-1)^{-1/2}\,\partial_t$ and induced spatial metric

$$ds^2\Big|_{t=0} = \frac{d\rho^2}{\rho^2-1} + \rho^2\left(du^2 + \sinh^2(u)\,d\Omega_{d-2}^2\right) \equiv h_{ab}\,dx^a dx^b\,. \tag{6.1.21}$$

The holographic result for the entanglement asymmetry is then

$$\Delta S = \int_1^\infty d\rho \int_0^\infty du \int_{S^{d-2}} d\Omega_{d-2}\,\sqrt{h}\,n^\mu \boldsymbol{\omega}_\mu(\phi, \mathcal{L}_\xi\phi) + O(\lambda^4)\,. \tag{6.1.22}$$

Inserting the solutions (6.1.16), the integrand takes the explicit form[3]

$$\int d\Omega_{d-2}\,\sqrt{h}\,n^\mu \boldsymbol{\omega}_\mu(\phi, \mathcal{L}_\xi\phi)\Big|_{t=0} = \tag{6.1.23}$$
$$= \lambda^2\,\frac{C_\Delta^2\,\mathrm{Vol}_{S^{d-2}}\,\pi\,\Delta\,\rho^{d-1}\,\sinh^{d-2}(u)\left(1 + 2\Delta\sin^2(\tau_0) + \rho\,(\rho^2-1)^{-\frac{1}{2}}\cos(\tau_0)\cosh(u)\right)}{4^{\Delta-1}\left(\rho\cosh(u) + \sqrt{\rho^2-1}\,\cos(\tau_0)\right)^{2(\Delta+1)}}\,.$$

Note that the integral in ρ converges if Δ is larger than the unitarity bound. Although the integral is hard to perform analytically, it is easy to evaluate numerically and we verified that it precisely reproduces the CFT answer:

$$\int_1^\infty d\rho \int_0^\infty du \int d\Omega_{d-2}\,\sqrt{h}\,n^\mu \boldsymbol{\omega}_\mu(\phi, \mathcal{L}_\xi\phi) = \lambda^2\,\Delta S^{(2)}_{\text{hyper}} \tag{6.1.24}$$

as given explicitly by eqn. (5.4.3).

6.1.2 Relation to the bulk charge

In holography a bulk gauge field A_μ is dual to a boundary current operator. However, there also exists a *bulk* current which, for the action in (6.1.4), takes the form

$$j_\mu = -i\left(\phi^\dagger D_\mu\phi - \phi\,D_\mu\phi^\dagger\right). \tag{6.1.25}$$

This is written in Lorentzian signature where Hermitian conjugation acts in the standard way. Notice that the bulk current is a rather mysterious quantity from the point of view of the boundary CFT. A natural observable is the bulk charge of the Rindler wedge:

$$Q_{\text{bulk}} = \int_\Sigma \star j\,. \tag{6.1.26}$$

[3]Recall that $\mathrm{Vol}_{S^{d-2}} = 2\pi^{(d-1)/2}/\,\Gamma\left(\frac{d-1}{2}\right)$.

In AdS_{d+1} it takes the explicit form $Q_{\text{bulk}} = \int_1^\infty d\rho \int_0^\infty du \int d\Omega_{d-2}\sqrt{h}\, n^\mu j_\mu$ and the integrand reads

$$\int d\Omega_{d-2}\sqrt{h}\, n^\mu j_\mu\Big|_{t=0} = -\lambda^2 \frac{C_\Delta^2 \,\mathrm{Vol}_{S^{d-2}}\, 2\Delta\, \rho^{d-1} \sinh^{d-2}(u) \sin(\tau_0)}{4^\Delta \sqrt{\rho^2-1}\left(\rho\cosh(u) + \sqrt{\rho^2-1}\,\cos(\tau_0)\right)^{2\Delta+1}} \,. \tag{6.1.27}$$

Using the equation of motion $d\star F = \star j$ we can write the integral as

$$Q_{\text{bulk}} = \int_A \star F - \int_{\widetilde{A}} \star F \,, \tag{6.1.28}$$

where we used that the boundary of the surface Σ is the union of the boundary subsystem A and the Ryu–Takayanagi surface $\widetilde{A}$. The first term simply computes the expectation value of the $U(1)$ charge Q in the CFT:

$$\int_A \star F = \mathrm{Tr}(\rho\, Q) \,, \tag{6.1.29}$$

while the second term is the electric flux through the Ryu–Takayanagi surface.

Now, one might expect a relation between bulk charge and entanglement asymmetry. Indeed we observe that, in our setup, the following simple relation holds:

$$\lambda^2\, \Delta S^{(2)} = -2\pi\, \partial_{\tau_0} Q_{\text{bulk}} \,. \tag{6.1.30}$$

This follows from the fact that the integrand satisfies (for any t):

$$\boldsymbol{\omega}_\mu(\phi, \mathcal{L}_\xi \phi) = -2\pi\, \partial_{\tau_0} j_\mu \,. \tag{6.1.31}$$

This can be checked explicitly from the formulas given above. It can also been argued from the fact that ∂_{τ_0} acts as $i\partial_t$ on ϕ while it acts as $-i\partial_t$ on $\phi^\dagger$ in (6.1.16), due to the general form of the bulk-to-boundary propagator. Indeed a simple calculation shows that

$$\boldsymbol{\omega}_\mu(\phi, \mathcal{L}_\xi \phi) = \left((\partial_\mu \phi)\left(2\pi \partial_t \phi^\dagger\right) - \left(2\pi \partial_\mu \partial_t \phi\right)\phi^\dagger\right) + \text{h.c.} = -2\pi\, \partial_{\tau_0} j_\mu \,. \tag{6.1.32}$$

This equation is reminiscent of the general analysis carried out in the context of black hole mechanics and Noether charges associated with the symmetries on the black-hole horizon [63, 102]. It would be interesting to investigate this point more systematically.

Notice that τ_0 parametrizes a one-parameter family of solutions as in (6.1.16), with delta-function sources. One could generalize this setting to a one-parameter family of smeared complex sources labelled by a parameter α:

$$\lambda_\alpha(\tau, Y) = \lambda_0(\tau - \alpha, Y)\,, \qquad\qquad \lambda^*_\alpha(\tau, Y) = \lambda^*_0(\tau + \alpha, Y)\,, \tag{6.1.33}$$

where λ_0 and λ^*_0 are some reference sources. The effect of α is to shift the boundary conditions along the modular flow. The bulk solutions are then labelled by α as follows:

$$\phi_\alpha(\rho, t, Y) = \int d\tau'\, dY'\; K_E\Big(\rho, it, Y \;\Big|\; \tau', Y'\Big)\, \lambda_\alpha(\tau', Y')\,. \tag{6.1.34}$$

Since $\partial_\tau \lambda_\alpha = -\partial_\alpha \lambda_\alpha$ and K_E has translational invariance, one can trade the derivatives with respect to t, τ' and α using integration by parts:

$$\mathcal{L}_\xi\, \phi_\alpha = -2\pi i\, \partial_\alpha \phi_\alpha\,, \qquad\qquad \mathcal{L}_\xi\, \phi^\dagger_\alpha = 2\pi i\, \partial_\alpha \phi^\dagger_\alpha\,. \tag{6.1.35}$$

With this, the holographic answer can be written as

$$\Delta S^{(2)} = -2\pi\, \partial_\alpha \int_\Sigma \star\, j_\alpha\,, \tag{6.1.36}$$

where both sides are of order λ^2. In other words, the holographic formula (6.1.30) for the quadratic entanglement asymmetry can be interpreted as the derivative of the bulk charge of the entanglement wedge, with respect to a modular flow of the sources that create the state. It would be interesting to better understand the physical meaning of this observation.

Chapter 7

Entanglement Asymmetry for generalized symmetries

In this chapter, we would like to define asymmetry for *generalized symmetries*, which include the cases of both higher-form [64] and noninvertible [65] symmetries.[1] In the modern formulation, the (finite internal) symmetries of a local quantum field theory are described by topological defects of various dimensions [64]. These objects fit naturally into mathematical structures known as (higher) fusion categories [65, 67, 105–108]. The latter not only encode which defects are present in a given theory, but also how they can fuse and join together, as well as various manifestations of anomalies (*e.g.*, braiding phases and transformations produced by manipulations of the topological defects). Such a generalized definition of "symmetry" goes well beyond ordinary symmetry groups. For the finite internal symmetries of unitary QFTs, we propose to define asymmetry through the following construction.

A QFT associates a Hilbert space of states to each possible spatial manifold. Consider thus a (possibly mixed) state, whose asymmetry one wishes to compute, described by a density matrix. One might be interested in studying the asymmetry of the full system, or of a subsystem. In the latter case, to each spatial subregion A and choice of boundary conditions, one can associate another Hilbert space and a reduced density matrix [109]. Moreover, one may choose whether or not to include the twisted sectors in these Hilbert spaces. In any case, one ends up with a (sub)system Hilbert space $\mathcal{H}$ and a (reduced) density matrix ρ. The symmetry defects, when laid parallel to the spatial manifold, give rise to an action on the (sub)system Hilbert space through a finite-dimensional C^*-algebra $\mathcal{A}$. We then propose to construct a

[1] The asymmetry for higher-form symmetries is studied in greater detail, from a different perspective, in [47]. On the other hand, a generalized Landau paradigm for noninvertible symmetries was advocated in [104].

"symmetrizer" S, that produces a symmetrized density matrix ρ_{S} from ρ. Concisely, S is the projector to the space of operators on $\mathcal{H}$ that commute with the symmetry algebra $\mathcal{A}$ (which turns out to be a quantum channel). Lastly, one quantifies how much ρ_{S} differs from ρ. Following [3], we use relative entropy or its Rényi version.[2] This defines, respectively, entanglement and Rényi asymmetries with respect to generalized symmetries.

In fact, this definition applies even beyond local quantum field theories — for instance, to lattice models. Once the relevant Hilbert space and finite-dimensional C^*-algebra of symmetry operators have been identified, our definition of asymmetry can be used.

To be concrete, we analyze in detail the case of two-dimensional unitary quantum field theories, where symmetries are implemented by the topological lines of a unitary fusion category $\mathscr{C}$. First, we consider QFTs placed on a spatial circle S^1 and study the asymmetry of the full system. The simplest setup is to restrict to the untwisted Hilbert space, on which the symmetry acts through a fusion algebra. On the other hand, one can encompass the total Hilbert space of untwisted and twisted sectors, on which a noninvertible symmetry has a more sophisticated action that mixes the untwisted sector with the twisted ones, and that is described by the so-called tube algebra $\mathsf{Tube}(\mathscr{C})$ [112]. We compare the asymmetries computed with respect to the fusion and tube algebras, finding that the latter is a more refined detector of symmetry breaking, especially in the case of noninvertible symmetries. We investigate this issue in the context of a class of excited states in CFTs, created by the insertion of local operators.

Moreover, we compute entanglement asymmetry in two-dimensional gapped phases with spontaneous symmetry breaking (SSB), employing a topological quantum field theory (TQFT) description. We find that vacua related by noninvertible symmetries need not have the same asymmetry, whereas for group-like symmetries they always do. This is another manifestation of the fact that vacua arising from the spontaneous breaking of a noninvertible symmetry can exhibit different physics [113, 114].

Next, we study the asymmetry of subsystems when the subregion A is an interval. In order to properly define a subsystem Hilbert space and a symmetry action on it, one needs to specify boundary conditions, mathematically described by a $\mathscr{C}$-module category $\mathscr{M}$. The noninvertible symmetry then acts through the so-called strip

[2] First, one could define what a symmetric density matrix is in different ways, see for instance [110, 111]. Second, other functions that quantify the difference between two density matrices could be used as well; see, for instance, [39] for a discussion.

algebra $\mathsf{Strip}_{\mathscr{C}}(\mathscr{M})$ [115–118].[3] When the theory admits (strongly or weakly [68]) symmetric boundary conditions, the definition of asymmetry is straightforward — otherwise,[4] we implement an averaging protocol over the boundary conditions related by symmetry. For excited states in CFTs (*e.g.*, in the Ising CFT), we investigate how the asymmetry varies with the subsystem size, and compare it with the asymmetry of the full system. Interestingly, we observe that Rényi asymmetries are not always monotonically increasing with the subsystem size (whereas entanglement asymmetry is, see *e.g.* [47]). For group-like symmetries, we find that the choice of boundary conditions eventually does not affect the asymmetry, thus validating previous, less rigorous approaches in the literature in which the boundary conditions (and the possible influence of 't Hooft anomalies) were not taken into account. For noninvertible symmetries, instead, a proper account of the boundary conditions seems inevitable in order to compute the asymmetry explicitly.

Finally, we note that when the symmetry algebra $\mathcal{A}$ has special properties or additional structure, there might exist other equivalent presentations of the symmetrizer S (and hence of the asymmetries). For instance, for those symmetry algebras that are Hopf algebras (including certain strip algebras) we find an alternative formula for S.

The rest of the thesis is organized as follows. In 7.1 we put forward our definition of asymmetry for generalized symmetries, whose core is the symmetrizer S with respect to a finite-dimensional semisimple algebra. In 8.1, focusing on two-dimensional theories, we study the asymmetry of states on a spatial circle, with respect to both the fusion and tube algebras. In Sec. 8.2, instead, we study the asymmetry of states on an interval with respect to the strip algebra. The possible definitions of the symmetrizer depend strongly on the available types of boundary conditions. We also present an alternative formula valid in the case of Hopf and weak Kac algebras. The asymmetry on the circle is applied in 9 to the detection of spontaneous symmetry breaking in 2d gapped phases. Finally, 10 is devoted to concrete examples that we work out in detail: group-like symmetries, as well as a collection of fusion categories including the Ising, $\mathsf{Rep}(H_8)$, Fibonacci, and Haagerup ones. More technical aspects are collected in appendices.

In the modern formulation, the finite internal symmetries of a quantum field theory are described by a (higher) fusion category. Its objects, the morphisms between objects, the morphisms between morphisms, and so on, describe the topological operators of various codimensions in the quantum field theory and their intersections,

[3] See also [119–121].

[4] For instance, the presence of 't Hooft anomalies in the theory prevents the existence of symmetric boundary conditions [68, 122, 123], in a sense that we spell out more precisely in Sec. 8.2.

and correspond to the symmetry elements. The full structure of the fusion category encodes phase factors (such as braiding phases and 't Hooft anomalies) as well as more general transformations produced by moves of the topological operators, which constitute the symmetry structure.

Depending on the physical setup, the symmetry category gives rise to different algebras of symmetry operators, as we now describe. A quantum field theory associates a Hilbert space of states to each spatial manifold. If we are interested in a subsystem (*i.e.*, a subregion) A, we can use the procedure of [109] (that we review in 8.2) to produce the Hilbert space of the QFT on a spatial manifold A with boundaries. Besides, we may want to include or not to include twisted sectors, *i.e.*, to allow the insertion of topological operators along the time direction so that they pierce the spatial manifold. In all cases, we end up with a Hilbert space $\mathcal{H}$. We can construct symmetry operators acting on this space by taking topological defects laid along the spatial slice. Under the multiplication given by fusing the defects, they give rise to an algebra $\mathcal{A}$. We call $\{\mathcal{X}_a\}$ a basis of the algebra.

For technical reasons, we focus on unitary quantum field theories with finite internal symmetries. These are described by a unitary (higher) fusion category, which contains a finite number of simple objects. As a result, the algebra $\mathcal{A}$ is a finite-dimensional C^*-algebra, which in particular is semisimple.

7.1 Symmetrizer

It turns out that such a symmetrizer has a simple and universal construction[5] when the symmetry action on the Hilbert space gives rise to a *strongly-separable algebra*. Consider a unital associative algebra $\mathcal{A}$ over the complex field $\mathbb{C}$ defined by the product

$$\mathcal{X}_a \times \mathcal{X}_b = \textstyle\sum_c T^c_{ab}\, \mathcal{X}_c \,, \tag{7.1.1}$$

where $\{\mathcal{X}_a\}$ is a basis while $T^c_{ab} \in \mathbb{C}$ are the structure coefficients. We will often omit the product sign $\times$. Associativity corresponds to the identity $\sum_m T^m_{ab}\, T^d_{mc} = \sum_m T^d_{am}\, T^m_{bc}$. We indicate the unit element, which in general is a linear combination of the basis elements, as $\mathcal{X}_{\mathbb{1}}$. The regular representation is defined by the left action of the algebra on itself, and is explicitly given by the matrices $(T_a)^c{}_b = T^c_{ab}$. Define a

[5]What we mean by "universal" is that the symmetrizer can be constructed using just elements of the symmetry algebra under consideration, without other specific knowledge of the particular theory.

trace $\mathrm{Tr}\colon \mathcal{A} \to \mathbb{C}$ for every element $X = \sum_a x^a \mathcal{X}_a \in \mathcal{A}$ as

$$\mathrm{Tr}(X) = \mathrm{Tr}\Big(\sum_a x^a \mathcal{X}_a\Big) \equiv \sum_a x^a \,\mathrm{Tr}(T_a) = \sum_{am} x^a \, T^m_{am} \,. \tag{7.1.2}$$

Then consider the symmetric bilinear form

$$K_{ab} = \mathrm{Tr}(\mathcal{X}_a \mathcal{X}_b) = \mathrm{Tr}(T_a T_b) = \sum_{mn} T^m_{an} \, T^n_{bm} \,. \tag{7.1.3}$$

As explained above, we will be dealing with finite-dimensional unital semisimple algebras over the complex field $\mathbb{C}$. For such algebras, using the Wedderburn–Artin theorem (see App. A.6), one can verify that the bilinear form (7.1.3) is non-degenerate. The inverse matrix $K^{-1} \equiv \tilde{K}$ allows one to construct a special element $e \in \mathcal{A} \otimes \mathcal{A}$ called the *symmetric separability idempotent* (SSI):

$$e = \sum_{ab} \tilde{K}^{ab} \, \mathcal{X}_a \otimes \mathcal{X}_b \,, \tag{7.1.4}$$

whose defining properties will be discussed shortly. An algebra for which such an object exists is called strongly separable. One can also prove (we give some details in App. A.6) that the structure coefficients satisfy the pivotal relation

$$T^b_{ca} = \sum_{b'c'} \tilde{K}^{bb'} \, K_{cc'} \, T^{c'}_{ab'} \,. \tag{7.1.5}$$

Besides, one can explicitly construct the identity (or unit) element

$$\mathcal{X}_{\mathbb{1}} = \sum_{abc} T^b_{ab} \, \tilde{K}^{ac} \mathcal{X}_c = \sum_{abc} \tilde{K}^{ab} \, T^c_{ab} \, \mathcal{X}_c \tag{7.1.6}$$

and verify that $\mathcal{X}_{\mathbb{1}} \mathcal{X}_a = \mathcal{X}_a \mathcal{X}_{\mathbb{1}} = \mathcal{X}_a$ for all $\mathcal{X}_a \in \mathcal{A}$, as well as $\mathrm{Tr}(\mathcal{X}_{\mathbb{1}}) = \dim \mathcal{A}$. The SSI has the following properties. First, it is symmetric under the exchange of the two factors in the tensor product. Second, denoting the product as $XY = \mu(X \otimes Y)$ in terms of $\mu\colon \mathcal{A} \otimes \mathcal{A} \to \mathcal{A}$, the contraction of the SSI gives the unit element: $\mu(e) = \mathcal{X}_{\mathbb{1}}$. Third, the SSI commutes with every element of the algebra, $\mathcal{X}_a \, e = e \, \mathcal{X}_a$, where multiplication from the left/right acts on the first/second factor. Fourth, the SSI is idempotent as an element of $\mathcal{A} \otimes \mathcal{A}^{\mathrm{op}}$ (where $\mathcal{A}^{\mathrm{op}}$ is the same as $\mathcal{A}$ but elements are multiplied in the opposite order): $e^2 = e$. The one in (7.1.4) is the unique element [124] with these properties.

The algebras we are interested in are also C^*-algebras and in particular have a $*$-structure, namely an anti-linear involution $\dagger\colon \mathcal{A} \to \mathcal{A}$ such that $(XY)^\dagger = Y^\dagger X^\dagger$. By a version of the Wedderburn–Artin theorem [125], one can show that the SSI is Hermitian, $e^\dagger = e$, and that there exists a special basis $\{\mathcal{X}_{\underline{a}}\}$ in which it takes the simple form $e = \sum_{\underline{a}} \mathcal{X}_{\underline{a}}^\dagger \otimes \mathcal{X}_{\underline{a}}$. See App. A.6 for more details.

The SSI provides then the general formula for the symmetrizer S: $\rho_{\mathsf{S}} = e(\rho)$, where the first factor of e acts on ρ from the left while the second factor from the right. More explicitly:

$$\boxed{\rho_{\mathsf{S}} = \sum\nolimits_{ab} \tilde{K}^{ab}\, \mathcal{X}_a\, \rho\, \mathcal{X}_b} \,. \tag{7.1.7}$$

One can easily verify that the properties of the SSI guarantee the properties 1. – 4. of the symmetrizer. Besides, assuming that $\rho^\dagger = \rho$ and $\rho \geq 0$, one verifies that $\rho_{\mathsf{S}}^\dagger = \rho_{\mathsf{S}}$ (using that $e^\dagger = e$) and that $\rho_{\mathsf{S}} \geq 0$ (using the simple form of e in the special basis). In fact, it turns out that ρ_{S} is a trace-preserving quantum channel. As we will show, one can also find equivalent alternative expressions for the SSI when the algebra $\mathcal{A}$ has extra properties or extra structure. For instance, for commutative algebras one can rewrite (7.1.7) as a sum over projectors on one-dimensional representations, while for Hopf and weak Kac algebras one can rewrite (7.1.7) in terms of the coproduct and antipode operations.

In the special case that the symmetry is a standard 0-form invertible symmetry given by a group G,[6] previous literature has studied the simplest algebra $\mathcal{A}$ that can describe the symmetry action, namely the group algebra $\mathbb{C}[G]$, which is the fusion algebra associated to this symmetry. Its basis elements (and generators) $\mathcal{X}_g$ correspond to the group elements $g \in G$ and to the simple objects $\mathcal{L}_g$ of the fusion category Vec_G. The structure coefficients are $T_{gh}^k = \delta_{(gh)}^k$, where (gh) is the group multiplication. The bilinear form is then $K_{gh} = |G|\, \delta_{g,h^{-1}}$ and its inverse is $\tilde{K}^{gh} = |G|^{-1}\, \delta^{g,h^{-1}}$. The symmetrizer reads:

$$\rho_{\mathsf{S}} = \frac{1}{|G|} \sum\nolimits_{g\in G} \mathcal{L}_g\, \rho\, \mathcal{L}_{g^{-1}} \,. \tag{7.1.8}$$

This expression agrees with what already used in previous literature (*e.g.* [3,19,27,32]).

For the symmetrizer (7.1.7) it is easy to prove that the two definitions (2.1.1) and (2.1.2) coincide. It is enough to notice that

$$\operatorname{Tr}\Big(\rho_{\mathsf{S}} \log \rho_{\mathsf{S}}\Big) = \sum\nolimits_{ab} \tilde{K}_{ab} \operatorname{Tr}\Big(\mathcal{X}_a\, \rho\, \mathcal{X}_b \log \rho_{\mathsf{S}}\Big) = \sum\nolimits_{ab} \tilde{K}_{ab} \operatorname{Tr}\Big(\rho\, \mathcal{X}_b \log(\rho_{\mathsf{S}})\, \mathcal{X}_a\Big) = \operatorname{Tr}\Big(\rho\, (\log \rho_{\mathsf{S}})_{\mathsf{S}}\Big) \,, \tag{7.1.9}$$

but $(\log \rho_{\mathsf{S}})_{\mathsf{S}} = \log \rho_{\mathsf{S}}$ because $\log \rho_{\mathsf{S}}$ commutes with the algebra, as does ρ_{S}.

Finally, given the algebra $\mathcal{A}$ corresponding to a chosen symmetry action, to what extent is the symmetrizer (7.1.7) unique? If we require that the symmetrizer be expressible solely in terms of the symmetry operators $\mathcal{X}_a$ — *i.e.*, that it be universal

[6] In the modern language of [64], a 0-form symmetry is a standard symmetry that acts on local operators and is implemented by spacetime-codimension-1 topological operators.

— then the uniqueness of the SSI e implies the uniqueness of S. Equivalently, as we show in App. A.6.2, the form of the symmetrized density matrix is fixed as in Fig. 2.1, and this completely specifies the action of the symmetrizer. One can verify that it is self-adoint with respect to Hilbert Schmidt. One could relax the requirement of universality and look for more general maps (which would require theory-specific operators). Yet one can argue that S, being a self-adjoint projector onto the space of operators that commute with $\mathcal{A}$, is completely determined.

Chapter 8

Towards Generalized symmetry actions

In chapter 4, we provided an introduction to generalized symmetries in $1+1$D. It is now time to use that to study the action of these symmetries on hilbert spaces.

8.1 Fusion Algebra

Associated to every fusion category $\mathscr{C}$ is a fusion algebra $\mathcal{A}$ spanned by the objects $\mathcal{L}_a$, which are to be thought of as the action . Such an algebra is unital and associative and takes the general form (7.1.1), however in the basis in which $\mathcal{X}_a$ are the simple lines $\mathcal{L}_a$, the coefficients T^c_{ab} are constrained to be nonnegative integer numbers $N^c_{ab} \in \mathbb{N}$. We thus write the fusion algebra as

$$\mathcal{L}_a \times \mathcal{L}_b = \sum\nolimits_c N^c_{ab}\, \mathcal{L}_c \ . \tag{8.1.1}$$

Besides, associated to the rigid structure of $\mathscr{C}$ is a conjugation operation on $\mathcal{A}$: there exists an element of the chosen basis, that we call $\mathcal{L}_1$, such that the matrix $C_{ab} \equiv N^1_{ab}$ is involutive, namely $C^2 = \mathbb{1}$. Since the coefficients are natural numbers, this implies that for every a there exists a unique $\bar{a}$ such that $N^1_{ab} = \delta_{b\bar{a}}$ and $\bar{\bar{a}} = a$. Conjugation is then the map

$$\mathcal{L}_a \ \mapsto \ \mathcal{L}^\dagger_a \equiv \mathcal{L}_{\bar{a}} = \sum\nolimits_b C_{ab}\, \mathcal{L}_b = \sum\nolimits_b N^1_{ab}\, \mathcal{L}_b \ . \tag{8.1.2}$$

This is also called duality. Conjugation is required to be an algebra anti-automorphism: $N^{\bar{c}}_{\bar{a}\bar{b}} = N^c_{ba}$. This is then extended to the whole fusion algebra by anti-linearity. Conjugation and associativity allow one to derive that $N^c_{ab} = N^{\bar{a}}_{b\bar{c}}$, hence one obtains the

Figure 8.1: Left: action of the fusion algebra (8.1.1) of the symmetry category $\mathscr{C}$ on the untwisted Hilbert space on S^1. The product of two elements of the algebra is realized by stacking the corresponding lines on the cylinder and fusing them. Right: the corresponding action of the fusion algebra on local operators.

pivotal relations

$$N_{ab}^{c} = N_{\bar{a}c}^{b} = N_{c\bar{b}}^{a} = N_{b\bar{c}}^{\bar{a}} = N_{\bar{c}a}^{\bar{b}} = N_{\bar{b}\bar{a}}^{\bar{c}} \ . \tag{8.1.3}$$

When applied to the conjugation matrix, they imply that $N_{1a}^{b} = N_{a1}^{b} = \delta_a^b$ so that $\mathcal{L}_1$ is in fact the unit element for the fusion algebra, it is unique and self-dual, and indeed it corresponds to the transparent identity line of $\mathscr{C}$.

The fusion algebra describes the action of the symmetry on the untwisted Hilbert space $\mathcal{H}_1$ on S^1, as depicted in Fig. 8.1 on the left. It also describes the action of the symmetry on untwisted local operators, as depicted in Fig. 8.1 on the right.[1] One can prove (as we review in App. A.6.1) that finite-dimensional fusion algebras are automatically C^*-algebras and thus semisimple and strongly separable. Therefore, if we are interested in defining and computing the asymmetry of (possibly mixed) states on $\mathcal{H}_1$ with respect to the fusion algebra, we can define the symmetrizer S — and hence entanglement and Rényi asymmetries — using the universal formula (7.1.7). We will describe some concrete results in 8.1, 9, and present detailed computations in various examples in chapter 10.

Commutative case. In the case of an Abelian algebra, the symmetrizer S can be described in an alternative but equivalent way, that we now present. The irreducible representations of a commutative algebra are one-dimensional. Therefore, the blocks shown in Fig. 2.1 are one-dimensional and the symmetrizer simply acts by setting to zero all blocks that connect different irreducible representations. Let $P_r \colon \mathcal{H} \to \mathcal{H}$ denote the projector onto the r-th irreducible representation. The symmetrizer then reads[2]

$$\rho_{\mathsf{S}} = \sum\nolimits_r P_r \, \rho \, P_r \ . \tag{8.1.4}$$

[1] In CFTs there is a one-to-one correspondence between untwisted states on S^1 and untwisted local operators. In generic QFTs there is no such a correspondence, but it is still true that both states and local operators transform in representations of the fusion algebra.

[2] The expression (8.1.4) agrees with the formula originally proposed in [3] for invertible Abelian symmetries.

If we further assume that the algebra is a commutative *fusion algebra*, an explicit formula for P_r in terms of simple lines is available. This was discussed in [126] in the context of fusion algebras of modular fusion categories, but in fact it holds more generally for arbitrary fusion algebras. In the following we review the construction, partially based on [127].

The matrices $(N_a)^b{}_c \equiv N_{ac}^b$ give the regular representation of the algebra. They satisfy $N_{\bar{a}} = N_a^{\mathsf{T}} = N_a^\dagger$ and in the Abelian case they all commute. It follows that they are normal matrices and can be simultaneously diagonalized with a unitary transformation. Let us call $w^{(r)}$ the common eigenvectors, that are orthogonal with respect to the standard Hermitian product, and $\nu_{a(r)}$ the eigenvalues:

$$N_a\, w^{(r)} = \nu_{a(r)}\, w^{(r)} \; . \tag{8.1.5}$$

Note that $r = 1, \ldots, \dim \mathcal{A}$. For each r, the eigenvalues provide a one-dimensional representation of the fusion algebra, namely

$$\nu_{a(r)}\, \nu_{b(r)} = \sum\nolimits_c N_{ab}^c\, \nu_{c(r)} \; . \tag{8.1.6}$$

This also shows that the eigenvectors can be taken to be equal to the eigenvalues: $w_a^{(r)} = \nu_{\bar{a}(r)}$, as one can check. Orthogonality of the vectors implies that $\sum_a \nu_{a(r)}^*\, \nu_{a(m)} = |s_r|^{-2}\, \delta_{rm}$ for some numbers s_r that we can take in $\mathbb{R}_{>0}$. One defines the matrix

$$S_{ar} = \nu_{a(r)}\, s_r \; . \tag{8.1.7}$$

Note that $\nu_{1(r)} = 1$ in all representations r since $\mathcal{L}_1$ is the identity, thus $s_r = S_{1r}$. The action of the fusion algebra on its representations is usually written as

$$N_a\, w^{(r)} = \frac{S_{ar}}{S_{1r}}\, w^{(r)} \; , \tag{8.1.8}$$

and the matrix S_{ar} is called the S-matrix. One checks that it is unitary, $S^\dagger S = \mathbb{1}$, and therefore also $SS^\dagger = \mathbb{1}$. Such identities correspond to the orthogonality and completeness of characters. The relations (8.1.6) can then be written as

$$N_{ab}^c = \sum\nolimits_r \frac{S_{ar}\, S_{br}\, S_{cr}^*}{S_{1r}} \; , \tag{8.1.9}$$

which is the Verlinde formula. It also shows that S^{T} diagonalizes the matrices N_a, and that $\nu_{\bar{a}(r)} = \nu_{a(r)}^*$. Notice that when $\mathscr{C}$ is a modular fusion category, the S-matrix is also symmetric, but in general it is not.

The projector onto the r-th irreducible representation is then given by

$$P_r = S_{1r} \sum\nolimits_a S^*_{ar} \, \mathcal{L}_a \; . \tag{8.1.10}$$

One can verify, using the Verlinde formula and unitarity of the S-matrix, that the set $\{P_r\}$ forms a family of orthogonal projectors, *i.e.* they satisfy $P_r P_s = \delta_{rs} P_r$, and that if $|\psi\rangle$ belongs to the r-th irreducible representation then $P_{r'}|\psi\rangle = \delta_{rr'}|\psi\rangle$. Finally, one can verify that the expression (8.1.4) with P_r given by (8.1.10) agrees with (7.1.7).[3]

Note that for a noncommutative algebra the formula (8.1.4) would fail. From Fig. 2.1 it is clear that this would only put the density matrix in a block-diagonal form, without further projection to the identity matrix inside each sub-block. In Sec. 10.4.2 we study the simplest noninvertible and non-Abelian example: the Haagerup fusion algebra $H_{(3)}$.

8.1.1 Tube algebra

On a spatial S^1, a noninvertible symmetry can map (un)twisted sectors to other (un)twisted sectors. One can thus construct a more sophisticated and complete action of the symmetry on the total Hilbert space

$$\mathcal{H}_{\text{Tube}} = \bigoplus\nolimits_{a \,\in\, \text{Irr}(\mathscr{C})} \mathcal{H}_a \; , \tag{8.1.11}$$

where $\mathcal{H}_a$ are the Hilbert spaces on S^1 twisted by the lines $\mathcal{L}_a$ (and thus $\mathcal{H}_1$ is the untwisted sector), and $\text{Irr}(\mathscr{C})$ is the set of simple objects in $\mathscr{C}$. The finite-dimensional C^*-algebra $\mathcal{A}$ that is obtained in this way is called the *tube algebra* $\mathsf{Tube}(\mathscr{C})$ [112]. This algebra does not only depend on the fusion rules of $\mathscr{C}$, but rather also on its F-symbols (which are the components of the associator).

In order to describe the algebra, let us first fix our notation (that follows [128]). The nonnegative integers N_{ab}^c represent the dimensions of the vector spaces of morphisms between lines: $N_{ab}^c = \dim\Big(\text{Hom}(\mathcal{L}_a \otimes \mathcal{L}_b, \mathcal{L}_c)\Big) = \dim\Big(\text{Hom}(\mathcal{L}_{\bar c}, \mathcal{L}_{\bar b} \otimes \mathcal{L}_{\bar a})\Big)$. The second equality is because conjugation corresponds to inverting the direction of a line:

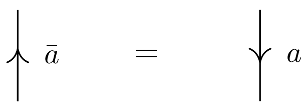

(8.1.12)

[3]The expression in (8.1.4) is $\rho_{\mathsf{S}} = \sum_{ab}\Big(\sum_r S_{1r}^2 S^*_{ar} S^*_{br}\Big)\, \mathcal{L}_a \rho \mathcal{L}_b$. We need to show that $\sum_r S_{1r}^2 S^*_{ar} S^*_{br} = \tilde{K}^{ab}$. This is easily verified by multiplying both sides by the matrix K_{bc}, using its definition (7.1.3) and the Verlinde formula (8.1.9) twice.

Figure 8.2: Left: action of the tube algebra $\mathsf{Tube}(\mathscr{C})$ on the total Hilbert space on S^1 (left) and on (un)twisted point operators (right). The product of two elements of the algebra is realized by stacking the corresponding elements on the cylinder and then resolving the configuration.

which physically is realized by a 180-degree rotation. The tensor product is associative, however it involves a change of basis in the vector spaces of morphisms described by the F-symbols:

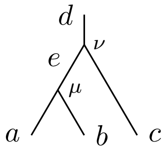

$$= \sum_{f,\rho,\sigma} \left[F^d_{abc}\right]_{(e;\mu\nu)(f;\rho\sigma)} \tag{8.1.13}$$

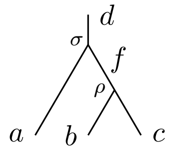

Here and in the following, unless stated otherwise, all lines have implicit arrows oriented from bottom to top. Roman letters label the lines, while Greek letters label the basis of morphisms. The F-symbol F^d_{abc} is an element of $\mathrm{End}\big(\mathrm{Hom}(\mathcal{L}_a \otimes \mathcal{L}_b \otimes \mathcal{L}_c, \mathcal{L}_d)\big)$ represented by an invertible square matrix of size $N^d_{abc} = \sum_e N^e_{ab}\, N^d_{ec}$. As in [128], we choose the bases of morphisms in such a way that the F-symbols are *unitary* matrices[4] and $[F^d_{abc}] = \mathbb{1}$ whenever a, b, or c is 1 (and fusion is possible). The F-symbols satisfy the pentagon equation. We spell it out, together with other details, in App. A.8. The bases are normalized so that the following hold:

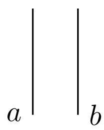

$$= \sum_{c,\mu} \sqrt{\frac{d_c}{d_a d_b}}$$

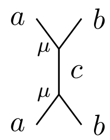

,

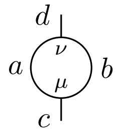

$$= \delta_{cd}\, \delta_{\mu\nu} \sqrt{\frac{d_a d_b}{d_c}} \tag{8.1.14}$$

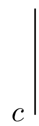

The positive real numbers d_a are the quantum dimensions, which are associated to each line $\mathcal{L}_a$ and furnish a 1d representation of the fusion algebra: $d_a d_b = \sum_c N^c_{ab}\, d_c$.

The tube algebra is generated by topological configurations in which a simple line $\mathcal{L}_a$ — stretched horizontally — can interpolate between two (un)twisted sectors $\mathcal{H}_g$ and $\mathcal{H}_h$, as in Fig. 8.2 left. Equivalently, the generators map (un)twisted local

[4]The existence of such bases is guaranteed by the fact that the fusion category is unitary. Without such an assumption, our formulas below would still be correct but in terms of inverse matrices, as opposed to Hermitian conjugate matrices.

operators $\mathcal{O}_g$ (that live at the end of a line $\mathcal{L}_g$) to (un)twisted operators $\mathcal{O}_h$ via the so-called lasso action, as in Fig. 8.2 right. The configuration is described by a "cross", where the horizontal line $\mathcal{L}_a$ is closed in a circle, while the vertical line $\mathcal{L}_g$ lies below and $\mathcal{L}_h$ lies above. The intersection Δ is an element of $\mathrm{Hom}(\mathcal{L}_a \otimes \mathcal{L}_g, \mathcal{L}_h \otimes \mathcal{L}_a)$, which has dimension $\sum_d N_{ag}^d \, N_{ha}^d$ (note that $N_{ha}^d = N_{\bar{h}d}^a$). It is convenient to decompose the intersection into trivalent junctions:

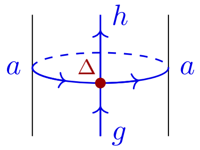

$$\equiv$$

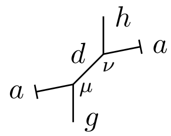

$$. \tag{8.1.15}$$

We will use the graphical notation on the r.h.s., and use the indicated basis for the tube algebra. All lines have an implicit arrow from bottom to top, and the tick at the beginning or end of a line indicates the "trace" described in [128]. The dimension of the tube algebra is

$$\dim\Big(\mathsf{Tube}(\mathscr{C})\Big) = \textstyle\sum_{g,a,d,h} N_{ag}^d \, N_{ha}^d \,. \tag{8.1.16}$$

In the tube algebra we multiply elements by placing one cylinder on top of the other (the product is such that bottom acts first, top acts second). The product is zero if there is no possible junction between adjacent vertical lines. In the case of the basis elements (8.1.15), because only simple lines are involved, this forces the vertical lines to be the same. We define a product matrix:

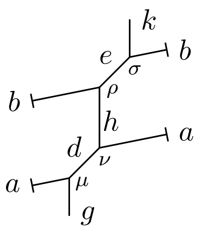

$$= \sum_{c,s,\alpha,\beta} M^{c,(s;\alpha\beta)}_{g,a,(d;\mu\nu),h,b,(e;\rho\sigma),k}$$

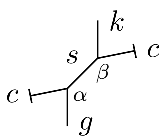

$$. \tag{8.1.17}$$

The computation of M is performed in App. A.8, and the result is:

$$M^{c,(s;\alpha\beta)}_{g,a,(d;\mu\nu),h,b,(e;\rho\sigma),k} = \sqrt{\frac{d_a d_b d_h d_s}{d_d d_e d_c}} \sum_{\gamma,\eta,\lambda} \Big[F^s_{kba}\Big]^*_{(e;\sigma\eta)(c;\gamma\beta)} \Big[F^s_{bha}\Big]_{(e;\rho\eta)(d;\nu\lambda)} \Big[F^s_{bag}\Big]^*_{(c;\gamma\alpha)(d;\mu\lambda)} \,. \tag{8.1.18}$$

The sums are over a basis of morphisms $\mathcal{L}_b \otimes \mathcal{L}_a \xrightarrow{\gamma} \mathcal{L}_c$, $\mathcal{L}_e \otimes \mathcal{L}_a \xrightarrow{\eta} \mathcal{L}_s$, and $\mathcal{L}_b \otimes \mathcal{L}_d \xrightarrow{\lambda} \mathcal{L}_s$. In the special case that all $N_{ab}^c \in \{0,1\}$ and thus junctions are multiplicity free, we have:

$$M^{c,s}_{g,a,d,h,b,e,k} = \sqrt{\frac{d_a d_b d_h d_s}{d_d d_e d_c}} \left[F^s_{kba}\right]^*_{ec} \left[F^s_{bha}\right]_{ed} \left[F^s_{bag}\right]^*_{cd} . \tag{8.1.19}$$

In App. A.8 we verify that the product is associative. One can also check that the generators of the tube algebra that map the untwisted sector to itself, *i.e.*, the elements with $g = h = 1$ in (8.1.15), form a subalgebra[5] that is identical to the fusion algebra.

Tube algebras are finite-dimensional C^*-algebras (see, *e.g.*, [129] for a proof) and so in particular they are semisimple. Given the product in (8.1.17), one constructs the bilinear form K and then the symmetrizer S with respect to the tube algebra using the universal formula (7.1.7). Since the fusion algebra is a subspace of the tube algebra closed under multiplication, we expect the asymmetry with respect to the tube algebra to be bigger or equal to the asymmetry with respect to the fusion algebra.[6] In other words, we expect $\mathsf{Tube}(\mathscr{C})$ to be a more accurate detector of symmetry breaking. We discuss explicit examples of this fact in the next section.

8.2 Interval Hilbert space

The entanglement entropy, and likewise the entanglement asymmetry, of a subsystem is normally defined assuming that the Hilbert space factorizes: $\mathcal{H} = \mathcal{H}_A \otimes \mathcal{H}_B$. Here A is the subsystem of interest, while B is its complement. This allows one to define the reduced density matrix $\rho_A = \mathrm{Tr}_B(\rho)$ from the complete density matrix ρ (that could be pure or mixed), and then compute the entropy or the asymmetry of ρ_A. In quantum field theory one usually takes A to be a spatial subregion, and here we will consider the case that A is an interval. However, in quantum field theory the Hilbert space does not actually factorize. A consequence is that entanglement entropy is divergent and it requires a regularization.

A convenient regularization was proposed in [109]. One constructs a linear map

$$\psi_{\mathcal{B}} \colon \mathcal{H} \to \mathcal{H}_A \otimes \mathcal{H}_B \tag{8.2.1}$$

and computes the entanglement entropy in the image of $\psi_{\mathcal{B}}$. Such a map can be constructed as the path-integral on a strip, in which the lower (or incoming) boundary

[5] By subalgebra we simply mean a subspace of the algebra that is closed under product. We do not require that the identity of the subalgebra be equal to that of the original algebra, which indeed does not happen in this case.

[6] It would be interesting to prove this expectation, or to find a counterexample.

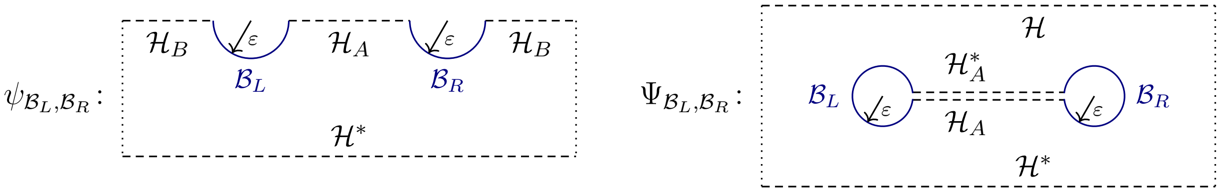

Figure 8.3: Left: the map $\psi_{\mathcal{B}_L,\mathcal{B}_R}\colon \mathcal{H} \to \mathcal{H}_A \otimes \mathcal{H}_B$ constructed with the path-integral on a strip, where $\mathcal{B}_{L,R}$ are boundary conditions at two removed half-discs of radius ε. Right: the map $\Psi_{\mathcal{B}_L,\mathcal{B}_R}\colon \operatorname{End}(\mathcal{H}) \to \operatorname{End}(\mathcal{H}_A)$ constructed via the path-integral on a strip with a finite-size cut, with the same boundary conditions imposed.

has the geometry underlying $\mathcal{H}$, while the upper (or outgoing) boundary is the union of two disjoint parts with geometries underlying $\mathcal{H}_A$ and $\mathcal{H}_B$, respectively. In the case that $\mathcal{H}_A$ is an interval, one removes two small half-discs of radius ε at the two entangling points that bound A, and specifies some boundary conditions $\mathcal{B}_{L,R}$ there.[7] Eventually, the limit $\varepsilon \to 0$ is taken. We depict the setup in Fig. 8.3 left. Given the map $\psi_{\mathcal{B}}$ between Hilbert spaces, one also constructs the linear map

$$\Psi_{\mathcal{B}}\colon \operatorname{End}(\mathcal{H}) \to \operatorname{End}(\mathcal{H}_A) \tag{8.2.2}$$

that acts on density matrices and already includes the partial trace on $\mathcal{H}_B$. It can be constructed as the path-integral on a strip obtained from a copy of $\psi_{\mathcal{B}}$ and a copy of its dual, glued along B. We depict the setup in Fig. 8.3 right. The path-integral constructions of those maps are particularly useful when also the states we want to analyze have a path-integral preparation, as we will see.

Once we have a (generically mixed) state in $\mathcal{H}_A$, we can define asymmetry in the general way described in Sec. 7.1. We need to identify how the symmetry acts on $\mathcal{H}_A$, which is the Hilbert space on an interval with boundary conditions $\mathcal{B}_{L,R}$. Such an action is given by the strip algebra, that we describe next. Note that $\mathcal{H}_A$ could also describe the asymmetry of the full system on an interval with boundary conditions; in this case one would not take the limit $\varepsilon \to 0$. For invertible symmetries, asymmetry with boundaries have been studied in [30, 31].

8.2.1 Strip algebra

The action of the symmetry on the interval Hilbert space is described by the strip algebra $\mathsf{Strip}_{\mathscr{C}}(\mathscr{M})$ [116–118]. Let us first recall how the symmetry properties of boundary conditions are described in terms of *module categories*. In a left-module category $\mathscr{M}$ the simple objects $\mathcal{B}_m$ correspond to right boundary conditions. The

[7] In (8.2.1) we used the compact notation $\mathcal{B}$ to indicate the collection of boundary conditions used.

fusion of simple bulk lines $\mathcal{L}_a$ (from the left) with simple boundaries $\mathcal{B}_m$ is described by a fusion algebra:

$$\mathcal{L}_a \times \mathcal{B}_m = \sum\nolimits_n \tilde{N}_{am}^n \, \mathcal{B}_n \;, \qquad\qquad \text{depicted as} \tag{8.2.3}$$

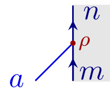

and where the fusion coefficients $\tilde{N}_{am}^n \in \mathbb{N}$. The number $\tilde{N}_{am}^n$ measures the dimension of the vector space of morphisms $\mathrm{Hom}(\mathcal{L}_a \otimes \mathcal{B}_m, \mathcal{B}_n)$, and the index ρ labels a basis of vectors when such a dimension is larger than 1. Simplicity of the objects $\mathcal{B}_m$ and the pivotal relation state that

$$\tilde{N}_{1m}^n = \delta_m^n \;, \qquad\qquad \tilde{N}_{am}^n = \tilde{N}_{\bar{a}n}^m \;. \tag{8.2.4}$$

Associativity of the product $\mathcal{L}_a \times \mathcal{L}_b \times \mathcal{B}_m$ requires

$$\sum\nolimits_p \tilde{N}_{ap}^n \, \tilde{N}_{bm}^p = \sum\nolimits_c N_{ab}^c \, \tilde{N}_{cm}^n \;\equiv\; \tilde{N}_{abm}^n \;. \tag{8.2.5}$$

This means that the matrices $(\tilde{N}_a)^n{}_m$ furnish a nonnegative-integer-valued matrix representation (NIM-rep) of the bulk fusion algebra. There is a change of basis involved in the associativity of the tensor product, described by the $\tilde{F}$-symbols:

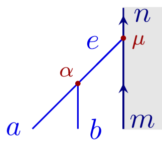

$$= \sum_{p,\nu,\rho} \Big[\tilde{F}_{abm}^n \Big]_{(e;\alpha\mu)(p;\nu\rho)} \tag{8.2.6}$$

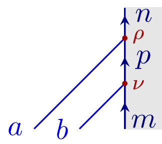

We indicate right boundaries with upward arrows, while all bulk lines run from bottom to top. The $\tilde{F}$-symbols are unitary square matrices of size $\tilde{N}_{abm}^n$ and hence relations similar to (8.2.6) can be obtained using unitarity or the associator diagram. We work in a basis in which $\tilde{F}_{abm}^n = \mathbb{1}$ whenever a or b are equal to 1. The $\tilde{F}$-symbols satisfy a left-module pentagon equation, that also involves the F-symbols, reported in (A.9.1). One can define the quantum dimension $\tilde{d}_m$ of a boundary condition as the disc partition function with that boundary condition. Those quantum dimensions satisfy the relations:

$$d_a \, \tilde{d}_m = \sum\nolimits_n \tilde{N}_{am}^n \, \tilde{d}_n \;. \tag{8.2.7}$$

Thus the boundary quantum dimensions are the components of a common eigenvector of the matrices $\tilde{N}_a$ (with eigenvalues d_a).[8] In a unitary theory $\tilde{d}_m > 0$. Notice that the quantum dimensions $\tilde{d}_m$ are ambiguous by a common rescaling: this is because

[8]Indeed, using that $d_a = d_{\bar{a}}$ and the pivotal relation, (8.2.7) can be rewritten as $d_{\bar{a}} \, \tilde{d}_m = \sum_n \tilde{N}_{\bar{a}n}^m \, \tilde{d}_n$.

the disc partition functions can be rescaled by adding an Euler counterterm to the action.

A right-module category is defined in a similar way, but the objects correspond to left boundary conditions and bulk lines act on them from the right. We describe the associativity of the tensor product with symbols ${}^R\tilde{F}$:

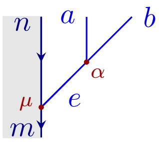

$$= \sum_{p,\nu,\rho} \left[{}^R\tilde{F}^{\bar{m}}_{\bar{n}ab}\right]_{(\bar{p};\rho\nu)(e;\alpha\mu)}$$

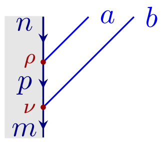

$$. \tag{8.2.8}$$

We use downward arrows to indicate left boundary conditions. The symbols ${}^R\tilde{F}$ satisfy their own right-module pentagon equation, that we report in (A.9.2). For simplicity, we will restrict to the case that the same module is used on the right and on the left. If $[\tilde{F}]$ solves the left-module pentagon equation (A.9.1), then $[{}^R\tilde{F}]$ defined as

$$\left[{}^R\tilde{F}^{\bar{m}}_{\bar{n}ab}\right]_{(\bar{p};\rho\nu)(e;\alpha\mu)} \equiv \left[\tilde{F}^{n}_{abm}\right]^*_{(e;\alpha\mu)(p;\nu\rho)} \qquad \text{or simply} \qquad \left[{}^R\tilde{F}^{\bar{m}}_{\bar{n}ab}\right]_{\bar{p}e} \equiv \left[\tilde{F}^{n}_{abm}\right]^*_{ep} \tag{8.2.9}$$

solves the right-module pentagon equation (A.9.2). Besides, this identification guarantees that if right boundary conditions are bent into left boundary conditions, their junctions with bulk lines can be moved from right to left. We thus regard this $[{}^R\tilde{F}]$ symbols as the right-module version of the left-module $[\tilde{F}]$.

A module category that always exists is the *regular module*, in which we identify the boundary conditions with the bulk lines, $\mathcal{B}_m = \mathcal{L}_m$, and thus also the boundary and bulk fusion algebras are identified: $\tilde{N} = N$. This is the module in which the fusion category $\mathscr{C}$ acts on itself. The $\tilde{F}$-symbols are simply identified with the F-symbols:

$$\text{regular module:} \qquad \tilde{F} = F\ . \tag{8.2.10}$$

For the right module, one could either use the gauge (8.2.9) as we will do, or use a different gauge in which $\tilde{F} = {}^R\tilde{F} = F$. Both solve the right-module pentagon equation (A.9.2).

The strip algebra is generated by the following basis elements:

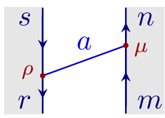

$$\tag{8.2.11}$$

where the line $\mathcal{L}_a$ acts both on the bulk as well as on the boundary by changing the boundary conditions. We will always make the same choice of module category for the left and right boundary condition. It is however easy to extend all formulas to the general case. The dimension of the algebra is

$$\dim\Big(\mathsf{Strip}_{\mathscr{C}}(\mathscr{M})\Big) = \textstyle\sum_{m,r,a,n,s} \tilde{N}^n_{am}\,\tilde{N}^s_{ar}\;. \tag{8.2.12}$$

The product in the algebra is easily computed using the two moves above and (8.1.14):

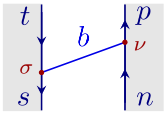

$\times$

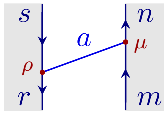

$$= \sum_{c,\tau,\pi} Q^{(c;\tau\pi)}_{m,r,(a;\rho\mu),n,s,(b;\sigma\nu),p,t}$$

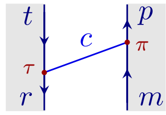

, (8.2.13)

where

$$Q^{(c;\tau\pi)}_{m,r,(a;\rho\mu),n,s,(b;\sigma\nu),p,t} = \textstyle\sum_\alpha \sqrt{\dfrac{d_a d_b}{d_c}}\,\left[\tilde{F}^t_{bar}\right]_{(c;\alpha\tau)(s;\rho\sigma)}\left[\tilde{F}^p_{bam}\right]^*_{(c;\alpha\pi)(n;\mu\nu)}\;. \tag{8.2.14}$$

The sum is over a basis of morphisms $\mathcal{L}_b \otimes \mathcal{L}_a \xrightarrow{\alpha} \mathcal{L}_c$. With no multiplicities this simplifies to

$$Q^c_{m,r,a,n,s,b,p,t} = \sqrt{\frac{d_a d_b}{d_c}}\;\left[\tilde{F}^t_{bar}\right]_{cs}\left[\tilde{F}^p_{bam}\right]^*_{cn}\;. \tag{8.2.15}$$

We verify in App. A.9 that such a product is associative.

Since, in our context, the boundary conditions are introduced as a tool to regularize the entanglement entropy, it is desirable to use symmetry-invariant boundary conditions, in order not to contaminate the measurement of symmetry breaking coming from the state with an effect due to the boundaries.[9] The type of symmetry-invariant boundary conditions available in a given theory depends on the structure of the symmetry, and in particular on the presence of 't Hooft anomalies [122, 123]. For noninvertible symmetries, one can distinguish three situations [68]: theories with strongly-symmetric simple boundaries, theories with only weakly-symmetric simple boundaries, and theories with no symmetric simple boundaries. We will discuss these three cases in turn.

8.2.2 Strongly-symmetric boundary conditions

The most favorable case is when there exists a module category made of a single simple boundary. Such a boundary condition is automatically symmetry-invariant, meaning that it is invariant (up to rescaling) under parallel fusion with the lines

[9] On the other hand, as previously mentioned, it is an interesting question to study the asymmetry of boundary conditions. This has been analyzed in [30, 31].

$\mathcal{L}_a \in \mathscr{C}$. Yet, there might be multiple junctions between a given bulk line $\mathcal{L}_a$ and the boundary. Such a boundary condition was called "strongly-symmetric" in [68]. It makes the definition and computation of entanglement asymmetry particularly simple. Such a boundary condition exists if and only if the symmetry is free from 't Hooft anomalies.[10]

A strongly-symmetric boundary condition is described by a module category in which there is a single simple object: $\mathcal{B}$. Since the boundary index takes a single value, we henceforth indicate it with a dot. The fusion coefficients and the $\tilde{F}$-symbols simplify:

$$\tilde{N}_{1\,\cdot}^{\,\cdot} = 1 \;, \qquad \tilde{N}_{a\,\cdot}^{\,\cdot} = \tilde{N}_{\bar{a}\,\cdot}^{\,\cdot} = d_a \geq 1 \;, \qquad \Big[\tilde{F}_{ab\,\cdot}^{\,\cdot}\Big]^*_{(c;\delta\rho)(\,\cdot\,;\nu\mu)} \equiv m_{a\mu,b\nu}^{c\rho;\delta} \;. \tag{8.2.16}$$

The fact that the boundary fusion coefficients are equal to the quantum dimensions immediately follows from (8.2.7). Thus a necessary condition for the existence of strongly-symmetric boundary conditions in $\mathscr{C}$ is that all quantum dimensions are integer. Notice that when $\tilde{N}_{a\,\cdot}^{\,\cdot} > 1$ there are multiple junctions between the line $\mathcal{L}_a$ and the boundary. It turns out that there is a one-to-one correspondence between:

- left-module categories over $\mathscr{C}$ with only one simple object;
- fiber functors of the fusion category $\mathscr{C}$;
- maximal haploid algebra objects $\mathfrak{A}$ in $\mathscr{C}$.[11]

The first entry corresponds to a strongly-symmetric boundary condition. The second entry corresponds to a trivially-gapped phase (*a.k.a.* SPT phase, or invertible TQFT) for the symmetry, and thus the symmetry is non-anomalous. We see that strongly-symmetric boundary conditions exist if and only if the symmetry is non-anomalous. The third entry corresponds to a maximal gauging of the whole symmetry (possible only in the absence of anomalies).

The redefinitions in (8.2.16) make the correspondence with the maximal algebra object $\mathfrak{A}$ explicit. This is

$$\mathfrak{A} = \bigoplus\nolimits_a d_a \, \mathcal{L}_a \;, \tag{8.2.17}$$

[10] More precisely, when the 't Hooft anomaly vanishes there always exists a module category with a single simple object, that can describe a strongly-symmetric boundary condition. Whether such a boundary condition actually exists in a given theory depends on the theory itself and on extra properties we might require to the boundary condition, for instance conformality. A similar comment applies to the regular module category that always exists, irrespective of 't Hooft anomalies.

[11] More precisely, one is typically interested in equivalence classes of the objects listed above. The relevant equivalence relations are, respectively: equivalence of $\mathscr{C}$-module categories; equivalence of tensor functors; Morita equivalence of algebras. In particular, the last one turns out to be the correct equivalence that corresponds to equivalent module categories, as opposed to the stronger isomorphism of algebras [69, 115].

where $d_a \in \mathbb{N}$ counts the dimension of $\mathrm{Hom}(\mathcal{L}_a, \mathfrak{A})$.[12] The symbols m are the components of the multiplication morphism $m \colon \mathfrak{A} \otimes \mathfrak{A} \to \mathfrak{A}$:

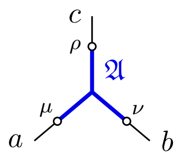

$$= \sum_{\delta} m^{c\rho;\delta}_{a\mu,b\nu} \tag{8.2.18}$$

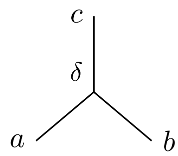

The requirement that m be associative, namely that $m\big(m(x \otimes y) \otimes z\big) = m\big(x \otimes m(y \otimes z)\big)$ for all $x, y, z \in \mathfrak{A}$, when written in components, boils down to the constraint [130]:

$$\sum\nolimits_{e,\epsilon,\alpha,\beta} m^{e\epsilon;\alpha}_{a\mu,b\nu}\, m^{d\sigma;\beta}_{e\epsilon,c\rho} \left[F^d_{abc}\right]_{(e;\alpha\beta)(f;\gamma\delta)} = \sum\nolimits_{\phi} m^{d\sigma;\delta}_{a\mu,f\phi}\, m^{f\phi;\gamma}_{b\nu,c\rho} \,. \tag{8.2.19}$$

Using the correspondence in (8.2.16) and unitarity, this equation is equivalent to the left-module pentagon equation (A.9.1) (for module categories with one simple object). Notice that a fusion category $\mathscr{C}$ can admit multiple inequivalent maximal algebra objects $\mathfrak{A}$: they will have the same decomposition (8.2.17), but would differ in the product m.[13]

The corresponding strip algebra is generated by the basis elements

$$H_{(a;\rho\mu)} \equiv \tag{8.2.20}$$

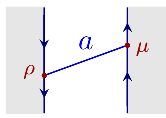

and the product is given by

$$\begin{aligned} Q^{(c;\tau\pi)}_{(a;\rho\mu)(b;\sigma\nu)} &= \sum\nolimits_{\alpha} \sqrt{\frac{d_a d_b}{d_c}} \left[\tilde{F}^{\,\cdot}_{ba\,\cdot}\right]_{(c;\alpha\tau)(\,\cdot\,;\rho\sigma)} \left[\tilde{F}^{\,\cdot}_{ba\,\cdot}\right]^*_{(c;\alpha\pi)(\,\cdot\,;\mu\nu)} \\ &= \sum\nolimits_{\alpha} \sqrt{\frac{d_a d_b}{d_c}} \left(m^{c\tau;\alpha}_{b\sigma,a\rho}\right)^* \left(m^{c\pi;\alpha}_{b\nu,a\mu}\right) . \end{aligned} \tag{8.2.21}$$

The sum is over a basis of morphisms $\mathcal{L}_b \otimes \mathcal{L}_a \xrightarrow{\alpha} \mathcal{L}_c$. This defines a finite-dimensional semisimple algebra $\mathcal{A}$, whose symmetrizer can be constructed using the universal formula (7.1.7).

[12] Haploid means that $\dim\big(\mathrm{Hom}(\mathcal{L}_1, \mathfrak{A})\big) = 1$.

[13] The construction is more general, see App. A of [68] as well as [65, 115, 131]. For any module, choose a simple object (a boundary), then the so-called internal Hom construction produces a (in general not maximal) haploid algebra object in $\mathscr{C}$. The algebra objects one obtains from the various simple objects (boundaries) of a given module can be different, but are all Morita equivalent. All haploid, semisimple, indecomposable algebra objects are obtained in this way, by considering all possible indecomposable module categories. Indeed, from the algebra object one can construct a module category such that the internal Hom construction gives back that algebra.

8.2.3 Weakly-symmetric boundary conditions

When strongly-symmetric boundary conditions do not exist, we are forced to consider modules with multiple simple objects. This means that we have to deal with a set of boundary conditions that form a "multiplet" under fusion with the bulk symmetry lines. It might happen, however, that the module contains one particular simple boundary $\hat{\mathcal{B}}$ (equal to $\mathcal{B}_m$ for a particular value $m = \hat{m}$) such that the fusion of any bulk line $\mathcal{L}_a$ with $\hat{\mathcal{B}}$ contains $\hat{\mathcal{B}}$ itself: $\mathcal{L}_a \otimes \hat{\mathcal{B}} \supseteq \hat{\mathcal{B}}$. This happens when

$$\tilde{N}_{a\hat{m}}^{\hat{m}} \geq 1 \qquad \text{for all } a \,. \tag{8.2.22}$$

This means that every bulk like $\mathcal{L}_a$ has at least one topological junction with the boundary $\hat{\mathcal{B}}$. Such a boundary condition was called "weakly-symmetric" in [68]. It allows us to restrict to a subspace of the strip algebra in which we have all bulk lines but only the boundary $\hat{\mathcal{B}}$, and that is closed under strip-algebra product. When multiple junctions exist, $N_{a\hat{m}}^{\hat{m}} > 1$, in general one has to keep all of them in order to obtain a closed algebra.[14] We call the resulting algebra a *reduced strip algebra*.

Note that the reduced strip algebra always admits a symmetrizer. Indeed, its C^*-structure is simply the restriction of the C^*-structure of the full strip algebra. In particular, the C^* condition (A.6.23) is still satisfied and the reduced strip algebra is thus semisimple and strongly separable. The symmetrizer can be constructed using the universal formula (7.1.7).

It turns out [68] that a fusion category $\mathscr{C}$ admits a weakly-symmetric boundary condition if and only if there exists a (not necessarily maximal) haploid algebra object

$$\mathfrak{A} = \bigoplus_a N_a^{(\mathfrak{A})} \mathcal{L}_a \qquad\qquad \text{such that } N_a^{(\mathfrak{A})} \geq 1 \text{ for all } a \,. \tag{8.2.23}$$

We introduced the nonnegative integer numbers $N_a^{(\mathfrak{A})} \equiv \dim\Big(\mathrm{Hom}(\mathcal{L}_a, \mathfrak{A})\Big)$, that for haploid algebra objects always satisfy $N_a^{(\mathfrak{A})} \leq d_a$ [132]. The connection between boundaries and algebra objects goes through the internal Hom construction (see fn. 13). Haploid algebra objects are the noninvertible generalization of anomaly-free subgroups of an invertible symmetry group with a choice of discrete torsion. Thus, a weakly-symmetric boundary condition exists if and only if there exists a gauging of $\mathscr{C}$ that involves all simple lines in $\mathscr{C}$. When the gauging is maximal, $N_a^{(\mathfrak{A})} = d_a$, which is possible only in the absence of 't Hooft anomalies, the boundary condition is actually strongly symmetric.

[14] In some cases it might be possible to restrict to a subspace of the junction space.

8.2.4 Non-symmetric boundary conditions

It might happen that a given theory does not admit neither strongly- nor weakly-symmetric boundary conditions, either because the symmetry has a severe enough 't Hooft anomaly to prevent them, or because we insist on some extra property, for instance conformality, of the boundary conditions. In such cases, the boundary condition at the entangling surface necessarily breaks the symmetry, implying a nonzero asymmetry on subsystems even when the original state is invariant. To overcome this, and to detect symmetry breaking of states independently of the boundary conditions at the entangling surface, we consider a map $\Psi_{\mathcal{B}}$ (see (8.2.2)) that produces a statistical mixture of density matrices with different boundary conditions. We show that there exists a choice of coefficients such that the invariant state prepared by the empty path-integral exhibits indeed vanishing asymmetry. The procedure can be carried out for any choice of module category $\mathscr{M}$, as we show here. However, in the examples in chapter 10 we specialize to the regular module category.

At a formal level, we could define a symmetric "composite" boundary condition $|\mathcal{B}_{\mathsf{S}}\rangle$ if we allow for arbitrary linear combinations of boundaries (which we denote here as kets because we regard them as element of a vector space):

$$|\mathcal{B}_{\mathsf{S}}\rangle = \sum\nolimits_m \tilde{d}_m \, |\mathcal{B}_m\rangle \qquad \text{so that} \qquad \mathcal{L}_a \, |\mathcal{B}_{\mathsf{S}}\rangle = d_a \, |\mathcal{B}_{\mathsf{S}}\rangle \ . \tag{8.2.24}$$

Here d_a and $\tilde{d}_m$ are the bulk and boundary quantum dimensions, and we used (8.2.7) to prove the second equality.[15]

We exploit this idea — in the case of unitary and normalizable CFTs and insisting on conformal boundary conditions — to construct a symmetric density matrix ρ on the interval Hilbert space starting from an invariant state, even in the absence of invariant simple boundary conditions. Consider a module category $\mathscr{M}$, and let ρ_{mn} be the reduced density matrix of the vacuum (or of another state invariant under the symmetry) constructed with simple boundary conditions $\mathcal{B}_m, \mathcal{B}_n \in \mathscr{M}$. We construct an "average" over boundary conditions as follows:

$$\rho = \frac{1}{D} \sum_{m,n \,\in\, \mathrm{Irr}(\mathscr{M})} \tilde{d}_m \, \tilde{d}_n \, \rho_{mn} = \frac{1}{D} \sum_{m,n \,\in\, \mathrm{Irr}(\mathscr{M})} \frac{\tilde{d}_m \, \tilde{d}_n}{Z_{mn}} \, \tilde{\rho}_{mn} \ , \qquad D = \Big(\sum\nolimits_{m \in \mathrm{Irr}(\mathscr{M})} \tilde{d}_m \Big)^2 . \tag{8.2.25}$$

Here $\tilde{\rho}_{mn}$ is the unnormalized density matrix produced by the path-integral realization of $\Psi_{\mathcal{B}}$ in (8.2.2) with boundary conditions $\mathcal{B}_m$ and $\mathcal{B}_n$, as depicted in Fig. 10.8, while $Z_{mn} = \mathrm{Tr}(\tilde{\rho}_{mn})$. We show that in the limit $\varepsilon \to 0$, ρ commutes with the strip algebra

[15] One also uses the pivotal relation: $\mathcal{L}_a \, |\mathcal{B}_{\mathsf{S}}\rangle = \sum_{mn} \tilde{d}_m \tilde{N}^n_{am} \, |\mathcal{B}_n\rangle = \sum_{mn} \tilde{N}^m_{\bar{a}n} \tilde{d}_m \, |\mathcal{B}_n\rangle$, as well as $d_a = d_{\bar{a}}$.

and thus it has vanishing asymmetry. The interval Hilbert space $\mathcal{H}$ decomposes in the various sectors with simple boundary conditions as $\mathcal{H} = \bigoplus_{m,n} \mathcal{H}_{m,n}$. We want to show that, for every $O \in \mathrm{End}(\mathcal{H})$:

$$\lim_{\varepsilon\to 0} \mathrm{Tr}\Big(\rho\, H^{r,s}_{m,n}\, O\Big) = \lim_{\varepsilon\to 0} \mathrm{Tr}\Big(H^{r,s}_{m,n}\, \rho\, O\Big)\ . \tag{8.2.26}$$

Here $H^{r,s}_{m,n}$ is a basis element of the strip algebra in $\mathrm{Hom}(\mathcal{H}_{m,n}, \mathcal{H}_{r,s})$. By matching boundary conditions and using (8.2.25), the previous equation is equivalent to

$$\lim_{\varepsilon\to 0} \frac{\tilde{d}_r\, \tilde{d}_s}{Z_{rs}}\ \mathrm{Tr}\Big(\tilde{\rho}_{rs}\, H^{r,s}_{m,n}\, O^{m,n}_{r,s}\Big) = \lim_{\varepsilon\to 0} \frac{\tilde{d}_m\, \tilde{d}_n}{Z_{mn}}\ \mathrm{Tr}\Big(H^{r,s}_{m,n}\, \tilde{\rho}_{mn}\, O^{m,n}_{r,s}\Big)\ , \tag{8.2.27}$$

where $O^{m,n}_{r,s}$ is the component of O in $\mathrm{Hom}(\mathcal{H}_{r,s}, \mathcal{H}_{m,n})$. Notice that $\tilde{\rho}_{rs}\, H^{r,s}_{m,n} = H^{r,s}_{m,n}\, \tilde{\rho}_{mn}$ since, by assumption, lines can be slid past the matrices $\tilde{\rho}_{mn}$ (even for finite ε). Thus, because the operators $O^{m,n}_{r,s}$ are completely arbitrary, we only need to check that

$$\lim_{\varepsilon\to 0} \frac{\tilde{d}_r\, \tilde{d}_s}{Z_{rs}} = \lim_{\varepsilon\to 0} \frac{\tilde{d}_m\, \tilde{d}_n}{Z_{mn}}\ . \tag{8.2.28}$$

This equation is indeed satisfied because

$$\lim_{\varepsilon\to 0} Z_{rs} = \tilde{d}_r\, \tilde{d}_s\, Z(\mathbb{C})\ , \tag{8.2.29}$$

where $Z(\mathbb{C})$ is the Euclidean partition function on the plane. This can be argued as follows. Recall that Z_{rs} is the partition function on the plane with two discs of radius ε removed (see Fig. 10.8). The discs are centered, say, at $z = 0$ and $z = \ell$. Following [109], this geometry can be mapped to a cylinder of length $2\log(\ell/\varepsilon)$ with the transformation $w = \log\big(z/(\ell - z)\big)$. The partition function can then be rewritten as a closed-channel amplitude:

$$Z_{rs} = W \left\langle s \right| (\varepsilon/\ell)^{L_0 + \bar{L}_0 - c/12)} \left| r \right\rangle\ , \tag{8.2.30}$$

where W is a Weyl factor, while $|r\rangle, |s\rangle$ are Cardy states. Inserting a resolution of the identity with eigenstates of the cylinder Hamiltonian, in the limit $\varepsilon \to 0$ (which corresponds to a cylinder of infinite length) only the ground state $|0\rangle$ remains.[16] Thus one gets

$$\lim_{\varepsilon\to 0} Z_{rs} = \lim_{\varepsilon\to 0} g_r\, g_s\, W \left\langle 0 \right| (\varepsilon/\ell)^{L_0 + \bar{L}_0 - c/12} \left| 0 \right\rangle\ , \tag{8.2.31}$$

where $g_r \equiv \langle r|0|r|0\rangle$ is the g-factor [133]. Because of the state/operator correspon-

[16] For unitary CFTs with discrete spectrum, $|0\rangle$ is the ground state. More generally, $|0\rangle$ is the lowest-dimension state that overlaps with the Cardy states $|r\rangle, |s\rangle$. See the discussion in [109].

dence, the term $\lim_{\varepsilon\to 0}\left\langle 0\right| (\varepsilon/\ell)^{L_0+\bar{L}_0-c/12} \left|0\right\rangle$ becomes the partition function of an infinite cylinder, with no insertions at infinity. We can then undo the Weyl transformation, reabsorbing the factor W, to obtain $\lim_{\varepsilon\to 0} Z_{rs} = g_r\, g_s\, Z(\mathbb{C})$. The g-factors can be interpreted as disc partition functions [134] for a specific choice of Euler counterterm, and thus they satisfy the equation of boundary quantum dimensions (8.2.7) (see also [135]). Hence we can choose a normalization such that $\tilde{d}_r = g_r$, and obtain (8.2.29).[17]

Large subsystem limits. Given the asymmetry of some state, computed on the interval subsystem using one of the types of boundary conditions discussed above, what is the relation between its large subsystem limit and the asymmetry of the full system, computed using the fusion or tube algebras?

In Sec. 10.1 we analyze invertible group-like symmetries. In particular, we consider excited CFT states created by the insertion of local operators in Euclidean time. We find that the entanglement and Rényi asymmetries on an interval, as long as our "averaging" protocol is used, are independent of the choice of boundary conditions. Moreover, for untwisted states, the large subsystem limits of the asymmetries coincide with the asymmetries of the full system, computed with respect to either the fusion or the tube algebra (since they coincide for untwisted states).

In Sec. 10.3 we study certain excited states in two copies of the Ising CFT, utilizing the $\mathsf{Rep}(H_8)$ (*a.k.a.* $\mathbb{Z}_2\times\mathbb{Z}_2$ Tambara–Yamagami) noninvertible symmetry that admits a strongly-symmetric boundary condition. The result is similar: the second Rényi entropy on the interval subsystem asymptotes in the large subsystem limit to the second Rényi entropy of the full system, computed with respect to the tube algebra (not the fusion algebra, which in general is different).

On the other hand, in Secs. 10.2 and 10.4 we study certain excited states in the Ising CFT, utilizing its Ising fusion category (*a.k.a.* $\mathbb{Z}_2$ Tambara–Yamagami) symmetry, which does not admit symmetric boundary conditions and which then forces us to resort to the averaging protocol. This time we find that the large subsystem limit of the second Rényi asymmetry on an interval is qualitatively similar to, but slightly smaller than, the asymmetry of the full system with respect to the tube algebra. A similar behavior is found in Sec. 10.4.1 when studying the Fibonacci fusion category symmetry with its weakly-symmetric boundary condition. It would be interesting to understand these results more systematically.

[17] With a generic normalization (*i.e.*, choice of Euler counterterm), the g-factors g_m are proportional to the boundary quantum dimensions $\tilde{d}_m$ and thus they satisfy (8.2.7). This implies that $\lim_{\varepsilon\to 0}\, \tilde{d}_m\tilde{d}_n/Z_{mn}$ is independent from m, n. This is enough to prove (8.2.28), even with generic normalization.

8.2.5 Symmetrizer from (weak) Hopf algebra structure

We can find an alternative, but equivalent, formula for the symmetrizer by leveraging the following reasoning that holds in the invertible case for a symmetry group G (or equivalently, for the group algebra $\mathbb{C}[G]$). Consider a Hilbert space $\mathcal{H}$ that carries a representation of G. A density matrix $\rho \in \mathrm{End}(\mathcal{H})$ is an element of $\mathcal{H} \otimes \mathcal{H}^\vee$ (the second factor being the dual space). This tensor product itself carries a representation of G, which decomposes into a sum of irreducible representations. Then, the symmetrization operation is reproduced by applying to this space the projector onto the trivial representation. The obstacle in generalizing this reasoning to the noninvertible case is that for a generic algebra $\mathcal{A}$ the concepts of tensor product of representations, of dual (or conjugate) representation, and of trivial representation, are not defined. In the special case that the algebra is *Hopf*, however, these concepts are available and the symmetrizer can be written as the projector onto the trivial representation. Moreover, we will see that if the algebra is only weak Hopf but its antipode map is involutive (such an algebra is called *weak Kac* [136]), a formula similar to that of the Hopf case applies, even though it lacks that interpretation. It was shown in [116, 117] that the strip algebras are always weak Hopf, therefore when they satisfy the weak Kac condition we can apply the strategy above to the case of the interval Hilbert space.[18]

Let us first consider the case that a strip algebra $\mathcal{A}$ is constructed using a strongly-symmetric boundary condition. We can show that such a strip algebra is a Hopf algebra. We provide definitions and basic properties in App. A.7 and prove the claim in App. A.7.1.

Concisely, a Hopf algebra comes equipped with (besides its unit and its associative product) the following algebra homomorphisms: a coassociative coproduct $\Delta\colon \mathcal{A} \to \mathcal{A} \otimes \mathcal{A}$ such that $\Delta(\mathbb{1}) = \mathbb{1} \otimes \mathbb{1}$ and a counit $\epsilon\colon \mathcal{A} \to \mathbb{C}$. In addition, it comes with an antipode $S\colon \mathcal{A} \to \mathcal{A}$, which is a linear algebra anti-homomorphism, *i.e.*, $S(xy) = S(y)\, S(x)$. In finite-dimensional semisimple Hopf algebras one proves that $S \circ S = \mathrm{id}$. The one-dimensional "trivial" representation $r_\epsilon\colon \mathcal{A} \to \mathrm{End}(\mathbb{C}) \cong \mathbb{C}$, which behaves as the identity under the tensor product of representations, is provided by the counit:

$$r_\epsilon(x) = \epsilon(x) \qquad \forall\, x \in \mathcal{A}\,. \tag{8.2.32}$$

The tensor product of representations is constructed using the coproduct Δ. Given two representations $r_1\colon \mathcal{A} \to \mathrm{End}(V_1)$ and $r_2\colon \mathcal{A} \to \mathrm{End}(V_2)$ on vector spaces $V_{1,2}$,

[18] On the contrary, the tube algebra is in general not a weak Hopf algebra. One can still define a tensor product of representations using the so-called Day convolution product [137]. We do not explore such a possibility here.

their tensor product representation $r_{12}\colon \mathcal{A} \to \mathrm{End}(V_1 \otimes V_2)$ is defined as

$$r_{12} = (r_1 \otimes r_2) \circ \Delta \qquad i.e. \qquad r_{12}(x)\, v_1 \otimes v_2 = \sum\nolimits_i \Big[r_1\Big(x^i_{(1)}\Big)\, v_1 \Big] \otimes \Big[r_2\Big(x^i_{(2)}\Big)\, v_2 \Big] \,, \tag{8.2.33}$$

where $v_{1,2} \in V_{1,2}$ and we used Sweedler's notation to write $\Delta(x) = \sum_i x^i_{(1)} \otimes x^i_{(2)}$. Using (A.7.2), one sees that the representation r_ϵ multiplies trivially with any other representation. Finally, given a representation $r\colon \mathcal{A} \to \mathrm{End}(V)$, its conjugate representation $r^*\colon \mathcal{A} \to \mathrm{End}(V^\vee)$ is constructed using the antipode:

$$\Big\langle r^*(x)\, f,\, v \Big\rangle \equiv \Big\langle f,\, r\Big(S(x)\Big)\, v \Big\rangle \qquad\qquad \forall\, x \in \mathcal{A}, \quad v \in V, \quad f \in V^\vee, \tag{8.2.34}$$

where the angular brackets denote the evaluation of a functional on a vector. More compactly, this can be written as $r^* = (r \circ S)^\mathsf{T}$. Using (A.7.6) one sees that the trivial representation is self-conjugate.

Associated to r_ϵ there is a minimal central idempotent (MCI) $P_\epsilon \in \mathcal{A}$, *i.e.*, the projector to the trivial representation. It satisfies[19]

$$P_\epsilon\, x = x\, P_\epsilon = \epsilon(x)\, P_\epsilon \qquad\qquad \forall\, x \in \mathcal{A}\,. \tag{8.2.35}$$

Taking x equal to one of the MCIs P_i (*i.e.*, a projector to an irreducible representation of $\mathcal{A}$), one obtains $\epsilon(P_i) = \delta_{i\epsilon}$, confirming that P_ϵ projects to the trivial representation.

We claim that the symmetric separability idempotent can be written as

$$e = (\mathrm{id} \otimes S) \circ \Delta(P_\epsilon) \tag{8.2.36}$$

which was proven to be a separability idempotent for a Hopf algebra in [138]. When acting on the space $\mathcal{H} \otimes \mathcal{H}^\vee \cong \mathrm{End}(\mathcal{H})$, this operator is precisely the action of the projector to the trivial representation P_ϵ on density matrices. More explicitly:

$$\rho_\mathsf{S} = \sum\nolimits_i (P_\epsilon)^i_{(1)}\; \rho\; S\Big((P_\epsilon)^i_{(2)} \Big) \tag{8.2.37}$$

where $\Delta(P_\epsilon) = \sum_i (P_\epsilon)^i_{(1)} \otimes (P_\epsilon)^i_{(2)}$. The disadvantage of this formula is that one needs to explicitly construct the projector P_ϵ to the trivial representation. In App. A.7.2 we prove that (8.2.37) satisfies properties 1. – 4. listed in 7.1. The expression in (8.2.37) is also universal, in the sense that it is written solely in terms of the elements

[19] The first equality is the centrality of projectors. For the second equality, since $P_\epsilon^2 = P_\epsilon$ and the trivial representation is one-dimensional, then P_ϵ is a basis for the image of the projector in the regular representation (recall that a 1d representation occurs only once inside the regular representation), and thus $P_\epsilon\, x = \alpha(x)\, P_\epsilon$ for some $\alpha \in \mathbb{C}$. Applying ϵ to both sides we find $\alpha(x) = \epsilon(x)$.

of $\mathcal{A}$. As we commented at the end of Sec. 7.1, this completely fixes the symmetrizer and thus (8.2.37) agrees with (7.1.7). Notice that the universal formula (7.1.7) only depends on the product structure on $\mathcal{A}$, therefore different Hopf algebras that share the same product structure will give rise, through (8.2.37), to the same symmetrizer.

For weak Hopf algebras a similar recipe exists to compute the symmetric separability idempotent, provided they satisfy the additional condition $S^2 = \mathrm{id}$ (such algebras are called weak Kac).[20] Referring to [139], one introduces the left and right projectors $\Pi^{\mathrm{L}}, \Pi^{\mathrm{R}} \colon \mathcal{A} \to \mathcal{A}$ as

$$\Pi^{\mathrm{L}}(x) = \textstyle\sum_i \epsilon\Big(\mathbb{1}^i_{(1)}\, x\Big)\, \mathbb{1}^i_{(2)} \;, \qquad\qquad \Pi^{\mathrm{R}}(x) = \textstyle\sum_i \mathbb{1}^i_{(1)}\, \epsilon\Big(x\, \mathbb{1}^i_{(2)}\Big) \;, \tag{8.2.38}$$

acting on $x \in \mathcal{A}$. Then one defines the left and right normalized integrals as those elements $\ell, r \in \mathcal{A}$ such that

$$x\,\ell = \Pi^{\mathrm{L}}(x)\,\ell \;, \qquad \Pi^{\mathrm{L}}(\ell) = \mathbb{1} \;, \qquad\quad \text{or} \qquad\quad r\,x = r\,\Pi^{\mathrm{R}}(x) \;, \qquad \Pi^{\mathrm{R}}(r) = \mathbb{1} \;, \tag{8.2.39}$$

for all $x \in \mathcal{A}$. In general, being a left integral does not imply being a right integral. When this happens, one talks about *Haar integrals*. That is, a Haar integral h is defined as a simultaneous left and right normalized integral. When it exists, it is unique. The necessary and sufficient conditions for its existence are spelled out in Th. 3.27 of [139]. Such conditions are indeed satisfied under our working hypotheses.[21] The symmetric separability idempotent is then given by

$$e = (\mathrm{id} \otimes S) \circ \Delta(h) \;, \tag{8.2.40}$$

where $h \in \mathcal{A}$ is the Haar integral. In App. A.7.2 we verify that such an expression satisfies the properties 1. – 4. and thus, being also universal, it agrees with (7.1.7).[22]

Note that in the case of a Hopf algebra, both the left and right projectors reduce to

$$\Pi^{\mathrm{L}}(x) = \Pi^{\mathrm{R}}(x) = \epsilon(x)\,\mathbb{1} \tag{8.2.41}$$

[20]This is not the case for a generic strip algebra (see [111], eq. (D.14)). We thank the authors of [111] for bringing to our attention a few inaccuracies on this point in the first version of this manuscript.

[21]In the notation of Th. 3.27 in [139], since we are assuming $S^2 = \mathrm{id}$, we have $g = \mathbb{1}$. Then, the second condition therein is satisfied because the trace of $\mathbb{1}$ in any representation is the dimension of that representation.

[22]Note that, had we not required the property $S^2 = \mathrm{id}$, the object (8.2.40) could still be defined. However, the resulting separability idempotent would not be symmetric. Hence, the symmetrized density matrix will fail to satisfy property 4. In this case, the existence of the Haar integral is guaranteed provided the weak Hopf algebra also possesses a C^*-structure compatible with the former, see Th. 4.5 of [139].

because $\Delta(\mathbb{1}) = \mathbb{1} \otimes \mathbb{1}$. Then the Haar integral h is equal to the projector P_ϵ.

Chapter 9

Spontaneous symmetry breaking

A natural application of entanglement asymmetry is to detect spontaneous symmetry breaking in gapped phases. In the far IR, a gapped phase is described by a topological field theory on which the symmetry acts. Therefore, for a given fusion category $\mathscr{C}$, the possible indecomposable and inequivalent (from the symmetry point of view) two-dimensional gapped phases are in one-to-one correspondence with indecomposable two-dimensional $\mathscr{C}$-symmetric TQFTs. In turn, the latter are in one-to-one correspondence with indecomposable module categories $\mathscr{M}$ for $\mathscr{C}$ [140]. We can then use entanglement asymmetry to try to distinguish the various phases.

Consider a 2d gapped phase described by a certain 2d $\mathscr{C}$-symmetric TQFT in the IR, and let $\mathscr{M}$ be the corresponding left-module category. On the circle S^1 the TQFT has a finite number of states. If the symmetry is unbroken, the circle Hilbert space is one-dimensional and the entanglement asymmetry with respect to the fusion algebra vanishes.[1] On the other hand, when a finite symmetry is spontaneously broken we expect a higher-dimensional circle Hilbert space on which the symmetry acts. We are not interested in computing the asymmetry of generic vectors in that Hilbert space, but only of very special vectors that we call "vacua": these are the states that satisfy the cluster decomposition property. Such states form a preferred basis of the Hilbert space. It turns out that they are in correspondence with the simple boundaries $\mathcal{B}_m$ of the corresponding module category $\mathscr{M}$, and can be constructed using open/closed duality [131]: one simply considers the cylinder with the boundary condition $\mathcal{B}_m$ in the past, as in Fig. 9.1 left.

To prove that the states created by simple boundaries satisfy cluster decomposition

[1] Here we only consider indecomposable gapped phases.

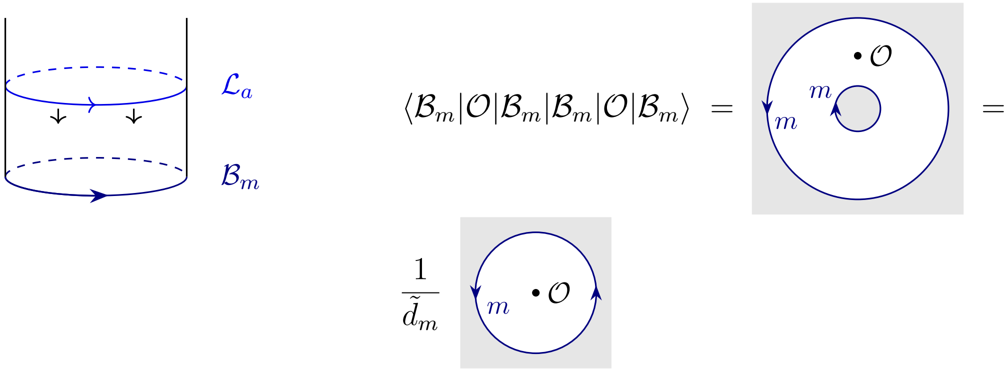

Figure 9.1: Left: the clustering states, or vacua, $|\mathcal{B}_m\rangle$ on the circle are created by the simple boundaries. Right: Correlation functions in those states are computed by disc partition functions.

one uses a boundary crossing relation proven in [131]:

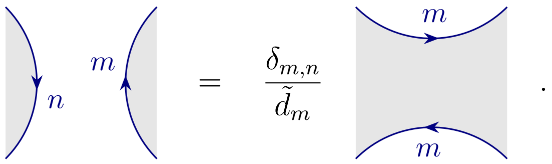

(9.0.1)

A correlator $\langle \mathcal{B}_m | \mathcal{O} | \mathcal{B}_m \rangle$ is the annulus partition function with boundaries $\mathcal{B}_m$ and with the insertion of a local operator $\mathcal{O}$, as in Fig. 9.1 right. Using the crossing relation, such a correlator is equal to $1/\tilde{d}_m$ times the disc one-point function of $\mathcal{O}$ with boundary $\mathcal{B}_m$, that we call $Z_{D_2}[\mathcal{O}]$. If $\mathcal{O}$ is the identity operator, the latter is equal to $\tilde{d}_m$ and thus the correlator is normalized. The crossing relation can then be used to break a disc into two discs, hence one obtains:

$$\langle \mathcal{B}_m | \mathcal{O}_1 \mathcal{O}_2 | \mathcal{B}_m \rangle = \frac{1}{\tilde{d}_m} Z_{D_2}[\mathcal{O}_1 \mathcal{O}_2] = \frac{1}{\tilde{d}_m^2} Z_{D_2}[\mathcal{O}_1] \, Z_{D_2}[\mathcal{O}_2] = \langle \mathcal{B}_m | \mathcal{O}_1 | \mathcal{B}_m \rangle \, \langle \mathcal{B}_m | \mathcal{O}_2 | \mathcal{B}_m \rangle \, . \tag{9.0.2}$$

This shows that in the states $|\mathcal{B}_m\rangle$ all correlation functions are equal to products of one-point functions, which is cluster decomposition for topological theories.

The fusion category $\mathscr{C}$ acts on the untwisted circle Hilbert space according to its fusion algebra, as described in Sec. 8.1. As is clear from Fig. 9.1 left, the action of the lines on the states is dictated by the fusion coefficients $\tilde{N}_{am}^n$ (8.2.3) of the corresponding module category $\mathscr{M}$:

$$\mathcal{L}_a \, |\mathcal{B}_m\rangle = \textstyle\sum_n \tilde{N}_{am}^n \, |\mathcal{B}_n\rangle \, . \tag{9.0.3}$$

Thus the clustering states of a gapped phase furnish a NIM-rep of the fusion algebra. This allows one to easily compute the entanglement asymmetry of the various vacua.

In chapter 10 we analyze various examples of spontaneous symmetry breaking and compute the asymmetry of the different vacua. In Sec. 10.1 we consider an invertible finite symmetry group G spontaneously broken to a subgroup H, and reproduce the result of [33] that the entanglement and Rényi asymmetries are equal to $\Delta S = \log(N_{\text{vac}})$, where $N_{\text{vac}} = |G|/|H|$ is the number of vacua.[2] In the rest of chapter 10 we study broken noninvertible symmetries. One of the outcomes is that the asymmetries can take more general values, and are not directly related to the number of vacua. Another outcome is that, as opposed to the invertible case, different vacua can exhibit inequivalent physical properties (as already anticipated in [113, 114]), and in particular can have different asymmetries. For instance, in a theory that spontaneously breaks the Ising symmetry, one vacuum has $\Delta S = \log 2$ while two other vacua (which are related by the invertible part of the symmetry) have $\Delta S = \frac{3}{2} \log 2$ (see Sec. 10.2).

9.1 Detecting SPT phases

In the case of an invertible anomaly-free finite symmetry G, two-dimensional gapped phases are classified by the conjugacy class of an unbroken subgroup $H \subseteq G$ as well as an SPT phase for H (see App. A.10 for the precise classification and construction). In particular, even when the full group G is unbroken, one could have inequivalent trivially-gapped phases with a single vacuum but distinguished by the SPT phase. Since they have a single vacuum, ordinary order parameters cannot detect the different SPT phases, and the asymmetries necessarily vanish. Interestingly, it was noted in [66] that in some examples twisted order parameters can distinguish different SPT phases. Can, likewise, one of the symmetry algebras $\mathcal{A}$ introduced so far be used to distinguish those phases? This question clearly generalizes to anomalous as well as noninvertible symmetries.

Below we show in one example that, indeed, the action of the tube algebra can often distinguish different gapped phases. For that, we need the tube algebra action on TQFT states, including the twisted states. By open/closed duality, this is computed from the data of the corresponding module category $\mathscr{M}$. Using the various moves already discussed in the case of fusion categories, in particular those in (8.1.14) and in Figs. A.1 and A.2, adapted to module categories, we find the

[2]The result of [33] used matrix product states. Our derivation, that uses the low-energy TQFT description, is valid in two or more spacetime dimensions.

following relation:

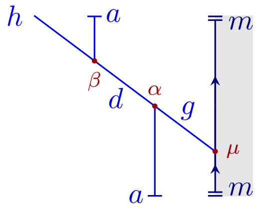

$$= \sum_{n,\nu,\rho,\sigma} \sqrt{\frac{d_g d_a}{d_d}} \left[\tilde{F}^n_{agm}\right]_{(d;\alpha\rho)(m;\mu\sigma)} \left[\tilde{F}^n_{ham}\right]^*_{(d;\beta\rho)(n;\sigma\nu)}$$

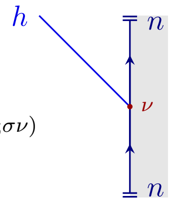

. (9.1.1)

The sum is over a basis of morphisms $\mathcal{L}_h \otimes \mathcal{B}_n \xrightarrow{\nu} \mathcal{B}_n$, $\mathcal{L}_d \otimes \mathcal{B}_m \xrightarrow{\rho} \mathcal{B}_n$, $\mathcal{L}_a \otimes \mathcal{B}_m \xrightarrow{\sigma} \mathcal{B}_n$, while the ticks indicate the "trace" of [128], *i.e.*, that the lines are attached. The configuration on the r.h.s., if rotated clockwise by 90 degrees, represents a twisted state $\left|\mathcal{B}^{(h)}_{n,\nu}\right\rangle \in \mathcal{H}_h$, where $\mathcal{H}_h$ is an h-twisted sector of dimension

$$\dim(\mathcal{H}_h) = \sum\nolimits_n \tilde{N}^n_{hn} \; . \tag{9.1.2}$$

The configuration on the l.h.s. of (9.1.1), on the other hand, represents the action of the tube algebra basis element (8.1.15) on a twisted state $\left|\mathcal{B}^{(g)}_{m,\mu}\right\rangle$. In the special case that $g = h = 1$ and $d = a$, (9.1.1) reproduces the fusion algebra action on the untwisted circle Hilbert space $\mathcal{H}_1$.

Example: SPT phases. In order to exhibit how the tube algebra action distinguishes different phases, consider the example, proposed in [66], of an invertible symmetry group $G = \mathbb{Z}_2 \times \mathbb{Z}_2$ with no anomaly, $\omega = 1$. The indecomposable gapped phases are labeled by conjugacy classes of subgroups $H \subseteq G$ and cocycles $\psi \in H^2\big(H, U(1)\big)$. In this case the possibilities are: for $H = \{1\}$ the completely broken phase; for the three inequivalent subgroups $H = \mathbb{Z}_2$ a broken phase with unbroken $\mathbb{Z}_2$; for $H = G$ two unbroken phases distinguished by the cocycle $\psi \in H^2\big(\mathbb{Z}_2 \times \mathbb{Z}_2, U(1)\big) = \mathbb{Z}_2$.

Let us focus on the two unbroken phases, which are SPT phases. The corresponding module categories have a single simple object that we indicate with a dot, the modules are multiplicity-free since $N^{\cdot}_{g\,\cdot} = 1$ for all $g \in G$, and the $\tilde{F}$-symbols are

$$\left[\tilde{F}^{\cdot}_{ab\,\cdot}\right] = \psi(a,b) \tag{9.1.3}$$

where $a, b \in G$ and the missing indices are fixed. The trivial cocycle, corresponding to the trivial SPT phase, is $\psi = 1$. The non-trivial cocycle, instead, corresponding to the nontrivial SPT phase, has a representative

$$\psi\Big((a_1, a_2)\,,\,(b_1, b_2)\Big) = (-1)^{a_1 b_2} \tag{9.1.4}$$

where $a_i, b_j \in \{0,1\}$. Both phases have four (un)twisted sectors, each with a single state. Since the symmetry is invertible and Abelian, the tube algebra basis elements (8.1.15) have $g = h$: we label them by $g, a \in G$. They do not change the sector of the state, but, in the nontrivial SPT phase, they act according to the following table:

$g \backslash a$	$(0,0)$	$(1,0)$	$(0,1)$	$(1,1)$
$(0,0)$	1	1	1	1
$(1,0)$	1	1	-1	-1
$(0,1)$	1	-1	1	-1
$(1,1)$	1	-1	-1	1

(9.1.5)

This reproduces the results in Sec. 4.5.4 of [66]. In the untwisted sector $g = (0,0)$, all elements a of G act trivially. On the other hand, in each nontrivial twisted sector $\mathcal{H}_g$, the element with $a = g$ acts trivially but the other two flip the sign of the state.

Extrapolating to the general case, one can often distinguish different SPT phases by the tube algebra representations under which their untwisted and twisted states transform. Unfortunately it may happen that two inequivalent SPT phases realize exactly the same tube algebra representation.This happens if the Lagrangian algebras in the Drinfeld center of $\mathscr{C}$ that determine the gapped phases have exactly the same decomposition in simple lines, and only differ by the product morphism. It would be interesting to be able to overcome this issue, and use Tube algebras to diagnose SPT order.

Chapter 10

Examples in 2D CFTs

In this chapter we collect a number of examples in two-dimensional theories with details about the computation of entanglement and Rényi asymmetries, in order to exhibit general features.

10.1 Group-like symmetries

Consider an invertible symmetry given by a finite group G. The corresponding fusion category is Vec_G^ω, whose simple lines $\mathcal{L}_g$ are in correspondence with the elements $g \in G$ and they all have dimension $d_g = 1$. The fusion coefficients are $N_{gh}^k = \delta_{(gh)}^k$ where (gh) denotes the group multiplication of g with h. In particular, there are no multiplicities at the junctions. The symmetrizer with respect to the fusion algebra is

$$\rho_{\mathsf{S}} = \frac{1}{|G|} \sum\nolimits_{g \in G} \mathcal{L}_g \, \rho \, \mathcal{L}_{g^{-1}} \; . \tag{10.1.1}$$

A possible 't Hooft anomaly is described by a class $\omega \in H^3\Big(G, U(1)\Big)$, which fixes the nonvanishing F-symbols to be

$$\Big[F^{ghk}_{g,h,k}\Big]_{gh,hk} = \omega(g,h,k) \; . \tag{10.1.2}$$

We use normalized representatives ω, meaning that $\omega(g,h,k) = 1$ whenever one or more of g, h, k are equal to the identity $1 \in G$. Different representatives of the same class produce the F-symbols in different gauges.

Spontaneous symmetry breaking. The possible indecomposable G-symmetric TQFTs, in correspondence with the possible indecomposable $\mathscr{C}$-module categories, are characterized by the conjugation class of a subgroup $H \subseteq G$ (besides a cochain

ψ, which however will not play a role here), as reviewed in App. A.10. They describe the SSB pattern $G \to H$ at very low energies. The clustering vacua $|m\rangle$, in correspondence with the simple boundaries $\mathcal{B}_m$, are labeled by the cosets $m \in G/H$. The vacua furnish a simple NIM-rep of the fusion algebra:

$$\mathcal{L}_g \, |m\rangle = |gm\rangle \; . \tag{10.1.3}$$

Here gm is the coset with representative ga, if $a \in G$ is a representative of m.

Consider the pure state $\rho = |m\rangle\langle m|$ of a vacuum on the circle. Using (10.1.1), the corresponding symmetrized density matrix with respect to the fusion algebra is

$$\rho_{\mathsf{S}} = \frac{1}{|G|} \sum\nolimits_{g \in G} \mathcal{L}_g \, \rho \, \mathcal{L}_{g^{-1}} = \frac{1}{|G|} \sum\nolimits_{g \in G} |gm\rangle\langle gm| = \frac{1}{|G/H|} \sum\nolimits_{p \in G/H} |p\rangle\langle p| \; . \tag{10.1.4}$$

In the second equality we used that $\mathcal{L}_{g^{-1}} = \mathcal{L}_g^\dagger$. Because of the crossing relation (9.0.1), the vacua are orthonormal and thus $\mathrm{Tr}(\rho_{\mathsf{S}}^n) = \big|G/H\big|^{1-n}$. The asymmetries easily follow:

$$\Delta S[\rho] = \Delta S^{(n)}[\rho] = \log \Big|G/H\Big| \; . \tag{10.1.5}$$

This computation reproduces the result of [33], obtained using matrix product states. Notice that the derivation here applies verbatim to spacetime dimensions higher than two as well.

Tube algebra

The tube algebra of Vec_G^ω (which is given by the twisted quantum double of G) is generated by the basis elements:

$$\tau_{g,a} \;\equiv \tag{10.1.6}$$

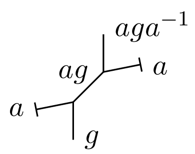

The product is given by:

$$\tau_{h,b} \times \tau_{g,a} = \delta_{h,aga^{-1}} \, \frac{\omega(b, aga^{-1}, a)}{\omega(baga^{-1}b^{-1}, b, a) \, \omega(b, a, g)} \, \tau_{g,ba} \; . \tag{10.1.7}$$

From here the structure constants $T^{k,c}_{h,b;\, g,a}$ are immediately read off. The phase factor appearing in the product can be interpreted as a twisted 2-cocycle. Indeed, define

$$\beta_g(x, y) = \frac{\omega(g, x, y) \, \omega(x, y, y^{-1}x^{-1}gxy)}{\omega(x, x^{-1}gx, y)} \; . \tag{10.1.8}$$

One verifies that this is a normalized twisted 2-cocycle, where x has an adjoint action on $g \in G$ (this also appeared in [141] Sec. 4.B).[1] We can write the tube algebra product as

$$\tau_{h,b} \times \tau_{g,a} = \frac{\delta_{h,aga^{-1}}}{\beta_{baga^{-1}b^{-1}}(b,a)} \, \tau_{g,ba} \; . \tag{10.1.9}$$

The identity element is $\mathcal{X}_{\mathbb{1}} = \sum_g \tau_{g,1}$. Associativity of the product coincides with the twisted cocycle condition for β. The non-degenerate bilinear form can be written as

$$K_{h,b;\,g,a} = \frac{|G| \; \delta_{h,aga^{-1}} \, \delta_{b,a^{-1}}}{\beta_g(a^{-1},a)} \; . \tag{10.1.10}$$

From its inverse matrix $\tilde{K}^{g,a;\,h,b}$ one obtains the symmetrizer:

$$\rho_{\mathsf{S}} = \frac{1}{|G|} \sum\nolimits_{g,a} \beta_g(a^{-1},a) \; \tau_{g,a} \, \rho \, \tau_{aga^{-1},a^{-1}} \; . \tag{10.1.11}$$

Using the twisted cocycle condition one proves the relation $\beta_{aga^{-1}}(a,a^{-1}) = \beta_g(a^{-1},a)$ which is useful to check directly some properties of the symmetrizer.

Strip algebras

Let us now study the case of the interval Hilbert space using the strip algebras. The possible boundary conditions are given in terms of module categories, whose classification in the case of invertible finite symmetries is reviewed in App. A.10.

In the non-anomalous case, one can always choose strongly-symmetric boundary conditions (but see fn. 10). From App. A.10, those are classified by $\psi \in H^2\big(G, U(1)\big)$. Explicitly, one has

$$\tilde{N}_{a\cdot}^{\cdot} = 1 \; , \qquad\qquad \big[\tilde{F}_{a,b,\cdot}^{\cdot}\big]_{c,\cdot} = \big(m_{a,b}^{c}\big)^{*} = \delta_{ab}^{c} \; \psi(a,b) \; . \tag{10.1.12}$$

Note that there are no multiplicities at the boundary junctions. In terms of the basis elements H_g defined in (8.2.20), we see that the cocycle cancels out from the product (8.2.21) so that $H_g \times H_h = H_{gh}$. The strip algebra $\mathsf{Strip}_{\mathsf{Vec}_G}(\mathsf{Vec})$ is thus isomorphic to the group algebra $\mathbb{C}[G]$ (which is also the fusion algebra) regardless of the class of ψ.[2] One finds the symmetrizer

$$\rho_{\mathsf{S}} = \frac{1}{|G|} \sum\nolimits_{g\in G} H_g \, \rho \, H_{g^{-1}} \; . \tag{10.1.13}$$

[1] The twisted cocycle condition is $d\beta_g(x,y,z) = \beta_{x^{-1}gx}(y,z)\, \beta_g(x,yz)/\beta_g(xy,z)\beta_g(x,y) = 1$. See also App. A of [142] for a review on twisted cocycles.

[2] Alternatively, the cocycle can be reabsorbed with a change of basis of the junction vector spaces [117].

On the other hand, a boundary condition that can always be chosen regardless of the value of the anomaly cocycle $\omega \in H^3\big(G, U(1)\big)$ is the regular module (but see fn. 10). In this case we obtain the algebra $\mathsf{Strip}_{\mathsf{Vec}_G^\omega}(\mathsf{Vec}_G^\omega)$, generated by the basis elements:

$$H^g_{r,m} \equiv$$

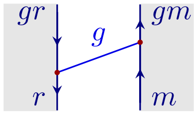

(10.1.14)

with $g, m, r \in G$ and $\tilde{N}^n_{gm} = \delta^n_{(gm)}$. The product is given by:

$$H^b_{s,n} \times H^a_{r,m} = \delta_{s,ar}\, \delta_{n,am}\, \frac{\omega(b,a,r)}{\omega(b,a,m)}\, H^{ba}_{r,m} \, . \tag{10.1.15}$$

Also in this case the phase can be interpreted as a twisted cocycle (in which the action on r, m is in the regular representation) and associativity as its closure. In this case, however, there exists an isomorphism with $\mathsf{Strip}_{\mathsf{Vec}_G}(\mathsf{Vec}_G)$, namely, with the strip algebra of the symmetry without anomaly [117]. The isomorphism is given by [3]

$$\begin{gathered} \varphi\colon \mathsf{Strip}_{\mathsf{Vec}_G}(\mathsf{Vec}_G) \to \mathsf{Strip}_{\mathsf{Vec}_G^\omega}(\mathsf{Vec}_G^\omega) \, , \\ \varphi\Big(H^a_{r,m}\Big) = \omega(a, r, r^{-1}m)\, H^a_{r,m} \, , \end{gathered} \tag{10.1.16}$$

then extended by linearity. Indeed one verifies that

$$\varphi\Big(H^b_{ar,am}\Big) \times_\omega \varphi\Big(H^a_{r,m}\Big) = \varphi\Big(H^b_{ar,am} \times_{\omega=1} H^a_{r,m}\Big) \tag{10.1.17}$$

using that $d\omega(b, a, r, r^{-1}m) = 1$. Here we made explicit where we used the anomalous product (10.1.15) or the non-anomalous one. The non-degenerate bilinear form can be written as

$$K_{s,n,b;\,r,m,a} = |G|\, \frac{\omega(a^{-1},a,r)}{\omega(a^{-1},a,m)}\, \delta_{s,ar}\, \delta_{n,am}\, \delta_{b,a^{-1}} \, . \tag{10.1.18}$$

From its inverse one obtains the symmetrizer

$$\rho_{\mathsf{S}} = \frac{1}{|G|} \sum_{r,m,a} \frac{\omega(a^{-1},a,m)}{\omega(a^{-1},a,r)}\, H^a_{r,m}\, \rho\, H^{a^{-1}}_{ar,am} = \frac{1}{|G|} \sum_{r,m,a} \varphi(H^a_{r,m})\, \rho\, \varphi(H^{a^{-1}}_{ar,am}) \, . \tag{10.1.19}$$

The rewriting in terms of φ makes it manifest that the symmetrizers for the two strip algebras are the same up to a phase redefinition of the basis elements.

Asymmetries in CFTs. Consider a CFT and a state on the real line $\mathbb{R}$ created by the Euclidean path-integral on a half space with the insertion of local operators.

[3]The two algebras share the same underlying vector space, hence we denote a basis of both with the same notation $H^a_{r,m}$.

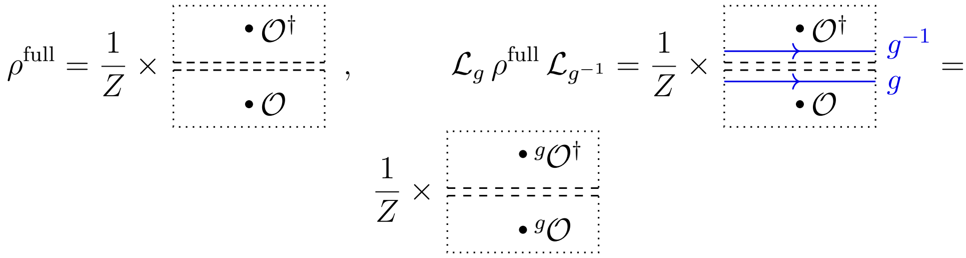

Figure 10.1: Left: path-integral representation of the state on the real line. The operator $\mathcal{O}$ is inserted at $z = x - i\tau$, while the operator $\mathcal{O}^\dagger$ is inserted at the specular image $\bar{z} = x + i\tau$. The normalization by the partition function Z ensures that $\mathrm{Tr}\big(\rho^{\text{full}}\big) = 1$. Right: path-integral representation of $\mathcal{L}_g\, \rho^{\text{full}}\, \mathcal{L}_{g^{-1}}$.

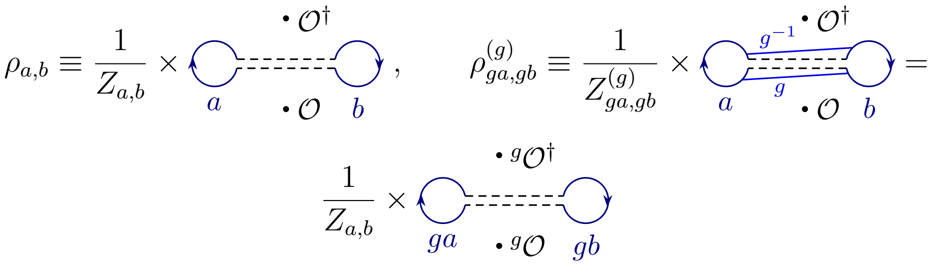

Figure 10.2: Left: path-integral construction of the reduced density matrix $\rho_{a,b}$. The dashed lines are the two open boundaries (cuts). The constant $Z_{a,b}$ is the partition function obtained by gluing the two cuts, so as to ensure that $\mathrm{Tr}(\rho_{a,b}) = 1$. Right: path-integral construction of the rotated density matrix $\rho^{(g)}_{ga,gb}$ where $Z^{(g)}_{ga,gb} \equiv Z_{a,b}\, \omega(g^{-1}, g, a)/\omega(g^{-1}, g, b)$.

The corresponding density matrix ρ^{full} is prepared by a Euclidean path-integral in which the future half-space is the specular image of the past half-space, and there is a cut along the real line. This is depicted in Fig. 10.1 left. There, Z is the partition function on the plane obtained by closing the cut, so as to ensure that $\mathrm{Tr}\Big(\rho^{\text{full}}\Big) = 1$.

To construct the reduced density matrix for a single interval along the real line, we apply the procedure of Sec. 8.2. Consider first the case that we use boundary conditions a, b chosen from the regular module. We depict the path-integral construction of $\rho_{a,b}$ in Fig. 10.2 left, where $Z_{a,b}$ is the partition function obtained by closing the cut so as to ensure that $\mathrm{Tr}(\rho_{a,b}) = 1$. For simplicity, in the figures we indicate only one operator insertion $\mathcal{O}$ and its specular image $\mathcal{O}^\dagger$, but the argument applies to any number of insertions. To obtain the symmetrized density matrix we apply (10.1.19). Since the symmetry elements $H^g_{r,m}$ project to zero when their boundary conditions do not match those of the state, we remain with a single sum:

$$\rho_{\mathsf{S}} = \frac{1}{|G|} \sum\nolimits_g \frac{\omega(g^{-1}, g, b)}{\omega(g^{-1}, g, a)}\, H^g_{a,b}\, \rho_{a,b}\, H^{g^{-1}}_{ga,gb} \equiv \frac{1}{|G|} \sum\nolimits_g \rho^{(g)}_{ga,gb}\,. \tag{10.1.20}$$

In the last equality we introduced the rotated density matrices $\rho^{(g)}_{ga,gb}$ whose path-integral construction is depicted in Fig. 10.2 right. They belong to $\mathrm{End}(\mathcal{H}_{ga,gb})$. The constant prefactor is $Z^{(g)}_{ga,gb} = Z_{a,b}\ \omega(g^{-1},g,a)/\omega(g^{-1},g,b)$. To obtain the second presentation one moves the line of $H^g_{a,b}$ through infinity and then annihilates it with $H^{g^{-1}}_{ga,gb}$. When the line crosses an operator $\mathcal{O}$, the latter gets transformed to ${}^g\mathcal{O}$. Since Hilbert spaces constructed with different simple boundary conditions are orthogonal, the moments of ρ_{S} simplify:

$$\mathrm{Tr}\Big(\rho_{\mathsf{S}}^n\Big) = \frac{1}{|G|^n}\sum\nolimits_g \mathrm{Tr}\Big[(\rho^{(g)}_{ga,gb})^n\Big] = \frac{1}{|G|^{n-1}}\ \mathrm{Tr}\Big(\rho^n_{a,b}\Big)\ . \tag{10.1.21}$$

The Rényi and entanglement asymmetries are then

$$\Delta S^{(n)}[\rho_{a,b}] = \Delta S[\rho_{a,b}] = \log|G| \qquad\qquad \text{for all } n\,. \tag{10.1.22}$$

This result does not depend on the state, and in particular it applies to the vacuum as well. Its interpretation is that the boundary conditions completely break the symmetry, therefore $\Delta S^{(n)}$ and ΔS reach their maximal value irrespective of the state. This observable is clearly not very interesting. To make it interesting, we should rather use a symmetric combination of boundary conditions, as described in Sec. 8.2.4.

Consider then the "averaged" reduced density matrix

$$\rho = \frac{1}{|G|^2}\sum\nolimits_{a,b}\rho_{a,b}\ . \tag{10.1.23}$$

The symmetrized matrix this time can be written as

$$\rho_{\mathsf{S}} = \frac{1}{|G|^3}\sum\nolimits_{a,b,g}\rho^{(g)}_{a,b}\ , \tag{10.1.24}$$

where $\rho^{(g)}_{a,b}$ is defined in Fig. 10.2 right. One computes

$$\mathrm{Tr}\Big(\rho^n\Big) = \frac{1}{|G|^{2n}}\sum\nolimits_{a,b}\mathrm{Tr}\Big(\rho^n_{a,b}\Big)\ , \qquad \mathrm{Tr}\Big(\rho^n_{\mathsf{S}}\Big) = \frac{1}{|G|^{3n}}\sum_{a,b}\ \sum_{g_1,\dots,g_n}\mathrm{Tr}\bigg(\rho^{(g_1)}_{a,b}\cdots\rho^{(g_n)}_{a,b}\bigg)\ . \tag{10.1.25}$$

From the path-integral representation of $\rho_{a,b}$ (see Fig. 10.2), $\mathrm{Tr}\Big(\rho^n_{a,b}\Big)$ is equal to $Z^{-n}_{a,b}$ times the partition function on an n-sheeted Riemann surface with operators $\mathcal{O}$ and $\mathcal{O}^\dagger$ inserted in each replica. In this manifold, the n copies of the boundary with boundary condition a are glued together to form a single boundary that spans all replicas, and the same holds for the boundaries with boundary condition b. Similarly, $\mathrm{Tr}\Big(\rho^{(g_1)}_{a,b}\cdots\rho^{(g_n)}_{a,b}\Big)$ is equal to $\prod_i 1/Z_{g_i^{-1}a,g_i^{-1}b}$ times the partition function on an n-

$$\left\langle {}^{g_1}\mathcal{O}^\dagger\, {}^{g_1}\mathcal{O} \;\ldots\; {}^{g_n}\mathcal{O}^\dagger\, {}^{g_n}\mathcal{O} \right\rangle_{\mathcal{M}_n} \equiv$$

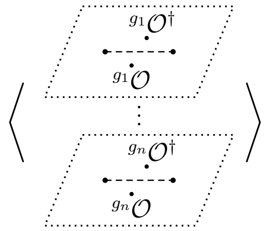

Figure 10.3: Correlator on the n-sheeted Riemann surface $\mathcal{M}_n$. It is understood that the lower rim of each cut (denoted by a dashed segment) is glued to the upper rim of the cut of the sheet above it (and the uppermost sheet is connected to the lowermost sheet). Two branch points sit at the ends of the branch cut. In the j-th replica the operator $^{g_j}\mathcal{O}$ is inserted at $z = x - i\tau$ while the operator $^{g_j}\mathcal{O}^\dagger$ is inserted at $\bar{z} = x + i\tau$.

sheeted Riemann surface with operators $^{g_j}\mathcal{O}$ and $^{g_j}\mathcal{O}^\dagger$ inserted in the j-th replica and with one a and one b boundary.

In the limit $\varepsilon \to 0$, the dependence of the traces on the boundary conditions becomes very simple. As described in (8.2.29), in the limit each partition function produces a factor of the boundary quantum dimension from each shrinking disc. Thus, the partition function on the n-sheeted Riemann surface becomes $\tilde{d}_a \tilde{d}_b$ times the partition function on a similar Riemann surface, where the boundary discs are shrunk to a branch point and all insertions of fields remain at the same position. For a group-like symmetry all boundary quantum dimensions $\tilde{d}$ are equal. We thus obtain the same factor $\tilde{d}^{2(1-n)}$ from both $\lim_{\varepsilon\to 0} \mathrm{Tr}(\rho^n)$ and $\lim_{\varepsilon \to 0} \mathrm{Tr}(\rho_{\mathbb{S}}^n)$, which simplifies in the ratio. Besides, once the $\varepsilon \to 0$ limit is taken, there is no dependence on a and b left and we can easily sum over them. The result can be expressed in terms of correlation functions on a Riemann surface with branch points:

$$\lim_{\varepsilon \to 0} \Delta S^{(n)}[\rho] = \frac{1}{1-n} \log\left[\frac{1}{|G|^n} \sum_{g_1,\ldots,g_n} \frac{\langle\, {}^{g_1}\mathcal{O}^\dagger\, {}^{g_1}\mathcal{O} \;\ldots\; {}^{g_n}\mathcal{O}^\dagger\, {}^{g_n}\mathcal{O} \,\rangle_{\mathcal{M}_n}}{\langle\, \mathcal{O}^\dagger\, \mathcal{O} \cdots \mathcal{O}^\dagger\, \mathcal{O} \,\rangle_{\mathcal{M}_n}} \right], \tag{10.1.26}$$

where the notation $\langle \cdot \rangle_{\mathcal{M}_n}$ indicates a correlation function on the branched Riemann surface, as detailed in Fig. 10.3.

We make three observations. First, if there are no insertions, *i.e.*, if we compute the asymmetry of the vacuum, then all correlators in (10.1.26) are equal to 1 and thus $\Delta S^{(n)} = \Delta S = 0$, as expected from the general discussion in Sec. 8.2.4. Second, the asymmetries have no explicit dependence on the anomaly, as already anticipated in [1]. Third, in the absence of an anomaly, one could compute the asymmetries using the strongly-symmetric boundary condition, and this would lead to exactly the same formula. In particular, earlier works on asymmetry for groups ignored the entangling surface and used the group algebra instead of the strip algebra; we see here that those less rigorous approaches are in fact validated by our more rigorous approach of using the strip algebra.

Large subsystem limit. In the limit of a large subsystem of size ℓ, the branch cut extends along the whole real axis. Then effectively each sheet gets split into two half-planes, and each lower half-plane is glued to the upper half-plane of the next sheet (*cfr.* with Fig. 10.3). One can perform a conformal block expansion of the $2n$-point functions appearing in (10.1.26), in the channel in which each operator is first contracted with the operator found across the cut after the gluing. When that channel is dominated by exchanges of the identity operator, the $2n$-point function factorizes into the product of n two-point functions. This is always the case for the $2n$-point function at denominator in (10.1.26). When exchanges of the identity operator are not possible in the numerator, the contribution to the sum in (10.1.26) is subdominant — and on the other hand some of the two-point functions vanish. Therefore, in the large subsystem limit we find the formula:

$$\lim_{\ell\to\infty}\lim_{\varepsilon\to 0}\Delta S^{(n)}[\rho] = \frac{1}{1-n}\log\left[\frac{1}{|G|^n}\sum_{g_1,\dots,g_n}\frac{\langle {}^{g_1}\mathcal{O}^\dagger\,{}^{g_2}\mathcal{O}\rangle_{\mathbb{C}}\cdots\langle {}^{g_n}\mathcal{O}^\dagger\,{}^{g_1}\mathcal{O}\rangle_{\mathbb{C}}}{\langle\mathcal{O}^\dagger\mathcal{O}\rangle_{\mathbb{C}}^n}\right]. \quad (10.1.27)$$

We claim that this is the same as the Rényi asymmetry of the full system, *i.e.*, of the state on the real line symmetrized with respect to the fusion algebra $\mathbb{C}[G]$. Indeed, let ρ^{full} be the state on the real line, depicted in Fig. 10.1 left. The symmetrized density matrix for the full system is

$$\rho_{\mathsf{S}}^{\text{full}} = \frac{1}{|G|}\sum\nolimits_{g\in G}\mathcal{L}_g\,\rho^{\text{full}}\,\mathcal{L}_{g^{-1}}\,. \quad (10.1.28)$$

The summand $\mathcal{L}_g\,\rho^{\text{full}}\,\mathcal{L}_{g^{-1}}$ is depicted in Fig. 10.1 right. The Rényi asymmetry is then

$$\Delta S^{(n)}\Big[\rho^{\text{full}}\Big] = \frac{1}{1-n}\log\left\{\frac{1}{|G|^n}\,\mathrm{Tr}\left[\frac{1}{Z^n}\left(\sum_{g\in G}\begin{array}{c}\bullet\,{}^{g}\mathcal{O}^\dagger\\ \hdashline \bullet\,{}^{g}\mathcal{O}\end{array}\right)^n\right]\right\}. \quad (10.1.29)$$

We used that ρ^{full} is pure and thus $\mathrm{Tr}\Big[(\rho^{\text{full}})^n\Big] = 1$. The n-th power of the operator appearing inside the trace is obtained by taking n copies of the cut plane and then connecting the lower rim of each cut (which is the "output" of the operator) to the upper rim of the next sheet (which is the "input"). The trace connects them cyclically, in a fashion similar to Fig. 10.3. The partition functions can then be replaced by expectation values, since both at numerator and denominator the required normalization is given by the same partition function with no operator insertions.

We conclude that (10.1.29) can be written as in (10.1.27) and therefore

$$\lim_{\ell\to\infty}\lim_{\varepsilon\to 0}\Delta S^{(n)}[\rho]=\Delta S^{(n)}\left[\rho^{\text{full}}\right] . \tag{10.1.30}$$

10.2 Ising symmetry — circle Hilbert space

The internal symmetry of the two-dimensional Ising CFT is described by a fusion category $\mathscr{C}$ (that we call the Ising fusion category) with 3 simple lines, that we indicate as $\mathcal{L}_1$, $\mathcal{L}_\eta$, $\mathcal{L}_\mathcal{N}$, satisfying the commutative fusion ring:

$$\mathcal{L}_\eta\times\mathcal{L}_\eta=\mathcal{L}_1 , \qquad \mathcal{L}_\eta\times\mathcal{L}_\mathcal{N}=\mathcal{L}_\mathcal{N} , \qquad \mathcal{L}_\mathcal{N}\times\mathcal{L}_\mathcal{N}=\mathcal{L}_1+\mathcal{L}_\eta . \tag{10.2.1}$$

Here $\mathcal{L}_1$ is the identity, $\mathcal{L}_\eta$ generates the $\mathbb{Z}_2$ spin-flip symmetry, and $\mathcal{L}_\mathcal{N}$ is the line of Kramers–Wannier duality. The junctions have no multiplicities. The nontrivial F-symbols are:

$$\left[F^{\mathcal{N}}_{\eta\mathcal{N}\eta}\right]_{\mathcal{N}\mathcal{N}}=\left[F^{\eta}_{\mathcal{N}\eta\mathcal{N}}\right]_{\mathcal{N}\mathcal{N}}=-1 , \qquad \left[F^{\mathcal{N}}_{\mathcal{N}\mathcal{N}\mathcal{N}}\right]_{ab}=\frac{1}{\sqrt{2}}\begin{pmatrix}1&1\\1&-1\end{pmatrix} , \tag{10.2.2}$$

where $a,b\in\{1,\eta\}$, while all other F-symbols allowed by fusion are equal to 1. All lines are self-dual. One reads off the Frobenius–Schur (FS) indicators $\varkappa_\eta=\varkappa_\mathcal{N}=1$ and the quantum dimensions $d_\eta=1$, $d_\mathcal{N}=\sqrt{2}$. The category $\mathscr{C}$ is the Tambara–Yamagami fusion category $\mathsf{TY}(\mathbb{Z}_2,\chi,+)$ [143] where $\chi(a,b)=e^{i\pi ab}$ is a symmetric nondegenerate $\mathbb{Z}_2$ bicharacter that equals -1 only if a,b are both the nontrivial element η, otherwise it equals 1.[4]

Fusion algebra

The fusion algebra has three 1-dimensional representations that we indicate as $\mathbb{1}$, ε, σ. In the Ising CFT these are realized in the Verma module of the identity, the energy, and the spin operator, respectively. The fusion algebra acts on them through (8.1.8), in terms of the unitary and symmetric modular S-matrix:

$$S=\frac{1}{2}\begin{pmatrix}1&1&\sqrt{2}\\1&1&-\sqrt{2}\\\sqrt{2}&-\sqrt{2}&0\end{pmatrix} . \tag{10.2.3}$$

[4] The $\mathsf{TY}(\mathbb{Z}_2,\chi,+)$ symmetry appears, for instance, in a system of $\nu=1,7,9,15 \pmod{16}$ Dirac fermions. A slight generalization is $\mathsf{TY}(\mathbb{Z}_2,\chi,-)$, whose only difference is that $\left[F^{\mathcal{N}}_{\mathcal{N}\mathcal{N}\mathcal{N}}\right]_{ab}=-\chi(a,b)/\sqrt{2}$ and thus $\varkappa_\mathcal{N}=-1$, which appears, for instance, in a system of $\nu=3,5,11,13 \pmod{16}$ Dirac fermions.

The symmetrizer for the fusion algebra is given by the inverse bilinear form:

$$\tilde{K} = \begin{pmatrix} \frac{3}{8} & -\frac{1}{8} & 0 \\ -\frac{1}{8} & \frac{3}{8} & 0 \\ 0 & 0 & \frac{1}{4} \end{pmatrix} , \tag{10.2.4}$$

and in particular it takes the form:

$$\rho_{\mathsf{S}} = \frac{1}{8}\Big[3\,\rho + 3\,\mathcal{L}_\eta\,\rho\,\mathcal{L}_\eta - \mathcal{L}_\eta\,\rho - \rho\,\mathcal{L}_\eta + 2\,\mathcal{L}_\mathcal{N}\,\rho\,\mathcal{L}_\mathcal{N}\Big] . \tag{10.2.5}$$

Asymmetry of excited states in CFTs. We consider a CFT whose symmetry includes the Ising fusion category. This could be the Ising CFT itself, or a more complicated one (for instance, the tricritical Ising model). The local operators fall into representations of the fusion algebra, that we indicate as $\mathbb{1}$, ε, σ as in (10.2.3). We consider excited states on the line $\mathbb{R}$ produced using a scalar operator $\varepsilon(z)$ of dimension Δ_ε in the Euclidean past, which by definition transforms in the representation ε:

$$|\psi\rangle \;=\; \boxed{\bullet\; 1+\lambda\,\varepsilon} \;. \tag{10.2.6}$$

Here λ is a constant of mass dimension $-\Delta_\varepsilon$. Notice that this state is neutral under the $\mathbb{Z}_2$ spin-flip symmetry. To compute its asymmetry with respect to the fusion algebra we can use (8.1). Setting the operator insertion at $z = -i\tau$ with $\tau > 0$ (thus $\bar{z} = i\tau$), the relevant two-point function is $\big\langle \varepsilon(\bar{z})\,\varepsilon(z)\big\rangle \equiv \langle\varepsilon^2\rangle = 1/(2\tau)^{2\Delta_\varepsilon}$. The second Rényi and entanglement asymmetries are then

$$\Delta S^{(2)}\big[|\psi\rangle\langle\psi|\big] = -\log\left[\frac{1+\lambda^4\langle\varepsilon^2\rangle^2}{\big(1+\lambda^2\langle\varepsilon^2\rangle\big)^2}\right] , \qquad \Delta S\big[|\psi\rangle\langle\psi|\big] = f\left[\frac{1}{1+\lambda^2\langle\varepsilon^2\rangle}\right] + f\left[\frac{\lambda^2\langle\varepsilon^2\rangle}{1+\lambda^2\langle\varepsilon^2\rangle}\right] , \tag{10.2.7}$$

where we used the function $f(x) = -x\log x$.

In the case of the Ising CFT we can take $\varepsilon(x)$ to be the energy conformal primary operator of dimension $\Delta_\varepsilon = 1$. In Fig. 10.4 we plot the entanglement asymmetry as a function of τ/λ.

Spontaneous symmetry breaking. The only indecomposable $\mathscr{C}$-module category of the Ising fusion category is the regular one.[5] This means that in a gapped phase the Ising symmetry is always completely spontaneously broken, and this is due to

[5] By Th. 6 of [115] (where the Ising category is called $\mathscr{C}_2$ and the module is of type A_3), the Ising fusion category admits only one indecomposable module category. Hence, this must be the regular module, which always exists.

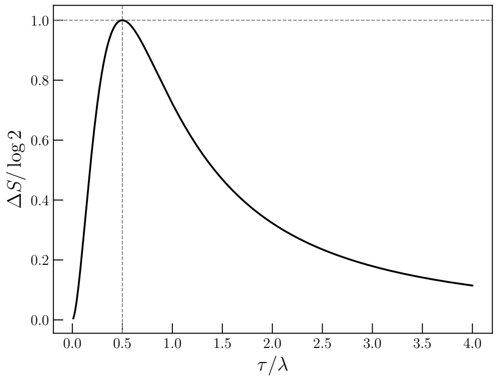

Figure 10.4: Entanglement asymmetry ΔS with respect to the Ising fusion algebra of a state on the real line prepared by inserting $(1+\lambda\,\varepsilon)$ with $\Delta_\varepsilon = 1$ in the path-integral. The asymmetry is plotted as a function of τ/λ, where $-\tau$ is the Euclidean time of the insertion. In the limit $\tau/\lambda \to \infty$ only the identity contributes, so the state becomes symmetric and the asymmetry vanishes. Similarly, in the limit $\tau/\lambda \to 0$ only ε contributes, leading again to a symmetric state with vanishing asymmetry. The asymmetry reaches its maximum at $\tau/\lambda = 1/2$.

the presence of an 't Hooft anomaly. In the regular module one could indicate both lines and boundary conditions using the same set of labels. However, in order to adhere to a more commonly used notation, we relabel the boundary conditions as:[6]

$$1 \;\to\; + \,, \qquad\qquad \eta \;\to\; - \,, \qquad\qquad \mathcal{N} \;\to\; f \,. \tag{10.2.8}$$

Correspondingly, we indicate the three normalized vacua (*i.e.*, the three clustering states) as $\Big\{|+\rangle\,,\,|-\rangle\,,\,|f\rangle\Big\}$. They furnish a NIM-rep of the fusion algebra:

$$\begin{aligned} &\mathcal{L}_\eta\,|+\rangle = |-\rangle\,, &&\mathcal{L}_\eta\,|-\rangle = |+\rangle\,, &&\mathcal{L}_\eta\,|f\rangle = |f\rangle\,, \\ &\mathcal{L}_\mathcal{N}\,|+\rangle = |f\rangle\,, &&\mathcal{L}_\mathcal{N}\,|-\rangle = |f\rangle\,, &&\mathcal{L}_\mathcal{N}\,|f\rangle = |+\rangle + |-\rangle\,. \end{aligned} \tag{10.2.9}$$

The gapped phase (some curious properties thereof were already noticed in [113]) can be obtained, for instance, from the tricritical Ising model deforming it by the relevant operator ε', as explained in Sec. 7.2.3 of [67].

Consider the pure state $\rho = |f\rangle\langle f|$ for the vacuum $|f\rangle$. Using the symmetrizer (10.2.5) with respect to the fusion algebra, one computes ρ_S. Its diagonalization is $\rho_\mathsf{S} \sim \mathrm{diag}\big(\frac{1}{2},\frac{1}{2},0\big)$ and therefore $\mathrm{Tr}(\rho_\mathsf{S}^n) = 2^{1-n}$. The Rényi and entanglement asymmetries are then

$$\Delta S^{(n)} = \Delta S = \log 2\,. \tag{10.2.10}$$

Notice that this is the same asymmetry as for a spontaneously broken $\mathbb{Z}_2$ symmetry

[6]These boundary conditions have a counterpart in a lattice spin model: $\pm$ correspond to up/down fixed boundary conditions for the spins, while f corresponds to the free boundary condition.

[32].[7] On the other hand, consider the pure state $\rho = |+\rangle\langle+|$ for the vacuum $|+\rangle$ (the vacuum $|-\rangle$ would give the same result). The symmetrized matrix ρ_{S} has diagonalization $\rho_{\mathsf{S}} \sim \mathrm{diag}\big(\frac{1}{2}, \frac{1}{4}, \frac{1}{4}\big)$ and hence $\mathrm{Tr}(\rho_{\mathsf{S}}^n) = \big(2^{n-1}+1\big)/2^{2n-1}$, from which the Rényi and entanglement asymmetries are

$$\Delta S^{(n)} = \frac{1}{1-n} \log \frac{2^{n-1}+1}{2^{2n-1}} \,, \qquad\qquad \Delta S = \frac{3}{2} \log 2 \,. \tag{10.2.11}$$

This time the entanglement asymmetry is larger than for a broken $\mathbb{Z}_2$, but smaller than for a broken $\mathbb{Z}_3$. We conclude that, while for a completely broken invertible symmetry G the entanglement asymmetry of a vacuum is $\Delta S = \log|G|$ [33], for noninvertible symmetries the asymmetry may take more general values. We also observe that different vacua in the same gapped phase can have inequivalent physical properties (as already stressed in [113, 114]) and in particular different asymmetries.

Tube algebra

The tube algebra is generated by the following 12 basis elements (see also [144]):

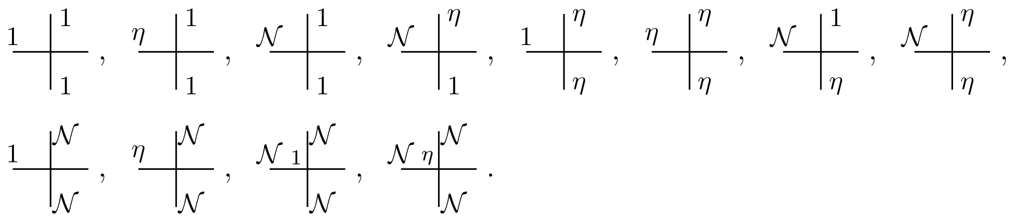

(10.2.12)

By applying the formula (8.1.19) we compute the algebra product. We use the bicharacter $\chi(a,b)$ defined on $\mathbb{Z}_2 = \{1, \eta\}$ above. As in the general discussion, we adopt the convention that the element on the left is stacked on top of the one on the right. We find:

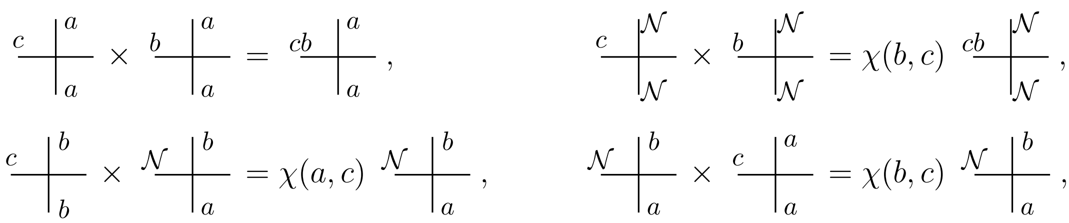

(10.2.13)

[7] This is explained by the fact that the "orbit" of $|f\rangle$ under the noninvertible symmetry is given by two rays, the ones of $|f\rangle$ and $\big(|+\rangle + |-\rangle\big)$, as it happens for a $\mathbb{Z}_2$ symmetry.

as well as

$$
\begin{aligned}
&{}^{b}{+}^{\mathcal{N}}_{\mathcal{N}} \times {}^{\mathcal{N}\,a}{+}^{\mathcal{N}}_{\mathcal{N}} = {}^{\mathcal{N}\,a}{+}^{\mathcal{N}}_{\mathcal{N}} \times {}^{b}{+}^{\mathcal{N}}_{\mathcal{N}} = \chi(b, ab)\ {}^{\mathcal{N}\,ab}{+}^{\mathcal{N}}_{\mathcal{N}}\ , \\
&{}^{\mathcal{N}}{+}^{c}_{b} \times {}^{\mathcal{N}}{+}^{b}_{a} = \delta_{ac} \sum_{d} \chi(b, da)\ {}^{d}{+}^{a}_{a}\ , \qquad\qquad (10.2.14) \\
&{}^{\mathcal{N}\,b}{+}^{\mathcal{N}}_{\mathcal{N}} \times {}^{\mathcal{N}\,a}{+}^{\mathcal{N}}_{\mathcal{N}} = \sum_{d} \frac{\chi(a, b)\chi(ab, d)}{\sqrt{2}}\ {}^{d}{+}^{\mathcal{N}}_{\mathcal{N}}\ .
\end{aligned}
$$

The unit of the algebra is

$$
\mathcal{X}_{\mathbb{1}} = {}^{1}{+}^{1}_{1} + {}^{1}{+}^{\eta}_{\eta} + {}^{1}{+}^{\mathcal{N}}_{\mathcal{N}}\ , \qquad (10.2.15)
$$

which agrees with (7.1.6).

Untwisted and twisted point operators fall into representations of the tube algebra. Such representations are in one-to-one correspondence with simple objects in the Drinfeld center of $\mathscr{C}$. Because $\mathscr{C}$ is modular, its Drinfeld center is isomorphic to the product of two copies of the TY fusion category, therefore it has 9 simple lines, listed in [144].

The total circle Hilbert space (8.1.11) is decomposed as a sum of twisted sectors, each graded by a simple element $a \in \mathrm{Irr}(\mathscr{C})$ of the symmetry category. Similarly, one can show that (see *e.g.* [145]) any representation of the tube algebra has a grading by elements in $\mathrm{Irr}(\mathscr{C})$: $V = \bigoplus_a V_a$. This grading is such that elements of the tube algebra that have g as the lower vertical line act as zero on those $V_{g'}$ with $g' \neq g$. In other words, the twist of the tube algebra must be compatible with that of the state it is acting on. When listing the irreducible representations of the tube algebra, we thus explicitly report how each vector space decomposes in graded components. In this case one finds:

- Two 1-dimensional irreducible representations $\mathcal{F}_1^{\pm}$ with space $V = \mathbb{C}_1$, and

$$
\mathcal{F}_1^{\pm}\left({}^{a}{+}^{1}_{1}\right) = 1\ , \qquad \mathcal{F}_1^{\pm}\left({}^{\mathcal{N}}{+}^{1}_{1}\right) = \pm\sqrt{2}\ , \qquad (10.2.16)
$$

  while all other ones are mapped to zero. They represent genuine local operators, not charged under $\mathbb{Z}_2$, which could be charged under $\mathcal{N}$ but that remain genuine local operators under its action.

- Two 1-dimensional irreducible representations $\mathcal{F}_\eta$ and $\mathcal{F}_\eta^*$ with space $V = \mathbb{C}_\eta$, and

$$\mathcal{F}_\eta\left(\begin{array}{c|c} a & \eta \\ \hline & \eta \end{array}\right) = \chi(a,\eta)\ , \qquad\qquad \mathcal{F}_\eta\left(\begin{array}{c|c} \mathcal{N} & \eta \\ \hline & \eta \end{array}\right) = i\sqrt{2}\ , \tag{10.2.17}$$

while all other ones are mapped to zero. They represent η-twisted operators that are charged under $\mathbb{Z}_2$, and that remain twisted-sector operators under the action of $\mathcal{N}$.

- Four 1-dimensional irreducible representations $\mathcal{F}_\mathcal{N}^\pm$ and $(\mathcal{F}_\mathcal{N}^\pm)^*$ with space $V = \mathbb{C}_\mathcal{N}$, and

$$\begin{aligned} &\mathcal{F}_\mathcal{N}^\pm\left(\begin{array}{c|c} 1 & \mathcal{N} \\ \hline & \mathcal{N} \end{array}\right) = 1\ , &&\mathcal{F}_\mathcal{N}^\pm\left(\begin{array}{c|c} \eta & \mathcal{N} \\ \hline & \mathcal{N} \end{array}\right) = i\ , \\ &\mathcal{F}_\mathcal{N}^\pm\left(\begin{array}{c|c} \mathcal{N}\ 1 & \mathcal{N} \\ \hline & \mathcal{N} \end{array}\right) = \pm e^{\frac{i\pi}{8}}\ , &&\mathcal{F}_\mathcal{N}^\pm\left(\begin{array}{c|c} \mathcal{N}\ \eta & \mathcal{N} \\ \hline & \mathcal{N} \end{array}\right) = \pm e^{-\frac{3i\pi}{8}}\ , \end{aligned} \tag{10.2.18}$$

while all other ones are mapped to zero. They represent $\mathcal{N}$-twisted operators, charged under η and $\mathcal{N}$, that remain $\mathcal{N}$-twisted operators under the action of $\mathcal{N}$.

- One 2-dimensional irreducible representation $\mathcal{F}_2$ with space $V = \mathbb{C}_1 \oplus \mathbb{C}_\eta$, and

$$\begin{aligned} &\mathcal{F}_2\left(\begin{array}{c|c} 1 & 1 \\ \hline & 1 \end{array}\right) = \begin{pmatrix} 1 & 0 \\ 0 & 0 \end{pmatrix}, &&\mathcal{F}_2\left(\begin{array}{c|c} \eta & 1 \\ \hline & 1 \end{array}\right) = \begin{pmatrix} -1 & 0 \\ 0 & 0 \end{pmatrix}, &&\mathcal{F}_2\left(\begin{array}{c|c} \mathcal{N} & \eta \\ \hline & 1 \end{array}\right) = \begin{pmatrix} 0 & 0 \\ \sqrt{2} & 0 \end{pmatrix} \\ &\mathcal{F}_2\left(\begin{array}{c|c} 1 & \eta \\ \hline & \eta \end{array}\right) = \begin{pmatrix} 0 & 0 \\ 0 & 1 \end{pmatrix}, &&\mathcal{F}_2\left(\begin{array}{c|c} \eta & \eta \\ \hline & \eta \end{array}\right) = \begin{pmatrix} 0 & 0 \\ 0 & 1 \end{pmatrix}, &&\mathcal{F}_2\left(\begin{array}{c|c} \mathcal{N} & 1 \\ \hline & \eta \end{array}\right) = \begin{pmatrix} 0 & \sqrt{2} \\ 0 & 0 \end{pmatrix} \end{aligned} \tag{10.2.19}$$

while all other ones are mapped to zero. It represents a doublet of a genuine local operator $\mathcal{O}_1$ and an η-twisted operator $\mathcal{O}_\eta$ that are exchanged by $\mathcal{N}$. Note that $\mathcal{O}_1$ is charged under $\mathbb{Z}_2$ while $\mathcal{O}_\eta$ is neutral.

Asymmetry of the tube algebra. The inverse bilinear form, in the ordered basis (10.2.12), reads: $\tilde{K} = \frac{1}{4}\operatorname{diag}\Big(1,1,1,0,1,1,0,-1,1,-1,\frac{1}{\sqrt{2}},-\frac{1}{\sqrt{2}}\Big) + \frac{1}{4}\operatorname{offdiag}_{[4,7]} + \frac{1}{4\sqrt{2}}\operatorname{offdiag}_{[11,12]}$, where the first term is a diagonal matrix while $\operatorname{offdiag}_{[i,j]}$ is an off-diagonal matrix with a 1 at positions (i,j) and (j,i). The symmetrizer can be computed from $\tilde{K}$.

Let us specialize to a state belonging to the 2d irreducible representation (10.2.19) of the tube algebra. For example, we can choose a pure state $\mathcal{O}_1(z)|0\rangle$ created by the untwisted local operator $\mathcal{O}_1$, which in the Ising model is $\sigma(z)$. In this case the only terms that survive in the symmetrized density matrix are

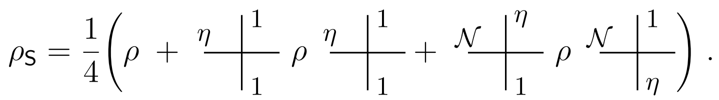

(10.2.20)

One immediately obtains $\Delta S = \log(2)$. More in general, the asymmetry of a pure state that belongs to a single d-dimensional irreducible representation of an algebra is $\Delta S = \log(d)$. Indeed, following the discussion in Fig. 2.1, the symmetrized density matrix is supported on a single block, where it takes the form $\frac{1}{\mathrm{d}}\mathbb{1}_{d\times d}$. Because the entropy of the initial state is zero, one obtains that both the entanglement and Rényi asymmetries are equal to $\log(d)$.

10.3 $\mathbb{Z}_2 \times \mathbb{Z}_2$ Tambara–Yamagami fusion category

The Ising (or $\mathbb{Z}_2$ TY) fusion category does not admit a fiber functor. This can be seen, for example, from the fact that the noninvertible line has non-integer quantum dimension. Therefore, the symmetry carries an 't Hooft anomaly and does not admit strongly-symmetric boundary conditions (in the language of [68]). Furthermore, it does not admit weakly-symmetric boundary conditions either, because the only indecomposable module is the regular one, which is not weakly symmetric.

However, one can take the stacking of two decoupled copies of the Ising symmetry and then look at a subsymmetry therein [68, 146, 147]. The full set of simple lines of the stacking is made of objects of the form $a_1 \boxtimes a_2$ with $a_j \in \{1, \eta, \mathcal{N}\}$. We consider the subcategory generated by

$$\mathcal{L}_1 = 1\boxtimes 1\ , \quad \mathcal{L}_\eta = \eta\boxtimes 1\ , \quad \mathcal{L}_{\eta'} = 1\boxtimes\eta\ , \quad \mathcal{L}_{\eta\eta'} = \eta\boxtimes\eta\ , \quad \mathcal{L}_\mathcal{V} = \mathcal{N}\boxtimes\mathcal{N}\ . \tag{10.3.1}$$

Their fusion ring is Abelian and given by:

$$\begin{aligned} &\mathcal{L}_\eta^2 = \mathcal{L}_{\eta'}^2 = \mathcal{L}_{\eta\eta'}^2 = \mathcal{L}_1\ , && \mathcal{L}_\eta\times\mathcal{L}_\mathcal{V} = \mathcal{L}_{\eta'}\times\mathcal{L}_\mathcal{V} = \mathcal{L}_\mathcal{V}\ , \\ &\mathcal{L}_\eta\times\mathcal{L}_{\eta'} = \mathcal{L}_{\eta\eta'}\ , && \mathcal{L}_\mathcal{V}\times\mathcal{L}_\mathcal{V} = \mathcal{L}_1 + \mathcal{L}_\eta + \mathcal{L}_{\eta'} + \mathcal{L}_{\eta\eta'}\ . \end{aligned} \tag{10.3.2}$$

This is in fact the fusion ring of $\mathbb{Z}_2\times\mathbb{Z}_2$ Tambara–Yamagami fusion categories [143]. In this case, the $\mathbb{Z}_2\times\mathbb{Z}_2$ symmetric bilinear character is $\gamma\Big((s_1,s_2),(s_3,s_4)\Big) = e^{i\pi(s_1s_3+s_2s_4)}$ where each $s_j \in \{0,1\}$, the Frobenius–Schur indicator is $\varkappa_\mathcal{V} = 1$, therefore the nontrivial F-symbols are

$$\Big[F^{\mathcal{V}}_{i\,\mathcal{V}\,j}\Big]_{\mathcal{V}\mathcal{V}} = \Big[F^{j}_{\mathcal{V}\,i\,\mathcal{V}}\Big]_{\mathcal{V}\mathcal{V}} = \gamma(i,j)\ , \qquad \Big[F^{\mathcal{V}}_{\mathcal{V}\mathcal{V}\mathcal{V}}\Big]_{ij} = \frac{1}{2}\,\gamma(i,j)\ , \tag{10.3.3}$$

where $i,j \in \mathbb{Z}_2^2$. The four invertible lines have quantum dimension 1, while $\mathcal{L}_{\mathcal{V}}$ has quantum dimension 2. This fusion category is also equivalent to $\mathsf{Rep}(H_8)$, where H_8 is the Kac–Paljutkin Hopf algebra [148]. As all categories of representations of a Hopf algebra, it admits at least one fiber functor given by the forgetful functor that maps a representation to its underlying vector space [69]. In this case one can show that this is the only fiber functor.[8] We conclude that the $\mathsf{Rep}(H_8)$ symmetry admits one (and only one) strongly-symmetric boundary condition. This is our motivation to study this example.

Fusion algebra

The fusion algebra has five 1-dimensional representations that we call $\mathbb{1}$, ε, σ, σ', σ''.[9] The unitary (but not symmetric) S-matrix is

$$S = \frac{1}{2\sqrt{2}} \begin{pmatrix} 1 & 1 & \sqrt{2} & \sqrt{2} & \sqrt{2} \\ 1 & 1 & -\sqrt{2} & \sqrt{2} & -\sqrt{2} \\ 1 & 1 & \sqrt{2} & -\sqrt{2} & -\sqrt{2} \\ 1 & 1 & -\sqrt{2} & -\sqrt{2} & \sqrt{2} \\ 2 & -2 & 0 & 0 & 0 \end{pmatrix} . \tag{10.3.4}$$

The symmetrizer for the fusion algebra is

$$\rho_{\mathsf{S}} = \frac{1}{32}\left(8 \sum_{a\,\in\,\mathbb{Z}_2\times\mathbb{Z}_2} \mathcal{L}_a\,\rho\,\mathcal{L}_a - B\,\rho\,B + 4\,\mathcal{L}_{\mathcal{V}}\,\rho\,\mathcal{L}_{\mathcal{V}} \right) \qquad \text{with} \qquad B = \sum_{a\,\in\,\mathbb{Z}_2\times\mathbb{Z}_2} \mathcal{L}_a \,. \tag{10.3.5}$$

Asymmetry of an excited state in CFT. Let us compute the asymmetry of excited states on the line $\mathbb{R}$ produced by Euclidean operator insertions in CFTs. For concreteness, consider the states

$$|\psi\rangle = \Big(1 + \lambda\, \varepsilon(-i\tau) \Big)\, |0\rangle \,, \tag{10.3.6}$$

that are neutral under the invertible part of the symmetry. Using (8.1), we obtain exactly the same formula (10.2.7) as before. In the case of two decoupled copies of the Ising CFT, we can take $\varepsilon(z)$ to be the energy operator of one of the two copies of Ising, so that $\Delta_\varepsilon = 1$. We obtain exactly the same function as in Fig. 10.4.

[8] Indeed, there is a unique maximal haploid algebra object in $\mathsf{Rep}(H_8)$ as shown in [147].

[9] In the case of two decoupled copies of the Ising CFT, the nine conformal primaries split as $1 \supset 1 \boxtimes 1, \varepsilon \boxtimes \varepsilon$; $\varepsilon \supset \varepsilon \boxtimes 1, 1 \boxtimes \varepsilon$; $\sigma \supset \sigma \boxtimes 1, \sigma \boxtimes \varepsilon$; $\sigma' \supset 1 \boxtimes \sigma, \varepsilon \boxtimes \sigma$; $\sigma'' \supset \sigma \boxtimes \sigma$.

Strip algebra

Strongly-symmetric boundary condition. The left-module category with a single object is described by the fusion coefficients $\tilde{N}_{a\cdot}^{\cdot} = \{1,1,1,1,2\}$. This means that the $\mathbb{Z}_2^2$ lines $\mathcal{L}_{\eta^m\eta'^n}$ have a single junction to the boundary, while the noninvertible line $\mathcal{L}_{\mathcal{V}}$ has two. Writing the $\tilde{F}$-symbols in terms of m-symbols,

$$\left[\tilde{F}_{ab\cdot}^{\cdot}\right]_{(c;-\rho)(\cdot\,;\nu\mu)} = \left(m_{a\mu,b\nu}^{c\rho}\right)^* , \tag{10.3.7}$$

the nontrivial ones are given by [146, 147]:[10]

$$\begin{gathered} m_{i,j}^{(ij)} = K_{ij} , \qquad m_{\eta,\mathcal{V}\mu}^{\mathcal{V}\rho} = m_{\mathcal{V}\rho,\eta}^{\mathcal{V}\mu} = \sqrt{2}\, m_{\mathcal{V}\mu,\mathcal{V}\rho}^{\eta} = m_{\eta',\mathcal{V}\rho}^{\mathcal{V}\mu} = m_{\mathcal{V}\mu,\eta'}^{\mathcal{V}\rho} = \sqrt{2}\, m_{\mathcal{V}\rho,\mathcal{V}\mu}^{\eta'} = M_{\mu\rho} , \\ m_{1,\mathcal{V}\mu}^{\mathcal{V}\rho} = m_{\mathcal{V}\mu,1}^{\mathcal{V}\rho} = \sqrt{2}\, m_{\mathcal{V}\mu,\mathcal{V}\rho}^{1} = \delta_{\mu\rho} , \qquad m_{\eta\eta',\mathcal{V}\mu}^{\mathcal{V}\rho} = m_{\mathcal{V}\mu,\eta\eta'}^{\mathcal{V}\rho} = \sqrt{2}\, m_{\mathcal{V}\mu,\mathcal{V}\rho}^{\eta\eta'} = (\sigma_z)_{\mu\rho} , \end{gathered} \tag{10.3.8}$$

in terms of matrices

$$K_{ij} = \begin{pmatrix} 1 & 1 & 1 & 1 \\ 1 & 1 & -i & i \\ 1 & i & 1 & -i \\ 1 & -i & i & 1 \end{pmatrix} , \quad M_{\mu\rho} = \begin{pmatrix} 0 & \xi^{-1} \\ \xi & 0 \end{pmatrix} , \quad \xi = e^{\frac{3\pi i}{4}} , \quad (\sigma_z)_{\mu\rho} = \begin{pmatrix} 1 & 0 \\ 0 & -1 \end{pmatrix} . \tag{10.3.9}$$

The m-symbols satisfy the associativity condition (8.2.19), while the $\tilde{F}$-symbols satisfy the left-module pentagon equation (A.9.1). We chose a gauge in which the $\tilde{F}$-symbols are unitary.

Strip algebra. For the unique strongly-symmetric boundary condition described above, the strip algebra $\mathsf{Strip}_{\mathsf{Rep}(H_8)}(\mathsf{Vec})$ has dimension 8. The fusion coefficients are $\tilde{N}_{a\cdot}^{\cdot} = d_a$ and the basis elements are

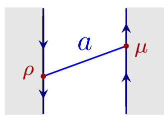

(10.3.10)

where $a \in \{1, \eta, \eta', \eta\eta', \mathcal{V}\}$, and for $a = \mathcal{V}$ the junctions are labeled by $\rho, \mu \in \{0,1\}$. We will use the notation H_i with $i \in \mathbb{Z}_2 \times \mathbb{Z}_2$ and $H_{\mathcal{V}}^{\rho,\mu}$ for the basis elements.

[10] Which we have adapted to our choice of unitary gauge.

Applying (8.2.21) we find the following algebra product (see also [121]):

$$\begin{aligned}
H_{\mathcal{V}}^{s,s'} \times H_{\eta^m\eta'^n} &= e^{-\frac{i\pi}{2}(s-s')(m-n+2mn)}\, H_{\mathcal{V}}^{s+m+n,s'+m+n} \,, \qquad\qquad H_i \times H_j = H_{(ij)} \,, \\
H_{\eta^m\eta'^n} \times H_{\mathcal{V}}^{s,s'} &= e^{\frac{i\pi}{2}(s-s')(m-n+2mn)}\, H_{\mathcal{V}}^{s+m+n,s'+m+n} \,, \\
H_{\mathcal{V}}^{s_1,s_2} \times H_{\mathcal{V}}^{s_3,s_4} &= \delta_{s_1s_3}\delta_{s_2s_4}\Big(H_1 + (-1)^{s_1+s_2} H_{\eta\eta'}\Big) \\
&\qquad + \delta_{s_1,1-s_3}\delta_{s_2,1-s_4}\Big(e^{\frac{i\pi}{2}(s_1-s_2)} H_\eta + e^{\frac{i\pi}{2}(s_2-s_1)} H_{\eta'}\Big) \,.
\end{aligned} \tag{10.3.11}$$

The symmetrizer, computed with (7.1.7), reads:

$$\rho_{\mathsf{S}} = \frac{1}{8}\left[\sum_{j\,\in\,\mathbb{Z}_2\times\mathbb{Z}_2} H_j\,\rho\,H_j + \sum_{s,\,s'\,\in\,\{0,1\}} H_{\mathcal{V}}^{s,s'}\,\rho\,H_{\mathcal{V}}^{s,s'}\right] . \tag{10.3.12}$$

Strip algebras constructed using strongly-symmetric boundary conditions are Hopf algebras. We review the definition and some properties of Hopf algebras in App. A.7. In this case one obtains an eight-dimensional Hopf algebra which is neither commutative nor cocommutative. It is known that there is only one such Hopf algebra, the Kac–Paljutkin H_8 Hopf algebra [148]. This algebra is not isomorphic to the group algebra of some group, nor to the dual of a group algebra, and it is the smallest-dimensional algebra with such properties [149, 150]. The coproduct is given by

$$\Delta(H_i) = H_i \otimes H_i \,, \qquad\qquad \Delta\Big(H_{\mathcal{V}}^{s,s'}\Big) = \frac{1}{\sqrt{2}} \textstyle\sum_{t\,\in\,\{0,1\}} H_{\mathcal{V}}^{s,t} \otimes H_{\mathcal{V}}^{t,s'} \,. \tag{10.3.13}$$

The counit and the antipode map are

$$\epsilon(H_i) = 1 \,, \qquad \epsilon\Big(H_{\mathcal{V}}^{s,s'}\Big) = \sqrt{2}\,\delta^{s,s'} \,, \qquad S(H_i) = H_i \,, \qquad S\Big(H_{\mathcal{V}}^{s,s'}\Big) = H_{\mathcal{V}}^{s',s} \,. \tag{10.3.14}$$

In the mathematical literature, the algebra H_8 is usually presented (see, *e.g.*, Sec. 4.2 of [150]) as generated by the elements $1, x, y, z$ where 1 is the identity while

$$x^2 = y^2 = 1 \,, \quad z^2 = \tfrac{1}{2}\Big(1 + x + y - xy\Big) \,, \quad xy = yx \,, \quad xz = zy \,, \quad yz = zx \,. \tag{10.3.15}$$

The basis elements are thus $\{1, x, y, z, xy, xz, yz, xyz\}$. The Hopf algebra structure is

$$\begin{aligned}
&\epsilon(x) = 1\,, && S(x) = x\,, && \Delta(x) = x\otimes x\,,\\
&\epsilon(y) = 1\,, && S(y) = y\,, && \Delta(y) = y\otimes y\,,\\
&\epsilon(z) = 1\,, && S(z) = z\,, && \Delta(z) = \tfrac{1}{2}\Big(z\otimes z + z\otimes xz + yz\otimes z - yz\otimes xz\Big)\,.
\end{aligned} \tag{10.3.16}$$

An isomorphism is given by

$$1 = H_1\,,\quad x = H_\eta\,,\quad y = H_{\eta'}\,,\quad z = \frac{1-i}{\sqrt{8}}\,H_{\mathcal{V}}^{0,0} + \frac{1}{2}\Big(H_{\mathcal{V}}^{1,0} + H_{\mathcal{V}}^{0,1}\Big) + \frac{1+i}{\sqrt{8}}\,H_{\mathcal{V}}^{1,1}\,. \tag{10.3.17}$$

The algebra has four 1-dimensional and one 2-dimensional irreducible representations. The four 1d representations $\mathcal{F}_1^\pm$ and $\mathcal{F}_\eta^\pm$ are

$$\begin{aligned}
\mathcal{F}_1^\pm:&\qquad H_i \mapsto 1\,,\, H_{\mathcal{V}}^{s,s'} \;\mapsto\; \pm\sqrt{2}\,\delta^{s,s'}\,,\\
\mathcal{F}_\eta^\pm:&\qquad H_1\,,\, H_{\eta\eta'} \mapsto 1\,,\quad H_\eta\,,\, H_{\eta'} \mapsto -1\,,\quad H_{\mathcal{V}}^{s,s'} \;\mapsto\; \pm\sqrt{2}\,\delta^{s,s'}\,e^{i\pi ss'}\,.
\end{aligned} \tag{10.3.18}$$

The 2d representation is given by

$$\mathcal{F}_2:\qquad H_{\eta^m\eta'^n} \;\mapsto\; \begin{pmatrix} (-1)^m & 0\\ 0 & (-1)^n\end{pmatrix}\,,\qquad H_{\mathcal{V}}^{s,s'} \;\mapsto\; \delta^{s,1-s'}\,\sqrt{2}\,\begin{pmatrix} 0 & (i)^{s'}\\ (-i)^{s'} & 0\end{pmatrix}\,. \tag{10.3.19}$$

The projector, or minimal central idempotent (MCI), to the trivial representation is

$$P_\epsilon = \frac{1}{8}\Big(H_1 + H_\eta + H_{\eta'} + H_{\eta\eta'} + \sqrt{2}\,H_{\mathcal{V}}^{0,0} + \sqrt{2}\,H_{\mathcal{V}}^{1,1}\Big)\,. \tag{10.3.20}$$

This is the only MCI on which the counit ϵ takes value 1. Applying the formula (8.2.37) for the symmetrizer with respect to a Hopf algebra, one reproduces the result (10.3.12) obtained using the general formula.

Example: the (Ising)^2 CFT

Consider the theory given by two decoupled copies of the Ising CFT (which has central charge $c = 1$ and is equivalent to an orbifold of the free compact boson at radius $\sqrt{2}$ times the self-dual radius). We study a subsymmetry of this theory, given by the $\mathbb{Z}_2\times\mathbb{Z}_2$ Tambara–Yamagami fusion category for the specific choice of bicharacter and Frobenius–Schur indicator already made after (10.3.2), and equivalent to the $\mathsf{Rep}(H_8)$ fusion category. This category admits a strongly-symmetric boundary condition, with which we construct the strip algebra H_8.

Case $\mathbf{1} \boxtimes \mathbf{1} + \boldsymbol{\lambda}\, \boldsymbol{\varepsilon} \boxtimes \mathbf{1}$. We study the state on the real line prepared by inserting the operator $\mathcal{O}(z) = 1 \boxtimes 1 + \lambda\, \varepsilon(z) \boxtimes 1$ at position $z = x - i\tau$. Since ε has scaling dimension $\Delta_\varepsilon = 1$, the coefficient λ has dimensions of a length. The path-integral that prepares the state is done on a half-plane. We study the asymmetry of the reduced density matrix on an interval $A = \left[-\frac{\ell}{2}, \frac{\ell}{2}\right]$, using the setup of Sec. 8.2.2: to prepare the state we cut out two discs of size ε around the entangling surface centered at $\left(\pm\frac{\ell}{2}, 0\right)$ and impose the strongly-symmetric boundary condition $|\mathcal{B}\rangle$ there. We compute the second Rényi asymmetry using the symmetrization formula derived above. This produces

$$\mathrm{Tr}\left(\rho_{\mathsf{S}}^2\right) = \frac{1}{8}\,\mathrm{Tr}\left[\sum_{j\,\in\,\mathbb{Z}_2\times\mathbb{Z}_2} \rho\, H_j\, \rho\, H_j + \sum_{s,s'} \rho\, H_{\mathcal{V}}^{s,s'}\, \rho\, H_{\mathcal{V}}^{s,s'}\right] = \frac{1}{2}\,\mathrm{Tr}\left(\rho^2 + \rho\rho'\right)\,. \quad (10.3.21)$$

Here ρ' is obtained by swiping a line $\mathcal{L}_{\mathcal{V}}$ across the whole density matrix, transforming the operator $\mathcal{O} = 1 \boxtimes 1 + \lambda\, \varepsilon \boxtimes 1$ to $\mathcal{O}' = 1 \boxtimes 1 - \lambda\, \varepsilon \boxtimes 1$. We thus get:

$$\Delta S^{(2)}[\rho] = -\log \frac{\mathrm{Tr}\left(\rho_{\mathsf{S}}^2\right)}{\mathrm{Tr}\left(\rho^2\right)} = \log 2 - \log\left[1 + \frac{\mathrm{Tr}\left(\rho\rho'\right)}{\mathrm{Tr}\left(\rho^2\right)}\right]\,. \quad (10.3.22)$$

We can express $\mathrm{Tr}(\rho\rho')/\,\mathrm{Tr}(\rho^2)$ as a ratio of partition functions on a Riemann surface obtained by gluing two copies of the complex plane with the entangling discs cut out. In the $\varepsilon \to 0$ limit, each entangling disc is replaced by a branch point and the partition functions are multiplied by the g-factor $g_{\mathcal{B}} = \langle \mathcal{B}|0\rangle$ (we already discussed such a procedure in Sec. 8.2.4). The g-factors at numerator and denominator are equal and cancel out. The same procedure is discussed in the paragraph above (10.1.26). In turn, the ratio of partition functions is equal to a ratio of correlation functions on a Riemann surface $\mathcal{M}_2$ with two branch points. We denote a point on $\mathcal{M}_2$ by z_j where $z \in \mathbb{C}$ denotes a point on the complex plane while $j \in \{1,2\}$ labels the sheet. We get:

$$\frac{\mathrm{Tr}(\rho\rho')}{\mathrm{Tr}(\rho^2)} = \frac{\left\langle 1 + 2\lambda^2\left(\varepsilon(z_1)\,\varepsilon(\bar{z}_1) - \varepsilon(z_1)\,\varepsilon(z_2) - \varepsilon(z_1)\,\varepsilon(\bar{z}_2)\right) + \lambda^4\,\varepsilon(z_1)\,\varepsilon(\bar{z}_1)\,\varepsilon(z_2)\,\varepsilon(\bar{z}_2)\right\rangle_{\mathcal{M}_2}}{\left\langle 1 + 2\lambda^2\left(\varepsilon(z_1)\,\varepsilon(\bar{z}_1) + \varepsilon(z_1)\,\varepsilon(z_2) + \varepsilon(z_1)\,\varepsilon(\bar{z}_2)\right) + \lambda^4\,\varepsilon(z_1)\,\varepsilon(\bar{z}_1)\,\varepsilon(z_2)\,\varepsilon(\bar{z}_2)\right\rangle_{\mathcal{M}_2}}. \quad (10.3.23)$$

We used the symmetry that cyclically exchanges the sheets, and that the 3-point function of ε vanishes. We can also write

$$\frac{\mathrm{Tr}(\rho_{\mathsf{S}}^2)}{\mathrm{Tr}(\rho^2)} = 1 - \frac{2\lambda^2 \left\langle \varepsilon(z_1)\varepsilon(z_2) + \varepsilon(z_1)\varepsilon(\bar{z}_2) \right\rangle_{\mathcal{M}_2}}{\left\langle 1 + 2\lambda^2 \Big(\varepsilon(z_1)\varepsilon(\bar{z}_1) + \varepsilon(z_1)\varepsilon(z_2) + \varepsilon(z_1)\varepsilon(\bar{z}_2) \Big) + \lambda^4 \, \varepsilon(z_1)\varepsilon(\bar{z}_1)\varepsilon(z_2)\varepsilon(\bar{z}_2) \right\rangle_{\mathcal{M}_2}} . \tag{10.3.24}$$

Correlation functions on $\mathcal{M}_2$ are obtained from the ones on the plane by a conformal transformation:

$$z_1 \mapsto \sqrt{\frac{z - \ell/2}{z + \ell/2}} \equiv g(z) , \qquad z_2 \mapsto -g(z) , \tag{10.3.25}$$

where the square root is taken with its branch cut along the negative real axis. The 2-point functions are then:

$$\left\langle \varepsilon(z_1)\, \varepsilon(\bar{z}_{1,2}) \right\rangle_{\mathcal{M}_2} = \frac{\left| g'(z) \right|^{2\Delta_\varepsilon}}{\left| g(z) \mp g(\bar{z}) \right|^{2\Delta_\varepsilon}} , \qquad \left\langle \varepsilon(z_1)\, \varepsilon(z_2) \right\rangle_{\mathcal{M}_2} = \frac{\left| g'(z) \right|^{2\Delta_\varepsilon}}{\left| 2g(z) \right|^{2\Delta_\varepsilon}} . \tag{10.3.26}$$

The 4-point function on $\mathcal{M}_2$ is related to the one on the complex plane as

$$\left\langle \varepsilon(z_1)\, \varepsilon(\bar{z}_1)\, \varepsilon(z_2)\, \varepsilon(\bar{z}_2) \right\rangle_{\mathcal{M}_2} = \left| g'(z) \right|^{4\Delta_\varepsilon} \left\langle \varepsilon\Big(g(z)\Big)\, \varepsilon\Big(g(\bar{z})\Big)\, \varepsilon\Big(-g(z)\Big)\, \varepsilon\Big(-g(\bar{z})\Big) \right\rangle_{\mathbb{C}} , \tag{10.3.27}$$

and the latter is given by [151]:

$$\left\langle \varepsilon(w_1)\, \varepsilon(w_2)\, \varepsilon(w_3)\, \varepsilon(w_4) \right\rangle_{\mathbb{C}} = \left| \frac{1 - \chi + \chi^2}{w_{14}\, w_{23}\, \chi} \right|^2 , \tag{10.3.28}$$

where $w_{ij} = w_i - w_j$ and $\chi = (w_{12}\, w_{34})/(w_{13}\, w_{24})$ is the conformal cross-ratio.

We report a few plots of the resulting second Rényi asymmetry in Fig. 10.5. Notice that the asymmetry takes values in the interval $[0, \log 2]$. The asymmetry vanishes in both limits $\tau \to \infty$ and $\tau \to 0$: indeed the state is dominated by $1 \boxtimes 1\, |0\rangle$ or by $\varepsilon \boxtimes 1\, |0\rangle$, respectively.

Large subsystem limit. When $\ell \to \infty$, the branch cut extends along the real line and correlation functions factorize. The 2-point functions behave as

$$\left\langle \varepsilon(z_1)\, \varepsilon(\bar{z}_1) \right\rangle_{\mathcal{M}_2} \sim \left\langle \varepsilon(z_1)\, \varepsilon(z_2) \right\rangle_{\mathcal{M}_2} \sim \frac{1}{\ell^2} , \qquad \left\langle \varepsilon(z_1)\, \varepsilon(\bar{z}_2) \right\rangle_{\mathcal{M}_2} \sim \frac{1}{(2\tau)^2} , \tag{10.3.29}$$

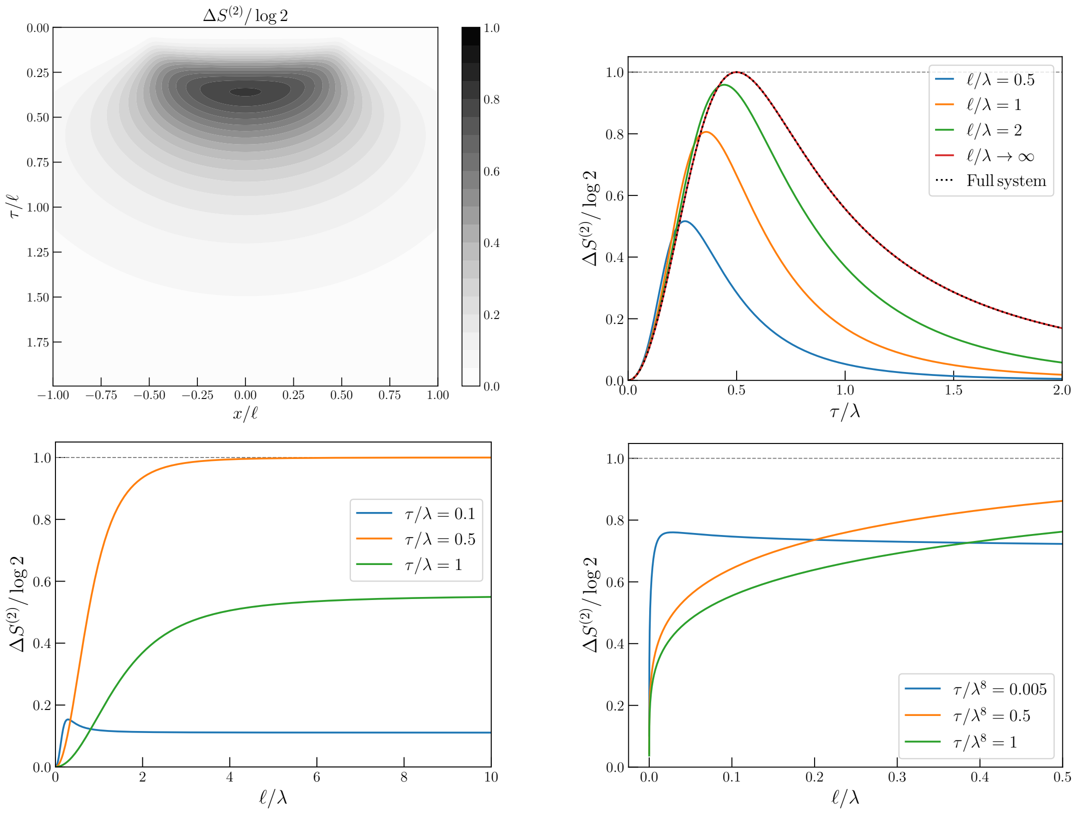

Figure 10.5: Top left: density plot of the second Rényi asymmetry of the state $\big(1\boxtimes 1 + \lambda\,\varepsilon(z)\boxtimes 1\big)|0\rangle$ for $\lambda = \ell = 1$ and with $z = x - i\tau$. Top right: second Rényi asymmetry when the field is inserted at $z = -i\tau$ as a function of τ, for different values of ℓ (in units of λ). Bottom left: second Rényi asymmetry as a function of ℓ, for different positions of the field insertion at $z = -i\tau$. Bottom right: second Rényi asymmetry of the state $\big(1 + \lambda\,\sigma(-i\tau)\big)|0\rangle$ in the Ising CFT with respect to the ordinary $\mathbb{Z}_2$ spin-flip symmetry (that acts as the strip algebra of the $\mathsf{Vec}_{\mathbb{Z}_2}$ fusion category on the interval Hilbert space with symmetric boundary conditions).

while the 4-point function factorizes through the identity channel:

$$\Big\langle \varepsilon(z_1)\,\varepsilon(\bar{z}_1)\,\varepsilon(z_2)\,\varepsilon(\bar{z}_2)\Big\rangle_{\mathcal{M}_2} \sim \frac{1}{(2\tau)^4}\,. \tag{10.3.30}$$

This gives the asymptotic behavior of the second Rényi asymmetry:

$$\Delta S^{(2)} = \log \frac{\Big[1 + \big(\frac{\lambda}{2\tau}\big)^2\Big]^2}{1 + \big(\frac{\lambda}{2\tau}\big)^4} + \mathcal{O}\Big(\lambda^2/\ell^2\Big)\,. \tag{10.3.31}$$

This expression matches with the Rényi asymmetry (10.2.7) with respect to the fusion algebra of the $\mathbb{Z}_2 \times \mathbb{Z}_2$ TY symmetry acting on the circle Hilbert space of the full system.

$\rho' \propto$ 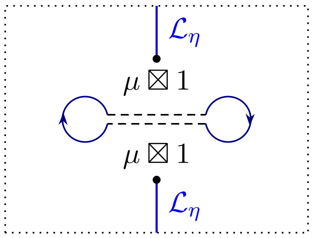

Figure 10.6: Path-integral representation of ρ', described above (10.3.32).

Non-monotonicity of Rényi asymmetry. It is interesting to notice that Rényi asymmetries are not always monotonic in the size of the subsystem. Indeed, when the field is inserted at $z = -i\tau$ and $\tau < \lambda$, the second Rényi asymmetry is not monotonic in ℓ, as shown in the bottom left panel of Fig. 10.5. This raises the question of whether such a counterintuitive behavior is a distinctive feature of asymmetries associated with noninvertible symmetries. The answer is negative: a simpler example involving a group-like symmetry also exhibits non-monotonic behavior. Specifically, we consider the state $\big(1 + \lambda\, \sigma(z)\big)|0\rangle$ in the Ising CFT (a single copy) and compute its second Rényi asymmetry with respect to the $\mathbb{Z}_2$ spin-flip symmetry over a subsystem, imposing symmetric conformal boundary conditions at the entangling surface — thus realizing a strip algebra isomorphic to $\mathbb{C}[\mathbb{Z}_2]$. The computation closely parallels the one described above: the second Rényi asymmetry is given by (10.3.22) and (10.3.23), with ε replaced by σ and λ assigned length dimension $\Delta_\sigma = \frac{1}{8}$. The relevant 4-point function of σ is provided in (10.3.33). In the bottom right panel of Fig. 10.5 we plot the second Rényi asymmetry as a function of the subsystem size ℓ, for a field insertion at $z = -i\tau$, showing a non-monotonic behavior for small values of τ.

Case $\boldsymbol{\sigma}\boxtimes$1. Consider now the state created by inserting the operator $\mathcal{O}(z) = \sigma(z)\boxtimes 1$ with dimension $\Delta_\sigma = \frac{1}{8}$ at $z = x - i\tau$. As before, let ρ be the reduced density matrix on $A = \left[-\frac{\ell}{2}, \frac{\ell}{2}\right]$ obtained using the strongly-symmetric boundary condition. The symmetrized matrix ρ_{S} is obtained applying (10.3.12). The invertible lines can freely pass through ρ_{S}, while the noninvertible one changes the untwisted operator σ to the twisted (or disorder) operator μ (with a line $\mathcal{L}_\eta$ attached). Therefore $\rho_{\mathsf{S}} = \frac{1}{2}\big(\rho + \rho'\big)$, where ρ' is the reduced density matrix of the state created by $\mathcal{O}' = \mu \boxtimes 1$. Such a density matrix contains a line $\mathcal{L}_\eta$ that goes through infinity, as depicted in Fig. 10.6.

The second Rényi asymmetry takes the form

$$\Delta S^{(2)}[\rho] = \log 2 - \log\left[1 + \frac{\big\langle \sigma(z_1)\, \sigma(\bar{z}_1)\, \mu(z_2)\, \mu(\bar{z}_2)\big\rangle_{\mathcal{M}_2}}{\big\langle \sigma(z_1)\, \sigma(\bar{z}_1)\, \sigma(z_2)\, \sigma(\bar{z}_2)\big\rangle_{\mathcal{M}_2}}\right], \tag{10.3.32}$$

where we have used the equality of 4-point functions $\langle\sigma^4\rangle = \langle\mu^4\rangle$ as a consequence of

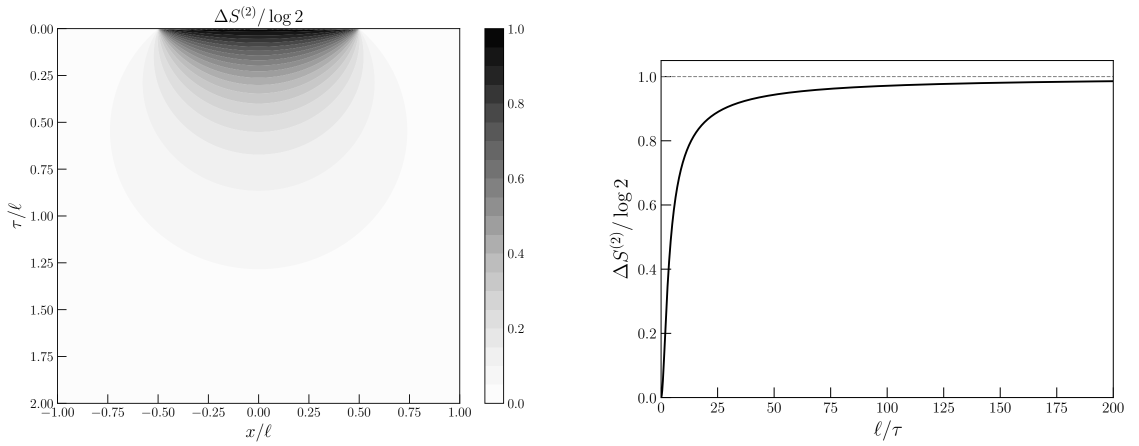

Figure 10.7: Second Rényi asymmetry of the state $\big(\sigma(z)\boxtimes 1\big)|0\rangle$ in two copies of the Ising CFT. Left: density plot of the Rényi asymmetry, as a function of the Euclidean insertion point $z = x - i\tau$. Right: Rényi asymmetry as a function of the subsystem size ℓ (measured in units of τ) for a field insertion at $z = -i\tau$.

Kramers–Wannier duality. On the plane one finds the following 4-point functions [58]:

$$\begin{aligned}
\Big\langle \sigma(w_1)\,\sigma(w_2)\,\sigma(w_3)\,\sigma(w_4)\Big\rangle_{\mathbb{C}} &= \frac{\big(1+|\chi|+|1-\chi|\big)^{1/2}}{\sqrt{2}\,\big|w_{14}\,w_{23}\,\chi\big|^{1/4}} = \frac{\big|1+\sqrt{\chi}\big|+\big|1-\sqrt{\chi}\big|}{2\big|w_{14}\,w_{23}\,\chi\big|^{1/4}}\,,\\
\Big\langle \sigma(w_1)\,\sigma(w_2)\,\mu(w_3)\,\mu(w_4)\Big\rangle_{\mathbb{C}} &= \frac{\big(1-|\chi|+|1-\chi|\big)^{1/2}}{\sqrt{2}\,\big|w_{14}\,w_{23}\,\chi\big|^{1/4}}\,,
\end{aligned} \tag{10.3.33}$$

where χ is the cross-ratio. The fields σ and μ, because of duality, have the same conformal dimension, therefore the conformal factors in the map between $\mathcal{M}_2$ and $\mathbb{C}$ simplify. This leads to the expression:

$$\Delta S^{(2)} = \log 2 - \log\left[1+\left(\frac{1-|\chi|+|1-\chi|}{1+|\chi|+|1-\chi|}\right)^{1/2}\right]\,, \tag{10.3.34}$$

where $w_1 = g(z)$, $w_2 = g(\bar{z})$, $w_3 = -g(z)$, $w_4 = -g(\bar{z})$. At finite subsystem size ℓ, the asymmetry vanishes in the limit $\tau \to \infty$ in which the field is inserted in the far Euclidean past. This is because symmetry breaking spreads over $\mathbb{R}$ and thus the subsystem only catches an infinitesimal fraction thereof. On the other hand, in the limit $\tau \to 0$ in which the field is inserted close to the real axis, the asymmetry is equal to $\log(2)$ if $x \in A$ and it vanishes if $x \notin A$. Finally, in the limit $\ell \to \infty$ that the subsystem size goes to infinity, the asymmetry is equal to $\log(2)$ irrespective of the insertion point. Plots of the Rényi asymmetry are in Fig. 10.7.

10.4 Ising symmetry — interval Hilbert space

As already mentioned in Sec. 10.2, the Ising fusion category admits only one indecomposable module category (that can describe boundary conditions): the regular one. In order to study the asymmetry on a subsystem, then, one has to employ the general procedure of Sec. 8.2.4. In the regular module the $\tilde{F}$-symbols are equal to the F-symbols, and we indicate the boundary conditions as $\{+, -, f\}$. Recall that the Ising symmetry has a multiplicity-free fusion ring, so no junction labels are necessary. Hence, we use the notation

$$H^{s,n}_{r,m}(a) \quad \equiv \tag{10.4.1}$$

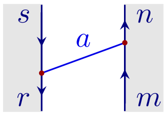

for basis elements of the strip algebra, which has dimension 34. The formula (8.2.13) for the strip-algebra product simplifies considerably, given the fact that every F-symbol is a symmetric and involutive matrix, and that every line is self-dual. We will not report it here, though.

The symmetrizer is given by a long expression. Let us write it sector by sector, in terms of the boundary conditions (r, m) for the reduced density matrix ρ.

- For a density matrix in the $(+,+)$ sector we have:

$$\rho_{\mathsf{S}} = \frac{1}{3}\Big(H^{++}_{++}(1)\,\rho\,H^{++}_{++}(1) \,+\, H^{--}_{++}(\eta)\,\rho\,H^{++}_{--}(\eta) \,+\, \frac{1}{\sqrt{2}}\,H^{ff}_{++}(\mathcal{N})\,\rho\,H^{++}_{ff}(\mathcal{N})\Big)\,. \tag{10.4.2}$$

- In the $(-,-)$ sector:

$$\rho_{\mathsf{S}} = \frac{1}{3}\Big(H^{--}_{--}(1)\,\rho\,H^{--}_{--}(1) \,+\, H^{++}_{--}(\eta)\,\rho\,H^{--}_{++}(\eta) \,+\, \frac{1}{\sqrt{2}}\,H^{ff}_{--}(\mathcal{N})\,\rho\,H^{--}_{ff}(\mathcal{N})\Big)\,. \tag{10.4.3}$$

- In the $(+,-)$ sector:

$$\rho_{\mathsf{S}} = \frac{1}{3}\Big(H^{+-}_{+-}(1)\,\rho\,H^{+-}_{+-}(1) \,+\, H^{-+}_{+-}(\eta)\,\rho\,H^{+-}_{-+}(\eta) \,+\, \frac{1}{\sqrt{2}}\,H^{ff}_{+-}(\mathcal{N})\,\rho\,H^{+-}_{ff}(\mathcal{N})\Big)\,. \tag{10.4.4}$$

- In the $(f,+)$ sector:

$$\rho_{\mathsf{S}} = \frac{1}{4}\Big(H^{f+}_{f+}(1)\,\rho\,H^{f+}_{f+}(1) \,+\, H^{f-}_{f+}(\eta)\,\rho\,H^{f+}_{f-}(\eta) \,+\, H^{+f}_{f+}(\mathcal{N})\,\rho\,H^{f+}_{+f}(\mathcal{N}) \,+\, H^{-f}_{f+}(\mathcal{N})\,\rho\,H^{f+}_{-f}(\mathcal{N})\Big)\,. \tag{10.4.5}$$

- In the $(f,-)$ sector:

$$\rho_{\mathsf{S}} = \frac{1}{4}\Big(H^{f-}_{f-}(1)\,\rho\,H^{f-}_{f-}(1) \,+\, H^{f+}_{f-}(\eta)\,\rho\,H^{f-}_{f+}(\eta) \,+\, H^{-f}_{f-}(\mathcal{N})\,\rho\,H^{f-}_{-f}(\mathcal{N}) \,+\, H^{+f}_{f-}(\mathcal{N})\,\rho\,H^{f-}_{+f}(\mathcal{N})\Big)\,. \tag{10.4.6}$$

- In the (f,f) sector:

$$\rho_{\mathsf{S}} = \frac{1}{6}\Big(H^{ff}_{ff}(1)\,\rho\,H^{ff}_{ff}(1) \,+\, H^{ff}_{ff}(\eta)\,\rho\,H^{ff}_{ff}(\eta)\Big) + \frac{1}{3\sqrt{2}}\sum_{s,\,s'\,\in\{+,-\}} H^{ss'}_{ff}(\mathcal{N})\,\rho\,H^{ff}_{ss'}(\mathcal{N})\,. \tag{10.4.7}$$

The sectors not reported are easily obtained by exchanging left and right boundary conditions.

We now proceed to compute the entanglement and Rényi asymmetries of the vacuum (*i.e.*, without operator insertions). The procedure is analogous to the group-like case in Sec. 10.1.

Consider first a generic density matrix ρ in the $(+,+)$ sector, that we indicate as ρ_{++} (as in Fig. 10.2 left), to which we apply the symmetrizer (10.4.2). Using the strip algebra products $\big[H^{++}_{++}(1)\big]^2 = H^{++}_{--}(\eta)H^{--}_{++}(\eta) = \frac{1}{\sqrt{2}}H^{++}_{ff}(\mathcal{N})H^{ff}_{++}(\mathcal{N}) = H^{++}_{++}(1)$ and orthogonality between different boundary conditions, we find $\mathrm{Tr}\big[(\rho_{++})^n_{\mathsf{S}}\big] = 3^{1-n}\,\mathrm{Tr}\big(\rho^n_{++}\big)$. Therefore the asymmetry of a state belonging to this sector is always

$$\Delta S^{(n)}[\rho_{++}] = \Delta S[\rho_{++}] = \log(3)\,. \tag{10.4.8}$$

Exactly the same result is found for ρ_{--} and ρ_{+-}. This result is valid for any state, and in particular also for the vacuum. By the same argument one finds $\mathrm{Tr}\big[(\rho_{f+})^n_{\mathsf{S}}\big] = 4^{1-n}\,\mathrm{Tr}\big(\rho^n_{f+}\big)$ and thus, for a generic density matrix ρ_{f+}:

$$\Delta S^{(n)}[\rho_{f+}] = \Delta S[\rho_{f+}] = \log(4)\,. \tag{10.4.9}$$

The same result is found for ρ_{f-}. Consider then the reduced density matrix of the vacuum in the (f,f) sector, that we indicate as ρ_{ff}, and whose symmetrizer is (10.4.7). When computing $\mathrm{Tr}\big[(\rho_{ff})^n_{\mathsf{S}}\big]$, to treat the first term in (10.4.7) one uses the products $H^{ff}_{ff}(a)H^{ff}_{ff}(b) = H^{ff}_{ff}(ab)$ for $a,b\in\{1,\eta\}\cong\mathbb{Z}_2$ and the fact that $H^{ff}_{ff}(a)$ commutes with ρ_{ff}. Since the number of lines $\mathcal{L}_\eta$ is always even, they annihilate among themselves. For the second term one uses $H^{ff}_{ss'}(\mathcal{N})H^{ss'}_{ff}(\mathcal{N}) = \frac{1}{\sqrt{2}}\Big(H^{ff}_{ff}(1)+(ss')H^{ff}_{ff}(\eta)\Big)$ with $s,s'=\pm1$. When expanding $\mathrm{Tr}\big[(\rho_{ff})^n_{\mathsf{S}}\big]$, those terms with an odd number of lines $\mathcal{L}_\eta$ cancel out. Eventually $\mathrm{Tr}\big[(\rho_{ff})^n_{\mathsf{S}}\big] = 3^{1-n}\,\mathrm{Tr}\big(\rho^n_{ff}\big)$ and hence

$$\Delta S^{(n)}[\rho_{ff}] = \Delta S[\rho_{ff}] = \log(3)\,. \tag{10.4.10}$$

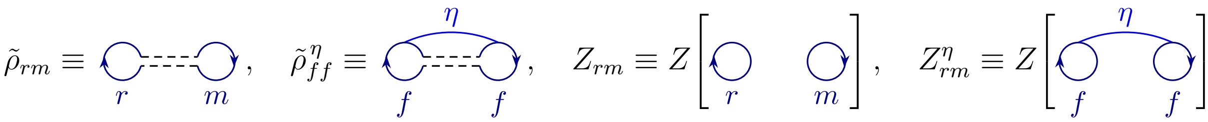

Figure 10.8: Path-integral definitions of various density matrices that enter in the symmetrization with respect to the strip algebra of the Ising fusion category with regular boundary conditions.

In all cases, the asymmetries of the vacuum in a subsystem with fixed simple boundary conditions attain a nonzero value. This is expected since each simple boundary condition breaks the symmetry.

On the other hand, let us apply the averaging procedure of Sec. 8.2.4 to the vacuum state and consider the matrix (recall that $\tilde{d}_m = d_m$ in the regular module):

$$\rho = \frac{1}{D} \sum\nolimits_{rm} d_r \, d_m \, \rho_{rm} \,. \tag{10.4.11}$$

Here ρ_{rm} is the reduced density matrix of the vacuum with boundary conditions (r,m), as in Fig. 10.2 left but without insertions, the sum is over $r, m \in \{+,-,f\}$, and $D = \left(\sum d_m\right)^2$. It is convenient to write $\rho_{rm} = Z_{rm}^{-1} \, \tilde{\rho}_{rm}$ where, as in Sec. 8.2.4, $\tilde{\rho}_{rm}$ is the unnormalized density matrix while Z_{rm} is its trace. They are depicted in Fig. 10.8. Since $\tilde{\rho}_{rm}$ come from the vacuum, the lines can move through them and the effect of the symmetrizer can be written as [11]

$$\begin{aligned}
(\tilde{\rho}_{++})_{\mathsf{S}} = (\tilde{\rho}_{--})_{\mathsf{S}} &= \frac{1}{3}\left(\tilde{\rho}_{++} + \tilde{\rho}_{--} + \frac{1}{2}\,\tilde{\rho}_{ff} + \frac{1}{2}\,\tilde{\rho}^{\eta}_{ff}\right) , \\
(\tilde{\rho}_{+-})_{\mathsf{S}} = (\tilde{\rho}_{-+})_{\mathsf{S}} &= \frac{1}{3}\left(\tilde{\rho}_{+-} + \tilde{\rho}_{-+} + \frac{1}{2}\,\tilde{\rho}_{ff} - \frac{1}{2}\,\tilde{\rho}^{\eta}_{ff}\right) , \\
(\tilde{\rho}_{f+})_{\mathsf{S}} = (\tilde{\rho}_{f-})_{\mathsf{S}} = (\tilde{\rho}_{+f})_{\mathsf{S}} = (\tilde{\rho}_{-f})_{\mathsf{S}} &= \frac{1}{4}\left(\tilde{\rho}_{f+} + \tilde{\rho}_{f-} + \tilde{\rho}_{+f} + \tilde{\rho}_{-f}\right) , \\
(\tilde{\rho}_{ff})_{\mathsf{S}} &= \frac{1}{3}\left(\tilde{\rho}_{++} + \tilde{\rho}_{--} + \tilde{\rho}_{+-} + \tilde{\rho}_{-+} + \tilde{\rho}_{ff}\right) .
\end{aligned} \tag{10.4.12}$$

Here $\tilde{\rho}^{\eta}_{ff}$ is a density matrix that contains a line $\mathcal{L}_\eta$ connecting the two boundaries of type f, as described in Fig. 10.8. To proceed, we use that $\lim_{\varepsilon \to 0} Z_{rm} \propto d_r d_m$, proven in Sec. 8.2.4. In the $\varepsilon \to 0$ limit, then, one immediately obtains the weak identity $\rho_{\mathsf{S}} = \rho$, valid when inserted into traces. We thus explicitly confirm that, in the limit, the asymmetries of the reduced vacuum density matrix vanish: $\Delta S^{(n)}[\rho] = \Delta S[\rho] = 0$.

[11] Using the tube algebra action (9.1.1) on boundary conditions, one can prove various relations among the vacuum traces, for $n \in \mathbb{Z}_{>0}$: $\mathrm{Tr}(\tilde{\rho}^n_{++}) = \mathrm{Tr}(\tilde{\rho}^n_{--})$, $\mathrm{Tr}(\tilde{\rho}^n_{+-}) = \mathrm{Tr}(\tilde{\rho}^n_{-+})$, $\mathrm{Tr}\left(\tilde{\rho}^n_{ff}\right) = \mathrm{Tr}(\tilde{\rho}^n_{++} + \tilde{\rho}^n_{+-})$, $\mathrm{Tr}\left(\tilde{\rho}^{n-1}_{ff}\tilde{\rho}^{\eta}_{ff}\right) = \mathrm{Tr}(\tilde{\rho}^n_{++} - \tilde{\rho}^n_{+-})$, as well as $\mathrm{Tr}\left(\tilde{\rho}^n_{f+}\right) = \mathrm{Tr}\left(\tilde{\rho}^n_{f-}\right) = \mathrm{Tr}\left(\tilde{\rho}^n_{+f}\right) = \mathrm{Tr}\left(\tilde{\rho}^n_{-f}\right)$. Besides, one finds the operator relations $\tilde{\rho}^{\eta}_{ff}\tilde{\rho}^{\eta}_{ff} = \tilde{\rho}_{ff}\tilde{\rho}_{ff}$ and $[\tilde{\rho}_{ff}, \tilde{\rho}^{\eta}_{ff}] = 0$. One can then verify that S is trace-preserving.

Case $1+\lambda\,\varepsilon$. We now wish to compute the asymmetry of an excited state $\mathcal{O}(z)|0\rangle$ obtained by the operator insertion $\mathcal{O}(z) = 1+\lambda\,\varepsilon(z)$ at $z = -i\tau$, along with its mirror image $\mathcal{O}^\dagger(\bar{z})$. The reduced density matrix is as in (10.4.11), but now ρ_{rm} contain the insertions. When we swipe a line $\mathcal{L}_\mathcal{N}$ through them, this time $\mathcal{O} \mapsto \mathcal{O}' = 1-\lambda\,\varepsilon$ and we call ρ'_{rm} the reduced density matrices with that insertion. The action of the symmetrizer can be written as

$$
\begin{aligned}
&(\tilde{\rho}_{++})_\mathsf{S} = (\tilde{\rho}_{--})_\mathsf{S} = \frac{\tilde{\rho}_{++}+\tilde{\rho}_{--}}{3} + \frac{\tilde{\rho}'_{ff}+\tilde{\rho}^{\eta\prime}_{ff}}{6}, \qquad (\tilde{\rho}_{f+})_\mathsf{S} = (\tilde{\rho}_{f-})_\mathsf{S} = \frac{\tilde{\rho}_{f+}+\tilde{\rho}_{f-}+\tilde{\rho}'_{+f}+\tilde{\rho}'_{-f}}{4},\\
&(\tilde{\rho}_{+-})_\mathsf{S} = (\tilde{\rho}_{-+})_\mathsf{S} = \frac{\tilde{\rho}_{+-}+\tilde{\rho}_{-+}}{3} + \frac{\tilde{\rho}'_{ff}-\tilde{\rho}^{\eta\prime}_{ff}}{6}, \qquad (\tilde{\rho}_{+f})_\mathsf{S} = (\tilde{\rho}_{-f})_\mathsf{S} = \frac{\tilde{\rho}'_{f+}+\tilde{\rho}'_{f-}+\tilde{\rho}_{+f}+\tilde{\rho}_{-f}}{4},\\
&(\tilde{\rho}_{ff})_\mathsf{S} = \frac{\tilde{\rho}'_{++}+\tilde{\rho}'_{--}+\tilde{\rho}'_{+-}+\tilde{\rho}'_{-+}+\tilde{\rho}_{ff}}{3}.
\end{aligned}
\tag{10.4.13}
$$

This allows one to compute traces of powers of ρ_S. For example, in the $\varepsilon \to 0$ limit, one can write the compact expression

$$
\lim_{\varepsilon\to 0} \frac{\mathrm{Tr}(\rho_\mathsf{S}^2)}{\mathrm{Tr}(\rho^2)} = \frac{1}{3}\,\frac{\mathrm{Tr}\Big[(3-\sqrt{2})\,\tilde{\rho}^{\,2} + \sqrt{2}\,\tilde{\rho}\,\tilde{\rho}'\Big]}{\mathrm{Tr}(\tilde{\rho}^{\,2})}\,. \tag{10.4.14}
$$

The notation on the r.h.s. should merely be interpreted as an instruction to construct a branched Riemann surface, obtained from the gluing of unnormalized density matrices followed by the $\varepsilon \to 0$ limit. The expression can be rewritten in terms of correlation functions on a two-sheeted Riemann surface $\mathcal{M}_2$:

$$
\frac{\mathrm{Tr}(\rho_\mathsf{S}^2)}{\mathrm{Tr}(\rho^2)} = 1 - \frac{\frac{4\sqrt{2}}{3}\,\lambda^2\,\Big\langle \varepsilon(z_1)\varepsilon(z_2)+\varepsilon(z_1)\varepsilon(\bar{z}_2)\Big\rangle_{\mathcal{M}_2}}{\Big\langle 1+2\lambda^2\Big(\varepsilon(z_1)\varepsilon(\bar{z}_1)+\varepsilon(z_1)\varepsilon(z_2)+\varepsilon(z_1)\varepsilon(\bar{z}_2)\Big)+\lambda^4\,\varepsilon(z_1)\varepsilon(\bar{z}_1)\varepsilon(z_2)\varepsilon(\bar{z}_2)\Big\rangle_{\mathcal{M}_2}} \tag{10.4.15}
$$

where we used the same notation as in Sec. 10.3 and cyclic permutation symmetry of the sheets. This can be used to obtain the second Rényi asymmetry, of which we present some plots in Fig. 10.9 (more generally, the n-th Rényi asymmetry can be written in terms of correlation functions up to $2n$ points). Comparing (10.4.15) with (10.3.24), the two expressions are very similar. Indeed, the second Rényi asymmetry $\Delta S^{(2)}[\rho] = -\log\big[\mathrm{Tr}(\rho_\mathsf{S}^2)/\,\mathrm{Tr}(\rho^2)\big]$ of $(1+\lambda\,\varepsilon)|0\rangle$ in the Ising CFT is very similar to (in fact, just slightly smaller than) the one of $(1+\lambda\,\varepsilon\boxtimes 1)|0\rangle$ in two copies of the Ising CFT, plotted in Fig. 10.5.

In the large subsystem limit $\ell\to\infty$, correlation functions factorize as discussed

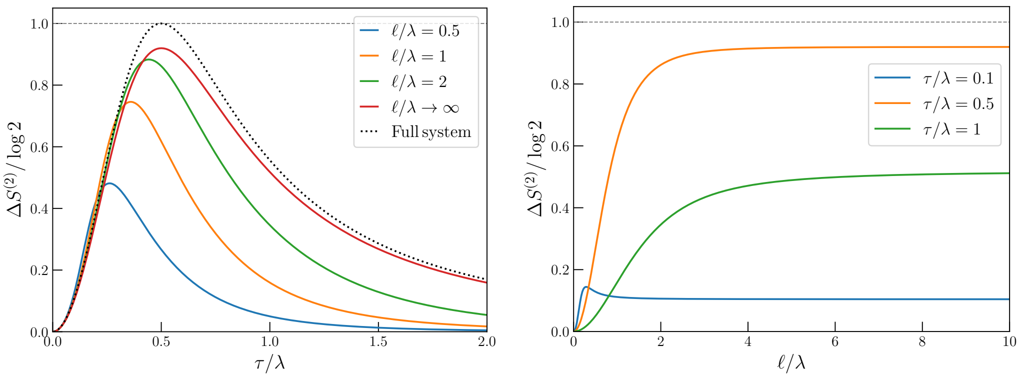

Figure 10.9: Second Rényi asymmetry of the state $\big(1+\lambda\,\varepsilon(z)\big)\,|0\rangle$ in the Ising CFT, with "averaged" boundary conditions at the entangling surface. Left: asymmetry when the field is inserted at $z = -i\tau$, as a function of τ, for different values of ℓ (in units of λ). We compare it with the asymmetry of the full system (dotted line) computed with respect to the fusion algebra. Right: asymmetry as a function of ℓ, for different positions of the field insertion at $z = -i\tau$.

around (10.3.31). For the Ising CFT, where $\Delta_\varepsilon = 1$, we obtain:

$$\lim_{\ell\to\infty} \Delta S^{(2)} = -\log\left[1 - \frac{\frac{4\sqrt{2}}{3}\left(\frac{\lambda}{2\tau}\right)^2}{\left(1+\left(\frac{\lambda}{2\tau}\right)^2\right)^2}\right]. \tag{10.4.16}$$

This, as a function of τ/λ, yields a very similar curve to the second Rényi asymmetry of the full system (10.2.7) computed with respect to the fusion algebra, just slightly smaller (the maximum of (10.4.16) is $\log\left(\frac{3}{3-\sqrt{2}}\right)$, smaller than $\log(2)$) . We compare them in Fig. 10.9. So in this case the large subsystem limit of the asymmetry computed with the averaging procedure is not identical to the asymmetry of the full system.

10.4.1 Fibonacci fusion category

The Fibonacci fusion category has 2 simple objects: $\mathcal{L}_1$, $\mathcal{L}_W$. Their fusion rule is [12]

$$\mathcal{L}_W \times \mathcal{L}_W = \mathcal{L}_1 + \mathcal{L}_W \tag{10.4.17}$$

and it is commutative. The quantum dimension of $\mathcal{L}_W$ is

$$d_W = \frac{1+\sqrt{5}}{2} \equiv \varphi \tag{10.4.18}$$

[12] The Fibonacci fusion category is also a specific instance ($N = 1$) of the Haagerup–Izumi categories, which we study in Sec. 10.4.2.

which is the golden ratio (*i.e.*, the positive solution of the equation $\varphi^2 = \varphi + 1$). Both lines are self-dual and $\varkappa_W = 1$. The only nontrivial F-symbol, in terms of $a, b \in \{1, W\}$, is [13]

$$\left[F^W_{WWW}\right]_{ab} = \begin{pmatrix} \varphi^{-1} & \varphi^{-1/2} \\ \varphi^{-1/2} & -\varphi^{-1} \end{pmatrix} , \tag{10.4.19}$$

while all other F-symbols allowed by fusion are equal to 1. The symmetrizer for the fusion algebra is determined by the inverse bilinear form $\tilde{K}$ and takes the form:

$$\rho_{\mathsf{S}} = \frac{1}{5}\Big(3\,\rho - \mathcal{L}_W\,\rho - \rho\,\mathcal{L}_W + 2\,\mathcal{L}_W\,\rho\,\mathcal{L}_W\Big) . \tag{10.4.20}$$

The fusion algebra has two one-dimensional representations $R_\pm$, where $R_+(\mathcal{L}_W) = \varphi$ while $R_-(\mathcal{L}_W) = -\varphi^{-1}$. The corresponding projectors are given by

$$P_+ = 5^{-\frac{1}{2}}\left(\varphi^{-1}\mathcal{L}_1 + \mathcal{L}_W\right) , \qquad P_- = 5^{-\frac{1}{2}}\left(\varphi\,\mathcal{L}_1 - \mathcal{L}_W\right) . \tag{10.4.21}$$

Spontaneous symmetry breaking. Like in the case of Ising, the only indecomposable module category over the Fibonacci fusion category is the regular one. This means that in a Fibonacci-symmetric gapped phase, the symmetry is always completely spontaneously broken. The clustering vacua form a 2-dimensional NIM-rep spanned by $|1\rangle$ and $|W\rangle$, and

$$\mathcal{L}_W\,|1\rangle = |W\rangle , \qquad \mathcal{L}_W\,|W\rangle = |1\rangle + |W\rangle , \tag{10.4.22}$$

where $\langle 1|1\rangle = \langle W|W\rangle = 1$. Consider the pure state $\rho = |1\rangle\langle 1|$. Using the symmetrizer (10.4.20), in the basis above we find

$$\rho = |1\rangle\langle 1| \qquad \Rightarrow \qquad \rho_{\mathsf{S}} = \frac{1}{5}\begin{pmatrix} 3 & -1 \\ -1 & 2 \end{pmatrix} . \tag{10.4.23}$$

Defining

$$\phi_+ = \frac{\sqrt{5}+1}{2\sqrt{5}} = \frac{\varphi}{\sqrt{5}} , \qquad \phi_- = \frac{\sqrt{5}-1}{2\sqrt{5}} = \frac{\varphi^{-1}}{\sqrt{5}} , \tag{10.4.24}$$

[13]There is a unique fusion category whose fusion ring is (10.4.17) and that has unitary F-symbols, see *e.g.* [129]. This category occurs for example as a subsymmetry of the tricritical Ising model [67].

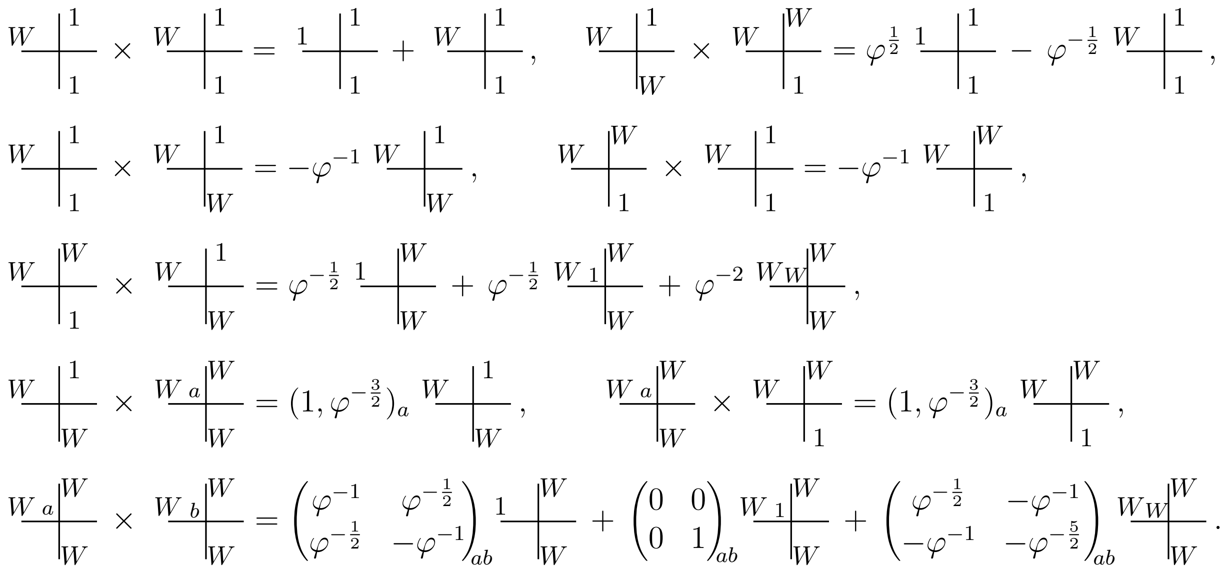

Figure 10.10: Nontrivial products in the tube algebra of the Fibonacci fusion category.

the eigenvalues of ρ_{S} are $\{\phi_+, \phi_-\}$. Then the Rényi asymmetries are $\Delta S^{(n)} = \frac{1}{1-n}\log\left(\phi_+^n + \phi_-^n\right)$ while the entanglement asymmetry is

$$\Delta S = -\phi_+ \log \phi_+ - \phi_- \log \phi_- = \frac{1}{2}\log 5 - \frac{1}{\sqrt{5}}\operatorname{arccoth}(\sqrt{5}) \simeq 0.5895 \,. \tag{10.4.25}$$

This value is smaller than $\log(2)$, the asymmetry for a spontaneously broken group of order 2. For the other vacuum:

$$\rho = |W\rangle\langle W| \qquad \Rightarrow \qquad \rho_{\mathsf{S}} = \frac{1}{5}\begin{pmatrix} 2 & 1 \\ 1 & 3 \end{pmatrix} \tag{10.4.26}$$

which gives the same asymmetries (because ρ_{S} has the same eigenvalues).

Tube algebra. This has been discussed, *e.g.*, in [129]. It has dimension 7. The elements

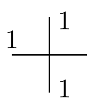 and 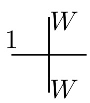 (10.4.27)

behave as the identity in the untwisted and twisted sector, respectively. The non-vanishing products are in Fig. 10.10. The algebra has three 1-dimensional and one 2-dimensional irreducible representations, that we now describe.

- A 1-dimensional representation $\mathcal{F}_1$ with space $V = \mathbb{C}_1$:

$$\mathcal{F}_1\left(\begin{smallmatrix} & 1 & \\ 1 & \!+\! & \\ & 1 & \end{smallmatrix}\right) = 1 \,, \qquad \mathcal{F}_1\left(\begin{smallmatrix} & 1 & \\ W & \!+\! & \\ & 1 & \end{smallmatrix}\right) = \varphi \,, \tag{10.4.28}$$

  while all other ones are mapped to zero. It represents genuine local operators invariant under the symmetry (up to multiplication by the quantum dimension of $\mathcal{L}_W$).

- Two 1-dimensional representations $\mathcal{F}_W$ and $\mathcal{F}_W^*$ with space $V = \mathbb{C}_W$, and

$$\mathcal{F}_W\left(\begin{smallmatrix} & W & \\ 1 & \!+\! & \\ & W & \end{smallmatrix}\right) = 1 \,, \quad \mathcal{F}_W\left(\begin{smallmatrix} & W & \\ W\,1 & \!+\! & \\ & W & \end{smallmatrix}\right) = e^{\frac{4\pi i}{5}} \,, \quad \mathcal{F}_W\left(\begin{smallmatrix} & W & \\ W\,W & \!+\! & \\ & W & \end{smallmatrix}\right) = e^{-\frac{3\pi i}{5}}\varphi^{\frac{1}{2}} \,, \tag{10.4.29}$$

  while all other ones are zero. It represents W-twisted operators, that remain W-twisted under the action of $\mathcal{L}_W$. Notice that there are two actions of $\mathcal{L}_W$ on these operators.

- One 2-dimensional representation $\mathcal{F}_2$ with space $V = \mathbb{C}_1 \oplus \mathbb{C}_W$ and

$$\mathcal{F}_2\left(\begin{smallmatrix} & 1 & \\ 1 & \!+\! & \\ & 1 & \end{smallmatrix}\right) = \begin{pmatrix} 1 & 0 \\ 0 & 0 \end{pmatrix}, \qquad \mathcal{F}_2\left(\begin{smallmatrix} & 1 & \\ W & \!+\! & \\ & 1 & \end{smallmatrix}\right) = \begin{pmatrix} -\varphi^{-1} & 0 \\ 0 & 0 \end{pmatrix}, \tag{10.4.30}$$

$$\mathcal{F}_2\left(\begin{smallmatrix} & W & \\ 1 & \!+\! & \\ & W & \end{smallmatrix}\right) = \begin{pmatrix} 0 & 0 \\ 0 & 1 \end{pmatrix}, \quad \mathcal{F}_2\left(\begin{smallmatrix} & W & \\ W\,1 & \!+\! & \\ & W & \end{smallmatrix}\right) = \begin{pmatrix} 0 & 0 \\ 0 & 1 \end{pmatrix}, \quad \mathcal{F}_2\left(\begin{smallmatrix} & W & \\ W\,W & \!+\! & \\ & W & \end{smallmatrix}\right) = \begin{pmatrix} 0 & 0 \\ 0 & \varphi^{-\frac{3}{2}} \end{pmatrix},$$

$$\mathcal{F}_2\left(\begin{smallmatrix} & W & \\ W & \!+\! & \\ & 1 & \end{smallmatrix}\right) = \begin{pmatrix} 0 & 0 \\ x & 0 \end{pmatrix}, \quad \mathcal{F}_2\left(\begin{smallmatrix} & 1 & \\ W & \!+\! & \\ & W & \end{smallmatrix}\right) = \begin{pmatrix} 0 & x \\ 0 & 0 \end{pmatrix}, \qquad x = 5^{\frac{1}{4}}\varphi^{-\frac{1}{4}} \,.$$

  It represents a doublet of an untwisted local operator $\mathcal{O}_1$ and a W-twisted operator $\mathcal{O}_W$ that get mixed under the action of $\mathcal{L}_W$.

Full and reduced strip algebras. The only indecomposable module category is the regular one. The corresponding strip algebra has dimension 13, and a basis is given by the elements:

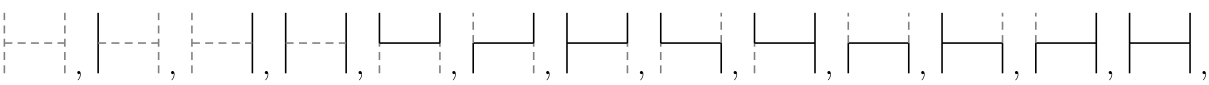

where dashed lines are $\mathcal{L}_1$ while solid lines are $\mathcal{L}_W$. One easily verifies that the boundary $\hat{\mathcal{B}} = \mathcal{L}_W$ provides a weakly-symmetric boundary condition [68], and the

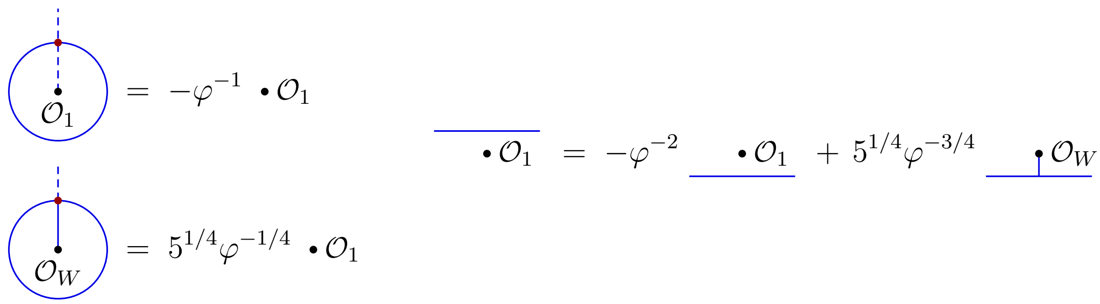

Figure 10.11: Left: lasso action of the Fibonacci tube algebra on the doublet of operators $(\mathcal{O}_1, \mathcal{O}_W)$, extracted from (10.4.30). Right: swiping action of the line $\mathcal{L}_W$ across $\mathcal{O}_1$. The coefficients have been fixed by separately completing the diagram from above and from below to form a circle, and by using the lasso actions on the left.

corresponding reduced strip algebra has dimension 2. In terms of the generators

$$\mathcal{S}_1 \; = \quad , \qquad\qquad \mathcal{S}_W \; = \quad , \tag{10.4.31}$$

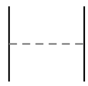

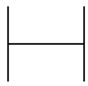

the reduced strip algebra is commutative, $\mathcal{S}_1$ is its identity, and the nontrivial product is

$$\mathcal{S}_W \times \mathcal{S}_W = \mathcal{S}_1 + \varphi^{-\frac{3}{2}}\, \mathcal{S}_W \; . \tag{10.4.32}$$

This algebra is very similar to the original fusion algebra (10.4.17), and it is semisimple. The symmetrizer with respect to the reduced strip algebra, computed using (7.1.7), takes the form

$$\rho_{\mathsf{S}} = \frac{1}{2}\left(\rho + \frac{1}{4\varphi^3+1}\left(1 - 2\varphi^{3/2}\mathcal{S}_W\right)\rho\left(1 - 2\varphi^{3/2}\mathcal{S}_W\right)\right) . \tag{10.4.33}$$

For the asymmetry of the vacuum, it is clear that the density matrix $\rho = \tilde{\rho}_{WW}/Z_{WW}$ (using the notation of Fig. 10.8) commutes with the action of the reduced strip algebra (10.4.31) (because there is a single boundary condition involved). Hence its asymmetry is zero.

We then compute the asymmetry of an excited state created by the insertion of an untwisted operator. We choose an operator transforming as $\mathcal{O}_1$ in the two-dimensional tube-algebra representation $\mathcal{F}_2$ in (10.4.30) (because the one-dimensional representations are either trivial or contain twisted-sector operators only). As above, we denote by $\mathcal{O}_1$ and $\mathcal{O}_W$ the two operators spanning the 2d irreducible representation, and we let ρ be the reduced density matrix for the state $\mathcal{O}_1(z)|0\rangle$. In order to compute the second Rényi asymmetry, we need to understand the swiping action of the line $\mathcal{L}_W$ across the operator $\mathcal{O}_1$. By looking at (10.4.30), it is clear that this will be a linear combination of $\mathcal{O}_1$ and $\mathcal{O}_W$. The result is reported in Fig. 10.11. When swiping $\mathcal{L}_W$ through ρ, which contains two instances of $\mathcal{O}_1$, it is also useful to perform an F-move described by the F-symbols (10.4.19). Consider now the limit $\varepsilon \to 0$ of small radius for the discs at the entangling surfaces. The traces of products of density matrices can be written in terms of partition functions on a replicated manifold, with the weakly-symmetric boundary condition at the entangling surfaces, and possibly with a line $\mathcal{L}_W$ connecting the two boundaries or connecting $\mathcal{O}_W$ to one of the boundaries. As discussed around (8.2.31), those partition functions can be analyzed by mapping the geometry to a cylinder and expressing them as amplitudes of Cardy states evolved in the closed channel. If the Cardy states are untwisted, the limit $\varepsilon \to 0$ simply produces two multiplicative g-factors, as in (8.2.29). If the Cardy states are twisted, instead, the ground state in the closed channel necessarily has higher energy than the untwisted vacuum, and the amplitude is suppressed by a positive power of ε. It follows that, in the $\varepsilon \to 0$ limit, partition functions involving a residual line $\mathcal{L}_W$ connected to one or both boundaries do not contribute.

For instance, in the computation of the second moment $\mathrm{Tr}(\rho_{\mathsf{S}}^2)$, we can write

$$\rho\left(1 - 2\varphi^{3/2}\mathcal{S}_W\right)\rho\left(1 - 2\varphi^{3/2}\mathcal{S}_W\right) = (1 + 4\varphi^{-1})\,\rho + 4\cdot 5^{1/2}\varphi\,\rho' + \dots\,, \tag{10.4.34}$$

where ρ' is as ρ but with $\mathcal{O}_W$ in place of $\mathcal{O}_1$ and with a line $\mathcal{L}_W$ connecting the two operators, similarly to Fig. 10.6, while the dots represent terms that are suppressed in the $\varepsilon \to 0$ limit once the trace is taken. In the end, up to an overall normalization which cancels in the ratio, we find:

$$\begin{aligned} \mathrm{Tr}\left(\rho_{\mathsf{S}}^2\right) \;&\propto\; \left(11\sqrt{5} - 24\right)\left\langle \mathcal{O}_1^\dagger\mathcal{O}_1\mathcal{O}_1^\dagger\mathcal{O}_1 \middle| \mathcal{O}_1^\dagger\mathcal{O}_1\mathcal{O}_1^\dagger\mathcal{O}_1\right\rangle_{\mathcal{M}_2} \\ &\quad + \left(25 - 11\sqrt{5}\right)\left\langle \mathcal{O}_1^\dagger\mathcal{O}_1\mathcal{O}_W^\dagger\mathcal{O}_W \middle| \mathcal{O}_1^\dagger\mathcal{O}_1\mathcal{O}_W^\dagger\mathcal{O}_W\right\rangle_{\mathcal{M}_2}\,, \\ \mathrm{Tr}\left(\rho^2\right) \;&\propto\; \left\langle \mathcal{O}_1^\dagger\mathcal{O}_1\mathcal{O}_1^\dagger\mathcal{O}_1 \middle| \mathcal{O}_1^\dagger\mathcal{O}_1\mathcal{O}_1^\dagger\mathcal{O}_1\right\rangle_{\mathcal{M}_2}\,, \end{aligned} \tag{10.4.35}$$

where the correlators are computed on the 2-sheeted Riemann surface $\mathcal{M}_2$. Hence:

$$\Delta S^{(2)} = -\log\left[\left(11\sqrt{5} - 24\right) + \left(25 - 11\sqrt{5}\right)\frac{\left\langle \mathcal{O}_1^\dagger\mathcal{O}_1\mathcal{O}_W^\dagger\mathcal{O}_W \middle| \mathcal{O}_1^\dagger\mathcal{O}_1\mathcal{O}_W^\dagger\mathcal{O}_W\right\rangle_{\mathcal{M}_2}}{\left\langle \mathcal{O}_1^\dagger\mathcal{O}_1\mathcal{O}_1^\dagger\mathcal{O}_1 \middle| \mathcal{O}_1^\dagger\mathcal{O}_1\mathcal{O}_1^\dagger\mathcal{O}_1\right\rangle_{\mathcal{M}_2}}\right]. \tag{10.4.36}$$

In the limit of a large subsystem, the correlation four-point functions factorize into two-point functions, see also the discussion around (10.1.27). While the correlator at denominator $\left\langle \mathcal{O}_1^\dagger\mathcal{O}_1\mathcal{O}_1^\dagger\mathcal{O}_1 \middle| \mathcal{O}_1^\dagger\mathcal{O}_1\mathcal{O}_1^\dagger\mathcal{O}_1\right\rangle_{\mathcal{M}_2}$ has a conformal block decomposition dominated by the identity channel and thus $\left\langle \mathcal{O}_1^\dagger\mathcal{O}_1\mathcal{O}_1^\dagger\mathcal{O}_1 \middle| \mathcal{O}_1^\dagger\mathcal{O}_1\mathcal{O}_1^\dagger\mathcal{O}_1\right\rangle_{\mathcal{M}_2} \simeq \left\langle \mathcal{O}_1^\dagger\mathcal{O}_1 \middle| \mathcal{O}_1^\dagger\mathcal{O}_1\right\rangle_{\mathbb{C}}^2$, in the numerator the OPE $\mathcal{O}_1^\dagger\mathcal{O}_W$ does not contain the identity channel and therefore, keeping into account that $\mathcal{O}_1$ and $\mathcal{O}_W$ have the same conformal dimension, the correlator $\left\langle \mathcal{O}_1^\dagger \mathcal{O}_1 \mathcal{O}_W^\dagger \mathcal{O}_W \middle| \mathcal{O}_1^\dagger \mathcal{O}_1 \mathcal{O}_W^\dagger \mathcal{O}_W \right\rangle_{\mathcal{M}_2}$ is further suppressed. We conclude that, in the large subsystem limit, the second Rényi asymmetry becomes

$$\Delta S^{(2)} = -\log\Big(11\sqrt{5} - 24\Big) \simeq 0.516 \,. \tag{10.4.37}$$

It is interesting to notice that this value is smaller than the second Rényi asymmetry of the full system computed with respect to the tube algebra. Indeed, by symmetrizing with respect to the tube algebra, one immediately gets $\Delta S^{(n)} = \Delta S = \log(2)$ because $\mathcal{O}_1$ belongs to an irreducible representation of dimension 2, see the discussion after (10.2.20).[14]

10.4.2 Haagerup fusion ring

The simplest fusion category whose product rules are both noninvertible and non-Abelian is the Haagerup fusion category [152–154], that we indicate as $H_{(3)}$. There exists a generalization to Haagerup–Izumi fusion categories [154–157] that we indicate as $H_{(N)}$, with $N > 3$. In this section we will only analyze the fusion algebra, hence we do not report the F-symbols of the category.[15] The fusion ring of $H_{(N)}$ is generated by the objects $\{\mathbb{1}, a, \varrho\}$ subject to the conditions

$$a^N = \mathbb{1} \,, \qquad a \times \varrho = \varrho \times a^{-1} \,, \qquad \varrho^2 = \mathbb{1} + \sum_{j=0}^{N-1} a^j \times \varrho \,. \tag{10.4.38}$$

We see that there is a $\mathbb{Z}_N$ subsymmetry and that, for $N \geq 3$, the element ϱ does not commute with a and thus the multiplication is non-Abelian. Conjugation is given by

$$\bar{a} = a^{-1} \,, \qquad \bar{\varrho} = \varrho \,, \qquad \overline{a^j \times \varrho} = a^j \times \varrho \,. \tag{10.4.39}$$

Notice that $H_{(1)}$ coincides with the Fibonacci (commutative) fusion ring that we already discussed in Sec. 10.4.1, while $H_{(2)}$ is the fusion ring of the $SO(3)_6$ WZW model.

---

[14] On the other hand, the asymmetry with respect to the fusion algebra vanishes: $\Delta S^{(n)} = \Delta S = 0$. To see this, we should restrict the 2d representation $\mathcal{F}_2$ of the tube algebra to its untwisted sector, corresponding to the fusion algebra, and determine how $\mathcal{O}_1$ decomposes in irreducible fusion-algebra representations. From (10.4.30), $\mathcal{O}_1$ lands in the single representation R_-. Since this is one-dimensional, the asymmetry vanishes.

[15] The F-symbols of $H_{(3)}$ can be found in [157, 158]. The F-symbols in [157] are in a particularly convenient gauge, which makes the expressions extremely compact. Numerical evidence for the existence of a CFT with Haagerup symmetry was given in [159]. The F-symbols of $H_{(N)}$ with $3 \leq N \leq 15$ odd can be found in [157].

The fusion algebra is $2N$-dimensional and a basis is given by the elements

$$\{\mathbb{1}, a, \ldots, a^{N-1}, \varrho, a\varrho, \ldots, a^{N-1}\varrho\} \ . \tag{10.4.40}$$

The symmetrizer with respect to it can be written as:

$$\rho_{\mathsf{S}} = \frac{1}{2N}\sum_{\mathcal{L}} \mathcal{L}\,\rho\,\mathcal{L}^\dagger + \frac{1}{2(N^2+4)}\Big(A\,\rho\,A - B\,\rho\,B\Big) - \frac{1}{N(N^2+4)}\Big(A\,\rho\,B + B\,\rho\,A\Big) \tag{10.4.41}$$

where in the first term we summed over all simple lines, while

$$A = \mathbb{1} + a + \ldots + a^{N-1} = A^\dagger \ , \qquad\qquad B = \varrho + a\varrho + \ldots + a^{N-1}\varrho = B^\dagger \ . \tag{10.4.42}$$

Let us list the irreducible representations of the fusion algebra. For N odd, there are two 1-dimensional representations R_+, R_- and $\frac{N-1}{2}$ 2-dimensional representations R_j. For N even, there are four 1-dimensional representations R_+, R_-, $R_{\tilde{+}}$, $R_{\tilde{-}}$ and $\frac{N-2}{2}$ 2-dimensional representations R_j. The 1-dimensional representations are:

$$\begin{aligned} &R_\pm : \qquad a = 1 \ , \qquad\quad \varrho = \tfrac{1}{2}\Big(N \pm \sqrt{N^2+4}\Big) \ , \\ &R_{\tilde{\pm}} : \qquad a = -1 \ , \qquad \varrho = \pm 1 \ . \end{aligned} \tag{10.4.43}$$

The 2-dimensional representations R_j with $j = 1, \ldots, \frac{N-1}{2}$ (for N odd) or $j = 1, \ldots, \frac{N-2}{2}$ (for N even) are:

$$R_j : \qquad a = \begin{pmatrix} \zeta^j & 0 \\ 0 & \zeta^{-j} \end{pmatrix} \ , \qquad \varrho = \begin{pmatrix} 0 & 1 \\ 1 & 0 \end{pmatrix} \ , \qquad \zeta = e^{\frac{2\pi i}{N}} \ . \tag{10.4.44}$$

Spontaneous symmetry breaking. For the Haagerup fusion ring with $N = 3$, let us consider a TQFT describing the full SSB of the symmetry, thus giving 6 vacua. These transform in the regular representation. The inverse bilinear form in the fusion algebra is given by

$$\tilde{K} = \frac{1}{39}\begin{pmatrix} 8 & \frac{3}{2} & \frac{3}{2} & -1 & -1 & -1 \\ \frac{3}{2} & \frac{3}{2} & 8 & -1 & -1 & -1 \\ \frac{3}{2} & 8 & \frac{3}{2} & -1 & -1 & -1 \\ -1 & -1 & -1 & 5 & -\frac{3}{2} & -\frac{3}{2} \\ -1 & -1 & -1 & -\frac{3}{2} & 5 & -\frac{3}{2} \\ -1 & -1 & -1 & -\frac{3}{2} & -\frac{3}{2} & 5 \end{pmatrix} \ . \tag{10.4.45}$$

We take a pure density matrix $\rho = |b\rangle\langle b|$. The symmetrized density matrix ρ_{S} has eigenvalues

$$\lambda_i = \left\{ \frac{\sqrt{13}+3}{6\sqrt{13}}, \frac{1}{6}, \frac{1}{6}, \frac{1}{6}, \frac{1}{6}, \frac{\sqrt{13}-3}{6\sqrt{13}} \right\} \tag{10.4.46}$$

for any of the six vacua. This leads to the entanglement asymmetry $\Delta S \simeq 1.6568$. This value is smaller than $\log(6)$, the asymmetry for a spontaneously broken group of order 6.

10.4.3 The $\frac{1}{2}E_6$ fusion ring

Finally, we briefly discuss the example of the $\frac{1}{2}E_6$ fusion ring, where a multiplicity greater than 1 appears. Since we limit ourselves to the study of the fusion ring, we will not be concerned with its categorifications, which do in fact exist (see [160] and Sec. 6.4 of [67]). One of the corresponding fusion categories appears as a subsymmetry of the non-diagonal $SU(2)_{10}$ WZW model of E_6 type, or of the (A_{10}, E_6) minimal model. Interestingly, the ring does not admit any braiding despite being Abelian.

The ring has three elements $\{\mathcal{L}_{\mathbb{1}}, \mathcal{L}_X, \mathcal{L}_Y\}$ with Abelian product rules

$$\mathcal{L}_X \times \mathcal{L}_X = \mathcal{L}_{\mathbb{1}} \ , \qquad \mathcal{L}_X \times \mathcal{L}_Y = \mathcal{L}_Y \times \mathcal{L}_X = \mathcal{L}_Y \ , \qquad \mathcal{L}_Y \times \mathcal{L}_Y = \mathcal{L}_{\mathbb{1}} + \mathcal{L}_X + 2\mathcal{L}_Y \ . \tag{10.4.47}$$

The non-degenerate inverse bilinear form, that provides the symmetrizer, is

$$\tilde{K} = \frac{1}{12} \begin{pmatrix} 5 & -1 & -1 \\ -1 & 5 & -1 \\ -1 & -1 & 2 \end{pmatrix} \ . \tag{10.4.48}$$

With this, we can compute the asymmetry in the case of fully broken symmetry. We get, for the three vacua, the following eigenvalues of ρ_{S} and the corresponding asymmetries:

$$\begin{aligned} |1\rangle, |X\rangle : \qquad & \lambda_i = \left\{ \frac{1}{2}, \frac{3+\sqrt{3}}{12}, \frac{3-\sqrt{3}}{12} \right\} \qquad & \Delta S \simeq 0.951 \ , \\ |Y\rangle : \qquad & \lambda_i = \left\{ \frac{3+\sqrt{3}}{6}, \frac{3-\sqrt{3}}{6}, 0 \right\} \qquad & \Delta S \simeq 0.516 \ . \end{aligned} \tag{10.4.49}$$

As in the case of the Ising symmetry, the first two vacua are related by a $\mathbb{Z}_2$ action and thus share the same asymmetry. The third vacuum, instead, has a different asymmetry.

Chapter 11

Discussion

There are several natural directions to pursue, bridging conformal field theories, holography, algebraic QFT, and condensed matter physics.

In [161] the relation between symmetric sectors of a theory and algebraic QFT axioms such as Haag duality were explored; it would be natural to connect this language of algebraic QFT with entanglement asymmetry [22, 24].

Following [48], it would be very interesting if something could be said about diagnosing long range entangled phases from entanglement asymmetry. Even in short range entangled phases like SPTs, there are situations where the asymmetry, as defined, doesn't quite fully capture the phase, as we discuss at the end of chapter 9; it would be interesting to find a way to diagnose them better.

Being a relative entropy, its monotonicity could be a useful constraint on RG flows of theories [162]. In a slightly different taste, it should have an interesting holographic description; if one were able to find a version of the gravitational replica trick of [95] to the case with topological defects inserted on the boundary. [163] would be a good place to start understanding this.

Appendix A

Appendix

A.1 Analytic continuation for renyi

We compute the Renyi asymmetries in (5.2.11) for a few semi-integer values of Δ. In particular we have to evaluate the sums

$$P_n = \sum_{j\neq k}^{n} \frac{1}{\left|2\sin\left[\frac{\pi}{n}\left(j-k+\frac{\tau_0}{\pi}\right)\right]\right|^{2\Delta}}\,. \tag{A.1.1}$$

We use the Mellin transform (5.2.12) of $1/\sin(\pi x)$.

Case $\boldsymbol{\Delta = 1/2}$. Taking into account that $\tau_0 \in (0,\pi)$ and therefore for $j>k$ the argument of the sine is between 0 and π while for $j<k$ it is between $-\pi$ and 0, we have

$$\begin{aligned}\Delta S_n^{(2)} &= \frac{n^{-1}}{n-1}\,\frac{1}{r}\int \frac{ds}{2\pi\,(1+e^s)}\left[\sum_{j>k}^{n} e^{\frac{s}{n}\left(j-k+\frac{\tau_0}{\pi}\right)} + \sum_{j<k}^{n} e^{\frac{s}{n}\left(j-k+\frac{\tau_0}{\pi}+n\right)}\right]\\ &= \frac{n^{-1}}{n-1}\,\frac{1}{r}\int ds\,\frac{n\,(e^{s/n}-e^s)}{2\pi\,(1+e^s)(1-e^{s/n})}\,e^{\frac{s\tau_0}{n\pi}}\,.\end{aligned} \tag{A.1.2}$$

We can now take the limit $\Delta S^{(2)} = \lim_{n\to 1}\Delta S_n^{(2)}$ yielding

$$\Delta S^{(2)} = \frac{1}{r}\int \frac{ds\, s\, e^{s\tau_0/\pi}}{4\pi\sinh(s)} = \frac{1}{r}\,\frac{\pi}{8\cos^2\left(\frac{\tau_0}{2}\right)}\,. \tag{A.1.3}$$

Case $\boldsymbol{\Delta = 1}$. We proceed as before, however this time there are two integrations:

$$\begin{aligned} P_n &= \frac{1}{4\pi^2}\int \frac{ds_1\,ds_2}{(1+e^{s_1})(1+e^{s_2})}\left[\sum_{j>k}^{n} e^{(s_1+s_2)\left(j-k+\frac{\tau_0}{\pi}\right)/n} + \sum_{j<k}^{n} e^{(s_1+s_2)\left(j-k+\frac{\tau_0}{\pi}+n\right)/n}\right] \\ &= \frac{1}{4\pi^2}\int ds_1\,ds_2\,\frac{n\left(e^{(s_1+s_2)/n}-e^{s_1+s_2}\right)}{(1+e^{s_1})(1+e^{s_2})(1-e^{(s_1+s_2)/n})}\,e^{\frac{(s_1+s_2)\tau_0}{n\pi}}\,. \end{aligned} \tag{A.1.4}$$

The integral can be computed analytically. First we change variables setting $s_2 = s - s_1$ and perform the integral in s_1, obtaining

$$P_n = \int ds\,\frac{ns}{8\pi^2}\,e^{\frac{s\tau_0}{n\pi}}\left(\frac{1}{\tanh(s/2n)} - \frac{1}{\tanh(s/2)}\right). \tag{A.1.5}$$

Then we shift the integration contour from $\mathbb{R}$ to $\mathbb{R}+\pi i$ by redefining $s \to s+\pi i$, as this does not cross any pole of the integrand. We perform indefinite integration in τ_0 to simplify the expression, and finally integrate in s. We obtain

$$P_n = \partial_{\tau_0}\left[\frac{n^2}{4}\left(\frac{1}{\tan(\tau_0/n)} - \frac{n}{\tan(\tau_0)} - i(n-1)\right)\right] = \frac{n^3}{4\sin^2(\tau_0)} - \frac{n}{4\sin^2(\tau_0/n)}\,. \tag{A.1.6}$$

This yields the Renyi asymmetry

$$\Delta S_n^{(2)} = \frac{1}{4r^2}\,\frac{n}{n-1}\left(\frac{1}{\sin^2(\tau_0)} - \frac{1}{n^2\sin^2(\tau_0/n)}\right) \tag{A.1.7}$$

and the entanglement asymmetry

$$\Delta S^{(2)} = \frac{1}{2r^2\sin^2(\tau_0)}\left(1 - \frac{\tau_0}{\tan(\tau_0)}\right). \tag{A.1.8}$$

Case $\boldsymbol{\Delta = 3/2}$. This time the Renyi asymmetry is given by three integrations:

$$\Delta S_n^{(2)} = \frac{n^{-2}}{n-1}\,\frac{1}{r^3}\int \frac{ds_1\,ds_2\,ds_3}{8\pi^3\,(1+e^{s_1})(1+e^{s_2})(1+e^{s_3})}\,\frac{(e^{s/n}-e^{s})}{(1-e^{s/n})}\,e^{\frac{s\tau_0}{n\pi}}\,, \tag{A.1.9}$$

where $s = s_1+s_2+s_3$. Taking the limit $n \to 1$ we obtain the entanglement asymmetry

$$\Delta S^{(2)} = \frac{1}{8\pi^3 r^3}\int \frac{ds_1\,ds_2\,ds_3}{(1+e^{s_1})(1+e^{s_2})(1+e^{s_3})}\,\frac{s\,e^{s\tau_0/\pi}}{(1-e^{-s})}\,. \tag{A.1.10}$$

It is convenient to change variables to s_1, s_2, s. The integral in s_1 can be easily performed:

$$\Delta S^{(2)} = \frac{1}{8\pi^3 r^3} \int ds_2\, ds\, \frac{s\,(s-s_2)\, e^{s\tau_0/\pi}}{(1+e^{-s_2})(e^s - e^{s_2})(1-e^{-s})}\,. \tag{A.1.11}$$

Then we shift the integration contour $s \to s + \pi i$. The integral in s_2 gives

$$\Delta S^{(2)} = \frac{e^{i\tau_0}}{8\pi^3 r^3} \int ds\, \frac{s(s+\pi i)(s+2\pi i)\, e^{s\tau_0/\pi}}{2\,(1+e^{-s})(1-e^s)}\,. \tag{A.1.12}$$

The final integral gives the entanglement asymmetry

$$\Delta S^{(2)} = \frac{3\pi}{128\, r^3 \cos^4\!\left(\frac{\tau_0}{2}\right)}\,. \tag{A.1.13}$$

Case $\boldsymbol{\Delta = 2}$. The Renyi asymmetry is given by four integrations. After taking the limit $n \to 1$ and changing variables to $s = s_1 + s_2 + s_3 + s_4$, we obtain the expression

$$\Delta S^{(2)} = \frac{1}{(2\pi r)^4} \int \frac{ds\, ds_1\, ds_2\, ds_3 \quad s\, e^{s_1+s_2+s_3}\, e^{s\tau_0/\pi}}{(1+e^{s_1})(1+e^{s_2})(1+e^{s_3})(e^{s_1+s_2+s_3}+e^s)(1-e^{-s})}\,. \tag{A.1.14}$$

We perform the integral in s_1, and then shift the integration contour $s \to s + \pi i$:

$$\Delta S^{(2)} = \frac{e^{i\tau_0}}{(2\pi r)^4} \int ds\, ds_2\, ds_3\, \frac{(s+\pi i)(s_2+s_3-s-\pi i)\, e^{s\tau_0/\pi}}{(1+e^{-s_2})(1+e^{-s_3})(e^{s_2+s_3}+e^s)(1+e^{-s})}\,. \tag{A.1.15}$$

We perform the integral in s_2, and then shift the integration contour back as $s \to s - \pi i$:

$$\Delta S^{(2)} = \frac{1}{(2\pi r)^4} \int ds\, ds_3\, \frac{s(s-s_3-\pi i)(s-s_3+\pi i)\, e^{s\tau_0/\pi}}{2(1+e^{-s_3})(e^{s_3}+e^s)(1-e^{-s})}\,. \tag{A.1.16}$$

We perform the integral in s_3:

$$\Delta S^{(2)} = \frac{1}{(2\pi r)^4} \int ds\, \frac{s^2(s^2+4\pi^2)\, e^{s\tau_0/\pi}}{6(e^s-1)(1-e^{-s})}\,. \tag{A.1.17}$$

The final integration gives the entanglement asymmetry

$$\Delta S^{(2)} = \frac{1}{4r^4 \sin^4(\tau_0)} \left(1 - \frac{1}{3}\sin^2(\tau_0) - \frac{\tau_0}{\tan(\tau_0)}\right). \tag{A.1.18}$$

A.2 Computation from relative entropy

Let us give some details on the evaluation of the integral (5.3.11):

$$I_\Delta = -\int_{\mathbb{R}} ds\, \frac{1}{4\sinh^2\!\left(\frac{s}{2}-i\varepsilon\right)\left[-4\sinh^2\!\left(\frac{s}{2}-i\tau_0\right)\right]^\Delta}\,, \tag{A.2.1}$$

in terms of the function $I_\Delta(x)$ in (5.3.12) with $x = \tan(\tau_0/2)$.

First notice that, calling $f(s)$ the integrand in (A.2.1), it satisfies $f(-s^*) = f(s)^*$. Since the operation $s \to -s^*$ maps the part of the contour with $s > 0$ to the part with $s < 0$, this implies that the integral can be written as

$$I_\Delta = \int_0^\infty \mathbb{R}\mathrm{e}\Big[f(s)\Big]\,, \tag{A.2.2}$$

showing that the integral is always real. The integrand has poles at $s = 2i\varepsilon + 2\pi ik$ and $s = 2i\tau_0 + 2\pi ik$ for any $k \in \mathbb{Z}$. We thus shift the contour as $s \to s + 2i\tau_0 - \pi i$. For $0 < \tau_0 < \frac{\pi}{2}$ the contour is moved downward and it does not cross any pole of $f(s)$. On the contrary, for $\frac{\pi}{2} < \tau_0 < \pi$ the contour is moved upward and it crosses the pole at $s = 2i\varepsilon$ where we pick up a residue. We thus obtain the expression

$$I_\Delta = J_\Delta - \delta_{\frac{\pi}{2}<\tau_0<\pi}\,\frac{2\pi\,\Delta}{4^\Delta \sin^{2\Delta}(\tau_0)\tan(\tau_0)} \tag{A.2.3}$$

where

$$J_\Delta = \int_0^\infty \mathbb{R}\mathrm{e}\left[\frac{2^{-2\Delta-1}\,ds}{\cosh^2\!\left(\frac{s}{2}+i\tau_0\right)\cosh^{2\Delta}\!\left(\frac{s}{2}\right)}\right] = \int_0^\infty \frac{\Big(1+\cos(2\tau_0)\cosh(s)\Big)\,ds}{2^\Delta\Big(\cos(2\tau_0)+\cosh(s)\Big)^2\Big(1+\cosh(s)\Big)^\Delta}\,. \tag{A.2.4}$$

To compute the integral we perform the change of variable $t = \tanh^2\!\left(\frac{s}{2}\right)$:

$$J_\Delta = \int_0^1 dt\,\frac{(1+X)(1-tX)(1-t)^\Delta}{2^{2\Delta+1}\sqrt{t}\,(1+tX)^2} \tag{A.2.5}$$

where we defined the parameter $X = \tan^2(\tau_0)$. This can be integrated as a hypergeometric function

$$J_\Delta = \frac{\sqrt{\pi}\,\Gamma(\Delta+1)}{4^\Delta\,\Gamma\!\left(\Delta+\frac{1}{2}\right)}\left(1 - \frac{\Delta}{\Delta+\frac{1}{2}}\,{}_2F_1\!\left[\tfrac{1}{2},1,\Delta+\tfrac{3}{2};-X\right]\right). \tag{A.2.6}$$

The hypergeometric function has a branch cut from 1 to infinity, conventionally taken along the positive real axis. When $0 < \tau_0 < \frac{\pi}{2}$ the argument $-X$ of the hypergeometric function goes from 0 to infinity along the negative real axis. For $\tau_0 = \frac{\pi}{2}$ the argument reaches the branch point at infinity and it moves to the second sheet. When $\frac{\pi}{2} < \tau_0 < \pi$ the argument goes from infinity to zero on the second sheet along the negative real axis. The fact that the argument is on the second sheet is implemented by the second term in (A.2.3).

In order to obtain an equivalent expression that does not require to move between different sheets, it is useful to use a different parameter $x = \tan\left(\frac{\tau_0}{2}\right)$, related to X by

$$X = \frac{4x^2}{(x^2-1)^2} \,. \tag{A.2.7}$$

Then one can use hypergeometric transformation identities (see for example [164]) to rewrite the answer in terms of x, obtaining (5.3.12). A simple way to implement the transformation is to use the fact that the hypergeometric function $y(z) = {}_2F_1(a,b,c;z)$ satisfies a second-order differential equation:

$$z(1-z)\,y''(z) + \Big(c - (a+b+1)z\Big)\,y'(z) - ab\,y(z) = 0\,. \tag{A.2.8}$$

This implies that the function $I_\Delta \equiv F(X)$ satisfies the differential equation

$$2X(X+1)\,F''(X) + (2\Delta + 5X + 3)\,F'(X) + F(X) = \frac{\sqrt{\pi}\,\Gamma(\Delta+1)}{4^\Delta \Gamma\left(\Delta + \frac{1}{2}\right)}\,. \tag{A.2.9}$$

We then use the change of variable (A.2.7) to write a differential equation for the function $I_\Delta \equiv f(x)$ in terms of the parameter x:

$$\frac{(x^2-1)^2}{8}\,f''(x) - \frac{(x^2-1)\Big(1+3x^2+(x^2-1)^2\Delta\Big)}{4x(x^2+1)}\,f'(x) + f(x) = \frac{\sqrt{\pi}\,\Gamma(\Delta+1)}{4^\Delta\Gamma\left(\Delta+\frac{1}{2}\right)}\,. \tag{A.2.10}$$

Solving this equation again gives the expression in (5.3.12).

A.3 Embedding formalism

In Poincaré coordinates, the metric of Euclidean AdS_{d+1} is

$$ds^2 = \frac{dz^2 + dx_1^2 + \ldots + dx_d^2}{z^2} \tag{A.3.1}$$

where $z > 0$. This can be obtained from the embedding formalism by introducing constrained coordinates $P_A = (P_{-1}, P_0, \ldots, P_d)$ that satisfy

$$P \cdot P \equiv -P_{-1}^2 + P_0^2 + \textstyle\sum_{i=1}^d P_i^2 = -1\,, \qquad\qquad P_{-1} \geq 1\,, \tag{A.3.2}$$

and projecting the flat metric $ds^2 = -dP_{-1}^2 + dP_0^2 + \sum_{i=1}^d dP_i^2$. This displays the $SO(d+1,1)$ isometry. The Poincaré coordinates are obtained from the parametrization

$$P_{-1} = \frac{1+z^2+\vec{x}^2}{2z}\,, \qquad P_0 = \frac{1-z^2-\vec{x}^2}{2z}\,, \qquad P_{i=1,\ldots,d} = \frac{x_i}{z}\,. \tag{A.3.3}$$

Here $\vec{x} = (x_i) = (x_1, \ldots, x_d)$. The conformal boundary is at $z = 0$.

The Rindler coordinates appearing in (6.1.12) are obtained from the parametrization

$$P_{-1} = \rho\, Y_0\,, \quad P_0 = \sqrt{\rho^2-1}\,\cos(\tau)\,, \quad P_d = \sqrt{\rho^2-1}\,\sin(\tau)\,, \quad P_{a=1,\ldots,d-1} = \rho\, Y_a\,, \tag{A.3.4}$$

where $\rho \geq 1$, the variable $\tau \in [0, 2\pi)$ is an angle, while (Y_0, Y_a) are auxiliary coordinates on $\mathbb{H}^{d-1}$ that satisfy $-Y_0^2 + \sum_{a=1}^{d-1} Y_a^2 = -1$ and $Y_0 \geq 1$. We parametrize them as

$$Y_0 = \cosh(u)\,, \qquad\qquad Y_{a=1,\ldots,d-1} = \sinh(u)\, \theta_a\,, \tag{A.3.5}$$

where $u \geq 0$ (although in the case of $d = 2$ we could set $\theta_1 = 1$ and use $u \in \mathbb{R}$) while θ_a satisfy $\sum_{a=1}^{d-1} \theta_a^2 = 1$ and describe a sphere S^{d-2} of radius 1. The induced metric is (6.1.12):

$$ds^2 = \left(\rho^2 - 1\right) d\tau^2 + \frac{d\rho^2}{\rho^2-1} + \rho^2 \left(du^2 + \sinh^2(u)\, d\Omega_{d-2}^2\right) \tag{A.3.6}$$

where $d\Omega_{d-2}^2$ is the metric on S^{d-2} induced from $ds^2 = \sum_a d\theta_a^2$. The two parametrizations of P_A given above define the change of coordinates.

In Poincaré coordinates the bulk-to-boundary propagator is as in (6.1.7):

$$K_E\left(z, \vec{x}\,\middle|\, \vec{x}\,'\right) = C_\Delta \left(\frac{z}{z^2 + (\vec{x} - \vec{x}\,')^2}\right)^{\Delta}. \tag{A.3.7}$$

In order to derive the propagator in Rindler coordinates we use the identity

$$\begin{aligned} -2\rho\, Y \cdot Y' - 2\sqrt{\rho^2-1}\cos(\tau - \tau') &= 2\Big[P_{-1} Y_0' - P_0 \cos(\tau') - P_a Y_a' - P_d \sin(\tau')\Big] \\ &= \left(Y_0' + \cos(\tau')\right) \frac{z^2 + (\vec{x} - \vec{x}\,')^2}{z} \end{aligned} \tag{A.3.8}$$

where[1]

$$x'_a = \frac{Y'_a}{Y'_0 + \cos(\tau')}\,, \qquad x'_d = \frac{\sin(\tau')}{Y'_0 + \cos(\tau')}\,, \qquad \vec{x}'^{\,2} = \frac{Y'_0 - \cos(\tau')}{Y'_0 + \cos(\tau')}\,. \tag{A.3.9}$$

The primed coordinates identify a point on the conformal boundary. In Poincaré coordinates, the metric induced on the conformal boundary at $z = 0$ from (A.3.1) is the flat one of $\mathbb{R}^d$, namely $ds^2_\partial = d\vec{x}'^{\,2}$. In these coordinates we regard x'_d as the Euclidean time, and consider the spherical spatial subregion $A = \left\{x'_d = 0,\ \vec{x}'^{\,2} < 1\right\}$ where the second term indicates the Euclidean norm of the spatial coordinates. The change of boundary coordinates (A.3.9) gives

$$ds^2_\partial = d\vec{x}'^{\,2} = \Omega^{-2}\Big(d\tau'^{\,2} + du'^{\,2} + \sinh^2(u')\, d\Omega'^{\,2}_{d-2}\Big)\,, \qquad \Omega = \cosh(u') + \cos(\tau')\,. \tag{A.3.10}$$

Here Ω is precisely the conformal factor (6.1.11), also appearing in (A.3.8). The metric in parenthesis is the one of $S^1 \times \mathbb{H}^{d-1}$, which is also the metric on the conformal boundary at $\rho = \infty$ induced from (A.3.6). The spherical spatial subregion A is mapped to a copy of $\mathbb{H}^{d-1}$ at $\tau' = 0$. Since the propagator transforms as a primary of dimension Δ, using (A.3.8) we conclude that

$$K_E\Big(\rho, \tau, Y \,\Big|\, \tau', Y'\Big) = \frac{C_\Delta}{\Big(-2\rho\, Y \cdot Y' - 2\sqrt{\rho^2 - 1}\cos(\tau - \tau')\Big)^{\Delta}}\,. \tag{A.3.11}$$

A.4 First and second law of entanglement

In the holographic context, a very natural observation is that every state (either the full system or a subregion) in the boundary CFT corresponds to some bulk AdS geometry. Not every CFT state, however, has a 'nice' or geometric bulk description. The vacuum state sure does; it corresponds to just empty AdS. Small perturbations around it do, too. Let us explore some very interesting consequences of such a duality. Starting from a (spacelike) subregion A with a normalized density matrix with $\mathrm{Tr}(\rho)_A = 1$ in a CFT_d. Then, note that we can always write an identity involving another density matrix ρ'_A :

---

[1]To invert these formulas (we omit primes) one can use $x_d = \dfrac{\sin(\tau)}{Y_0 + \cos(\tau)}$, $\dfrac{1 - \vec{x}^{\,2}}{2} = \dfrac{\cos(\tau)}{Y_0 + \cos(\tau)}$ from which one extracts $\tan(\tau) = \dfrac{2x_d}{1 - \vec{x}^{\,2}}$ and $Y_0 = \dfrac{1 + \vec{x}^{\,2}}{\sqrt{(1 - \vec{x}^{\,2})^2 + 4x_d^2}} \geq 1$.

$$\begin{aligned} S(\rho'_A) - S(\rho_A) &= \mathrm{Tr}(\rho_A \log \rho_A) - \mathrm{Tr}(\rho'_A \log \rho'_A) + \Big(\mathrm{Tr}(\rho'_A \log \rho'_A) - \mathrm{Tr}(\rho'_A \log \rho'_A) \Big) \\ &= \delta \langle H_A \rangle - S(\rho'_A || \rho_A) \\ \implies \delta S &\leq \delta \langle H_A \rangle \end{aligned}$$

where δ denotes quantities computed for ρ' minus those computed for ρ. In the last inequality, we used the positivity of relative entropy; this is an analog of the Bekenstein bound.

Let us now consider the above inequality for a *first* order perturbation to the state, $\rho_A(\lambda) = \rho_A(0) + \lambda \delta^{(1)} \rho_A + \mathcal{O}(\lambda)^2$. Then, $\rho'_A = \rho_A(\lambda), \rho_A = \rho_A(0)$ in the above equation. Then, to first order, the variation of entanglement entropy directly gives

$$\delta^{(1)} S(\rho_A) = \mathrm{Tr}\Big(\delta^{(1)} \rho_A H_A\Big) - \mathrm{Tr}\Big(\rho_A^{-1} \rho_A \; \delta^{(1)} \rho_A\Big) \tag{A.4.1}$$

$$\implies \delta^{(1)} S(\rho_A) \overset{!}{=} \delta^{(1)} \langle H \rangle \tag{A.4.2}$$

where the second term vanishes because $\rho_A(\lambda)$ and $\rho_A(0)$ is normalized to 1(all perturbations therefore have vanishing trace). Note that in the context of thermodynamic entropy this would be the first law; this equation is a generalization for entanglement entropy. Therefore, this equation is sometimes dubbed the *first law of entanglement entropy*. For ball shaped regions in CFTs, this equation is geometric.

Combining the general relations $\delta S = \delta H - S(\rho || \rho_0)$ along with the first law of entanglement above, we find that the *relative entropy* can only kick in at *second order* in perturbations. This yields the following interesting expression for the *second order* perturbations

$$\delta^{(2)} S(\rho || \rho_0) = \delta^{(2)} H(\rho) - \delta^{(2)} S(\rho)$$

These are CFT equations for reduced density matrices. These laws have very nice holographic counterparts [76, 165]. Those results are an extension of classic results of [63, 102] in the context of black hole mechanics, where the role of the black hole horizon is played by the horizon of the entanglement wedge associated to the subregion. Let us sketch the classic calculations in the case of black holes mechanics; the results extend immediately to the case of vacuum reduced density matrices and Rindler wedges.

A.4.1 Wald Iyer

Start with

$$\delta L = E(\phi)\,\delta\phi + d\Theta(\phi, \delta\phi), \tag{A.4.3}$$

Suppose ϕ solves the equations of motion, and we consider arbitrary variations $\delta\phi$, which may or not solve the linearized equations of motion about ϕ background. The variation to the Noether current from this perturbation can be computed (we will be on shell, $E(\phi) = 0$)

$$\begin{aligned}\delta J &= \delta\Theta(\phi, \mathcal{L}_\xi\phi) - \xi \cdot \delta L &(A.4.4)\\ &= \delta\Theta(\phi, \mathcal{L}_\xi\phi) - \xi \cdot d\Theta(\phi, \delta\phi) &(A.4.5)\\ &= \delta\Theta(\phi, \mathcal{L}_\xi\phi) - \mathcal{L}_\xi\Theta(\phi, \delta\phi) + d(\xi \cdot \Theta) &(A.4.6)\end{aligned}$$

Now, recall that

$$\omega(\phi, \delta_1\phi, \delta_2\phi) = \delta_1\Theta(\phi, \delta_2\phi) - \delta_2\Theta(\phi, \delta_1\phi) \tag{A.4.7}$$

and using, by construction, $\mathcal{L}_\xi\Theta = \delta_2\Theta$ whete $\delta_2\phi = \mathcal{L}_\xi\phi$, we land on the identity

$$\omega(\phi, \delta\phi, \mathcal{L}_\xi\phi) = \delta J - d(\xi \cdot \Theta) = d(\delta Q_\xi) - (\xi \cdot \Theta)) \tag{A.4.8}$$

In the last equality we further demand that $\delta\phi$ satisfy linearized equations of motion, so we may write $\delta J = d\delta Q_\xi$. Note that this is an exact form.

But recall that given a Cauchy surface Σ, recall that the Hamiltonian evolution generated by a field ξ is precisely[2]

$$\delta H_\xi = \int_\Sigma d\Sigma^\mu \omega_\mu(\phi, \delta\phi, \mathcal{L}_\xi\phi) \tag{A.4.9}$$

If ξ is a symmetry, then $\mathcal{L}_\xi\phi = 0$, and the RHS of the above equation vanishes. Therefore, integrating the RHS of A.4.8 from the bifurcation surface $\mathcal{B}$ to infinity via Stoke's theorem, we find m that the boundary terms must cancel, $\delta H_\infty + \delta H_{\mathcal{B}} = 0$.

$$\delta H_\xi|_\infty = \delta \int_{\mathcal{B}} Q_\xi \tag{A.4.10}$$

where we used that $\xi|_{\mathcal{B}} = 0$ when integrating the RHS. The left hand side is

[2]This is the field theory version of the classical mechanical statement that if X is a phase space transformation, then $\delta H_X = \int \star\omega(X)$. These are phase space variables on 'field space'.

precisely the (variation of) ADM energy E of the black hole[3]. Combining with Wald's entropy formula, we find precisely

$$\delta E = \frac{\kappa}{2\pi}\delta S \qquad \text{first law of black hole mechanics} \tag{A.4.11}$$

This is a bulk manifestation of the first law of thermodynamic entropy. The Rindler-horizon version of this result is precisely the first law of entanglement entropy. The ADM energy is replaced by the modular hamiltonian's energy, and the black hole is modelled by the Rindler wedge. The black hole temperature is the Unruh temperature of the Rindler observer, and the bifurcation surface is the area of the entangling surface.

What happens if we consider the next order variations to eq A.4.8? The key step there was the LHS vanishing when $\mathcal{L}_\xi \phi = 0$. But this needn't be true of the perturbations, and one can ask what is the fate of the quantity $\omega(\phi, \delta\phi, \mathcal{L}_\xi \delta\phi)$. Note that this symplectic current is *second order* in the perturbations; we are beyond the realm of entanglement first law. Now, the integral $\delta H_\xi = \int \omega(\delta\phi, \mathcal{L}_\xi \delta\phi) \neq 0$, and is called the *Hollands-Wald canonical energy* $\mathcal{E}$. In summary, we have demonstrated that

$$\delta^{(1)}(E - S) = 0 \qquad \Longleftrightarrow \text{Entanglement first law} \tag{A.4.12}$$

$$\delta^{(2)}(E - S) = \mathcal{E} \qquad \Longleftrightarrow S^{(2)}(\rho||\rho_0) = \mathcal{E} \tag{A.4.13}$$

This is the holographic dual to the perturbative relative entropy we used in our calculation in 6.1.

A.5 Some properties of (Rényi) asymmetry

Here, we first comment on the finiteness of the asymmetry. Recall that the relative entropy $S[\rho\|\sigma] \equiv \mathrm{Tr}[\rho\log\rho - \rho\log\sigma]$ is finite as long as the condition $\ker(\sigma) \subseteq \ker(\rho)$ holds. This guarantees finiteness of the second term in the relative entropy, while the first term is always finite.

We now aim to show that, for the specific choice $\sigma = \rho_{\mathsf{S}}$, such a condition always holds:

$$\ker(\rho_{\mathsf{S}}) \subseteq \ker(\rho) \ . \tag{A.5.1}$$

[3]There are also angular momentum terms for rotating black holes, which we have suppressed to keep the presentation simple

To show this, we first notice that $\mathsf{S}^\dagger = \mathsf{S}$ with respect to the Hilbert-Schmidt scalar product on operators:

$$\mathrm{Tr}\left[(\mathsf{S}(M))^\dagger N\right] = \mathrm{Tr}\left[M^\dagger \mathsf{S}(N)\right] \tag{A.5.2}$$

as can be checked by using (7.1.7), the self-adjointness of the SSI, and cyclicity of the trace. This also implies that the decomposition $\mathrm{End}(\mathcal{H}) = \ker(\mathsf{S}) \oplus \mathbb{I}\mathrm{m}(\mathsf{S})$ is orthogonal with respect to the same scalar product.

Let now P be the orthogonal projector[4] onto $\ker(\rho_{\mathsf{S}})$ and note that this commutes with the action of the algebra.[5] We thus have $\mathsf{S}(P) = P$. Then consider the following string of equalities:

$$\mathrm{Tr}[P\rho] = \mathrm{Tr}[\mathsf{S}(P)\rho] = \mathrm{Tr}[P\rho_{\mathsf{S}}] = \mathrm{Tr}[P\rho_{\mathsf{S}}P] = 0 \; . \tag{A.5.3}$$

Then, letting $\rho^\dagger = \rho$ and using the Hilbert-Schmidt norm we have:

$$\left\|\rho^{1/2}P\right\|^2 = \mathrm{Tr}\left[P\rho^{1/2}\rho^{1/2}P\right] = \mathrm{Tr}[P\rho] = 0 \; . \tag{A.5.4}$$

Therefore, $\rho^{1/2}P = 0$ as an operator, and thus also $\rho P = 0$. To conclude, take $|v\rangle \in \ker(\rho_{\mathsf{S}})$, so that $P|v\rangle = |v\rangle$. Then $0 = \rho P|v\rangle = \rho|v\rangle$, so also $|v\rangle \in \ker(\rho)$.

This establishes the finiteness of the asymmetry, as well as that of all quantities appearing in the computation (7.1.9).

We finally show here that all Rényi asymmetries turn out to be nonnegative. First, we write these as

$$\Delta S^{(n)}[\rho] = H_n(\rho_{\mathsf{S}}) - H_n(\rho) \; , \tag{A.5.5}$$

where $H_n[\rho] \equiv \frac{1}{1-n}\log \mathrm{Tr}[\rho^n]$ is the n-th Rényi entropy of a density matrix.

Following [53], let ρ be a Hermitian matrix, and let $\lambda(\rho)$ be the vector of its eigenvalues, sorted in decreasing order:

$$\lambda(\rho) = (\lambda_1(\rho), \cdots, \lambda_d(\rho)) \; . \tag{A.5.6}$$

A unital quantum channel is a linear, completely positive, trace preserving map

[4]Orthogonal with respect to the physical scalar product.

[5]To see this, write P as a function of ρ_{S}: $P = \prod_{j=1}^{\mathrm{rk}(\rho_{\mathsf{S}})}\left(\mathbb{1} - \frac{\rho_{\mathsf{S}}}{\lambda_j}\right)$, where λ_j are the distinct nonzero eigenvalues of ρ_{S}. One can check that $P|\lambda_k\rangle = 0$ for all k, and that $P|v\rangle = |v\rangle$ if $\rho_{\mathsf{S}}|v\rangle = 0$. It is then obvious that, since ρ_{S} commutes with the action of the algebra, the same must be true for P.

(between linear operators) Φ such that $\Phi(\mathbb{1}) = \mathbb{1}$. As we have already commented, our symmetrizer S is a trace-preserving quantum channel. It is furthermore unital, as a consequence of property 3. in 7.1. One can then apply Uhlmann's theorem (see Theorem 4.32 of [53]) to the channel S. The theorem implies, among other things, that

$$\lambda(\rho_{\mathsf{S}}) \prec \lambda(\rho) \ , \tag{A.5.7}$$

where $v \prec w$ means that

$$\sum\nolimits_{i=1}^{k} v_i \leq \sum\nolimits_{i=1}^{k} w_i \ , \tag{A.5.8}$$

for every $k = 1, \ldots, d$, provided that the entries of the real d-dimensional vectors v and w are ordered in decreasing order. Moreover, the equality holds for $k = d$ (as it should be since the trace is supposed to be preserved). A real function of such vectors is called Schur-convex if $x \prec y \Rightarrow f(x) \leq f(y)$ and Schur-concave when the inequalities are in opposite directions. Rényi entropies H_n are known to be Schur-concave functions [166]. This is precisely the statement of non-negativity of (A.5.5).

A.6 Strongly separable algebras and the symmetrizer

Consider a finite-dimensional unital semisimple associative algebra $\mathcal{X}_a \times \mathcal{X}_b = \sum_c T^c_{ab}\mathcal{X}_c$ (often we will omit the product sign $\times$) over $\mathbb{C}$ as in (7.1.1). Here $\{\mathcal{X}_a\}$ is a basis of the algebra, and one defines a trace as $\mathrm{Tr}(\mathcal{X}_a) = \sum_m T^m_{am}$ then extended by linearity. In the finite-dimensional case, such algebras are automatically strongly separable and the symmetric bilinear form K_{ab} defined in (7.1.3) is non-degenerate. We call $\tilde{K} \equiv K^{-1}$ its inverse. Indeed, the Wedderburn–Artin theorem states that every finite-dimensional unital semisimple associative algebra over $\mathbb{C}$ is isomorphic to a sum of matrix algebras,

$$\mathcal{A} \cong \bigoplus\nolimits_{\alpha=1}^{r} \mathrm{Mat}_{N_\alpha \times N_\alpha}(\mathbb{C}) \ , \tag{A.6.1}$$

where r is the number of blocks, N_α are the sizes of the matrices, and those numbers are unique up to permutation. Note that r is also the number of irreducible representations, and N_α are their dimensions. Using the isomorphism (A.6.1), all properties of the algebras can be explicitly checked. Following [124], we construct the dual basis $\{\mathsf{X}^a\}$ with respect to the bilinear form:

$$\mathsf{X}^a = \sum\nolimits_b \tilde{K}^{ab}\mathcal{X}_b \ . \tag{A.6.2}$$

It satisfies $\mathrm{Tr}\big(\mathcal{X}_a\, \mathsf{X}^b\big) = \delta_a^b$. Going to a basis, one proves that for every $x \in \mathcal{A}$:

$$x = \sum\nolimits_a \mathrm{Tr}(x\, \mathcal{X}_a)\, \mathsf{X}^a = \sum\nolimits_a \mathrm{Tr}(x\, \mathsf{X}^a)\, \mathcal{X}_a \; . \tag{A.6.3}$$

The symmetric separability idempotent (SSI) can be written as

$$e = \sum\nolimits_{ab} \tilde{K}^{ab} \mathcal{X}_a \otimes \mathcal{X}_b = \sum\nolimits_a \mathcal{X}_a \otimes \mathsf{X}^a = \sum\nolimits_a \mathsf{X}^a \otimes \mathcal{X}_a \; . \tag{A.6.4}$$

It is clearly symmetric in the exchange of the two factors. One proves that e commutes with every element of $\mathcal{A}$. Using the shorthand notations $\mathcal{X}_b\, e \equiv (\mathcal{X}_b \otimes \mathbb{1})\, e$ and $e\, \mathcal{X}_b \equiv e\, (\mathbb{1} \otimes \mathcal{X}_b)$:

$$\begin{aligned}\mathcal{X}_b\, e &= \sum\nolimits_a \mathcal{X}_b \mathcal{X}_a \otimes \mathsf{X}^a = \sum\nolimits_{ac} \mathrm{Tr}\big(\mathcal{X}_b \mathcal{X}_a \mathsf{X}^c\big) \mathcal{X}_c \otimes \mathsf{X}^a \\ &= \sum\nolimits_{ac} \mathcal{X}_c \otimes \mathrm{Tr}\big(\mathsf{X}^c \mathcal{X}_b \mathcal{X}_a\big) \mathsf{X}^a = \sum\nolimits_c \mathcal{X}_c \otimes \mathsf{X}^c \mathcal{X}_b = e\, \mathcal{X}_b \; . \end{aligned} \tag{A.6.5}$$

We can use K to obtain a pivotal relation. Consider the following element of $\mathcal{A} \otimes \mathcal{A}$:

$$\sum\nolimits_b \mathcal{X}_b \otimes \mathcal{X}_a \mathsf{X}^b = \sum\nolimits_b \mathcal{X}_b \mathcal{X}_a \otimes \mathsf{X}^b = \sum\nolimits_{bc} T^c_{ba} \mathcal{X}_c \otimes \mathsf{X}^b = \sum\nolimits_{bc} \mathcal{X}_b \otimes T^b_{ca} \mathsf{X}^c \; . \tag{A.6.6}$$

In the first equality we used that e commutes with $\mathcal{A}$ also "from the inside", which follows from the fact that e is symmetric. In the last equality we moved the scalars and renamed the indices. Since $\{\mathcal{X}_b\}$ are a basis on the first factor of $\mathcal{A} \otimes \mathcal{A}$, we conclude that

$$\mathcal{X}_a \times \mathsf{X}^b = \sum\nolimits_c T^b_{ca} \mathsf{X}^c \; . \tag{A.6.7}$$

This can be rewritten as the pivotal relation (7.1.5). One can also obtain

$$\sum\nolimits_{ab} T^c_{ab} \mathsf{X}^b \mathsf{X}^a = \mathsf{X}^c \; . \tag{A.6.8}$$

Using the trace relation (A.6.3), the identity element (7.1.6) can be written as

$$\mathcal{X}_{\mathbb{1}} = \sum\nolimits_a \mathrm{Tr}(\mathcal{X}_{\mathbb{1}} \mathcal{X}_a)\, \mathsf{X}^a = \sum\nolimits_{ab} T^b_{ab} \mathsf{X}^a = \sum\nolimits_b \mathcal{X}_b \mathsf{X}^b = \sum\nolimits_b \mathsf{X}^b \mathcal{X}_b \; . \tag{A.6.9}$$

In the third equality we used (A.6.7). Using the notation $xy \equiv \mu(x \otimes y)$ for the product, we can regard the previous relation as the contraction $\mu(e) = \mathcal{X}_{\mathbb{1}}$. Finally, let us show that e is idempotent as an element of $\mathcal{A} \otimes \mathcal{A}^{\mathrm{op}}$ (where $\mathcal{A}^{\mathrm{op}}$ is the same as $\mathcal{A}$ but elements are multiplied in the opposite order). In other words, $e^2 = e$ where e acts on itself from the outside:

$$e^2 = \sum\nolimits_{ab} \mathcal{X}_a \mathcal{X}_b \otimes \mathsf{X}^b \mathsf{X}^a = \sum\nolimits_{abc} T^c_{ab} \mathcal{X}_c \otimes \mathsf{X}^b \mathsf{X}^a = \sum\nolimits_c \mathcal{X}_c \otimes \mathsf{X}^c = e \; . \tag{A.6.10}$$

In the third equality we moved the scalars to the other side and used (A.6.8). We have thus shown that e is a *symmetric separability idempotent*, that commutes with the algebra and gives the identity upon contraction.

Relation with special Frobenius algebras. The strong separability condition allows one to make $\mathcal{A}$ into a special Frobenius algebra $(\mathcal{A}, \mu, u, \Delta, \epsilon)$. The product $\mu\colon \mathcal{A}\otimes\mathcal{A} \to \mathcal{A}$ is the one already defined. The unital map $u\colon \mathbb{C} \to \mathcal{A}$ is given by $u(1) = \mathcal{X}_{\mathbb{1}}$ and linearity. They satisfy $\mu\big(x\otimes u(1)\big) = \mu\big(u(1)\otimes x\big) = x$. The coproduct $\Delta\colon \mathcal{A} \to \mathcal{A}\otimes\mathcal{A}$ is defined as

$$\Delta(x) = x\, e = e\, x \; . \tag{A.6.11}$$

It satisfies $\mu\circ\Delta = \mathrm{id}_{\mathcal{A}}$ because $\mu\big(\Delta(x)\big) = \mu(xe) = \mu\big(\sum_a x\mathcal{X}_a \otimes \mathsf{X}^a\big) = \sum_a x\mathcal{X}_a\mathsf{X}^a = x\mathcal{X}_{\mathbb{1}}$. Note that $\Delta\circ\mu \neq \mathrm{id}_{\mathcal{A}\otimes\mathcal{A}}$. The Frobenius relation

$$(\mathrm{id}_{\mathcal{A}}\otimes\mu)\circ(\Delta\otimes\mathrm{id}_{\mathcal{A}}) = (\mu\otimes\mathrm{id}_{\mathcal{A}})\circ(\mathrm{id}_{\mathcal{A}}\otimes\Delta) = \Delta\circ\mu \tag{A.6.12}$$

simply follows from $xey = xye$. One can also define the counital map $\epsilon\colon \mathcal{A} \to \mathbb{C}$ using the trace, $\epsilon(x) = \mathrm{Tr}(x)$. It satisfies $(\mathrm{id}_{\mathcal{A}}\otimes\epsilon)\circ\Delta = \mathrm{id}_{\mathcal{A}} = (\epsilon\otimes\mathrm{id}_{\mathcal{A}})\circ\Delta$. The first equation is

$$(\mathrm{id}_{\mathcal{A}}\otimes\epsilon)\circ\Delta(x) = (\mathrm{id}_{\mathcal{A}}\otimes\epsilon)\Big(\textstyle\sum_a x\mathcal{X}_a\otimes\mathsf{X}^a\Big) = \displaystyle\sum\nolimits_a x\,\mathcal{X}_a\;\mathrm{Tr}(\mathsf{X}^a) = x\,\mathcal{X}_{\mathbb{1}} = x \; . \tag{A.6.13}$$

The second equation is similar. One finds $\Delta\big(u(1)\big) = e$ and $\epsilon\big(\mu(e)\big) = \dim\mathcal{A}$.

$*$-structure. A $*$-structure on an algebra $\mathcal{A}$ over the complex field $\mathbb{C}$ is an anti-linear involution $\dagger\colon \mathcal{A}\to\mathcal{A}$ (*i.e.*, such that $X^{\dagger\dagger} = X$ and $(\alpha X + \beta Y)^\dagger = \alpha^* X^\dagger + \beta^* Y^\dagger$ for $\alpha, \beta \in \mathbb{C}$) which is also an anti-homomorphism: $(XY)^\dagger = Y^\dagger X^\dagger$.

If $\mathcal{A}$ is a finite-dimensional C^*-algebra, a version of the Wedderburn–Artin theorem (see [125] Th. 6.3.8) states that the isomorphism to a sum of matrix algebras can be chosen such that the star operation is mapped to the standard matrix adjoint operation. Consider for simplicity the case of a single block of size N: $\mathcal{A} \cong \mathrm{Mat}_{N\times N}(\mathbb{C})$, which means that $\mathcal{A}$ is simple (the following arguments extend to the general case of multiple blocks with minimal modifications). Then we can represent the index a as $a \equiv ij$ with $i, j = 1, \ldots, N$. Let us work in a special basis in which $\mathcal{X}_a \equiv \mathcal{X}_{ij}$ is mapped by the $*$-algebra isomorphism to the matrix with a single 1 at position (i,j) and all other entries vanishing. In this basis the product is

$$\mathcal{X}_a \times \mathcal{X}_b \equiv \mathcal{X}_{ij}\times\mathcal{X}_{kl} = \delta_{jk}\,\mathcal{X}_{il} \; , \tag{A.6.14}$$

in other words the structure constants are

$$T_{ab}^{c} \equiv T_{ij,kl}^{mn} = \delta_i^m \delta_{jk} \delta_l^n \ . \tag{A.6.15}$$

The symmetric bilinear form is [6]

$$K_{ab} \equiv K_{ij,kl} = \sum\nolimits_{mnrs} T_{ij,mn}^{rs} \, T_{kl,rs}^{mn} = N \, \delta_{il} \delta_{jk} \ . \tag{A.6.16}$$

This is indeed invertible, and the inverse is

$$\tilde{K}^{ab} \equiv \tilde{K}^{ij,kl} = N^{-1} \, \delta^{il} \delta^{jk} \ . \tag{A.6.17}$$

In this basis the symmetric separability idempotent takes the simple form

$$e = \sum\nolimits_{ijkl} \tilde{K}^{ij,kl} \, \mathcal{X}_{ij} \otimes \mathcal{X}_{kl} = N^{-1} \sum\nolimits_{ij} \mathcal{X}_{ij} \otimes \mathcal{X}_{ji} \ . \tag{A.6.18}$$

The star operation takes a simple form as well:

$$\mathcal{X}_a^\dagger \equiv \mathcal{X}_{ij}^\dagger = \mathcal{X}_{ji} \ . \tag{A.6.19}$$

We see that e is Hermitian: $e^\dagger = e$. Since Hermiticity does not depend on the basis (it is invariant under isomorphism), we conclude that e is Hermitian in general:

$$e^\dagger = \sum\nolimits_{ab} (\tilde{K}^{ab})^* \, \mathcal{X}_a^\dagger \otimes \mathcal{X}_b^\dagger = e \ . \tag{A.6.20}$$

In the special basis the SSI can also be written as follows:

$$e = N^{-1} \sum\nolimits_{ij} \mathcal{X}_{ij}^\dagger \otimes \mathcal{X}_{ij} \ . \tag{A.6.21}$$

By a rescaling of the basis, $\mathcal{X}_{\underline{a}} \equiv N^{-\frac{1}{2}} \mathcal{X}_{ij}$, it reads $e = \sum_{\underline{a}} \mathcal{X}_{\underline{a}}^\dagger \otimes \mathcal{X}_{\underline{a}}$. This very simple form (which is reached also in the general case of multiple blocks) is not invariant under change of basis, however it is useful that such an expression exists. The special basis provides a Kraus representation of the symmetrizer. This implies that our symmetrizer is in fact a (trace preserving) quantum channel, and in particular is completely positive [167].

[6] In the general case (A.6.1), $\mathcal{A}$ is isomorphic to a sum of matrix algebras. The basis elements can be labeled as $\mathcal{X}_{\alpha ij}$. Then K_{ab} is as in (A.6.16) in each block, namely $K_{\alpha ij, \beta kl} = N_\alpha \, \delta_{\alpha\beta} \, \delta_{il} \delta_{jk}$. All the following formulas apply block by block.

Consequences for the symmetrizer. The symmetrizer can be defined in terms of the symmetric separability idempotent e as the linear map $\rho_{\mathsf{S}} = e(\rho) = \sum_{ab} \tilde{K}^{ab}\, \mathcal{X}_a \rho \mathcal{X}_b$. Idempotency of e implies that $(\rho_{\mathsf{S}})_{\mathsf{S}} = \rho_{\mathsf{S}}$ and thus the symmetrizer is a projector. The property $\mu(e) = \mathcal{X}_{\mathbb{1}}$ and symmetry of e imply that $\mathrm{Tr}(\rho_{\mathsf{S}}) = \mathrm{Tr}(\rho)$ and that, if ρ commutes with $\mathcal{A}$, then $\rho_{\mathsf{S}} = \rho$. Since e commutes with $\mathcal{A}$ then ρ_{S} commutes with $\mathcal{A}$. In other words, the image of the projector is precisely given by the matrices that commute with the action of the algebra, and not a subspace thereof.

Since $e = e^\dagger$, when $\rho = \rho^\dagger$ is Hermitian one finds that also ρ_{S} is Hermitian. Finally, assume that the density matrix ρ is nonnegative, namely that $\langle\psi|\rho|\psi\rangle \geq 0$ for every vector $|\psi\rangle$ in the Hilbert space. Then

$$\langle\psi|\rho_{\mathsf{S}}|\psi\rangle = \sum\nolimits_{ab} \tilde{K}^{ab} \langle\psi|\mathcal{X}_a \rho \mathcal{X}_b|\psi\rangle \overset{\text{special basis}}{=} \sum\nolimits_{\underline{a}} \langle\psi|\mathcal{X}_{\underline{a}}^\dagger \rho \mathcal{X}_{\underline{a}}|\psi\rangle \geq 0 \,. \tag{A.6.22}$$

In the second equality we used the special basis adapted to the $*$-structure. In that basis we find a sum of nonnegative numbers, which is nonnegative. This proves that also ρ_{S} is nonnegative.

A.6.1 C^*-structure of fusion algebras

A C^*-algebra $\mathcal{A}$ is a Banach algebra[7] over $\mathbb{C}$, with a $*$-structure $\dagger\colon \mathcal{A} \to \mathcal{A}$ and with a norm such that

$$\|x^\dagger x\| = \|x\|^2 \qquad \text{for all } x \in \mathcal{A} \,. \tag{A.6.23}$$

This condition is called the C^* relation and it is very restrictive, indeed, if it exists, such a norm is uniquely fixed by the algebraic structure as

$$\|x\|^2 = \|x^\dagger x\| = \sup\Big\{ |\lambda| \;\Big|\; (x^\dagger x - \lambda \mathbb{1}) \text{ is not invertible} \Big\} \,. \tag{A.6.24}$$

One can prove that C^*-algebras are semisimple.

Let us show that finite-dimensional fusion algebras are C^*-algebras. We show that

$$x^\dagger x = 0 \qquad \Rightarrow \qquad x = 0 \,. \tag{A.6.25}$$

For finite-dimensional unital $*$-algebras, this implies that they are C^* (see, *e.g.*, Prop. 2.1 in [168] or Th. 2.4.4 in [169]). Decompose $x = \sum_a x_a \mathcal{L}_a$. Then

$$x^\dagger x = \sum\nolimits_{abcd} x_a^* x_b \, N_{ac}^{1} \, N_{cb}^{d} \, \mathcal{L}_d \,. \tag{A.6.26}$$

[7]Meaning that it is associative, it has a norm such that $\|xy\| \leq \|x\| \cdot \|y\|$, and it is complete with respect to the metric induced by that norm.

Assume that $x^\dagger x = 0$, then $\sum_{abc} x_a^* x_b \, N_{ac}^1 \, N_{cb}^d = 0$ for all d. Taking $d = 1$ we get $\sum_a |x_a|^2 = 0$, therefore $x = 0$. We conclude that finite-dimensional fusion algebras are C^*-algebras, and thus they are also semisimple.

A.6.2 Explicit form of ρ_{S}

Let us consider an algebra $\mathcal{A}$, with the same hypotheses as above, which we identify with a matrix algebra by virtue of (A.6.1). We pick a basis of $\mathcal{A}$ given by $\{\mathcal{X}_{\alpha,ij}\}$ as above (A.6.14), where

$$\mathcal{X}_{\alpha,ij} = \left(\begin{array}{c|c|c} 0 & 0 & 0 \\ \hline 0 & e_{ij}^\alpha & 0 \\ \hline 0 & 0 & 0 \end{array}\right) \leftarrow \alpha\text{-th block} \qquad \begin{array}{c} \alpha = 1, \dots, r \\ i, j = 1, \dots, N_\alpha \end{array} \tag{A.6.27}$$

and e_{ij}^α is the $N_\alpha \times N_\alpha$ matrix that has a single 1 in position (i, j) and 0 elsewhere. The β-th representation of $\mathcal{A}$ merely selects the β-th diagonal block from the matrix above. The most generic representation $\mathfrak{R} \colon \mathcal{A} \to \mathrm{End}(V)$ is a direct sum of irreducible representations:

$$V = \bigoplus\nolimits_{\alpha=1}^{r} \, n_\alpha \, V_\alpha \ , \tag{A.6.28}$$

where $\dim(V_\alpha) = N_\alpha$, and thus the matrix that represents $\mathcal{X}_{\alpha,ij}$ is of the form:

$$\mathfrak{R}(\mathcal{X}_{\alpha,ij}) = \left(\begin{array}{c|c|c} 0 & 0 & 0 \\ \hline 0 & \begin{matrix} e_{ij}^\alpha & & 0 \\ & \ddots & \\ 0 & & e_{ij}^\alpha \end{matrix} & 0 \\ \hline 0 & 0 & 0 \end{array}\right) \leftarrow \alpha\text{-th block} \tag{A.6.29}$$

where e_{ij}^α is repeated n_α times. We now assume that the symmetrizer, which in principle can be any element of $\mathrm{End}\big(\mathrm{End}(V)\big)$, is written in the following form:[8]

$$M_{\mathsf{S}} = \sum\nolimits_{\alpha, i, j, \alpha', i', j'} \; c_{(\alpha,ij)(\alpha',i'j')} \;\; \mathfrak{R}(\mathcal{X}_{\alpha,ij}) \; M \; \mathfrak{R}(\mathcal{X}_{\alpha',i'j'}) \ , \tag{A.6.30}$$

where $M \in \mathrm{End}(V)$ is any matrix, that we also decompose in blocks $M^{\alpha\alpha'}$ according to (A.6.28). Thanks to property 2. and to Schur's lemma,[9] we can conclude that, as

[8] This assumption is referred to as "universality" in Sec. 7.1.

[9] Schur's lemma [52] can be stated (under our working hypotheses) as the fact that the module-endomorphisms of an irreducible $\mathcal{A}$-module form a division algebra. But there is only one such algebra over $\mathbb{C}$: the complex numbers themselves. Since the identity is clearly a module-endomorphism, we conclude that all such endomorphisms must be proportional to the identity. In more concrete terms, matrices that commute with all elements of an irreducible representation of $\mathcal{A}$ must be proportional to the identity matrix. This result generalizes the well-known analogous result for groups and group

a matrix, M_{S} has vanishing off-diagonal blocks, $(M_{\mathsf{S}})^{\alpha\alpha'} = 0$ for $\alpha \neq \alpha'$, while each diagonal block is of the form

$$(M_{\mathsf{S}})^{\alpha\alpha} = \begin{pmatrix} \lambda^{\alpha\alpha}_{11} \mathbb{1}_{N_\alpha} & \cdots & \lambda^{\alpha\alpha}_{1n_\alpha} \mathbb{1}_{N_\alpha} \\ \vdots & \ddots & \vdots \\ \lambda^{\alpha\alpha}_{n_\alpha 1} \mathbb{1}_{N_\alpha} & \cdots & \lambda^{\alpha\alpha}_{n_\alpha n_\alpha} \mathbb{1}_{N_\alpha} \end{pmatrix} . \tag{A.6.31}$$

In principle each coefficient $\lambda^{\alpha\alpha}_{ab}$ is completely generic. However, using the additional assumption (A.6.30), we have

$$M_{\mathsf{S}} = \sum_{\alpha,\, i,\, j,\, i',\, j'} c_{(\alpha,ij)(\alpha,i'j')} \left(\begin{array}{c|ccc|c} 0 & & 0 & & 0 \\ \hline 0 & e^\alpha_{ij} m^{\alpha\alpha}_{11} e^\alpha_{i'j'} & \cdots & e^\alpha_{ij} m^{\alpha\alpha}_{1n_\alpha} e^\alpha_{i'j'} & 0 \\ 0 & \vdots & \ddots & \vdots & 0 \\ 0 & e^\alpha_{ij} m^{\alpha\alpha}_{n_\alpha 1} e^\alpha_{i'j'} & \cdots & e^\alpha_{ij} m^{\alpha\alpha}_{n_\alpha n_\alpha} e^\alpha_{i'j'} & 0 \\ \hline 0 & & 0 & & 0 \end{array}\right) \begin{array}{l} \\ \\ \leftarrow \alpha\text{-th block} \\ \\ \\ \end{array} \tag{A.6.32}$$

where $m^{\alpha\alpha}_{ab}$ with $a, b \in \{1, \dots, n_\alpha\}$ are sub-blocks of $M^{\alpha\alpha}$. The symmetrization in each of the sub-blocks $m^{\alpha\alpha}_{ab}$ depends only on the entries of M of that same sub-block. Let us now focus on such a sub-block. Its symmetrized version is

$$\sum\nolimits_{i,\, j,\, i',\, j'} c_{(\alpha,ij)(\alpha,i'j')}\, e^\alpha_{ij}\, m^{\alpha\alpha}_{ab}\, e^\alpha_{i'j'} = \sum\nolimits_{i,\, j,\, i',\, j'} c_{(\alpha,ij)(\alpha,i'j')}\, (m^{\alpha\alpha}_{ab})_{ji'}\, e^\alpha_{ij'} \,. \tag{A.6.33}$$

This must be proportional to the identity, so it must be $c_{(\alpha,ij)(\alpha,i'j')} = \delta_{ij'}\, \tilde{c}^\alpha_{i'j}$. Consider now a matrix M that is nonzero only in the block $m^{\alpha\alpha}_{aa}$. Imposing conservation of the trace gives $\sum_j (m^{\alpha\alpha}_{aa})_{jj} = \mathrm{Tr}(M) \stackrel{!}{=} \mathrm{Tr}(M_{\mathsf{S}}) = N_\alpha \sum_{ji'} \tilde{c}^\alpha_{i'j} (m^{\alpha\alpha}_{aa})_{ji'}$. We conclude it must be $\tilde{c}^\alpha_{i'j} = \delta_{i'j}/N_\alpha$ and $c_{(\alpha,ij)(\alpha,i'j')} = \delta_{ij'}\delta_{i'j}/N_\alpha$. This means that the sub-block (a, b) of the block (α, α) is

$$\sum\nolimits_{i,\, j,\, i',\, j'} c_{(\alpha,ij)(\alpha,i'j')}\, e^\alpha_{ij}\, m^{\alpha\alpha}_{ab}\, e^\alpha_{i'j'} = \frac{1}{N_\alpha} \mathrm{Tr}(m^{\alpha\alpha}_{ab})\, \mathbb{1}^\alpha_{ab} \,. \tag{A.6.34}$$

Notice that conservation of the trace has also fixed those blocks with $a \neq b$.

Said in words, the matrix M_{S} is proportional to the identity in blocks that connect isomorphic irreducible representations, and is zero elsewhere. In each block, the proportionality constant is the trace of that block, divided by its dimension[10] (see also Fig. 2.1).

---

algebras.

[10]Implicit in this statement is a choice of basis such that all copies of a given representation use the same matrices, as was the case in (A.6.29). This choice implies that also the off-diagonal blocks are proportional to the identity (see fn. 9). Indeed, such blocks are nonzero module-endomorphisms between isomorphic representations and thus, as matrices, commute with all elements of the corresponding irreducible module of $\mathcal{A}$.

A.7 Hopf algebras, modules, and tensor products

We review here the definition of Hopf algebras, following [117,138,139]. An associative algebra $\mathcal{A}$ over $\mathbb{C}$ has an associative product $\mu\colon \mathcal{A}\otimes\mathcal{A}\to\mathcal{A}$ and a unit $u\colon \mathbb{C}\to\mathcal{A}$ such that

$$\mu\circ\Big(u(1)\otimes\mathrm{id}\Big)=\mathrm{id}=\mu\circ\Big(\mathrm{id}\otimes u(1)\Big)\,. \tag{A.7.1}$$

We will henceforth denote $u(1)\equiv\mathbb{1}$. Both μ and u are linear, and u is unique when it exists. A coassociative coalgebra $\mathcal{A}$ over $\mathbb{C}$, instead, has a coassociative coproduct $\Delta\colon\mathcal{A}\to\mathcal{A}\otimes\mathcal{A}$, such that $(\Delta\otimes\mathrm{id})\circ\Delta=(\mathrm{id}\otimes\Delta)\circ\Delta\equiv\Delta^2$, and a counit $\epsilon\colon\mathcal{A}\to\mathbb{C}$ such that

$$(\epsilon\otimes\mathrm{id})\circ\Delta=\mathrm{id}=(\mathrm{id}\otimes\epsilon)\circ\Delta\,. \tag{A.7.2}$$

Both Δ and ϵ are linear, and ϵ is unique. It is convenient to use Sweedler's notation: it is always possible to write (in a non-unique way) coproducts as sums: $\Delta(x)=\sum_i x^i_{(1)}\otimes x^i_{(2)}$. This is concisely written as $\Delta(x)=x_{(1)}\otimes x_{(2)}$ with the sum kept implicit.

A weak bialgebra $\mathcal{A}$ has both the algebra and coalgebra structures, which must be compatible in the following sense. The coproduct is an algebra homomorphism: $\Delta(xy)=\Delta(x)\,\Delta(y)$, where on the r.h.s. pairwise multiplication is used. The counit is weakly multiplicative:

$$\epsilon(xyz)=\epsilon\Big(x\,y_{(1)}\Big)\,\epsilon\Big(y_{(2)}\,z\Big)=\epsilon\Big(x\,y_{(2)}\Big)\,\epsilon\Big(y_{(1)}\,z\Big)\,, \tag{A.7.3}$$

where associativity is assumed. The unit is weakly comultiplicative, that can be written as

$$\Delta^2(\mathbb{1})=\Big(\Delta(\mathbb{1})\otimes\mathbb{1}\Big)\Big(\mathbb{1}\otimes\Delta(\mathbb{1})\Big)=\Big(\mathbb{1}\otimes\Delta(\mathbb{1})\Big)\Big(\Delta(\mathbb{1})\otimes\mathbb{1}\Big)\,, \tag{A.7.4}$$

where coassociativity is assumed in the first expression, while in the second and third expressions pairwise multiplication is used. A *weak Hopf algebra* is a weak bialgebra in which there exists an antipode map $S\colon\mathcal{A}\to\mathcal{A}$ satisfying the following three properties:

$$x_{(1)}\,S\Big(x_{(2)}\Big)=\epsilon\Big(\mathbb{1}_{(1)}\,x\Big)\,\mathbb{1}_{(2)}\,,\qquad S\Big(x_{(1)}\Big)\,x_{(2)}=\mathbb{1}_{(1)}\,\epsilon\Big(x\,\mathbb{1}_{(2)}\Big)\,,\qquad S\Big(x_{(1)}\Big)\,x_{(2)}\,S\Big(x_{(3)}\Big)=S(x)\,. \tag{A.7.5}$$

In the last equation we used Sweedler's notation for $\Delta^2(x)$. It follows [139] that the antipode map is unique, and that it is an algebra anti-homomorphism satisfying:

$$\begin{aligned} S(xy) &= S(y)\,S(x)\;, & S(\mathbb{1}) &= \mathbb{1}\;, \\ S(x)_{(1)} \otimes S(x)_{(2)} &= S\big(x_{(2)}\big) \otimes S\big(x_{(1)}\big)\;, & \epsilon \circ S &= \epsilon\;. \end{aligned} \tag{A.7.6}$$

In finite-dimensional weak Hopf algebras, S is always invertible. Weak C^*-Hopf algebras in which the antipode map is involutive, $S^2 = \mathrm{id}$, are called weak Kac algebras [136, 170].

A bialgebra (sometimes called strong bialgebra) is a weak bialgebra in which the counit is multiplicative and the unit is comultiplicative:

$$\epsilon(xy) = \epsilon(x)\,\epsilon(y)\;, \qquad\qquad \Delta(\mathbb{1}) = \mathbb{1} \otimes \mathbb{1}\;. \tag{A.7.7}$$

These stronger properties imply the corresponding weaker ones. A *Hopf algebra* (sometimes called a strong Hopf algebra) is a weak Hopf algebra in which one requires, equivalently, multiplicativity of the counit, comultiplicativity of the unit, or the hexagon diagram:

$$x_{(1)}\,S\big(x_{(2)}\big) = S\big(x_{(1)}\big)\,x_{(2)} = \epsilon(x)\,\mathbb{1}\;. \tag{A.7.8}$$

If one of these three properties holds for a weak Hopf algebra, then the other two follow automatically. This means that a Hopf algebra is in particular a bialgebra. Also in this case the antipode S is unique, it satisfies (A.7.6), and it is always invertible in the finite-dimensional case [171]. Besides,[11]

$$S^2 = \mathrm{id} \tag{A.7.9}$$

in finite-dimensional semisimple Hopf algebras over $\mathbb{C}$ [172, 173].

Group algebra. The group algebra $\mathbb{C}[G]$ is a typical example of Hopf algebra, where

$$\mu(g_1 \otimes g_2) = (g_1 g_2)\;, \quad u(1) = \mathbb{1}_G\;, \quad \Delta(g) = g \otimes g\;, \quad \epsilon(g) = 1\;, \quad S(g) = g^{-1}\;. \tag{A.7.10}$$

One easily verifies that all properties are satisfied.

[11] In finite-dimensional semisimple weak Hopf algebras over $\mathbb{C}$, S is not necessarily involutive.

Integrals. Following [139], in a weak Hopf algebra one introduces the left and right projectors

$$\begin{aligned} \Pi^{\mathrm{L}}(x) &= \epsilon\Big(\mathbb{1}_{(1)}\, x\Big)\, \mathbb{1}_{(2)} = x_{(1)}\, S\Big(x_{(2)}\Big) \,, \\ \Pi^{\mathrm{R}}(x) &= \mathbb{1}_{(1)}\, \epsilon\Big(x\, \mathbb{1}_{(2)}\Big) = S\Big(x_{(1)}\Big)\, x_{(2)} \,, \end{aligned} \tag{A.7.11}$$

acting on $x \in \mathcal{A}$. These are projectors because of (A.7.3), and the second equality is as in (A.7.5). They are related by the antipode map:[12]

$$\Pi^{\mathrm{L}} \circ S = \Pi^{\mathrm{L}} \circ \Pi^{\mathrm{R}} = S \circ \Pi^{\mathrm{R}} \,, \qquad\qquad \Pi^{\mathrm{R}} \circ S = \Pi^{\mathrm{R}} \circ \Pi^{\mathrm{L}} = S \circ \Pi^{\mathrm{L}} \,. \tag{A.7.12}$$

Then one defines left and right normalized integrals ℓ and r, respectively, such that:

$$x\, \ell = \Pi^{\mathrm{L}}(x)\, \ell \,, \qquad \Pi^{\mathrm{L}}(\ell) = \mathbb{1} \,, \qquad \text{or} \qquad r\, x = r\, \Pi^{\mathrm{R}}(x) \,, \qquad \Pi^{\mathrm{R}}(r) = \mathbb{1} \,, \tag{A.7.13}$$

for all $x \in \mathcal{A}$. Note that the normalized integrals ℓ, r are themselves projectors. Besides, $S(\ell)$ is a normalized right integral, and $S(r)$ is a normalized left integral (proven by applying S to (A.7.13) and using that S is invertible). An element that is simultaneously a left and right normalized integral is called a Haar integral h. When it exists, the Haar integral is unique. It follows that $S(h) = h$.

(Weak) Hopf algebra modules. A left-module, or representation, consists of a vector space V and a homomorphism $r \colon \mathcal{A} \to \mathrm{End}(V)$ that acts from the left and respects the algebra structure. For a general algebra there is no concept of conjugate representation or of tensor product of representations. Those concepts become available in a (weak) Hopf algebra [136].

Let $\mathcal{M} = (V, r)$ be a left-module for a weak Hopf algebra $\mathcal{A}$ over $\mathbb{C}$. There is a canonical right action on the dual space $V^\vee$, induced by the left action on V simply as $\langle f\, r(x), v\rangle \equiv \langle f, r(x)\, v\rangle$ for all $f \in V^\vee$, $v \in V$ and $x \in \mathcal{A}$. In order to construct a left action, instead, one uses the antipode map S:

$$r^*(x)\, f \equiv f\, r\Big(S(x)\Big) \,. \tag{A.7.14}$$

The fact that $S(xy) = S(y)\, S(x)$ guarantees that r^* is an algebra homomorphism. Thus $\mathcal{M}^* = (V^\vee, r^*)$ is a left-module that we call the conjugate representation to $\mathcal{M}$.

Let $\mathcal{M}_1$, $\mathcal{M}_2$ be two left-modules. The tensor product representation $\mathcal{M}_1 \otimes \mathcal{M}_2$

[12] Let us prove the first relation. First, notice that $\Pi^{\mathrm{L}}(\mathbb{1}) = \Pi^{\mathrm{R}}(\mathbb{1}) = \mathbb{1}$ and $\epsilon \circ \Pi^{\mathrm{L}} = \epsilon \circ \Pi^{\mathrm{R}} = \epsilon$. Then $\Pi^{\mathrm{L}} \circ \Pi^{\mathrm{R}}(x) = \epsilon\big(\mathbb{1}_{(1)} S(x_{(1)}) x_{(2)}\big)\mathbb{1}_{(2)} = \epsilon\big(\mathbb{1}_{(1)} S(x_{(1)})_{(2)}\big)\epsilon\big(S(x_{(1)})_{(1)} x_{(2)}\big)\mathbb{1}_{(2)} = \epsilon\big(\mathbb{1}_{(1)} S(x_{(1)})\big)\epsilon\big(S(x_{(2)}) x_{(3)}\big)\mathbb{1}_{(2)}$. Use $\epsilon\big(S(x_{(2)})x_{(3)}\big) = \epsilon \circ \Pi^{\mathrm{R}}(x_{(2)}) = \epsilon(x_{(2)})$, so that $\Pi^{\mathrm{L}} \circ \Pi^{\mathrm{R}}(x) = \epsilon\big(\mathbb{1}_{(1)} S(x)\big)\mathbb{1}_{(2)} = \Pi^{\mathrm{L}} \circ S(x)$.

on $V_1 \otimes V_2$ is constructed using the coproduct:

$$r_{12} \equiv (r_1 \otimes r_2) \circ \Delta \qquad \text{that is} \qquad r_{12}(x)\, v_1 \otimes v_2 \;\equiv\; \sum\nolimits_i \Big[r_1\big(x^i_{(1)}\big)\, v_1 \Big] \otimes \Big[r_2\big(x^i_{(2)}\big)\, v_2 \Big] \,. \tag{A.7.15}$$

This defines an algebra homomorphism $r_{12} \colon \mathcal{A} \to \mathrm{End}(V_1 \otimes V_2)$ in the case of Hopf algebras. In strictly weak Hopf algebras, since $\Delta(\mathbb{1}) \neq \mathbb{1} \otimes \mathbb{1}$, there are vectors annihilated by $r_{12}(\mathbb{1})$. To remedy, notice that $\Delta(\mathbb{1})$ is a projector, therefore one constructs the representation on the subspace of $V_1 \otimes V_2$ where $\Delta(\mathbb{1})$ acts as the identity.

In the case of Hopf algebras one can also define the so-called "trivial" one-dimensional representation $r_\epsilon \colon \mathcal{A} \to \mathbb{C}$ using the counit:

$$r_\epsilon(x) = \epsilon(x) \;. \tag{A.7.16}$$

This is an algebra homomorphism thanks to multiplicativity of the counit (A.7.7). The trivial representation multiplies trivially with all other representations (*i.e.*, it is the identity) under tensor product, since $\big((\epsilon \otimes r) \circ \Delta\big)(x) = \big((r \otimes \epsilon) \circ \Delta\big)(x) = r(x)$ using (A.7.2), and besides it is self-conjugate since $\epsilon \circ S = \epsilon$. In strictly weak Hopf algebras, a representation that multiplies trivially with all the other ones exists as well, however it is not one-dimensional.

A.7.1 Strip algebras with strongly-symmetric boundaries

It was shown in [116, 117] that strip algebras are weak Hopf algebras. Here we show that a strip algebra constructed using strongly-symmetric boundary conditions is actually a Hopf algebra. We only need to show that $\Delta(\mathbb{1}) = \mathbb{1} \otimes \mathbb{1}$.

A general formula to construct the coproduct Δ in strip algebras was provided in [117] Sec. 2.1. The identity element $\mathbb{1}$ (that we sometimes called $\mathcal{X}_{\mathbb{1}}$) of the strip algebra, and its coproduct computed using that formula, are:

$\mathbb{1} = \sum_{r,m}$ 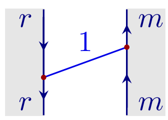

, $\quad \Delta(\mathbb{1}) = \sum_{r,n,m}$ 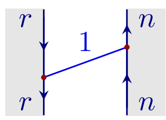

$\otimes$ 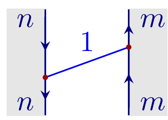

. (A.7.17)

For strongly-symmetric boundary conditions (and only in that case) the module has only one simple object, $r, m, n = \boldsymbol{\cdot}$, and therefore $\Delta(\mathbb{1}) = \mathbb{1} \otimes \mathbb{1}$.

A.7.2 Symmetrizer in Hopf and weak Kac algebras

In semisimple Hopf algebras, the symmetrizer is constructed using the object

$$\mathbb{P} = (\mathrm{id} \otimes S) \circ \Delta(P_\epsilon) \ \in \mathcal{A} \otimes \mathcal{A}^{\mathrm{op}} \ , \tag{A.7.18}$$

that we called e in (8.2.36). This is known to provide a separability idempotent with respect to the canonical Frobenius structure of a Hopf algebra, see [138] Remark 3.2.31. This implies that $\mathbb{P}$ satisfies the properties 1. – 3. listed in 7.1. Let us explicitly check 1., 3. and 4. Idempotency is

$$\begin{aligned} \mathbb{P} \times \mathbb{P} &= P_{\epsilon\,(1)'}\, P_{\epsilon\,(1)} \otimes S\Big(P_{\epsilon\,(2)}\Big)\, S\Big(P_{\epsilon\,(2)'}\Big) = P_{\epsilon\,(1)'}\, P_{\epsilon\,(1)} \otimes S\Big(P_{\epsilon\,(2)'}\, P_{\epsilon\,(2)}\Big) \\ &= (\mathrm{id} \otimes S)\Big(\Delta(P_\epsilon)\, \Delta(P_\epsilon)\Big) = (\mathrm{id} \otimes S) \circ \Delta\Big(P_\epsilon^2\Big) = \mathbb{P} \ . \end{aligned} \tag{A.7.19}$$

The preservation of symmetry-invariant matrices is $\mu(\mathbb{P}) = P_{\epsilon\,(1)}\, S\Big(P_{\epsilon\,(2)}\Big) = \mathbb{1}$, which immediately follows from (A.7.8) and $\epsilon(P_\epsilon) = 1$. The property of being trace-preserving follows from

$$S\Big(P_{\epsilon\,(2)}\Big)\, P_{\epsilon\,(1)} = S\bigg(S\Big(P_{\epsilon\,(1)}\Big)\, P_{\epsilon\,(2)}\bigg) = S\Big(\epsilon(P_\epsilon)\, \mathbb{1}\Big) = \mathbb{1} \ , \tag{A.7.20}$$

where we used $S^2 = \mathrm{id}$ repeatedly.

In semisimple weak Hopf algebras where $S^2 = \mathrm{id}$, the symmetrizer is constructed using

$$\mathbb{P} = (\mathrm{id} \otimes S) \circ \Delta(h) \ , \tag{A.7.21}$$

where h is the Haar integral. By Th. 3.13 of [139], the properties 1. – 3. are satisfied. In particular, the preservation of symmetry-invariant matrices follows from

$$\mu(\mathbb{P}) = h_{(1)}\, S\Big(h_{(2)}\Big) = \Pi^{\mathrm{L}}(h) = \mathbb{1} \ . \tag{A.7.22}$$

The property of being trace-preserving instead follows from

$$S\Big(h_{(2)}\Big)\, h_{(1)} = S\bigg(S\Big(h_{(1)}\Big)\, h_{(2)}\bigg) = S\Big(\Pi^{\mathrm{R}}(h)\Big) = S(\mathbb{1}) = \mathbb{1} \ , \tag{A.7.23}$$

where we used $S^2 = \mathrm{id}$.

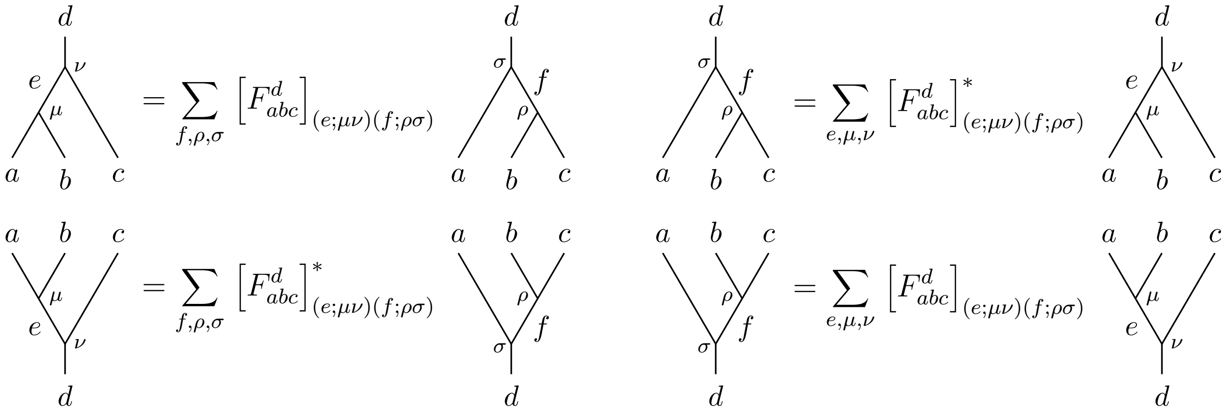

Figure A.1: Different ways of writing the F-move. All lines are oriented from bottom to top. We take as definition the one in the upper-left corner. The other ones are obtained using that F^d_{abc} is a unitary matrix, as well as manipulating the associator diagrams and .

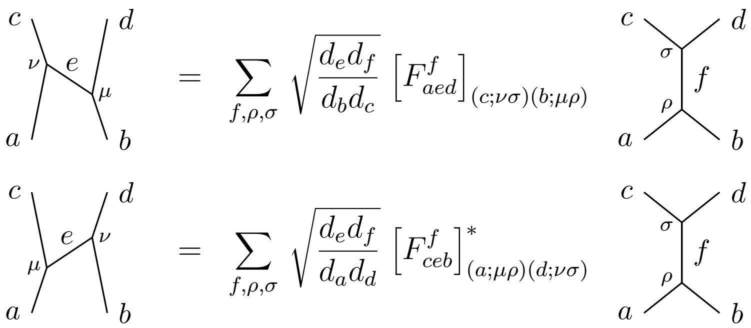

Figure A.2: Other F-moves, derived from the ones in Fig. A.1 by manipulating the associator diagrams. All lines run from bottom to top.

A.8 $\boldsymbol{F}$-symbols and the tube algebra

In the definition of the monoidal structure of $\mathscr{C}$ we follow the normalizations of [128]. The F-symbols F^d_{abc} are unitary isomorphisms

$$\bigoplus_e \mathrm{Hom}(\mathcal{L}_a \otimes \mathcal{L}_b, \mathcal{L}_e) \otimes \mathrm{Hom}(\mathcal{L}_e \otimes \mathcal{L}_c, \mathcal{L}_d) \xrightarrow{\sim} \bigoplus_f \mathrm{Hom}(\mathcal{L}_a \otimes \mathcal{L}_f, \mathcal{L}_d) \otimes \mathrm{Hom}(\mathcal{L}_b \otimes \mathcal{L}_c, \mathcal{L}_f) \tag{A.8.1}$$

represented by a unitary square matrix of size

$$N^d_{abc} = \sum\nolimits_e N^e_{ab}\, N^d_{ec} = \sum\nolimits_f N^d_{af}\, N^f_{bc} \,. \tag{A.8.2}$$

We use the definition in (8.1.13). The vector spaces of morphisms are normalized such that the relations in (8.1.14) hold. Those relations, together with unitarity, allow one to fix various moves that we summarize in Figs. A.1 and A.2.

The F-symbols satisfy the pentagon equation:

$$\sum_{\delta}[F^{e}_{fcd}]_{(g;\beta\gamma)(l;\nu\delta)}\,[F^{e}_{abl}]_{(f;\alpha\delta)(k;\mu\lambda)} = \sum_{h,\psi,\sigma,\rho}[F^{g}_{abc}]_{(f;\alpha\beta)(h;\psi\sigma)}\,[F^{e}_{ahd}]_{(g;\sigma\gamma)(k;\rho\lambda)}\,[F^{k}_{bcd}]_{(h;\psi\rho)(l;\nu\mu)}\,. \tag{A.8.3}$$

Unitarity can be used to move the first F-symbol and the sum over $(h;\psi\sigma)$ (or the last F-symbol and the sum over $(h;\psi\rho)$) from the right to the left, obtaining in this way many other equivalent relations.

The basis elements of the tube algebra are defined in (8.1.15), and the structure coefficients M of the algebra are introduced in (8.1.17). To compute them we proceed as follows. First we fuse b with a into c using (8.1.14), then we section the diagram horizontally intro three parts:

$$(8.1.17) = \sum_{c,\gamma}\sqrt{\frac{d_c}{d_a d_b}} \tag{A.8.4}$$

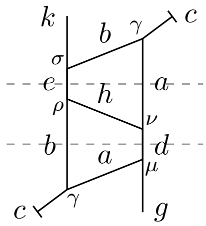

and finally we apply the F-moves in Fig. A.2. The resulting expression for M is in (8.1.18).

Case of an invertible symmetry. In the special case of an invertible symmetry group G, possibly with 't Hooft anomaly ω, the fusion category $\mathscr{C}$ is $\mathsf{Vec}^{\omega}_{G}$. The anomaly is parametrized by $\omega \in H^3\big(G, U(1)\big)$. The only nonvanishing F-symbols are

$$\Big[F^{(abc)}_{abc}\Big]_{(ab)(bc)} \equiv F_{abc} = \omega(a,b,c)\;. \tag{A.8.5}$$

On the left we used parenthesis (gh) to indicate the group multiplication, while in the middle we introduced a lighter notation for the F-symbols since they only depend on three group elements. The pentagon equation (A.8.3) is nonvanishing only if $e = (abcd)$, $f = (ab)$, $g = (abc)$, $h = (bc)$, $k = (bcd)$, $l = (cd)$, and it reads $F_{(ab)cd}\,F_{ab(cd)} = F_{abc}\,F_{a(bc)d}\,F_{bcd}$. This is precisely the cocycle condition $d\omega = 1$.

The elements of the tube algebra are specified by two labels: the vertical line incoming from below, and the horizontal line. Referring to (8.1.15), we specify g and a, while $d = ag$ and $h = aga^{-1}$. The nonvanishing structure coefficients of the tube algebra are then specified by three labels:

$$M^{ba,bag}_{g,a,ag,aga^{-1},b,baga^{-1},baga^{-1}b^{-1}} \;\equiv\; M_{g,a,b}\;. \tag{A.8.6}$$

Formula (8.1.19) gives:

$$M_{g,a,b} = \Big[F_{baga^{-1}b^{-1},b,a}\Big]^* \Big[F_{b,aga^{-1},a}\Big] \Big[F_{b,a,g}\Big]^* = \frac{\omega(b, aga^{-1}, a)}{\omega(baga^{-1}b^{-1}, b, a)\, \omega(b, a, g)} \ . \qquad \text{(A.8.7)}$$

Associativity of the tube algebra is guaranteed by the following identity:

$$M_{g,a,b}\, M_{g,ba,c} = M_{g,a,cb}\, M_{aga^{-1},b,c} \ . \qquad \text{(A.8.8)}$$

When expanded in terms of ω, this identity becomes equivalent to

$$\frac{d\omega(c, b, a, g)\ d\omega(c, baga^{-1}b^{-1}, b, a)}{d\omega(c, b, aga^{-1}, a)\ d\omega(cbaga^{-1}b^{-1}c^{-1}, c, b, a)} = 1 \ , \qquad \text{(A.8.9)}$$

which is indeed a true equation because ω is a cocycle.

Associativity in the noninvertible case. In the general case, the tube algebra product is given by (8.1.18). Using an argument similar to the previous one, but with lengthier algebra, and in particular applying the pentagon equation (A.8.3) four times, one can show that the product is associative. Let us sketch the proof in the case without multiplicities, *i.e.*, for $N_{ab}^c \in \{0, 1\}$. Associativity is the equation

$$\sum_{ds} M^{d,s}_{g,a,m,h,b,n,k}\, M^{f,t}_{g,d,s,k,c,p,l} = \sum_{er} M^{f,t}_{g,a,m,h,e,r,l}\, M^{e,r}_{h,b,n,k,c,p,l} \qquad \text{for}$$

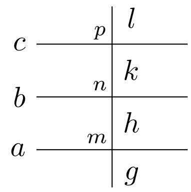

. (A.8.10)

Substituting the expression for M in (8.1.19), the quantum dimensions are the same on the two sides and can be dropped. One is left with the relation

$$\begin{aligned} &\textstyle\sum_{ds} \Big[F^s_{kba}\Big]^*_{nd} \Big[F^s_{bha}\Big]_{nm} \Big[F^s_{bag}\Big]^*_{dm} \cdot \Big[F^t_{lcd}\Big]^*_{pf} \Big[F^t_{ckd}\Big]_{ps} \Big[F^t_{cdg}\Big]^*_{fs} \\ &\qquad = \textstyle\sum_{er} \Big[F^t_{lea}\Big]^*_{rf} \Big[F^t_{eha}\Big]_{rm} \Big[F^t_{eag}\Big]^*_{fm} \cdot \Big[F^r_{lcb}\Big]^*_{pe} \Big[F^r_{ckb}\Big]_{pn} \Big[F^r_{cbh}\Big]^*_{en} . \end{aligned} \qquad \text{(A.8.11)}$$

This can be proven using the following set of four pentagon equations, obtained from (A.8.3) with various indices and possibly applying unitarity once or twice:

$$\begin{aligned} \left[F^t_{ckd}\right]_{ps} \left[F^s_{kba}\right]^*_{nd} &= \sum\nolimits_r \left[F^t_{pba}\right]^*_{rd} \left[F^r_{ckb}\right]_{pn} \left[F^t_{cna}\right]_{rs} \,, \\ \sum\nolimits_e \left[F^f_{cba}\right]^*_{ed} \left[F^t_{eag}\right]_{fm} \left[F^t_{cbm}\right]_{es} &= \left[F^t_{cdg}\right]_{fs} \left[F^s_{bag}\right]_{dm} \,, \\ \left[F^r_{cbh}\right]^*_{en} \left[F^t_{eha}\right]_{rm} &= \sum\nolimits_s \left[F^t_{cna}\right]_{rs} \left[F^s_{bha}\right]_{nm} \left[F^t_{cbm}\right]^*_{es} \,, \\ \sum\nolimits_d \left[F^t_{pba}\right]_{rd} \left[F^t_{lcd}\right]_{pf} \left[F^f_{cba}\right]^*_{ed} &= \left[F^r_{lcb}\right]_{pe} \left[F^t_{lea}\right]_{rf} \,. \end{aligned} \tag{A.8.12}$$

The first one and the complex conjugate of the second one are used on the l.h.s. of (A.8.11), while the third one and the complex conjugate of the fourth one are used on the r.h.s. On each side one ends up with a quadruple sum $\sum_{dser}$ of the same string, proving associativity.

A.9 $\tilde{F}$-symbols and the strip algebra

The $\tilde{F}$-symbols of a left-module category $\mathcal{M}$, as defined in (8.2.6), satisfy a pentagon equation that also involves the F-symbols of the underlying fusion category $\mathscr{C}$:

$$\sum_\rho \left[\tilde{F}^n_{dcm}\right]_{(e;\beta\mu)(p;\nu\rho)} \left[\tilde{F}^n_{abp}\right]_{(d;\alpha\rho)(q;\sigma\tau)} = \sum_{f,\gamma,\delta,\omega} \left[F^e_{abc}\right]_{(d;\alpha\beta)(f;\gamma\delta)} \left[\tilde{F}^n_{afm}\right]_{(e;\delta\mu)(q;\omega\tau)} \left[\tilde{F}^q_{bcm}\right]_{(f;\gamma\omega)(p;\nu\sigma)} \,. \tag{A.9.1}$$

Unitarity of the F and $\tilde{F}$ symbols allows one to move the first or third term on the l.h.s. and the sum to the r.h.s. Similarly, the symbols ${}^R\tilde{F}$ satisfy a right-module pentagon equation:

$$\begin{aligned} &\sum\nolimits_\omega \left[{}^R\tilde{F}^{\bar{m}}_{\bar{q}bc}\right]_{(\bar{p};\sigma\nu)(f;\gamma\omega)} \left[{}^R\tilde{F}^{\bar{m}}_{\bar{n}af}\right]_{(\bar{q};\tau\omega)(e;\delta\mu)} = \\ &\qquad = \sum\nolimits_{d\alpha\beta\rho} \left[{}^R\tilde{F}^{\bar{p}}_{\bar{n}ab}\right]_{(\bar{q};\tau\sigma)(d;\alpha\rho)} \left[{}^R\tilde{F}^{\bar{m}}_{\bar{n}dc}\right]_{(\bar{p};\rho\nu)(e;\beta\mu)} \left[F^e_{abc}\right]_{(d;\alpha\beta)(f;\gamma\delta)} \,. \end{aligned} \tag{A.9.2}$$

Associativity of the strip algebra. The strip algebra product was given in (8.2.13). Let us verify that it gives rise to an associative algebra, working for simplicity in the case that we use the same module on the right and on the left, and that there are no multiplicities. Associativity is the identity:

$$\sum\nolimits_d Q^d_{m,r,a,n,s,b,p,t}\, Q^f_{m,r,d,p,t,c,q,u} = \sum\nolimits_e Q^f_{m,r,a,n,s,e,q,u}\, Q^e_{n,s,b,p,t,c,q,u} \,. \tag{A.9.3}$$

Substituting the expression for Q, the quantum dimensions cancel out and we are left with

$$\sum_d \Big[\tilde F^t_{bar}\Big]_{ds} \Big[\tilde F^p_{bam}\Big]^*_{dn} \Big[\tilde F^u_{cdr}\Big]_{ft} \Big[\tilde F^q_{cdm}\Big]^*_{fp} = \sum_e \Big[\tilde F^u_{ear}\Big]_{fs} \Big[\tilde F^q_{eam}\Big]^*_{fn} \Big[\tilde F^u_{cbs}\Big]_{et} \Big[\tilde F^q_{cbn}\Big]^*_{ep} . \tag{A.9.4}$$

This identity can be verified using the module pentagon equation (A.9.1) twice, in particular in the following two forms:

$$\begin{aligned} \sum_e \Big[F^f_{cba}\Big]^*_{ed} \Big[\tilde F^u_{ear}\Big]_{fs} \Big[\tilde F^u_{cbs}\Big]_{et} &= \Big[\tilde F^u_{cdr}\Big]_{ft} \Big[\tilde F^t_{bar}\Big]_{ds} , \\ \Big[\tilde F^q_{eam}\Big]_{fn} \Big[\tilde F^q_{cbn}\Big]_{ep} &= \sum_d \Big[F^f_{cba}\Big]_{ed} \Big[\tilde F^q_{cdm}\Big]_{fp} \Big[\tilde F^p_{bam}\Big]_{dn} . \end{aligned} \tag{A.9.5}$$

The second one is used after complex conjugation. On both sides of (A.9.4) we obtain a double sum $\sum_{de}$ with the same string. This proves the identity.

A.10 Module categories over Vec_G^ω

Consider a symmetry group G. We first consider the case that there is no anomaly, $\omega = 1$, therefore the fusion category is Vec_G. Module categories are labeled by conjugacy classes of subgroups $H \subseteq G$ and cocycles $\psi \in H^2\big(H, U(1)\big)$ (see Example 7.4.10 in [69]). Let us explain how the modules are constructed.

The simple objects $\mathcal{B}_m$ correspond to the right-cosets G/H. We indicate them as $\mu \in G/H$. There is a projection map $[\,\cdot\,]\colon G \to G/H$ so that $[m] = \mu$ if m is a representative of the class μ. The module action is simply

$$a \times [m] = [am] \qquad \text{for } a \in G \;, \quad [m] \in G/H \;. \tag{A.10.1}$$

This product is well defined, in the sense that it does not depend on the representative m chosen, because the coset is a right-coset. We can then write $a \times \mu = a\mu$. Notice that H and kHk^{-1} (where $k \in G$) define equivalent module categories. If we denote $[g]_1 \in G/H$ and $[g]_k \in G/(kHk^{-1})$, an isomorphism is given by $\varphi\big([g]_1\big) = [gk^{-1}]_k$.

In order to construct the $\tilde F$-symbols we need a map $h\colon G \times G/H \to H$. First, choose a lift $r\colon G/H \to G$ of $[\,\cdot\,]$, that is a map

$$r(\mu) \qquad \text{such that} \qquad [r(\mu)] = \mu \;. \tag{A.10.2}$$

In general, $a \cdot r(\mu) \neq r(a\mu)$, however $[a \cdot r(\mu)] = a\mu = [r(a\mu)]$, therefore the two terms in the inequality differ by the action of H from the right. This allows us to define

$$h(a,\mu) \qquad \text{such that} \qquad a\cdot r(\mu) = r(a\mu)\cdot h(a,\mu)\ . \tag{A.10.3}$$

By considering $ab\cdot r(\mu)$ one obtains the identity

$$h(ab,\mu) = h(a,b\mu)\cdot h(b,\mu)\ . \tag{A.10.4}$$

Besides, $h(1,\mu)=1$ and so $h(a^{-1},\mu) = h(a,a^{-1}\mu)^{-1}$. We then define the $\tilde{F}$-symbols as

$$\tilde{F}_{ab\mu} = \psi\Big(h(a,b\mu),h(b,\mu)\Big)\ . \tag{A.10.5}$$

The indices not indicated are fixed. The left-module pentagon equation reads:

$$\tilde{F}_{ab,c,\mu}\,\tilde{F}_{a,b,c\mu} = F_{a,b,c}\,\tilde{F}_{a,bc,\mu}\,\tilde{F}_{b,c,\mu}\ . \tag{A.10.6}$$

As we are assuming that there are no anomalies, $\omega=1$, we have $F_{a,b,c}=1$. The remaining terms organize as

$$\frac{\psi\Big[h(b,c\mu),h(c,\mu)\Big]\,\psi\Big[h(a,bc\mu),h(bc,\mu)\Big]}{\psi\Big[h(ab,c\mu),h(c,\mu)\Big]\,\psi\Big[h(a,bc\mu),h(b,c\mu)\Big]} = d\psi\Big[h(a,bc\mu),h(b,c\mu),h(c,\mu)\Big] = 1\ . \tag{A.10.7}$$

This equation is satisfied because ψ is a cocycle. Thus the pentagon equation is satisfied.

There are two extreme cases. When $H=\{1\}$ we obtain the regular module, whose simple objects are all the elements of G. Such a module is completely fixed by G. Indeed $r(\mu)=\mu\in G$, $h(a,\mu)=1$, and ψ is trivial so that $\tilde{F}=\omega$ is trivial. When $H=G$, instead, the module has a single simple object (which is then a strongly-symmetric boundary condition) and the inequivalent consistent $\tilde{F}$-symbols parametrize the different SPT phases of G — or equivalently projective representations of G.

Consider now the general case that ω is not necessarily vanishing. This includes the case that ω vanishes in cohomology, but we have chosen a representative that is not identically 1. We will however use normalized cocycles. The fusion category is Vec_G^ω. Then module categories are labeled by:

- the conjugacy class of a subgroup $H\subseteq G$ such that $\omega\big|_H$ is trivial in $H^3\big(H,U(1)\big)$;
- a cochain $\psi\in C^2\big(H,U(1)\big)$ such that (using multiplicative notation):

$$d\psi = \omega^{-1}\big|_H\ . \tag{A.10.8}$$

Such cochains form a torsor over $H^2\Big(H, U(1)\Big)$.

As before, the simple objects are classes of G/H and fusion is defined in the natural way. Given a lift r of the projection and the map $h(a,\mu) \in H$ defined in (A.10.3), the $\tilde{F}$-symbols are

$$\tilde{F}_{ab\mu} = \psi\Big(h(a,b\mu), h(b,\mu)\Big)\, \frac{\omega\Big(r(ab\mu), h(a,b\mu), h(b,\mu)\Big)\, \omega\Big(a,b,r(\mu)\Big)}{\omega\Big(a, r(b\mu), h(b,\mu)\Big)} \;. \tag{A.10.9}$$

The only thing to check is that the left-module pentagon equation is satisfied. The condition (A.10.8) on ψ reads:

$$\frac{\psi\Big[h(b,c\mu), h(c,\mu)\Big]\, \psi\Big[h(a,bc\mu), h(bc,\mu)\Big]}{\psi\Big[h(ab,c\mu), h(c,\mu)\Big]\, \psi\Big[h(a,bc\mu), h(b,c\mu)\Big]} = d\psi = \omega\Big[h(a,bc\mu), h(b,c\mu), h(c,\mu)\Big]^{-1} \;. \tag{A.10.10}$$

When substituting into the pentagon equation, we obtain

$$\begin{aligned}&\Big\{\omega[a,b,c]\, \omega[a,bc,r(\mu)]\, \omega[a,r(bc\mu),h_{b,c\mu}]\, \omega[b,c,r(\mu)]\, \omega[ab,r(c\mu),h_{c,\mu}] \times \\ &\omega[r(bc\mu),h_{b,c\mu},h_{c,\mu}]\, \omega[r(abc\mu),h_{a,bc\mu},h_{bc,\mu}]\Big\} \Big/ \Big\{\omega[a,b,r(c\mu)]\, \omega[a,r(bc\mu),h_{bc,\mu}]\, \omega[b,r(c\mu),h_{c,\mu}] \times \\ &\omega[h_{a,bc\mu},h_{b,c\mu},h_{c,\mu}]\, \omega[ab,c,r(\mu)]\, \omega[r(abc\mu),h_{a,bc\mu},h_{b,c\mu}]\, \omega[r(abc\mu),h_{ab,c\mu},h_{c,\mu}]\Big\} \stackrel{?}{=} 1 \;,\end{aligned} \tag{A.10.11}$$

where we used a more compact notation for h. The expression on the left is indeed equal to 1, using that $d\omega[a,b,c,r(\mu)]$, $d\omega[a,b,r(c\mu),h_{c,\mu}]$, $d\omega[a,r(bc\mu),h_{b,c\mu},h_{c,\mu}]$, $d\omega[r(abc\mu),h_{a,bc\mu},h_{b,c\mu},h_{c,\mu}]$ are all equal to 1, as well as the multiplication properties of r and h given above.

Bibliography

[1] F. Benini, V. Godet, and A. H. Singh, "Entanglement asymmetry in conformal field theory and holography," *PTEP* **2025** no. 6, (2025) 063B05, arXiv:2407.07969 [hep-th].

[2] F. Benini, P. Calabrese, M. Fossati, A. H. Singh, and M. Venuti, "Entanglement asymmetry for higher and noninvertible symmetries," arXiv:2509.16311 [hep-th].

[3] F. Ares, S. Murciano, and P. Calabrese, "Entanglement asymmetry as a probe of symmetry breaking," *Nature Commun.* **14** (2023) 2036, arXiv:2207.14693 [cond-mat.stat-mech].

[4] X.-G. Wen, "Zoo of quantum-topological phases of matter," *Rev. Mod. Phys.* **89** no. 4, (2017) 041004, arXiv:1610.03911 [cond-mat.str-el].

[5] D. Tong, "Lectures on the Quantum Hall Effect," 6, 2016. arXiv:1606.06687 [hep-th].

[6] E. Fradkin, *Field Theories of Condensed Matter Physics*. Cambridge University Press, 2, 2013.

[7] H. Bethe, "Zur theorie der metalle. i. eigenwerte und eigenfunktionen der linearen atomkette," *Zeitschrift für Physik* **71** (1931) 205–226.

[8] F. D. M. Haldane, "Continuum dynamics of the 1-d heisenberg antiferromagnet: Identification with the o(3) nonlinear sigma model," *Phys. Lett. A* **93** (1983) 464–468.

[9] F. D. M. Haldane, "Nonlinear field theory of large-spin heisenberg antiferromagnets: Semiclassically quantized solitons of the one-dimensional easy-axis néel state," *Phys. Rev. Lett.* **50** (1983) 1153–1156.

[10] I. Affleck, T. Kennedy, E. H. Lieb, and H. Tasaki, "Rigorous results on valence-bond ground states in antiferromagnets," *Phys. Rev. Lett.* **59** (1987) 799–802.

[11] I. Affleck, T. Kennedy, E. H. Lieb, and H. Tasaki, "Valence bond ground states in isotropic quantum antiferromagnets," *Commun. Math. Phys.* **115** (1988) 477–528.

[12] M. den Nijs and K. Rommelse, "Preroughening transitions in crystal surfaces and valence-bond phases in quantum spin chains," *Phys. Rev. B* **40** (1989) 4709–4734.

[13] K. von Klitzing, G. Dorda, and M. Pepper, "New method for high-accuracy determination of the fine-structure constant based on quantized hall resistance," *Phys. Rev. Lett.* **45** (1980) 494–497.

[14] D. J. Thouless, M. Kohmoto, M. P. Nightingale, and M. den Nijs, "Quantized hall conductance in a two-dimensional periodic potential," *Phys. Rev. Lett.* **49** (1982) 405–408.

[15] D. C. Tsui, H. L. Störmer, and A. C. Gossard, "Two-dimensional magnetotransport in the extreme quantum limit," *Phys. Rev. Lett.* **48** (1982) 1559–1562.

[16] R. B. Laughlin, "Anomalous quantum hall effect: An incompressible quantum fluid with fractionally charged excitations," *Phys. Rev. Lett.* **50** (1983) 1395–1398.

[17] D. Arovas, J. R. Schrieffer, and F. Wilczek, "Fractional Statistics and the Quantum Hall Effect," *Phys. Rev. Lett.* **53** (1984) 722–723.

[18] A. Kitaev and J. Preskill, "Topological entanglement entropy," *Phys. Rev. Lett.* **96** (2006) 110404, `arXiv:hep-th/0510092`.

[19] J. A. Vaccaro, F. Anselmi, H. M. Wiseman, and K. Jacobs, "Tradeoff between extractable mechanical work, accessible entanglement, and ability to act as a reference system, under arbitrary superselection rules," *Phys. Rev. A* **77** (2008) 032114, `arXiv:quant-ph/0501121`.

[20] G. Gour, I. Marvian, and R. W. Spekkens, "Measuring the quality of a quantum reference frame: The relative entropy of frameness," *Phys. Rev. A* **80** (2009) 012307, `arXiv:0901.0943 [quant-ph]`.

[21] I. Marvian and R. W. Spekkens, "Extending Noether's theorem by quantifying the asymmetry of quantum states," *Nature Commun.* **5** (2014) 3821, `arXiv:1404.3236 [quant-ph]`.

[22] H. Casini, M. Huerta, J. M. Magán, and D. Pontello, "Entanglement entropy and superselection sectors. Part I. Global symmetries," *JHEP* **02** (2020) 014, `arXiv:1905.10487 [hep-th]`.

[23] J. M. Magán and D. Pontello, "Quantum complementarity through entropic certainty principles," *Phys. Rev. A* **103** (2021) 012211, arXiv:2005.01760 [hep-th].

[24] H. Casini, M. Huerta, J. M. Magán, and D. Pontello, "Entropic order parameters for the phases of QFT," *JHEP* **04** (2021) 277, arXiv:2008.11748 [hep-th].

[25] J. M. Magán, "Proof of the universal density of charged states in QFT," *JHEP* **12** (2021) 100, arXiv:2111.02418 [hep-th].

[26] S. Murciano, F. Ares, I. Klich, and P. Calabrese, "Entanglement asymmetry and quantum Mpemba effect in the XY spin chain," *J. Stat. Mech.* (2024) P013103, arXiv:2310.07513 [cond-mat.stat-mech].

[27] F. Ferro, F. Ares, and P. Calabrese, "Non-equilibrium entanglement asymmetry for discrete groups: the example of the XY spin chain," *J. Stat. Mech.* (2024) P023101, arXiv:2307.06902 [cond-mat.stat-mech].

[28] M. Fossati, F. Ares, J. Dubail, and P. Calabrese, "Entanglement asymmetry in CFT and its relation to non-topological defects," *JHEP* **05** (2024) 059, arXiv:2402.03446 [hep-th].

[29] M. Lastres, S. Murciano, F. Ares, and P. Calabrese, "Entanglement asymmetry in the critical XXZ spin chain," *J. Stat. Mech.* (2025) P013107, arXiv:2407.06427 [cond-mat.stat-mech].

[30] Y. Kusuki, S. Murciano, H. Ooguri, and S. Pal, "Entanglement asymmetry and symmetry defects in boundary conformal field theory," *JHEP* **01** (2025) 057, arXiv:2411.09792 [hep-th].

[31] M. Fossati, C. Rylands, and P. Calabrese, "Entanglement asymmetry in CFT with boundary symmetry breaking," *JHEP* **06** (2025) 089, arXiv:2411.10244 [hep-th].

[32] L. Capizzi and M. Mazzoni, "Entanglement asymmetry in the ordered phase of many-body systems: the Ising field theory," *JHEP* **12** (2023) 144, arXiv:2307.12127 [cond-mat.stat-mech].

[33] L. Capizzi and V. Vitale, "A universal formula for the entanglement asymmetry of matrix product states," *J. Phys. A: Math. Theor.* **57** (2024) 45LT01, arXiv:2310.01962 [quant-ph].

[34] C. Rylands, K. Klobas, F. Ares, P. Calabrese, S. Murciano, and B. Bertini, "Microscopic origin of the quantum Mpemba effect in integrable systems,"

Phys. Rev. Lett. **133** (2024) 010401, arXiv:2310.04419 [cond-mat.stat-mech].

[35] K. Klobas, "Non-equilibrium dynamics of symmetry-resolved entanglement and entanglement asymmetry: exact asymptotics in Rule 54*," *J. Phys. A* **57** (2024) 505001, arXiv:2407.21793 [cond-mat.stat-mech].

[36] F. Ares, S. Murciano, E. Vernier, and P. Calabrese, "Lack of symmetry restoration after a quantum quench: An entanglement asymmetry study," *SciPost Phys.* **15** (2023) 089, arXiv:2302.03330 [cond-mat.stat-mech].

[37] X. Turkeshi, P. Calabrese, and A. De Luca, "Quantum Mpemba effect in random circuits," *Phys. Rev. Lett.* **135** (2025) 040403, arXiv:2405.14514 [quant-ph].

[38] S. Liu, H.-K. Zhang, S. Yin, and S.-X. Zhang, "Symmetry restoration and quantum Mpemba effect in symmetric random circuits," *Phys. Rev. Lett.* **133** (2024) 140405, arXiv:2403.08459 [quant-ph].

[39] F. Ares, P. Calabrese, and S. Murciano, "The quantum Mpemba effects," *Nature Rev. Phys.* **7** (2025) 451–460, arXiv:2502.08087 [cond-mat.stat-mech].

[40] L. K. Joshi *et al.*, "Observing the quantum Mpemba effect in quantum simulations," *Phys. Rev. Lett.* **133** (2024) 010402, arXiv:2401.04270 [quant-ph].

[41] M. Chen and H.-H. Chen, "Rényi entanglement asymmetry in (1+1)-dimensional conformal field theories," *Phys. Rev. D* **109** (2024) 065009, arXiv:2310.15480 [hep-th].

[42] H. Fujimura and S. Shimamori, "Entanglement asymmetry and quantum Mpemba effect for non-Abelian global symmetry," arXiv:2509.05597 [hep-th].

[43] F. Ares, S. Murciano, L. Piroli, and P. Calabrese, "Entanglement asymmetry study of black hole radiation," *Phys. Rev. D* **110** (2024) L061901, arXiv:2311.12683 [hep-th].

[44] H.-H. Chen and Z.-J. Tang, "Entanglement asymmetry in the Hayden–Preskill protocol," *Phys. Rev. D* **111** (2025) 066003, arXiv:2411.17695 [hep-th].

[45] A. Russotto, F. Ares, and P. Calabrese, "Non-Abelian entanglement asymmetry in random states," *JHEP* **06** (2025) 149, arXiv:2411.13337 [hep-th].

[46] A. Russotto, F. Ares, and P. Calabrese, "Symmetry breaking in chaotic many-body quantum systems at finite temperature," *Phys. Rev. E* **112** (2025) L032101, arXiv:2504.06146 [quant-ph].

[47] F. Benini, E. García-Valdecasas, and S. Vitouladitis, "Higher-form entanglement asymmetry. Part I. The limits of symmetry breaking," arXiv:2512.15898 [hep-th].

[48] A. G. Lamas, J. Gliozzi, and T. L. Hughes, "Higher-form entanglement asymmetry and topological order," arXiv:2510.03967 [cond-mat.str-el].

[49] A. Florio and S. Murciano, "Entanglement asymmetry in gauge theories: Chiral anomaly in the finite temperature massless Schwinger model," *Phys. Rev. D* **113** no. 9, (2026) L091901, arXiv:2511.01966 [hep-th].

[50] Z. Ma, C. Han, Y. Meir, and E. Sela, "Symmetric inseparability and number entanglement in charge-conserving mixed states," *Phys. Rev. A* **105** (2022) 042416, arXiv:2110.09388 [quant-ph].

[51] C. Han, Y. Meir, and E. Sela, "Realistic protocol to measure entanglement at finite temperatures," *Phys. Rev. Lett.* **130** (2023) 136201, arXiv:2210.10713 [cond-mat.mes-hall].

[52] S. Lang, *Algebra*, vol. 211 of *Graduate Texts in Mathematics*. Springer, New York, 2002.

[53] J. Watrous, *The Theory of Quantum Information*. Cambridge University Press, 4, 2018.

[54] J. J. Bisognano and E. H. Wichmann, "On the duality condition for a hermitian scalar field," *J. Math. Phys.* **16** (1975) 985–1007.

[55] J. J. Bisognano and E. H. Wichmann, "On the duality condition for quantum fields," *J. Math. Phys.* **17** (1976) 303–321.

[56] H. Casini, M. Huerta, and R. C. Myers, "Towards a derivation of holographic entanglement entropy," *JHEP* **05** (2011) 036, arXiv:1102.0440 [hep-th].

[57] P. Calabrese and J. L. Cardy, "Entanglement entropy and quantum field theory," *J. Stat. Mech.* (2004) P06002, arXiv:hep-th/0405152.

[58] P. Di Francesco, P. Mathieu, and D. Senechal, *Conformal Field Theory*. Graduate Texts in Contemporary Physics. Springer-Verlag, New York, 1997.

[59] D. V. Fursaev and S. N. Solodukhin, "On the description of the riemannian geometry in the presence of conical defects," *Phys. Rev. D* **52** (1995) 2133–2143, arXiv:hep-th/9501127.

[60] M. B. Hastings, "An area law for one-dimensional quantum systems," *J. Stat. Mech.* **2007** (2007) P08024, arXiv:0705.2024 [quant-ph].

[61] S. Ryu and T. Takayanagi, "Holographic derivation of entanglement entropy from AdS/CFT," *Phys. Rev. Lett.* **96** (2006) 181602, arXiv:hep-th/0603001.

[62] V. E. Hubeny, M. Rangamani, and T. Takayanagi, "A covariant holographic entanglement entropy proposal," *JHEP* **07** (2007) 062, arXiv:0705.0016 [hep-th].

[63] R. M. Wald, "Black hole entropy is the Noether charge," *Phys. Rev. D* **48** (1993) R3427–R3431, arXiv:gr-qc/9307038.

[64] D. Gaiotto, A. Kapustin, N. Seiberg, and B. Willett, "Generalized global symmetries," *JHEP* **02** (2015) 172, arXiv:1412.5148 [hep-th].

[65] L. Bhardwaj and Y. Tachikawa, "On finite symmetries and their gauging in two dimensions," *JHEP* **03** (2018) 189, arXiv:1704.02330 [hep-th].

[66] L. Bhardwaj, L. E. Bottini, D. Pajer, and S. Schäfer-Nameki, "Gapped phases with non-invertible symmetries: (1+1)d," *SciPost Phys.* **18** (2025) 032, arXiv:2310.03784 [hep-th].

[67] C.-M. Chang, Y.-H. Lin, S.-H. Shao, Y. Wang, and X. Yin, "Topological defect lines and renormalization group flows in two dimensions," *JHEP* **01** (2019) 026, arXiv:1802.04445 [hep-th].

[68] Y. Choi, B. C. Rayhaun, Y. Sanghavi, and S.-H. Shao, "Remarks on boundaries, anomalies, and noninvertible symmetries," *Phys. Rev. D* **108** (2023) 125005, arXiv:2305.09713 [hep-th].

[69] P. Etingof, S. Gelaki, D. Nikshych, and V. Ostrik, *Tensor categories*, vol. 205 of *Mathematical Surveys and Monographs*. American Math. Soc., 2015. https://math.mit.edu/~etingof/egnobookfinal.pdf.

[70] S. H. Simon, *Topological Quantum*. Oxford University Press, 9, 2023.

[71] E. P. Verlinde, "Fusion Rules and Modular Transformations in 2D Conformal Field Theory," *Nucl. Phys. B* **300** (1988) 360–376.

[72] J. Frohlich, J. Fuchs, I. Runkel, and C. Schweigert, "Duality and defects in rational conformal field theory," *Nucl. Phys. B* **763** (2007) 354–430, arXiv:hep-th/0607247.

[73] S.-H. Shao, "What's Done Cannot Be Undone: TASI Lectures on Non-Invertible Symmetries," in *Theoretical Advanced Study Institute in Elementary Particle Physics 2023: Aspects of Symmetry*. 8, 2023. arXiv:2308.00747 [hep-th].

[74] M. Botta-Cantcheff, P. Martínez, and G. A. Silva, "On excited states in real-time AdS/CFT," *JHEP* **02** (2016) 171, arXiv:1512.07850 [hep-th].

[75] A. Christodoulou and K. Skenderis, "Holographic Construction of Excited CFT States," *JHEP* **04** (2016) 096, arXiv:1602.02039 [hep-th].

[76] T. Faulkner, F. M. Haehl, E. Hijano, O. Parrikar, C. Rabideau, and M. Van Raamsdonk, "Nonlinear gravity from entanglement in conformal field theories," *JHEP* **08** (2017) 057, arXiv:1705.03026 [hep-th].

[77] C. Holzhey, F. Larsen, and F. Wilczek, "Geometric and renormalized entropy in conformal field theory," *Nucl. Phys. B* **424** (1994) 443–467, arXiv:hep-th/9403108.

[78] P. Calabrese and J. Cardy, "Entanglement entropy and conformal field theory," *J. Phys. A* **42** (2009) 504005, arXiv:0905.4013 [cond-mat.stat-mech].

[79] N. Lashkari and M. Van Raamsdonk, "Canonical Energy is Quantum Fisher Information," *JHEP* **04** (2016) 153, arXiv:1508.00897 [hep-th].

[80] J. Cardy and E. Tonni, "Entanglement hamiltonians in two-dimensional conformal field theory," *J. Stat. Mech.* (2016) P123103, arXiv:1608.01283 [cond-mat.stat-mech].

[81] P. Calabrese and J. L. Cardy, "Time-dependence of correlation functions following a quantum quench," *Phys. Rev. Lett.* **96** (2006) 136801, arXiv:cond-mat/0601225.

[82] N. Laflorencie and S. Rachel, "Spin-resolved entanglement spectroscopy of critical spin chains and Luttinger liquids," *J. Stat. Mech.* (2014) P11013, arXiv:1407.3779 [cond-mat.str-el].

[83] M. Goldstein and E. Sela, "Symmetry-resolved entanglement in many-body systems," *Phys. Rev. Lett.* **120** (2018) 200602, arXiv:1711.09418 [cond-mat.stat-mech].

[84] J. C. Xavier, F. C. Alcaraz, and G. Sierra, "Equipartition of the entanglement entropy," *Phys. Rev. B* **98** (2018) 041106, arXiv:1804.06357 [cond-mat.stat-mech].

[85] M. Gutperle, Y.-Y. Li, D. Rathore, and K. Roumpedakis, "A note on entanglement entropy and topological defects in symmetric orbifold CFTs," *JHEP* **09** (2024) 010, arXiv:2406.10967 [hep-th].

[86] E. B. Mpemba and D. G. Osborne, "Cool?," *Phys. Educ.* **4** (1969) 172.

[87] Z. Lu and O. Raz, "Nonequilibrium thermodynamics of the Markovian Mpemba effect and its inverse," *PNAS* **114** (2017) 5083–5088, arXiv:1609.05271 [cond-mat.stat-mech].

[88] A. Kumar and J. Bechhoefer, "Exponentially faster cooling in a colloidal system," *Nature* **584** (2020) 64–68, arXiv:2008.02373 [cond-mat.stat-mech].

[89] J. Cardy, "Thermalization and Revivals after a Quantum Quench in Conformal Field Theory," *Phys. Rev. Lett.* **112** (2014) 220401, arXiv:1403.3040 [cond-mat.stat-mech].

[90] A. Belin, L.-Y. Hung, A. Maloney, S. Matsuura, R. C. Myers, and T. Sierens, "Holographic Charged Renyi Entropies," *JHEP* **12** (2013) 059, arXiv:1310.4180 [hep-th].

[91] H. Casini, C. D. Fosco, and M. Huerta, "Entanglement and alpha entropies for a massive Dirac field in two dimensions," *J. Stat. Mech.* (2005) P07007, arXiv:cond-mat/0505563.

[92] J. M. Maldacena, "The Large N limit of superconformal field theories and supergravity," *Adv. Theor. Math. Phys.* **2** (1998) 231–252, arXiv:hep-th/9711200.

[93] S. S. Gubser, I. R. Klebanov, and A. M. Polyakov, "Gauge theory correlators from noncritical string theory," *Phys. Lett. B* **428** (1998) 105–114, arXiv:hep-th/9802109.

[94] E. Witten, "Anti-de Sitter space and holography," *Adv. Theor. Math. Phys.* **2** (1998) 253–291, arXiv:hep-th/9802150.

[95] A. Lewkowycz and J. Maldacena, "Generalized gravitational entropy," *JHEP* **08** (2013) 090, arXiv:1304.4926 [hep-th].

[96] G. Penington, S. H. Shenker, D. Stanford, and Z. Yang, "Replica wormholes and the black hole interior," *JHEP* **03** (2022) 205, arXiv:1911.11977 [hep-th].

[97] A. Almheiri, T. Hartman, J. Maldacena, E. Shaghoulian, and A. Tajdini, "Replica Wormholes and the Entropy of Hawking Radiation," *JHEP* **05** (2020) 013, arXiv:1911.12333 [hep-th].

[98] D. Z. Freedman, S. D. Mathur, A. Matusis, and L. Rastelli, "Correlation functions in the $\mathrm{CFT}_d/\mathrm{AdS}_{d+1}$ correspondence," *Nucl. Phys. B* **546** (1999) 96–118, arXiv:hep-th/9804058.

[99] S. Hollands and R. M. Wald, "Stability of Black Holes and Black Branes," *Commun. Math. Phys.* **321** (2013) 629–680, arXiv:1201.0463 [gr-qc].

[100] N. Lashkari, J. Lin, H. Ooguri, B. Stoica, and M. Van Raamsdonk, "Gravitational positive energy theorems from information inequalities," *PTEP* **12** (2016) 12C109, arXiv:1605.01075 [hep-th].

[101] A. May and E. Hijano, "The holographic entropy zoo," *JHEP* **10** (2018) 036, arXiv:1806.06077 [hep-th].

[102] V. Iyer and R. M. Wald, "Some properties of Noether charge and a proposal for dynamical black hole entropy," *Phys. Rev. D* **50** (1994) 846–864, arXiv:gr-qc/9403028.

[103] J. Lee and R. M. Wald, "Local symmetries and constraints," *J. Math. Phys.* **31** (1990) 725–743.

[104] L. Bhardwaj, L. E. Bottini, D. Pajer, and S. Schafer-Nameki, "Categorical Landau paradigm for gapped phases," *Phys. Rev. Lett.* **133** (2024) 161601, arXiv:2310.03786 [cond-mat.str-el].

[105] C. L. Douglas and D. J. Reutter, "Fusion 2-categories and a state-sum invariant for 4-manifolds," arXiv:1812.11933 [math.QA].

[106] D. Gaiotto and T. Johnson-Freyd, "Condensations in higher categories," arXiv:1905.09566 [math.CT].

[107] T. Johnson-Freyd, "On the classification of topological orders," *Commun. Math. Phys.* **393** (2022) 989–1033, arXiv:2003.06663 [math.CT].

[108] L. Bhardwaj, L. E. Bottini, S. Schafer-Nameki, and A. Tiwari, "Non-invertible higher-categorical symmetries," *SciPost Phys.* **14** (2023) 007, arXiv:2204.06564 [hep-th].

[109] K. Ohmori and Y. Tachikawa, "Physics at the entangling surface," *J. Stat. Mech.* (2015) P04010, arXiv:1406.4167 [hep-th].

[110] S. Schäfer-Nameki, A. Tiwari, A. Warman, and C. Zhang, "SymTFT approach for mixed states with non-invertible symmetries," arXiv:2507.05350 [quant-ph].

[111] S. Ali Ahmad, M. S. Klinger, and Y. Wang, "The many faces of non-invertible symmetries," *JHEP* **05** (2026) 110, arXiv:2509.18072 [hep-th].

[112] A. Ocneanu, "Chirality for operator algebras," in *Subfactors: Proceedings of the Taniguchi Symposium on operator algebras*, H. Araki and others, eds., pp. 39–63. World Scientific, Singapore, 1994.

[113] D. A. Huse, "Exact exponents for infinitely many new multicritical points," *Phys. Rev. B* **30** (1984) 3908–3915.

[114] J. Aguilera-Damia, R. Argurio, F. Benini, S. Benvenuti, C. Copetti, and L. Tizzano, "Non-invertible symmetries along 4d RG flows," *JHEP* **02** (2024) 084, arXiv:2305.17084 [hep-th].

[115] V. Ostrik, "Module categories, weak Hopf algebras and modular invariants," *Transform. Groups* **8** (2003) 177–206, arXiv:math/0111139.

[116] A. Kitaev and L. Kong, "Models for gapped boundaries and domain walls," *Commun. Math. Phys.* **313** (2012) 351–373, arXiv:1104.5047 [cond-mat.str-el].

[117] C. Córdova, N. Holfester, and K. Ohmori, "Representation theory of solitons," *JHEP* **06** (2025) 001, arXiv:2408.11045 [hep-th].

[118] Y. Choi, B. C. Rayhaun, and Y. Zheng, "Generalized tube algebras, symmetry-resolved partition functions, and twisted boundary states," arXiv:2409.02159 [hep-th].

[119] C. Córdova, D. García-Sepúlveda, and N. Holfester, "Particle-soliton degeneracies from spontaneously broken non-invertible symmetry," *JHEP* **07** (2024) 154, arXiv:2403.08883 [hep-th].

[120] C. Copetti, L. Cordova, and S. Komatsu, "S-matrix bootstrap and non-invertible symmetries," *JHEP* **03** (2025) 204, arXiv:2408.13132 [hep-th].

[121] Y. Choi, B. C. Rayhaun, and Y. Zheng, "Noninvertible symmetry-resolved Affleck–Ludwig–Cardy formula and entanglement entropy from the boundary tube algebra," *Phys. Rev. Lett.* **133** (2024) 251602, arXiv:2409.02806 [hep-th].

[122] K. Jensen, E. Shaverin, and A. Yarom, "'t Hooft anomalies and boundaries," *JHEP* **01** (2018) 085, arXiv:1710.07299 [hep-th].

[123] R. Thorngren and Y. Wang, "Anomalous symmetries end at the boundary," *JHEP* **09** (2021) 017, arXiv:2012.15861 [hep-th].

[124] M. Aguiar, "A note on strongly separable algebras," *Boletín de la Academia Nacional de Ciencias* **65** (2000) 51–60. Journal page.

[125] G. J. Murphy, *C^*-algebras and operator theory*. Academic Press, 1990.

[126] Y.-H. Lin, M. Okada, S. Seifnashri, and Y. Tachikawa, "Asymptotic density of states in 2d CFTs with non-invertible symmetries," *JHEP* **03** (2023) 094, arXiv:2208.05495 [hep-th].

[127] J. Fuchs, "Fusion rules in conformal field theory," *Fortsch. Phys.* **42** (1994) 1–48, arXiv:hep-th/9306162.

[128] M. Barkeshli, P. Bonderson, M. Cheng, and Z. Wang, "Symmetry Fractionalization, Defects, and Gauging of Topological Phases," *Phys. Rev. B* **100** (2019) 115147, arXiv:1410.4540 [cond-mat.str-el].

[129] T. Bartsch, "Unitary Categorical Symmetries," arXiv:2502.04440 [hep-th].

[130] J. Fuchs, I. Runkel, and C. Schweigert, "TFT construction of RCFT correlators 1. Partition functions," *Nucl. Phys. B* **646** (2002) 353–497, arXiv:hep-th/0204148.

[131] T.-C. Huang, Y.-H. Lin, and S. Seifnashri, "Construction of two-dimensional topological field theories with non-invertible symmetries," *JHEP* **12** (2021) 028, arXiv:2110.02958 [hep-th].

[132] J. Fuchs, I. Runkel, and C. Schweigert, "TFT construction of RCFT correlators. 3. Simple currents," *Nucl. Phys. B* **694** (2004) 277–353, arXiv:hep-th/0403157.

[133] I. Affleck and A. W. W. Ludwig, "Universal noninteger 'ground state degeneracy' in critical quantum systems," *Phys. Rev. Lett.* **67** (1991) 161–164.

[134] A. Recknagel and V. Schomerus, *Boundary Conformal Field Theory and the Worldsheet Approach to D-Branes*. Cambridge Monographs on Mathematical Physics. Cambridge University Press, 2013.

[135] J. Fuchs and C. Schweigert, "Category theory for conformal boundary conditions," *Fields Inst. Commun.* **39** (2003) 25, arXiv:math/0106050.

[136] G. Böhm and K. Szlachányi, "Weak Hopf algebras: II. Representation theory, dimensions, and the Markov trace," *J. Algebra* **233** (2000) 156–212, arXiv:math/9906045 [math.QA].

[137] B. Day, "On closed categories of functors," in *Reports of the Midwest Category Seminar IV*, vol. 137 of *Lecture Notes in Mathematics*, pp. 1–38. Springer, Berlin, 1970.

[138] C. Schweigert, "Hopf Algebras, Quantum Groups and Topological Field Theory," 2023. https://www.math.uni-hamburg.de/home/schweigert/skripten/hskript.pdf.

[139] G. Böhm, F. Nill, and K. Szlachányi, "Weak Hopf algebras: I. Integral theory and C^*-structure," *J. Algebra* **221** (1999) 385–438, arXiv:math/9805116 [math.QA].

[140] R. Thorngren and Y. Wang, "Fusion category symmetry. Part I. Anomaly in-flow and gapped phases," *JHEP* **04** (2024) 132, arXiv:1912.02817 [hep-th].

[141] Y. Hu, Y. Wan, and Y.-S. Wu, "Twisted quantum double model of topological phases in two dimensions," *Phys. Rev. B* **87** (2013) 125114, arXiv:1211.3695 [cond-mat.str-el].

[142] F. Benini, C. Córdova, and P.-S. Hsin, "On 2-group global symmetries and their anomalies," *JHEP* **03** (2019) 118, arXiv:1803.09336 [hep-th].

[143] D. Tambara and S. Yamagami, "Tensor categories with fusion rules of self-duality for finite Abelian groups," *J. Algebra* **209** (1998) 692–707.

[144] T. Bartsch, M. Bullimore, and A. Grigoletto, "Representation theory for categorical symmetries," arXiv:2305.17165 [hep-th].

[145] K. Kawagoe, C. Jones, S. Sanford, D. Green, and D. Penneys, "Levin–Wen is a gauge theory: Entanglement from topology," *Commun. Math. Phys.* **405** (2024) 266, arXiv:2401.13838 [cond-mat.str-el].

[146] A. Perez-Lona, D. Robbins, E. Sharpe, T. Vandermeulen, and X. Yu, "Notes on gauging noninvertible symmetries. Part I. Multiplicity-free cases," *JHEP* **02** (2024) 154, arXiv:2311.16230 [hep-th].

[147] O. Diatlyk, C. Luo, Y. Wang, and Q. Weller, "Gauging non-invertible symmetries: topological interfaces and generalized orbifold groupoid in 2d QFT," *JHEP* **03** (2024) 127, arXiv:2311.17044 [hep-th].

[148] G. I. Kats and V. Palyutkin, “Finite ring groups,” *Trudy Moskovskogo Matematicheskogo Obshchestva* **15** (1966) 224–261.

[149] A. Masuoka, “Semisimple Hopf algebras of dimension 6, 8,” *Israel J. Math.* **92** (1995) 361–373.

[150] D. S. Sage and M. D. Vega, “Twisted Frobenius–Schur indicators for Hopf algebras,” *J. Algebra* **354** (2012) 136–147, arXiv:1107.0742 [math.QA].

[151] M. P. Mattis, “Correlations in two-dimensional critical theories,” *Nucl. Phys. B* **285** (1987) 671–686.

[152] U. Haagerup, “Principal graphs of subfactors in the index range $4 < [M : N] < 3 + \sqrt{2}$,” in *Subfactors: Proceedings of the Taniguchi Symposium on operator algebras*, H. Araki and others, eds., pp. 1–38. World Scientific, Singapore, 1994.

[153] M. Asaeda and U. Haagerup, “Exotic subfactors of finite depth with Jones indices $(5 + \sqrt{13})/2$ and $(5 + \sqrt{17})/2$,” *Commun. Math. Phys.* **202** (1999) 1–63, math/9803044 [math.OA].

[154] P. Grossman and N. Snyder, “Quantum subgroups of the Haagerup fusion categories,” *Commun. Math. Phys.* **311** (2012) 617–643, arXiv:1102.2631 [math.OA].

[155] M. Izumi, “The structure of sectors associated with Longo–Rehren inclusions. II: Examples,” *Rev. Math. Phys.* **13** (2001) 603–674.

[156] P. Grossman and M. Izumi, “Drinfeld centers of fusion categories arising from generalized Haagerup subfactors,” *Quantum Topol.* **13** (2023) 593–668, arXiv:1501.07679 [math.OA].

[157] T.-C. Huang and Y.-H. Lin, “The F-Symbols for Transparent Haagerup–Izumi Categories with $G = \mathbb{Z}_{2n+1}$,” arXiv:2007.00670 [math.CT].

[158] T. J. Osborne, D. E. Stiegemann, and R. Wolf, “The F-symbols for the $\mathcal{H}_3$ fusion category,” arXiv:1906.01322 [math.CT].

[159] T.-C. Huang, Y.-H. Lin, K. Ohmori, Y. Tachikawa, and M. Tezuka, “Numerical evidence for a Haagerup conformal field theory,” *Phys. Rev. Lett.* **128** (2022) 231603, arXiv:2110.03008 [cond-mat.stat-mech].

[160] T. J. Hagge and S.-M. Hong, “Some non-braided fusion categories of rank 3,” *Commun. Contemp. Math.* **11** (2009) 615–637.

[161] S.-H. Shao, J. Sorce, and M. Srivastava, "Additivity, Haag duality, and non-invertible symmetries," arXiv:2503.20863 [hep-th].

[162] H. Casini, E. Teste, and G. Torroba, "Relative entropy and the RG flow," *JHEP* **03** (2017) 089, arXiv:1611.00016 [hep-th].

[163] J. J. Heckman, M. Hübner, and C. Murdia, "On the holographic dual of a topological symmetry operator," *Phys. Rev. D* **110** no. 4, (2024) 046007, arXiv:2401.09538 [hep-th].

[164] G. E. Andrews, R. Askey, and R. Roy, *Special functions*. Encyclopedia of mathematics and its applications. Cambridge University Press, 1999.

[165] T. Faulkner, M. Guica, T. Hartman, R. C. Myers, and M. Van Raamsdonk, "Gravitation from Entanglement in Holographic CFTs," *JHEP* **03** (2014) 051, arXiv:1312.7856 [hep-th].

[166] A. W. Marshall, I. Olkin, and B. C. Arnold, *Inequalities: theory of majorization and its applications*. Springer, 2011.

[167] M. A. Nielsen and I. L. Chuang, *Quantum Computation and Quantum Information*. Cambridge University Press, 2010.

[168] M. Müger, "Galois theory for braided tensor categories and the modular closure," *Adv. Math.* **150** (2000) 151–201, arXiv:math/9812040 [math.CT].

[169] D. Penneys, "Operator algebras and their modules." Notes on Unitary quantum symmetries (Chapter 2), 2018. https://people.math.osu.edu/penneys.2/UQSL/PartI/UQSLPartIChapter2.pdf.

[170] D. Nikshych and L. Vainerman, "Algebraic versions of a finite-dimensional quantum groupoid," *Lecture Notes in Pure and Appl. Math.* (2000) 189–220, arXiv:math/9808054 [math.QA].

[171] R. G. Larson and M. E. Sweedler, "An associative orthogonal bilinear form for Hopf algebras," *Amer. J. Math.* **91** (1969) 75–94.

[172] R. G. Larson and D. E. Radford, "Semisimple cosemisimple Hopf algebras," *Amer. J. Math.* **110** (1988) 187–195.

[173] R. G. Larson and D. E. Radford, "Finite dimensional cosemisimple Hopf algebras in characteristic 0 are semisimple," *J. Alg.* **117** (1988) 267–289.